STATE OF CALIFORNIA • DEPARTMENT OF TRANSPORTATION

TECHNICAL REPORT DOCUMENTATION PAGE

TR0003 (REV 10/98)

ADA Notice

For individuals with sensory disabilities, this document is available in alternate formats. For information call (916) 654-6410 or TDD (916) 654-3880 or write Records and Forms Management, 1120 N Street, MS-89, Sacramento, CA 95814.

1. REPORT NUMBER	2. GOVERNMENT ASSOCIATION NUMBER	3. RECIPIENT'S CATALOG NUMBER
CA13-1665	N/A	N/A

4. TITLE AND SUBTITLE

High Occupancy Vehicle (HOV) System Analysis Tools-
Statewide High Occupancy Vehicle (HOV) Facility Performance Analysis

5. REPORT DATE

December 31, 2012

6. PERFORMING ORGANIZATION CODE

N/A

7. AUTHOR

UC Berkeley: C-Y Chan, Y-Q Du, K. Jang; UC Irvine: L. Chu, M-H Yang, W. Recker

8. PERFORMING ORGANIZATION REPORT NO.

UCB-0323

9. PERFORMING ORGANIZATION NAME AND ADDRESS

Institute of Transportation Studies
University of California, Berkeley
Berkeley, CA 94720

10. WORK UNIT NUMBER

65-3763

11. CONTRACT OR GRANT NUMBER

65A0323

12. SPONSORING AGENCY AND ADDRESS

California Department of Transportation
Division of Research, Innovation, and System Information (DRISI), MS-83
1227 O Street
Sacramento, CA. 95814

13. TYPE OF REPORT AND PERIOD COVERED

Final Report
May 2009 to December 2012

14. SPONSORING AGENCY CODE

N/A

15. SUPPLEMENTARY NOTES

None

16. ABSTRACT

This report describes the research findings of a study that includes the evaluation of operational performance of HOV facilities in several regions in California with different access types as well as a before-after comparative study of California facilities where access types were converted in recent years. The two most common types of HOV lanes in California are continuous access, prevalent in Northern California, and buffer-separated limited access, prevalent in Southern California. The objective of the study was to understand whether HOV facilities exhibited observable differences in their operational performance and if the conversion of access types resulted in noticeable differences.

The work, covering HOV facilities in the San Francisco Bay Area, Los Angeles County, and Orange County, was jointly carried out by research teams from the University of California, Berkeley and the University of California, Irvine. A separate but coordinated study, conducted by a research team from the University of California at Riverside, evaluates the HOV facilities in Riverside County.

The report documents the scope of the study and the data sources, and then presents the results of analysis based on real-world data and microsimulation. A set of performance measures were defined and selected to indicate how well the HOV facilities achieve its intended goals - that are the relief of congestion, saving of travel time, carrying more vehicle flows and passenger flows. Additionally, an alternative methodology of indicating how well the operations perform in terms of the traffic flow fundamental diagrams was also adopted.

17. KEY WORDS	18. DISTRIBUTION STATEMENT
High Occupancy Vehicle (HOV), Operational Performance, California Statewide HOV Facilities, Before-After Study, Continuous Access, Limited Access.	No restrictions. This document is available to the public through the National Technical Information Service, Springfield, VA 22161.

19. SECURITY CLASSIFICATION *(of this report)*	20. NUMBER OF PAGES	21. COST OF REPORT CHARGED
Unclassified	207	N/A

High Occupancy Vehicle (HOV) System Analysis Tools: Statewide HOV Facility Performance Analysis

- Final Report –

Federal Report No.: CA13-1665

University of California Report No.: UCB-0323

Prepared for:

California Department of Transportation

Division of Research, Innovation, and System Information (DRISI)

Prepared By:

Kitae Jang, Ching-Yao Chan, and Yao-Qiong Du

California PATH, University of California Berkeley

Lianyu Chu, Ming-Hsun Yang, and Will Recker

Institute of Transportation Studies (ITS), University of California Irvine

December 31, 2012

DISCLAIMER STATEMENT

This document is disseminated in the interest of information exchange. The contents of this report reflect the views of the authors who are responsible for the facts and accuracy of the data presented herein. The contents do not necessarily reflect the official views or policies of the State of California or the Federal Highway Administration. This publication does not constitute a standard, specification or regulation. This report does not constitute an endorsement by the Department of any product described herein.

For individuals with sensory disabilities, this document is available in Braille, large print, audiocassette, or compact disk. To obtain a copy of this document in one of these alternate formats, please contact: the Division of Research and Innovation, MS-83, California Department of Transportation, P.O. Box 942873, Sacramento, CA 94273-0001.

TABLE OF CONTENTS

LIST OF FIGURES

LIST OF TABLES

LIST OF ACRONYMS

- API: Application Programming Interface
- BPR: Bureau of Public Roads
- Caltrans: California Department of Transportation
- CERT-UCR: Center for Environmental Research and Technology at the University of California, Riverside
- CSMP: Corridor System Management Plan
- GP: General Purpose
- K-S: Kolmogorov-Smirnov
- FEP: Front End Processor
- FHWA: Federal Highway Administration
- LOS: Level of Service
- HCM: Highway Capacity Manual
- HOV: High-Occupancy Vehicle
- Micro-simulation: Microscopic simulation
- MPH: Miles Per Hour
- MPO: Metropolitan Planning Organization
- NB: North Bound
- OD: Origin Destination
- PATH: Partners for Advanced Transportation TecHnology
- PeMS: Freeway Performance Measurement System
- PMT: Person Miles Traveled
- PHT: Person Hours Traveled
- SATMS: Semi-Actuated Traffic Metering System
- SB: South Bound
- SR: State Route
- SOV: Single Occupancy Vehicle
- TAG: Technical Advisory Group
- TAP: Technical Advisory Panel
- TOPL: Tools for Operational Planning

- TT: Travel Time
- UC: University of California
- UCB: University of California Berkeley
- UCI: University of California Irvine
- Vcc: Vehicle Occupants
- VDS: Vehicle Detector Station
- VMT: Vehicle Miles Traveled
- VHT: Vehicle Hours Traveled
- VPH: Vehicles per hour

EXECUTIVE SUMMARY

This report documents research conducted under the sponsorship of the California Department of Transportation (Caltrans) Contract 65A323. The study period was from May 2009 to December 2012. The work was jointly carried out by research teams from the University of California, Berkeley and the University of California, Irvine. This study evaluated the performance of High-Occupancy Vehicle (HOV) operations in California, with an emphasis on investigating HOV facilities operational effectiveness according to their access configuration. The two most common types of HOV lanes in California are continuous access, prevalent in Northern California, and buffer-separated limited access, prevalent in Southern California.

This project was carried out in tandem with a separate project funded by Caltrans entitled, "HOV System Analysis Tools – District 8 HOV Facility Performance Analysis." That project was conducted by the Center for Environmental Research and Technology at the University of California, Riverside (CERT-UCR). The two projects were closely coordinated with frequent interactions among the researchers and joint quarterly meetings attended by the same Caltrans advisory panel and project managers. A report for the CERT-UCR project has been published. Readers of this report will benefit from referring to the documentation provided for the CERT-UCR project to understand the overall scope of HOV evaluation and the methodologies adopted.

This report is organized into two major parts. Part I evaluates real-world highway traffic data to identify the operating characteristics of HOV and general-purpose (GP) lanes. Key performance measures of HOV and GP lanes on a system-wide basis are calculated to offer comparisons by corridor, by region, and by access type. Part II compares the before-and-after performance of HOV facilities based on computer simulations and real-world data collected from five study sites in Orange County where the HOV lanes were converted from limited-access to continuous-access.

Part I includes the comparison of HOV and GP lane performance in Caltrans District 4, (San Francisco Bay area), District 7 (Los Angeles County area), and District 12 (Orange County area). The results can be summarized as follows:

1) HOV lanes generally have a higher traveling speed than GP lanes.
2) The VMT ratio for HOV lanes versus GP lanes is generally below 1, indicating that HOV lanes serve fewer vehicle-miles than GP lanes.
3) The PMT ratio for HOV lanes versus GP lanes is generally above 1, indicating HOV lanes carry more person-miles than GP lanes.

The results of the comparison between continuous and limited-access types are further summarized below. Please note that the compilation of results is based on specific study sites in Districts 4, 7, and 12 that have been selected for this report. The data are based on a six-month period of PeMS data in 2009 as well as corresponding vehicle occupancy count information from HOV reports of included districts. They are representative of operational performance in different districts but they do not encompass all HOV facilities. Thus, the evaluation results should be considered within the scope of data samples from the selected corridors.

1) Continuous- and limited-access HOV lanes offer similar levels of speed differentials in comparison to their adjacent GP lanes.
2) The VMT ratios in both types of HOV access are approximately equal. The detailed comparison of VMT values and ratios is given in the corresponding sections within the report.
3) The PMT ratios in both types of HOV access are approximately equal. The PMT ratios are heavily dependent on the occupancy requirements.

In reference to data sampling, methodologies and types of analysis for the conclusions offered above, the following similarities and differences when compared to those offered by the CERT-UCR report should be noted:

1) The technical approach in Part I of this report is similar to the "Corridor Level Analysis" and "Statistical Analysis" in the CERT-UCR study.
2) The data samples used for the primary body of analysis in Part I of this report are taken from HOV operational periods when there is a deteriorated level of service in the GP lanes (when the average speed in the GP lanes is below 45 mph). Thus, we only compared HOV/GP performance under constrained conditions. If traffic on the freeway is relatively free-flow, travelers have more flexibility to choose lanes of travel, which is particularly true for continuous-access types of facilities. Therefore, the comparison of

HOV/GP operational performance is more meaningful under the aforementioned degraded conditions, with the considerations that HOV is a congestion-relief measure and its performance is most critical when highways are operated under constrained conditions.

3) Since data points are filtered by the previously noted conditions, the overall sampling selection is different from the data set typically used, which commonly includes all operating hours from both types of HOV facilities.
4) In this report, no data from District 8 were used. We provide a discussion of our study sites from Districts 4, 7, and 12 in Section 3.
5) From a wide-ranging set of potential performance measures, the study in Part I focused on the selection and application of three key measures to evaluate HOV/GP performance: speed differential, vehicles-miles-traveled (VMT) ratio and passenger-miles-traveled (PMT) ratio.
    a. Speed differential provides a direct indicator of whether HOV lanes offer any advantage in travel speed and potential time saving.
    b. The VMT ratio compares how capacities in HOV and GP lanes fare against each other, and indicate how well the HOV is relatively utilized.
    c. The comparison of PMT ratio is similar to the idea of using VMT but with average passenger counts included in the calculation.
6) One challenge in making comparisons of operational performance is that each corridor has unique properties or special operating characteristics. The use of the VMT and PMT ratios allows us to explore the comparative performance of HOV versus GP lanes within individual corridors. For this reason, the VMT and PMT ratios are first calculated for each study site. Afterward, the calculated performance measures are then grouped by each district and each access type for comparison. However, we caution the reader that assessment of the grouped performance will be biased by the selection of corridors in the groups.
7) Supplementary information and detailed data from the study sites are also provided in the Appendices:
    a. Appendix A provides corridor bottlenecks as highlighted by speed-time contour maps for each corridor in the list of study sites.

b. Speed-flow maps that allow a comparative inspection of flows and speeds in GP and HOV lanes as well as the occurrence of congestion in each corridor, as in Appendix B-D for Districts 4, 7, and 12 respectively.
c. Speed differential, VMT ratio, and PMT ratio for each corridor, as in Appendix E-G for Districts 4, 7, and 12 respectively.
d. Distribution plots of various performance measures versus average general purpose lanes, as in Appendix H.

In Part II of the report, a real-world before- and- after study was performed for five study sites along the SR-55 and SR-57 corridors in District 12, Orange County, in which conversion of HOV lanes from limited-access to continuous-access has taken place. The performance measures include speed contour, speed differential, VMT ratio, demand flow, traffic flow fundamental diagram parameters, HOV lane changing rate and HOV violation. Among these measures, traffic flow fundamental diagram parameters are derived from the proposed traffic flow fundamental diagram based approach, which was adopted to analyze the detailed operational performance before and after the HOV lane conversion. The results of this analysis are summarized as follows:

1) The performance of HOV lane conversion from limited-access to continuous-access operation is site-specific and influenced by the local geometric attributes and associated traffic patterns.
2) Except for the SR-55 SB1 site, the continuous-access HOV facility has slightly lower throughputs for most detector stations in other study sites.
3) The conversion of HOV lane from limited-access to continuous-access leads to a faster shockwave speed on general-purpose lanes during the dissipation of congestion. In other words, a freeway with continuous-access HOV lane would see congestion clear faster.
4) The continuous-access HOV facility has a higher HOV lane changing rate. The limited-access HOV facility has a higher HOV lane changing intensity within the ingress/egress areas.
5) HOV lane conversion from limited-access to continuous-access increases the HOV lane violation rate based on the data collected along SR-55.

The simulation study was conducted based on the SR-57 freeway. We compared the southbound freeway's performance under the limited-access and continuous-access HOV configurations. We

also analyzed the freeway's performance under two different HOV lane striping strategies for the location with a HOV-to-HOV direct connector (based on the northbound SR-57 around the SR-91 interchange). The results from the simulation study are summarized as follows:

1) There are more lane change and weaving activities after converting the HOV lane from limited-access to continuous-access.
2) For the location with a freeway-to-freeway HOV direct connector, it is better to operate the HOV lane as a limited-access facility if HOV demands are high enough to cause congestion on the HOV lane.

1. Background

High-occupancy vehicle (HOV) facilities have been implemented on California freeways as one means of combating congestion in metropolitan areas. HOV facilities are a growing part of freeway infrastructure with significant effects on overall freeway performance. There are two primary HOV striping configurations employed in California: continuous and limited-access. These are shown in Figure 1.

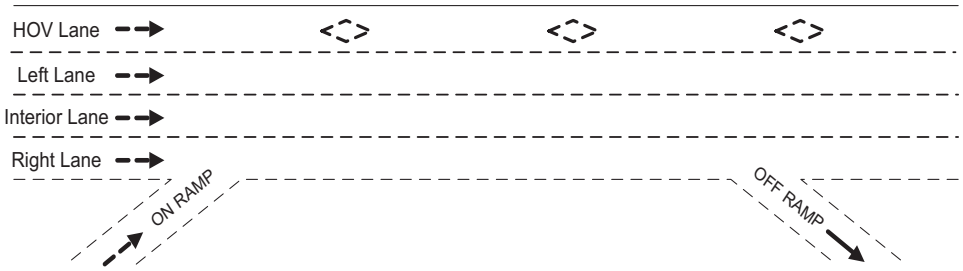

(a) Continuous Access HOV Lane

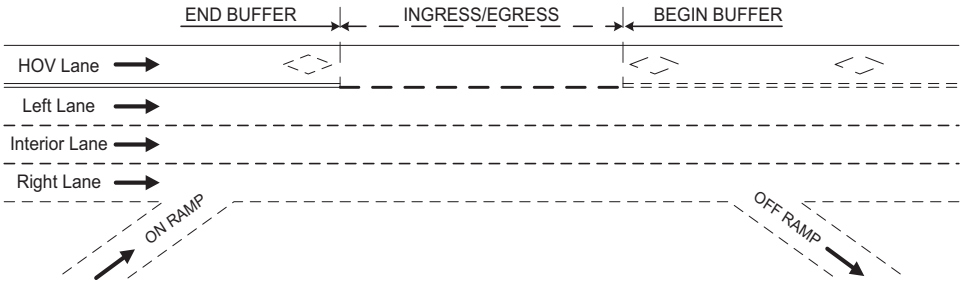

(b) Limited Access HOV Lane

Figure 1. Two Configurations for HOV Lanes: (a) Continuous and (b) Limited Access

Figure 1(a) shows **continuous-access HOV lanes (predominant in Northern California).** These lanes are normally implemented in areas that have short high-volume peak commute traffic periods, follow by a long off-peak period of low traffic volume. They generally operate only during peak hours. An example is the lane on Interstate 80 near San Francisco which operates from 5:00 a.m. to-10:00 a.m. and 3:00 p.m.to 7:00 p.m. The timed transition of HOV activation is equivalent to setting up a virtual partition between the HOV lane and the adjacent left lane that only allows HOV vehicles to enter. This influences driver lane-changing maneuvers, but imposes no fixed spatial restrictions on the movements. Continuous access HOV lanes may also be used when right-of-way limitations preclude buffer separation of the HOV

lane from General-Purpose (GP) lane traffic. Since continuous-access HOV lanes allow vehicles to enter or exit the HOV facility at any point along the freeway, traffic operation in the continuous HOV lane is more frequently interrupted by vehicles attempting to change lanes.

Limited access HOV lanes (predominant in Southern California), as shown in Figure 1(b), have specified locations for ingress and egress HOV maneuvers, and are separated from other freeway lanes by buffer zones demarcated by pavement markings or physical barriers. The limited-access configuration is designed to facilitate separate operation of traffic flows, typically at relatively high speeds within HOV lanes, and to lessen the impact from slower traffic in GP lanes. Conceptually, the ingress/egress areas serve as transition lanes, or virtual ramps, from the general-purpose lanes into the HOV lane, and vice versa. Concerns about limited-access lanes include possible impacts on traffic maneuvers due to vehicle lane-changing concentrated near ingress/egress locations, and extensive vehicle lane-changing between freeway ramps and HOV access points within a fixed and often relatively short distance.

Within the two primary categories of HOV lane access in California are four predominant operational strategies. These are:

(1) *Part-time continuous-access,* as used in Sacramento and the San Francisco Bay Area (Caltrans Districts 3 and 4).

(2) *Full-time limited-access buffer-separated with ingress/egress areas*, used in most HOV facilities in Southern California Caltrans districts: Districts 7, 8, 11 and 12).

(3) *Full-time continuous-access* in Orange County, used on State Route (SR)-22 and SR-55 and a portion of SR-57 southbound in Caltrans District 12 and a portion of SR-60/I-215 in Caltrans District 8.

(4) *Part-time limited-access buffer-separated with ingress/egress areas, used on* SR-14 in Caltrans District 7.

2. Project Objectives

HOV lanes have been regarded as a cost-effective and environmentally-friendly option to move travelers through congested routes. HOV facilities increase the total number of people moved through congested corridors by offering two travel incentives: travel time savings, and travel time reliability. Because HOV lanes carry vehicles with more occupants they move many more people during congested periods, even if the number of vehicles in the HOV lane is less than the number in the adjoining general purpose lanes. In general, carpoolers, vanpoolers, and bus patrons are the primary beneficiaries of HOV lanes.

This project focuses on the performance of California high occupancy vehicle (HOV) facilities performance in light of operational policies and access configurations. Specifically, we seek an understanding of the effects of HOV lane access control and operational policies on HOV facility performance.

Caltrans is currently considering the reconfiguration of the HOV lane system from full-time buffer-separated to full/part-time continuous-access. Before this is done, they must understand the potential benefits of both types of operation for system safety and operations. A recent study sponsored by Caltrans to investigate the safety of California freeways with HOV facilities provides some insight. Notably, the safety of the buffer-separated, limited-access HOV lanes typically seen in Southern California appeared to be no greater than the safety of the continuous-access limited-hour HOV lanes in Northern California (Jang, 2009). This is contrary to the common belief that buffer separation and restricted access provide additional protection for traffic in the HOV lanes. This project looks at whether or not a continuous-access HOV facility provides better operational performance than a buffer-separated facility.

This report summarizes our research, which was jointly undertaken by research teams from the University of California Berkeley (UCB) and the University of California Irvine (UCI). Part I focuses on system wide data analysis and Part II provides before-and-after comparisons.

PART I: PERFORMANCE MEASURES ANALYSIS OF STATEWIDE HOV OPERATION

3. Technical Approach

The approach taken in this report is to determine a set of performance measures that can be used to properly evaluate HOV performance by computing performance measures for various HOV system *scales* (district-level, corridor-level, and section-level) and comparing performance between different *types* of HOV facilities. The following sections outline the methodologies and calculations of performance measures adopted in the study.

3.1 List of Study Sites

To evaluate the performance of HOV facilities, the report uses real-world data and analyzes the performance of HOV facilities in a wide range of corridors (see Table 1). Figure 2 shows the geographic locations of these corridors. The corridors for this study were recommended by a Caltrans Technical Advisory Group (TAG) based on the group's familiarity with HOV facilities in their respective regions. In this report, we define a corridor as: *a unidirectional freeway segment with its accompanying HOV lanes*. Taking into consideration potential differences in directional traffic phenomena and geometric attributes, a corridor in our study is comprised of only one direction of a freeway segment with the associated ramps and HOV lanes.

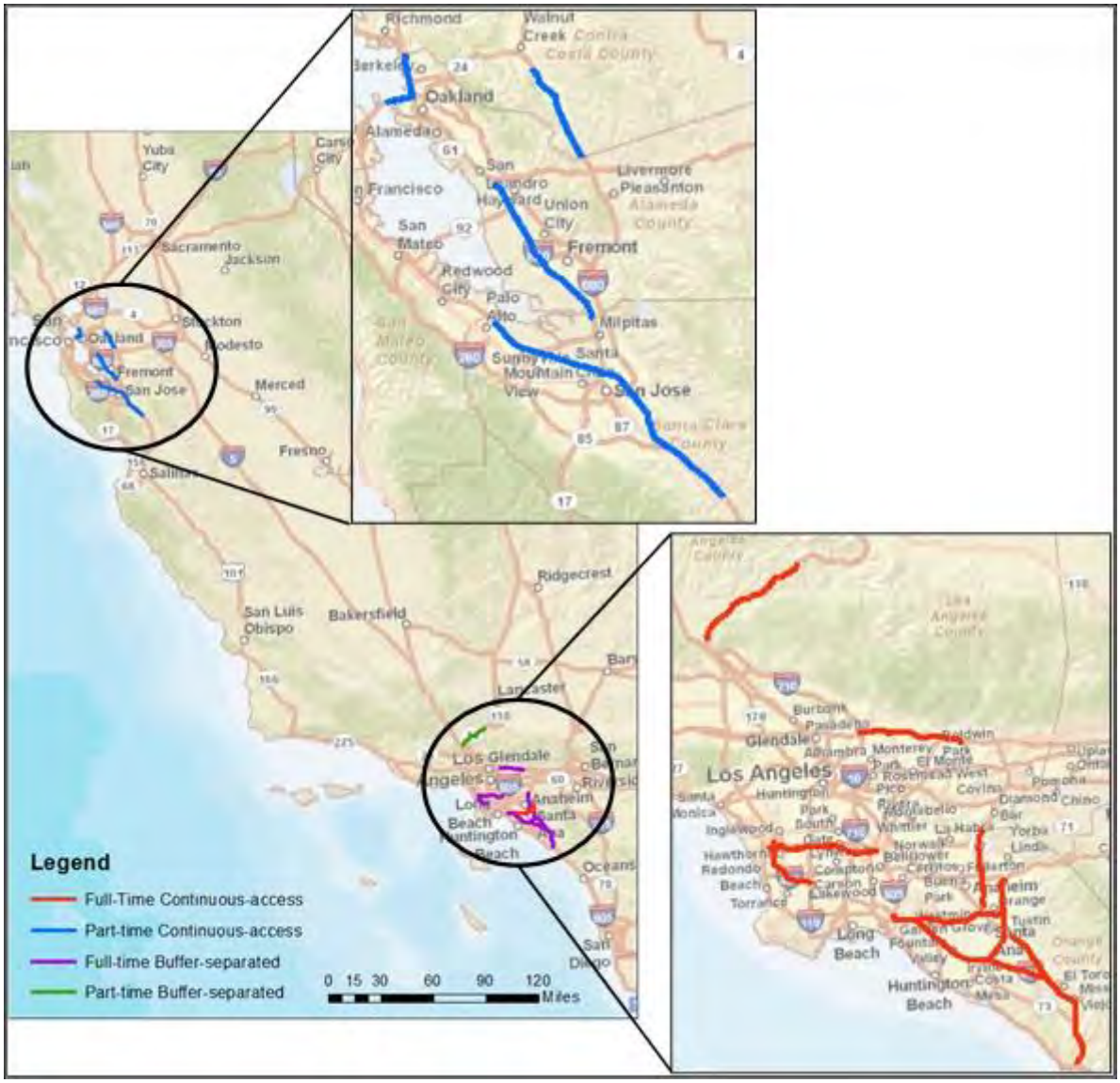

Figure 2. Study Corridors

Table 1. List of Study Corridors

HOV Type	District	County	Corridor	Direction	Study Boundaries (CA PM)	Operation Hours
Full-Time Continuous -access	12	ORA	SR-22	Both (E&W)	1.1-12.0	24 Hours, All Days
	12	ORA	SR-55	Both (N&S)	12.0-18.0	24 Hours, All Days
Full-time Buffer-separated	7	LA	I-105	West	2.6-16.8	24 Hours, All Days
	7	LA	I-105	East	1.2-16.9	24 Hours, All Days
	7	LA	I-210	East	24.8-39.6	24 Hours, All Days
	7	LA	I-405	South	12.9-22.2	24 Hours, All Days
	12	ORA	I-405	South	24.178-0.230E	24 Hours, All Days
	12	ORA	I-5	North	7-29	24 Hours, All Days
	12	ORA	I-405	North	0.230E-24.178	24 Hours, All Days
	12	ORA	I-5S	South	7.0-29.0	24 Hours, All Days
	12	ORA	SR-55	North	6.0-12.0	24 Hours, All Days
	12	ORA	SR-57	South	11.1-R22.6	24 Hours, All Days
Part-time Buffer-separated	7	LA	SR-14	North	25.0- 43.3	5-9 AM, Weekdays
	7	LA	SR-14	South	25.0- 43.3	3-7 PM, Weekdays
Part-time Continuous -access	4	ALA	I-80	West	0.0-9.8	5-10 AM & 3-7 PM, Weekdays
	4	SCL	US101	North	18.0-52.5	5-9 AM & 3-7 PM, Weekdays
	4	ALA	I-80	East	0.0-10.0	5-10 AM & 3-7 PM, Weekdays
	4	SCL	US101	South	18.1- 52.5	5-9 AM & 3-7 PM, Weekdays
	4	CC	I-680	North	0.0-11.4	5-9 AM & 3-7 PM, Weekdays
	4	CC	I-680	South	0.0-11.9	5-9 AM & 3-7 PM, Weekdays
	4	ALA	I-880	North	0.0-19.8	5-9 AM & 3-7 PM, Weekdays

3.2 Candidate Performance Measures

A freeway corridor with an HOV facility may have a variety of traffic and geometric attributes. At the same time, the performance of HOV systems can be evaluated from a number of key aspects. To address the primary objective of the current study, we first explored an extensive list of performance measures for analysis of HOV operations. The list was reviewed and established with input from the Caltrans TAG. The broad list of freeway corridor performance measures was then reduced to a selective list of key measures for use in detailed data analysis.

3.2.1 Measures of Freeway Performance Measures

Table 2 presents a list of all the performance measures reviewed in this study. Provided below are the detailed performance measures items that can be used, under each category, for an in-depth analysis of the HOV facilities.

Mobility

- VMT = segment length × traffic flow
- VMT (GP) = segment length × traffic flow in GP
- VMT (HOV) = segment length × traffic flow in HOV
- VHT = TT GP × traffic flow in GP + TT HOV × traffic flow in HOV
- VHT (GP) = TT GP × traffic flow in GP
- VHT (HOV) = TT HOV × traffic flow in HOV
- Travel time relative to TT at 65mph = TT – segment length / 65mph
- Travel time relative to TT at 35mph = TT – segment length / 35mph
- Person throughput = traffic flow in GP × Vcc in GP + traffic flow in HOV × Vcc in HOV
- Person throughput (GP) = traffic flow in GP × Vcc in GP
- Person throughput (HOV) = traffic flow in HOV × Vcc in HOV
- Headway (GP) = 300 / traffic flow in GP (flow data are aggregated in 5-min or 300 sec)
- Headway (GP Left) = 300 / traffic flow in GP left lane (GP left lane is the GP lane adjacent to HOV lane)
- Headway (HOV) = 300 / traffic flow in HOV
- Density (GP) = number of vehicles in GP / number of lanes in GP / segment length

- Density (GP Left) = number of vehicles in GP left / segment length
- Density (HOV) = number of vehicles in HOV / segment length

Table 2. List of Performance Measures

Category	Performance Measure
Mobility	VMT (at both system and lane level)
	VHT (at both system and lane level)
	Travel time delay (when compared to free-flowing conditions such as 65 MPH free-flowing conditions and when compared to congested states such as 35 MPH)
	Person throughput on HOV/GP lane(s)
	Vehicle throughput on HOV/GP lane(s)
	Vehicle density on HOV/GP lane(s)
	Vehicle headway on HOV/GP lane(s)
Reliability	Travel time statistics on HOV/GP lane(s)
	Absolute/relative travel time saving using HOV lane compared to GP lanes
	Travel speed statistics on HOV/GP lane(s)
	Travel speed differential between HOV/GP lane(s)
	Travel speed variation on HOV/GP lane(s) with time and space
Productivity	Level of service on HOV/GP lane(s)
	Presence of bottlenecks
	Duration and impact of bottlenecks
	Potential causes of bottlenecks
	Facility utilization on HOV/GP lane(s)
Maneuverability	Lane changing frequency between HOV and GP lanes
	Access types, barrier types
Conformance	Passenger occupancy rate on HOV/GP lanes
	HOV passenger occupancy violation rate
	Percent of HOV vehicles on HOV lanes
	Percent of HOV vehicles on GP lanes

Reliability

- TT (GP) = segment length / Speed in GP
- TT (HOV) = segment length / Speed in HOV
- Absolute TT Saving = TT (GP) – TT (HOV)
- Relative TT Saving = (TT (GP) – TT (HOV)) / TT (GP)
- Speed (GP) = ***f*** (traffic flow (GP), detector occupancy (GP))
  Where ***f*** () represents a certain functional relationship. Detector occupancy here is defined as the percentage of time that the detection zone of the instrument is occupied by a vehicle and is a measure of density.
- Speed (GP left) = ***f*** (traffic flow (GP left), detector occupancy (GP left))
- Speed (HOV) = ***f*** (traffic flow (HOV), detector occupancy (HOV))
- Speed Differential = Speed (HOV) – Speed (GP left)
- Speed Variation = Visualized from the *Speed Contour Diagram*

Productivity

- LOS (GP) = ***f*** (Speed GP) or ***f*** (Density GP)
- LOS (HOV) = ***f*** (Speed HOV) or ***f*** (Density HOV)
- Demand Volume GP
- Demand Volume HOV
- Presence of bottleneck = [Yes, No]
- Bottleneck Cause = 1 if HOV lane changing is related (may be caused by other factors simultaneously), 0 otherwise
- Bottleneck Duration = Percentage in time when the speed is under a certain threshold

Maneuverability

- Lane Changing Frequency = number of lane changing / (segment length × traffic flow) (unit: event per vehicle-mile)
- Qualitative ease of lane-changing due to presence or non-presence of separations or barriers

Conformance

- Vcc GP = obtained from Caltrans HOV Annual Report
- Vcc HOV = obtained from Caltrans HOV Annual Report
- HOV violation rates = obtained from Caltrans HOV Annual Report
- % of HOVs = (traffic flow in GP × % of HOV in GP + traffic flow in HOV × % of HOV in HOV) / (traffic flow in GP + traffic flow in HOV)

3.2.2 Specific Performance Measures for HOV Operations

Table 2 presents an extensive list of performance measures commonly used to evaluate the performance of freeway facilities. However, these measures are not necessarily tailored for comparing performance between the two access types, which is the intent of this study. In this section, we will pare this list down to a few measures that are most representative and allow system-level comparisons. The selection of measures is based on the following considerations:

1) The use of a large number of performance measures within the broad list in Table 2 makes it challenging to control some exposure variables.

2) Parameters such as speed, VMT and PMT are basic and representative factors to directly describe performance. These measures are independent by site and comparable for different HOV types.

3) The operational performance of both HOV and GP lanes are intertwined, thus the evaluation should allow the identification of situations when GP traffic conditions have a meaningful impact on HOV operations. For example, as will be explained in a later section, the performance comparison is considered most significant when the GP lanes are operating below 45 mph.

4) Due to the nature of heterogeneous travel patterns across corridors, it is important to investigate HOV operational performance at the system level as well at the corridor level.

5) Previous research has studied various aspects of HOV safety, including accident ratio and incident impact. This study focus on other aspects of performance.

Based on these considerations, we selected three focused, representative and comparable performance measures for our study. They are defined and explained below.

Speed differential = Speed (HOV) – Speed (GP)

Speed differential is a proxy for travel time savings, and comparable between samples. The speed differential definition chosen for this study is the difference between the speeds in the HOV and the GP lanes. For example, if traffic in the GP lane is moving faster than that in the HOV lane then the speed differential is negative. In other words, traffic in the HOV lane travels at slower speeds than that in GP lanes. In this case, HOV facilities do not provide travel time savings.

VMT ratio = (segment length × traffic flow in HOV lane) / (segment length × traffic flow in GP lanes)

This ratio measures the utilization level of the HOV lane by vehicle-miles (is equivalent to the ratio of HOV flow to GP flow). If the ratio is greater than 1, it means that the subject HOV lane carries more vehicle-miles than the average GP lane.

PMT ratio = (segment length × average Vcc in HOV × traffic flow in HOV lane) / (segment length × average Vcc in GP × traffic flow in GP lane)

This ratio measures the utilization level of the HOV lane by person-miles. If the ratio is greater than 1, it means that the subject HOV lane serves more person-miles than the average GP lane.

One of the objectives of implementing HOV lanes is to carry more passengers with fewer vehicles. Thus, both the PMT and the VMT ratios are of critical importance in evaluating the operational performance of HOV facilities. There are four possibilities when the VMT and PMT measures are combined. These are:

i) VMT ratio < 1 and PMT ratio < 1: This means that the HOV lane serves fewer vehicles and people than the average GP lane, which implies the potential of *relatively underutilized HOV facilities*. Although in this category, the HOV lane may still meet the minimum requirement by serving more than 800 vph or 1800 persons per hour according to the HOV guideline.

ii) VMT ratio < 1 and PMT ratio >= 1: This means that the HOV lane serves fewer vehicles but moves the same number or more people than an average GP lane.

iii) VMT ratio > 1 and PMT ratio < 1: This means that the HOV lane serves more vehicles but fewer people than the average GP lane. This situation is unlikely due to the nature of multiple occupancy requirements in HOV lanes, but it may occur only when the average occupancy of the GP lane traffic is greater than that of HOV lane traffic.

iv) VMT ratio > 1 and PMT ratio >= 1: This means that the HOV lane serves more vehicles and moves more people than the average GP lane, which implies the possibility of o*ver-utilized HOV facilities*. If an excessively large number of vehicles travels in the HOV lanes, it may cause the speed differential to be negative, resulting in a deterioration of operations in the HOV lane.

3.2.3 Conditions for Computing Performance Measures

For comparability, it is important to take congestion into account because different corridors may have different hours of HOV lane operation and have different patterns of congestion. In addition, since congestion is the primary reason for implementing HOV facilities, there is an additional incentive to understand the impact of congestion on the operational performance of HOV facilities in California.

Figure 3 shows the contour plots of average speed across GP lanes in time-space dimensions for two different corridors, 8 peak-hour only vs. 24 hour HOV operations. The X-axis is HOV operation hours and Y-axis is post-mile. The dash line on Figure 3(a) denotes the boundary of morning (5:00 a.m. - 9:00 a.m.) and afternoon (3:00 p.m. – 7:00 p.m.) rush hours. The color red denotes congested conditions while green indicates free-flow conditions. Although the two corridors are similar in length, they have quite different congestion patterns.

Visual inspection of Figure 3(a) shows that a recurrent bottleneck exists near post-mile 17 during morning and afternoon operating hours. In the morning hours, the bottleneck activates around 7:00 a.m. due to the increase in traffic demand while congestion exists throughout the HOV afternoon operation hours. On the other hand, as shown in Figure 3(b), congestion on the I-210 Eastbound spans over a 13-mile stretch and over 5 afternoon peak hours (2:00-7:00 p.m.). Based on the calculation of congestion hour-distance, I-210 Eastbound is considered more congested. However, if the congestion hour-distance is calculated by the percentage of congested samples within the total operational hours, 18.8% of samples from I-880 Northbound are below 45 mph

versus 16.2% of samples from I-210 Eastbound are below 45 mph. Without knowing the operational differences between the corridors, we may conclude that I-880 is more congested. This exercise suggests that the performance measures should control for the conditions of congestion in comparing performance measures between different types of HOV facilities.

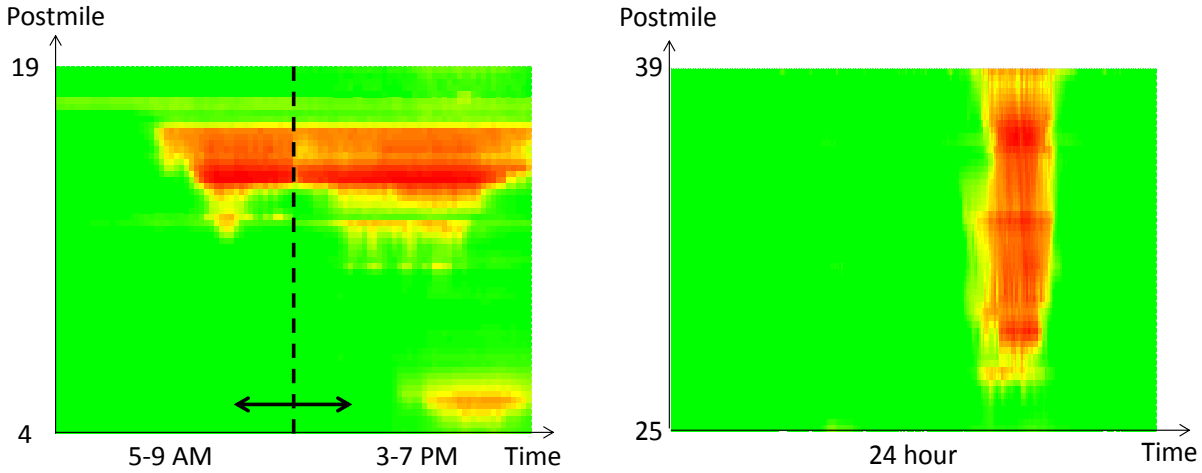

(a) Interstate 880 Northbound, District 4 (b) Interstate 210 Eastbound, District 7

Figure 3. Speed contour plots: (a) Interstate 880 Northbound, District 4, and (b) Interstate 210 Eastbound, District 7

There are many definitions of traffic congestion. These could include, for example, vehicles traveling below a certain speed threshold, existence of vehicle queuing, elongated trip times, etc. Our study adopts the definition from the Highway Capacity Manual (HCM, 2000), in which congestion is defined as *the state when the flow reaches the capacity of the segment and thus becomes slow*. Figure 4 shows a speed vs. flow diagram, showing that the flow reaches its maximum around 2,400 passenger-car/hour/lane at around 45 mph. In the current study, we will define congestion in the GP lanes when their speeds are below 45 mph. Thus, samples from the congested traffic states characterized by speeds below 45 mph will be used to compute performance measures.

It should be noted that congestion may be defined under different travel conditions. For example, in some Caltrans reports[1,2] congestion is described as a condition where travel speeds are below 35 mph.

[1] http://www.dot.ca.gov/hq/traffops/sysmgtpl/MPR/pdfs/MPR2009.pdf
[2] http://www.dot.ca.gov/dist3/departments/envinternet/topbus/final/chap1.pdf

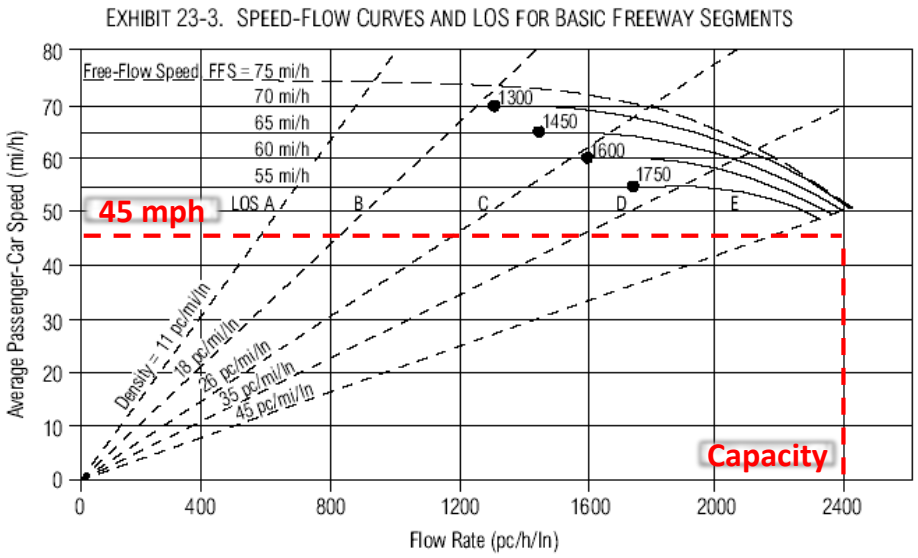

Figure 4. Speed-Flow Curves and Level of Service (LOS) for Basic Freeway Segment (Highway Capacity Manual, 2000)

3.3 Data Sources

As to the real-world evaluation, the performance analysis tool for statewide HOV facilities will be developed mainly based on the following data sources:

- *HOV facilities*
    - California Department of Transportation *Statewide HOV Map and Inventory* (2008)
    - California Department of Transportation *2008 HOV Annual Reports*
- *Traffic Information*
    - Freeway Performance Measurement System (PeMS), http://pems.dot.ca.gov, from May 2009 to October 2009

Most of the HOV facility data were taken from HOV reports from various districts. For example, the vehicle occupant counts in the HOV lanes were available from 2008, but not in subsequent years. To be consistent across different districts, data from 2008 were used in this study.

As for traffic data, the present study takes 5-minute samples from all weekdays between May

and October 2009; for part-time operational HOV facilities, only operational hours (5:00 a.m. to 10:00 a.m. and 3:00 p.m.to 7:00 p.m.) are included in the analysis and for full-time operational HOV facilities, hours from 5:00 a.m. to 9:00 p.m. are included in the analysis. Even though the data span a number of months, there may be certain seasonal patterns in different districts that may affect the analysis and interpretation of data. It should also be noted that the final evaluation is made by selecting data samples when GP lanes are congested or when speed is less than 45 mph. Therefore the data sets were further filtered even though different periods of data are extracted for continuous-access (9 hours) and limited-access (16 hours) types.

Other data sources (e.g., Tach Runs) for traffic information are also available. Data sources of this kind continuously measure traffic speed while some vehicles with special equipment are being driven with the real traffic. Hence, the data collected could include more accurate and detailed information than data from loop detectors (which are located sparsely along the freeway.) However, these data are available only for the selected corridors during limited times because of insufficient coverage and sample size, and therefore not appropriate for the computation of large-scale system-wide performance measures, as required in the current study. Thus, detector data were used for the computation and comparison of performance measures.

It has been brought to the attention of the Caltrans Technical Advisory Panel (TAP) and the research team that in some cases there have been observations and discussions regarding the fidelity and accuracy of PeMS data. A previous study sponsored by Caltrans also examined these data issues and also compared the use of PeMS and Tach Run data for congestion evaluation as well as its impact on accuracy (Kwon, McCullough, Petty, & and Varaiya, 2007).

3.4 Scale of Computation Samples

The scale of samples is a 5-minute sample from a loop detector. Each detector covers a segment length upstream and downstream from the detector location. For example, in Figure 5 the detector in the middle of the diagram will be used to represent the traffic sample data for the section designated as “Detector Coverage.” Five-minute total flow and average speed at each detector location are extracted from PeMS.

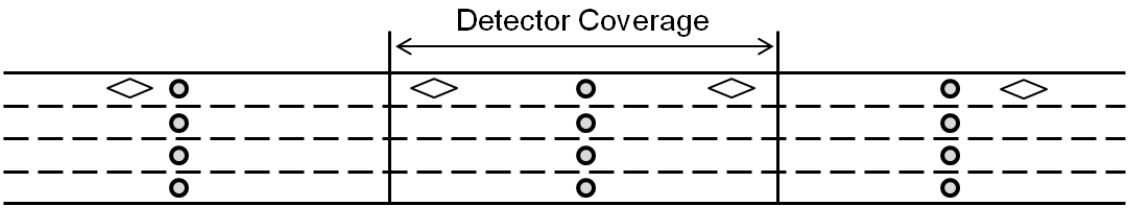

Figure 5. Detector coverage

The distribution of performance measures for the following three levels is constructed using samples collected from detectors.

1) Performance measures for district: all the samples from all detectors in the district
2) Performance measures for corridor: all the samples from all detectors in the corridor
3) Performance measures for segment: all the samples from all detectors in the segment

3.5 Comparison of Technical Approaches and Methodologies

This project was carried out in tandem with a separately-funded project by Caltrans, entitled "HOV System Analysis Tools – District 8 HOV Facility Performance Analysis," which is being conducted by the Center for Environmental Research and Technology at the University of California, Riverside. The two projects are closely coordinated with frequent interactions among the researchers and joint quarterly meetings attended by the same Caltrans advisory panel and project managers. A report for the CERT-UCR project has also been submitted. Readers of this report will benefit from referring to the documentation provided for the CERT-UCR project to understand the overall scope of the HOV evaluation and the methodologies adopted. Table 3 below highlights the differences in the use of data and technical approaches.

Table 3. Methodology Summary by Research Group

Research Group	UC Berkeley	UC Irvine	UC Riverside
Study Site	District 4,7,12	SR-55, SR-57 in District 12	District 8
Data Sampling	Filtered data when general purpose lanes are operating below 45 mph	Data in HOV operation hours	Data in HOV operation hours
Real-World Data Analysis	Corridor • Recurrent bottlenecks • Speed-flow joint probability A GP Lane Congested • Speed/ Flow • Speed Differential • VMT/PMT • VMT/PMT Ratio • Statistical Weaving Analysis	Before and After Comparison • Traffic flow fundamental diagram • Critical Detector Occupancy / Critical Flow • Free Flow Speed / Shockwave Speed • Speed contour map • Demand flows • HOV lane changing rate • HOV violation rate	Corridor • AVO /ratio • HOV violation rate • Proportion of carpool/ HOVL carpool • Recurrent bottlenecks • Q and identification of peak hour • VMT /PMT ratio • HOVL-MFL joint LOS matrix • Speed difference vs. density • Speed-flow joint probability Statistical Modeling (D4,7,8,12) • Capacity
Simulation		Existing Paramics model (SR 57) • Speed/Flow/ Density difference • Number of lane changes	Existing Paramics model (SR-91 I-15) • Q
Video			Lane change • Intensity • Gap Distribution

This chapter described research technical approach, list of study sites, list of performance measures, and data sources. The overall operation of study sites will be analyzed in following chapter.

4. General Evaluation of Study-Site Corridor Performance

In this section, we provide an overall evaluation of operational characteristics for the corridors included in the current study. This preliminary evaluation is necessary, prior to in-depth calculation of key HOV performance measures, to help us understand the traffic patterns on these corridors and to build a foundation for sound and objective interpretation of the final analysis.

4.1 Bottleneck and Congestion Analysis

To understand the spatio-temporal extents of congestion, speed contours were plotted. Contour plots shown in Appendix A are average speeds of weekdays in the 3rd quarter (from July to September) of 2009. Even if the demand of the 3rd quarter is higher than that in other times, the contour plot still represents the bottleneck location and relationship between the HOV and GP lanes. The contours were plotted in the PeMS website. Plots for all the corridors in Table 1 are provided in Appendix A. This section summarizes the findings from the contour plots.

- Accuracy of identifying bottleneck locations depends on the quality and quantity of loop detectors such as location, density, conditions, etc. Since a contour has a time dimension, temporal patterns of congestion can be explored.
- Demand exceeding capacity is the primary cause of congestion, but there are also some secondary causes for congestion in some corridors such as merging, diverging, weaving, etc.
- Congestion patterns are often different across corridors.
- Preliminary investigation of traffic conditions in HOV lanes, coupled with speed contours, indicates that degradation in HOV lanes is generally associated with congestion in the GP lanes,

4.2 Speed-Flow Probability Histogram Analysis

In this section, overall operating conditions in the HOV and GP lanes are measured with two traffic parameters – flow and speed:

1) Flow is the rate at which vehicles pass a fixed point (vehicles per hour, vph), and
2) Speed is the rate of change of a vehicle's position (miles per hour, mph).

To evaluate how the facility is being operated, we constructed a two-dimensional (speed vs. flow) joint probability histogram. The procedure is described below:

1) Partition the collected samples into two dimensional cells at increments of 2-mph (speed) and 50-vph (flow).
2) Count the number of samples that belong to each cell.
3) Divide the numbers by total sample size.

The equation below represents the value for each cell. The value for each cell represents what percentage of total samples falls into the corresponding cell based on the operating condition measured in flow and speed.

$$P_{i,j}(x) = \frac{\sum_{k=1}^{N} \mathrm{I}\{v_i \le x_k < v_{i+1}\} \cdot \mathrm{I}\{q_j \le x_k < q_{j+1}\}}{N}$$

Where, $P_{i,j}(x)$: Percent of total samples belonging to a cell (i, j),
v_i: i^{th} interval in speed,
q_j: j^{th} interval in flow,
I{}: indicator function,
N: total number of samples

The detailed results of this analysis for each corridor in individual districts are provided in Appendices B, C, and D. The following figures (Figure 6, Figure 7 and Figure 8) show probability histograms for HOV and GP lanes by district. Probability histograms for each district are simple aggregations of those for all the corridors in each district. The patterns shown in Figures 6, 7 and 8 are well representative of probability histograms of the corridors within the corresponding district. Visual inspection of the figures provides the findings below:

3) In all three districts, operating conditions in the HOV lanes indicate higher speed and lower flow than those in the GP lanes but the HOV lanes are often found to carry the flow

rate higher than 800 vehicles per hour or 1800 persons per hour given in the HOV guidelines.

4) In all three districts, there is significant congestion in both the HOV and GP lanes (shown as the grey color in low speed regimes). However, more samples from the GP lanes are plagued by congestion.

5) When comparing districts, it is apparent that the difference in speed between the HOV and GP lanes is higher in District 4 than other districts. However, this observation may be skewed because samples from District 4 were primarily collected from peak hours when the HOV facility is in operation while samples from other districts represent all operational hours including peak and non-peak hours. The peak hours in individual corridors may vary; therefore these figures are provided to show overall flow-speed patterns and are not meant for direct performance comparison.

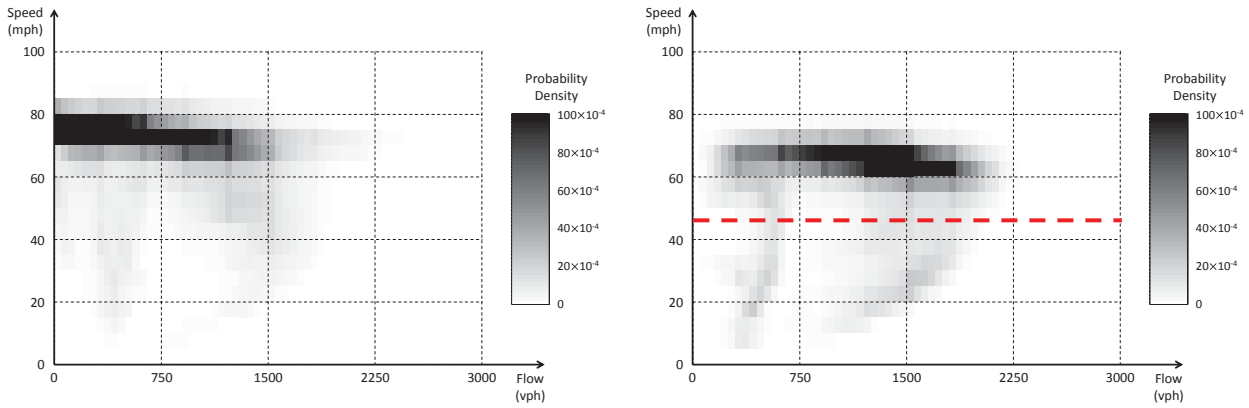

(a) HOV Lane (b) GP lane

Figure 6. Probability density of speed-flow for District 4: (a) HOV lane, (b) GP lane (All routes)

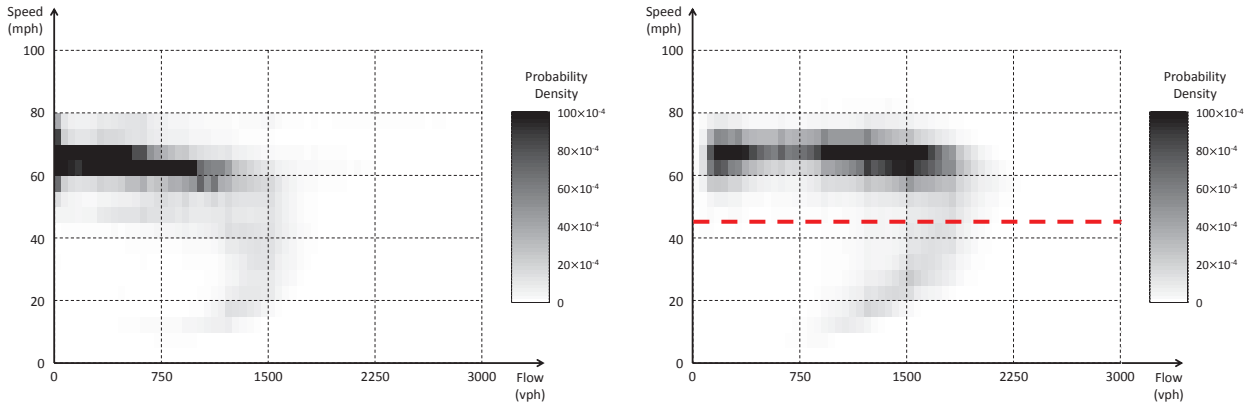

(a) HOV Lane (b) GP lane

Figure 7. Probability density of speed-flow for District 7: (a) HOV lane, (b) GP lane (All routes)

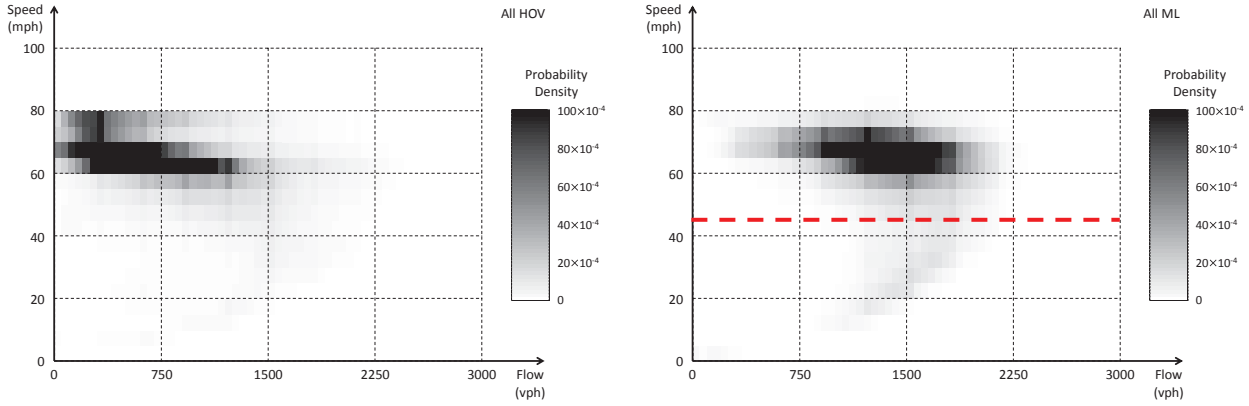

(a) HOV Lane (b) GP lane

Figure 8. Probability density of speed-flow for District 12: (a) HOV lane, (b) GP lane (All routes)

The third finding again emphasizes the importance of taking congestion into consideration when computing the performance measures. Hence, only samples collected when the GP lane speed is below 45 mph (marked by the red dotted line) were used to compute performance measures. Table 4 provides the summary statistics of selected samples. Samples from congestion are the number of samples when the GP lane speed was below 45 mph. Total samples = number of weekdays[3] × operation hours[4] × number of detectors. The percentage of samples from congestion equals samples from congestion divided by total samples.

[3] Total number of weekdays in this study is 131 days (from March 1st, 2009 to Oct. 31st, 2009)
[4] Each hour has 12 5-min samples. Operation hours for full-time facilities are 16 hours (from 5AM to 9PM).

Table 4. Summary statistics of samples from speed in the GP lane below 45 mph

District	Route	Samples from Congestion	Total Samples	% of Samples from Congestion
4	I-80W	119,837	384,912	31.13%
	I-80E	110,551	399,168	27.70%
	I-680N	30,097	392,832	7.66%
	I-680S	12,813	405,504	3.16%
	I-880N	83,825	468,864	17.88%
	SR-101N	29,518	468,864	6.30%
	SR-101S	55,497	468,864	11.84%
	Total	442,138	2,989,008	14.80%
7	I-105E	136,863	811,008	16.88%
	I-105W	87,781	811,008	10.82%
	I-210E	99,254	532,224	18.65%
	I-405S	87,192	506,880	17.20%
	SR-14N	3,264	50,688	6.44%
	SR-14S	6,435	57,024	11.28%
	Total	420,789	2,768,832	15.20%
12	I-5N	60,105	1,089,792	5.52%
	I-5S	48,016	1,013,760	4.74%
	I-405N	126,548	1,343,232	9.42%
	I-405S	109,098	1,368,576	7.97%
	SR-22E	58,172	836,352	6.96%
	SR-22W	19,567	734,976	2.66%
	SR-55N	4,184	228,096	1.83%
	SR-55N_Con	49,612	380,160	13.05%
	SR-55S	9,576	228,096	4.20%
	SR-57S	65,369	633,600	10.32%
	Total	550,247	7,856,640	7.0%

This chapter discussed the overall performance of HOV facilities. The performance by district, by corridor, and by access type will be presented in the next chapter.

5. Performance Measures

This section presents the analysis of performance measures that have been chosen to represent the comparisons of HOV operations: speed differential, VMT, and PMT. Outcomes of our data analysis are displayed in box plots (also known as box-and-whisker plots). The plots provide a convenient way of graphically depicting groups of numerical data with five summary statistics: minimum of samples, lower quartile (25^{th} percentile), median of samples, upper quartile (75^{th} percentile), and maximum of samples (See Figure 9). These plots display distribution of samples in a non-parametric fashion.

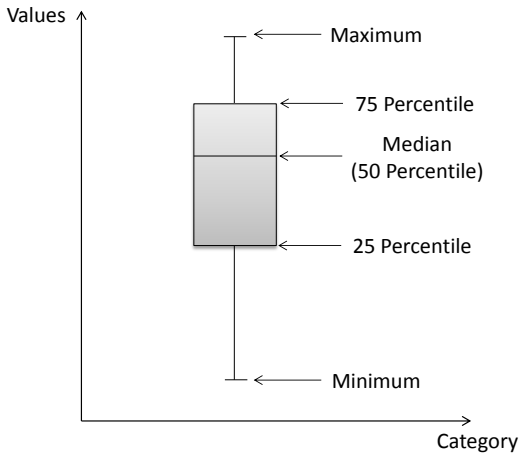

Figure 9. Hypothetical Box Plots

In the following sections, we present computed performance measures in box plots for different categorizations. Note that the samples used are only from the GP lane speed below 45 mph. The detailed results of this analysis for each corridor in individual districts are provided in Appendices E, F, and G. The following sections offer a summary of the analysis.

5.1 Comparison by District

This section aggregates samples by district-level and computes speed, flow, speed differential, VMT ratio and PMT ratio. When comparing data by district level, performance measures are fairly similar for all three districts.

5.1.1 Speed

In all three districts, median travel speed in the HOV lanes was between 40 and 50 mph (See Figure 10) when GP lane speed was below 45 mph while the median of GP lane speed was about 30 mph (See Figure 11). This shows that, when the GP lane was congested, HOV lanes could provide a 10~20 mph speed benefit to HOV lane travelers.

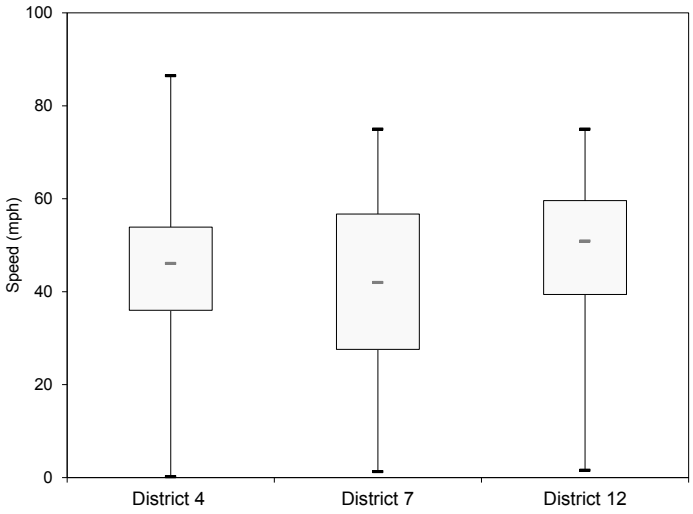

Figure 10. HOV Lane Speed (by District)

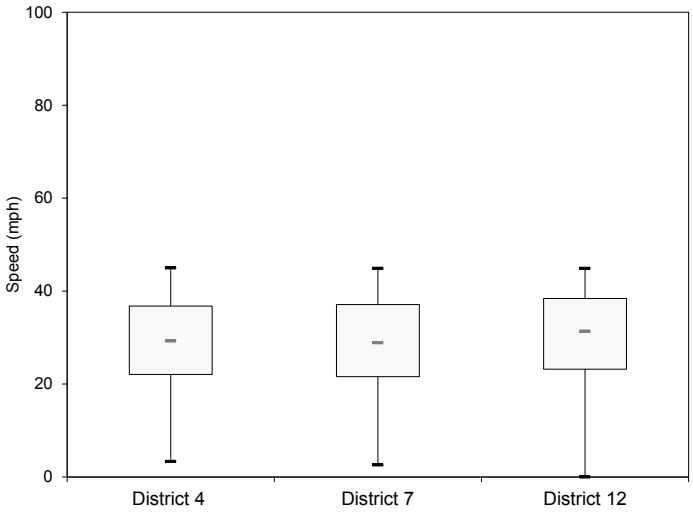

Figure 11. GP Lane Speed (by District)

5.1.2 Flow

In all three districts, median flow in HOV lanes was between 1100 and 1300 vph (See Figure 12) while the median of GP lane flow was between 1300 and 1500 vph when GP lane speed was below 45 mph (See Figure 13). Generally speaking, vehicle flow counts in HOV lanes were lower than GP lanes.

It should be noted, however, that there may be exceptions to the observation of lower flows in the HOV lanes. For example, in reviewing 2009 and 2010 HOV reports from District 7, at several detector stations the vehicle flow was greater on HOV lanes during certain rush hours.

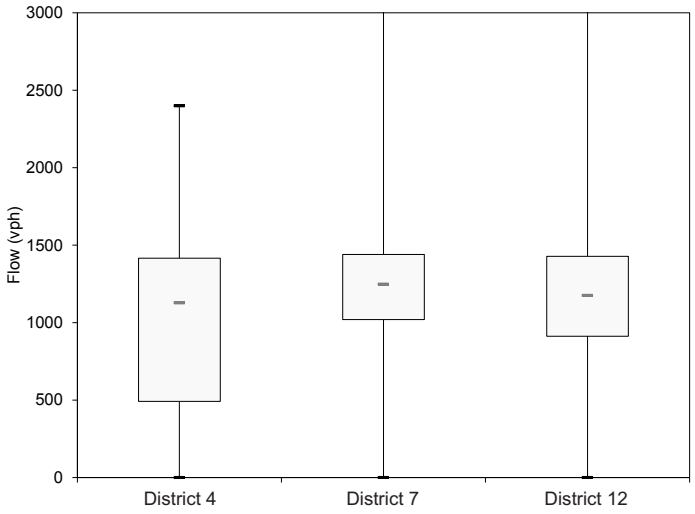

Figure 12. HOV Lane Flow (by District)

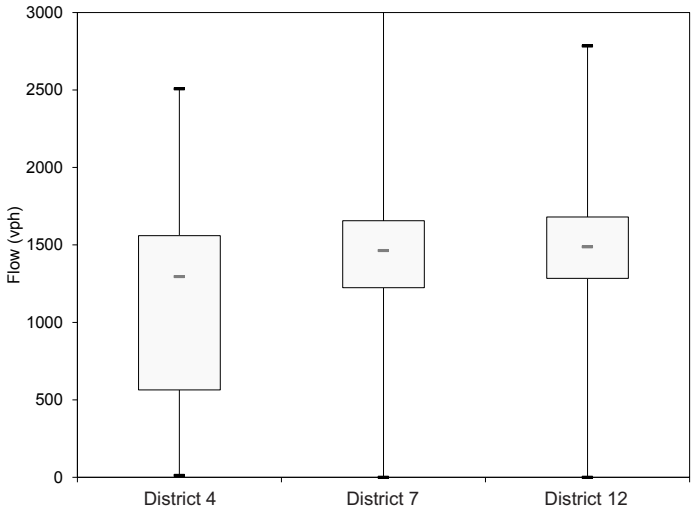

Figure 13. GP Lane Flow (by District)

5.1.3 Speed Differential

At the district-level, vehicle speeds in the HOV lanes were faster than average speeds across GP lanes for more than 75% of the examined samples in all three districts (See Figure 14).

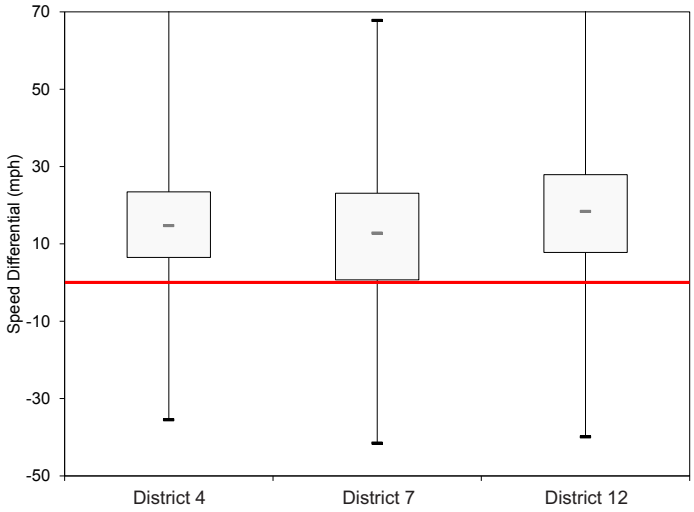

Figure 14. Speed Differential (by District)

5.1.4 VMT Ratio

At the district-level, about 75% of VMT ratios (representing the relative level of utilization by vehicles to average across GP lanes) in all three districts were below 1, meaning that a HOV lane serves fewer vehicle-miles traveled than a GP lane (See Figure 15).

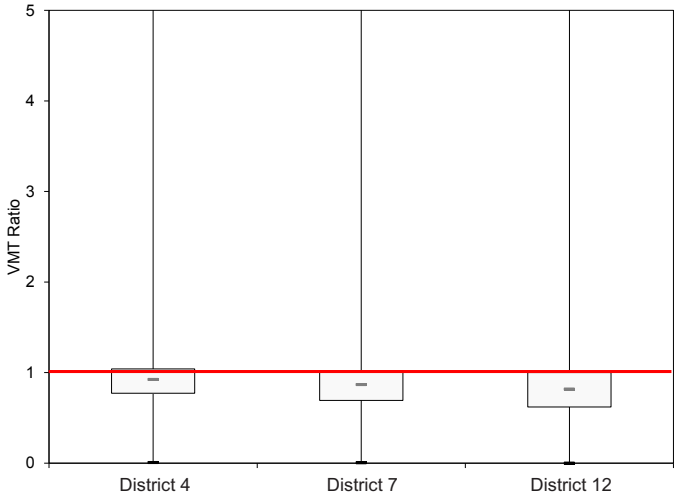

Figure 15. VMT Ratio (by District)

5.1.5 PMT Ratio

At the district-level, more than 75% of PMT ratios (representing relative level of utilization by people-miles to average across GP lanes) in all three districts were above 1, meaning that a HOV lane serves more person-miles traveled than a GP lane (See Figure 16). The occupancy requirement of I-80 eastbound and westbound (two out of 7 corridors) is 3 or more, which increases PMT in the HOV lane for District 4. For comparison of PMT for individual corridors, see the next section.

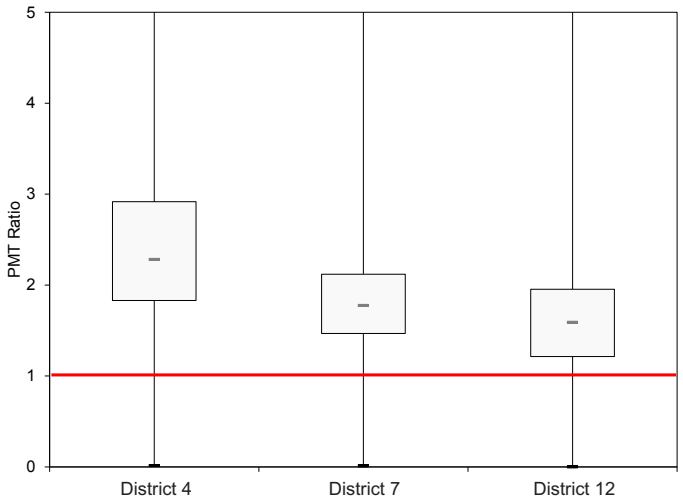

Figure 16. PMT ratio (by District)

5.2 Comparison by Corridor

This section breaks down district-level samples into corridors and computes speed, flow, speed differential, VMT ratio and PMT ratio.

5.2.1 District 4

- ***Speed***

Median speeds in the HOV lanes are between 40 and 60 mph while those in the GP lanes are between 20 and 40 mph, indicating that, when GP lanes are slow, HOV lanes provide faster speed by about 20 mph. (Figure 17 and Figure 18)

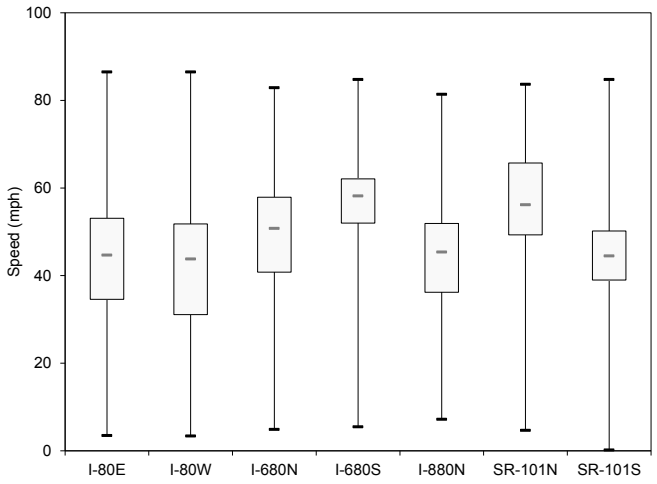

Figure 17. HOV Lane Speed (by Corridor, D4)

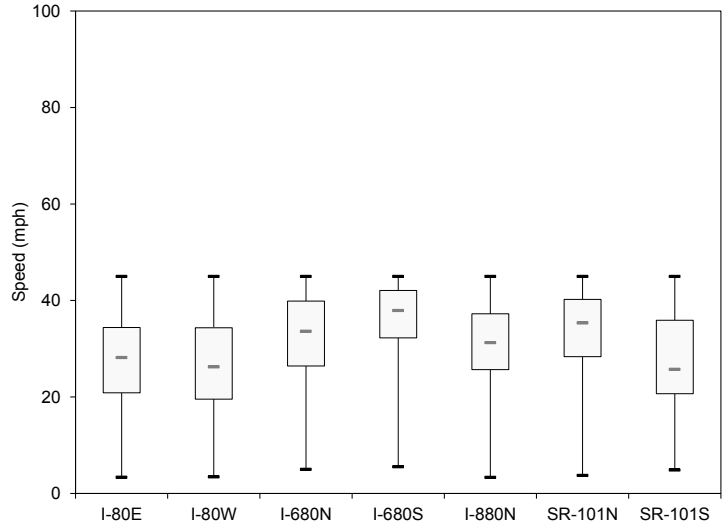

Figure 18. GP Lane Speed (by Corridor, D4)

- ***Flow***

Flows in HOV lanes vary across routes. Comparing HOV lane flows to GP-lane flows indicates that GP lane flows are higher. (Figure 19 and Figure 20)

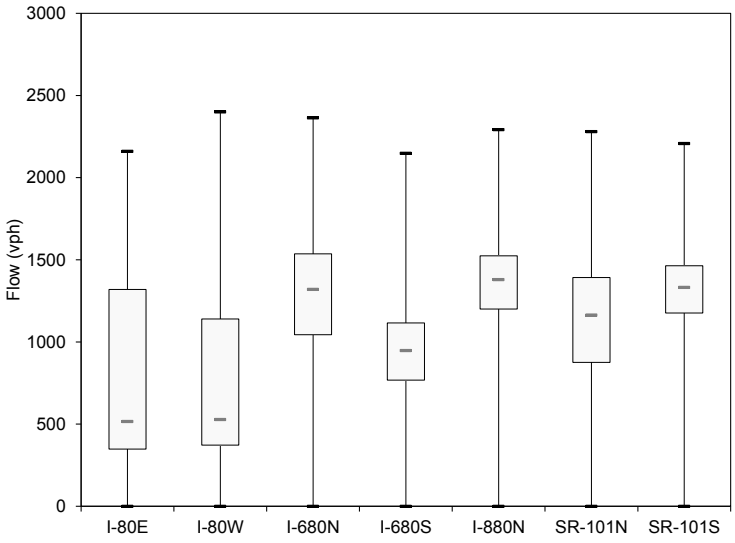

Figure 19. HOV Lane Flow (by Corridor, D4)

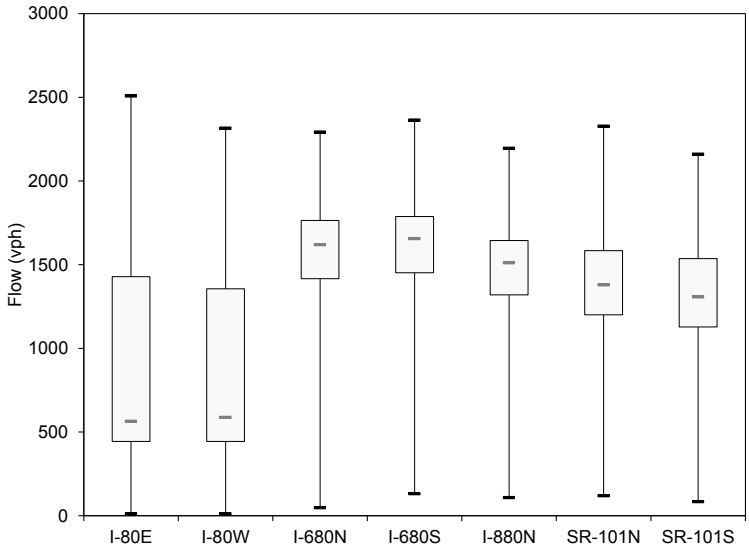

Figure 20. GP Lane Flow (by corridor, D4)

- ***Speed Differential***

At the corridor-level, vehicle speeds in the HOV lanes were faster than average speeds across GP lanes for more than 75% of the examined samples in all corridors in District 4. (Figure 21)

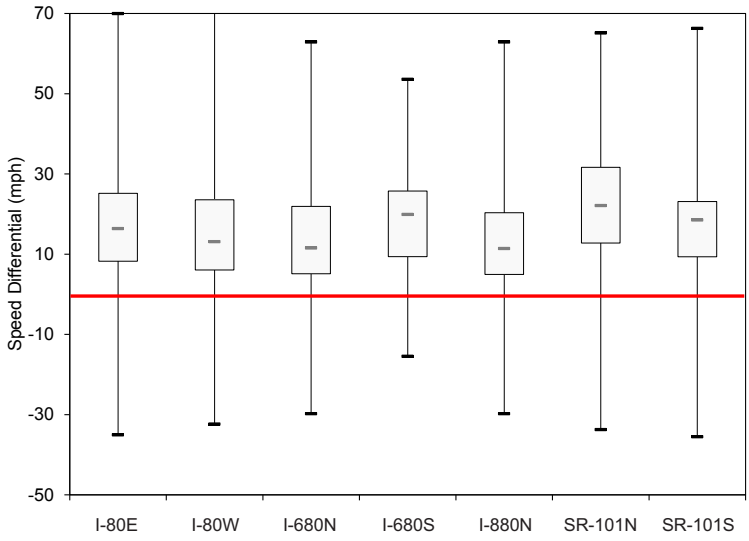

Figure 21. Speed differential (by Corridor, District 4)

- ***VMT Ratio***

At the corridor-level, about 75% of VMT ratios in all corridors, except SR-101S, were below 1; which means that a HOV lane serves fewer vehicle-miles traveled than a GP lane (Figure 22). At SR-101S, the red line traverses the middle of the box with 50% of samples below 1 and the remaining 50% above 1, indicating that the HOV lane serves as many VMT as a GP lane.

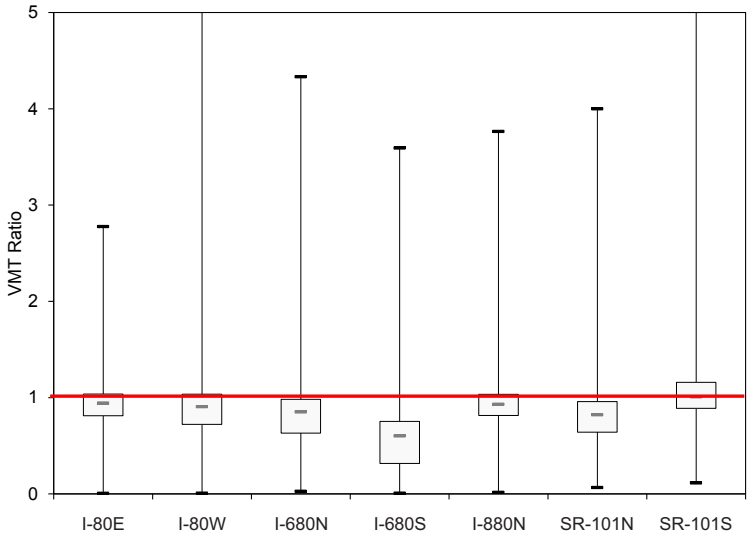

Figure 22. VMT Ratio (by Corridor, District 4)

- ***PMT Ratio***

At the corridor-level, all the corridors except I-680S exhibit a PMT ratio higher than 1. (Figure 23) However, it should be noted that as shown in Figure 19 I-680 has a median flow of 1000 vph, therefore it does meet the minimum HOV guideline.

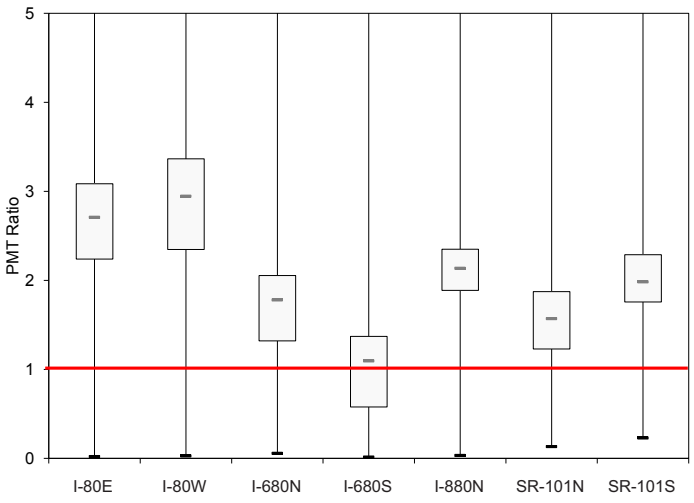

Figure 23. PMT Ratio (by Corridor, District 4)

5.2.2 District 7

- ***Speed***

Median speeds of HOV lanes in I-210E and I-405S are slower than those of other routes. (Figure 24 and Figure 25)

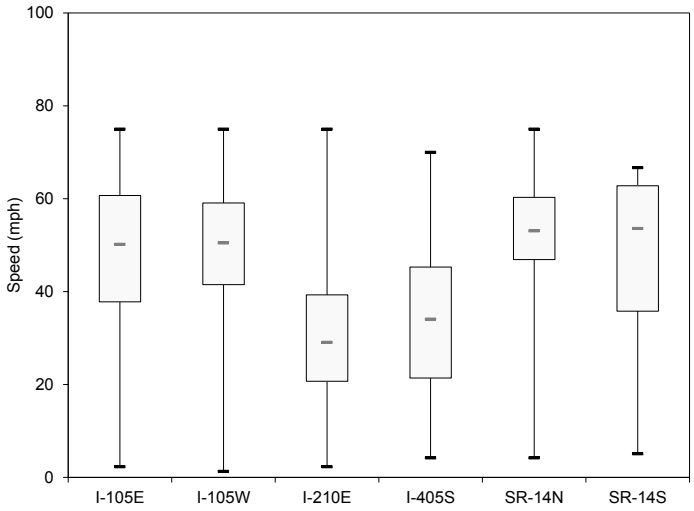

Figure 24. HOV Lane Speed (by Corridor, District 7)

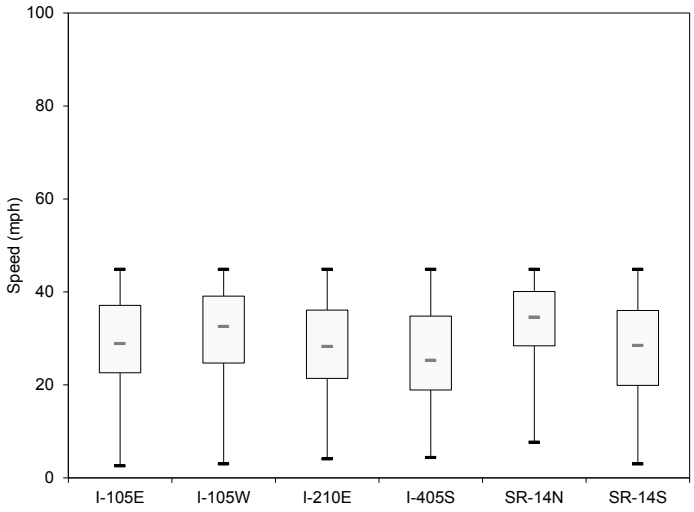

Figure 25. GP Lane Speed (by Corridor, District 7)

- ***Flow***

Slow speeds on I-210E and I-405S can be explained by the high utilization of these facilities. The flows in the HOV and GP lanes in I-210E and I-405S were approximately equal. (Figure 26 and Figure 27)

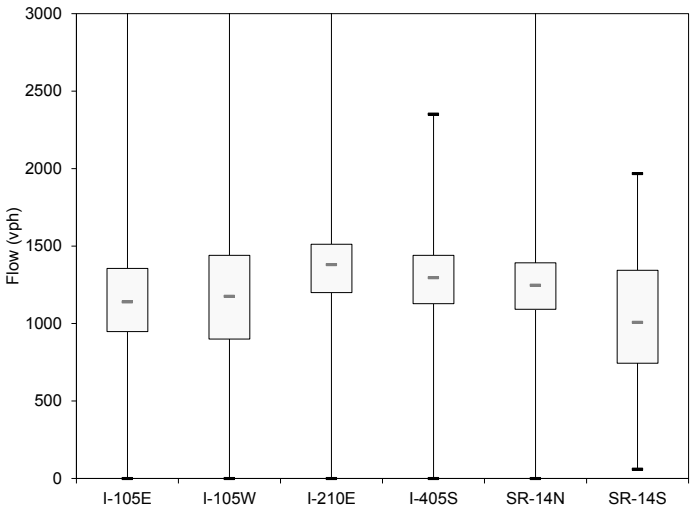

Figure 26. HOV Lane Flow (by Corridor, District 7)

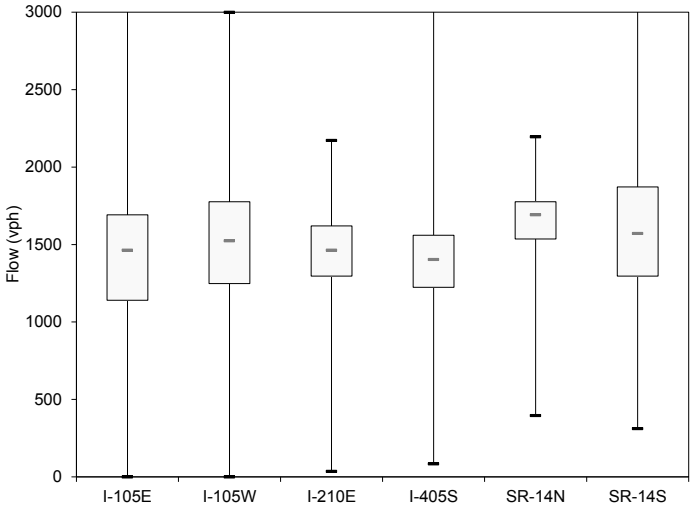

Figure 27. GP Lane Flow (by Corridor, District 7)

- ***Speed Differential***

At the corridor-level, vehicle speeds in the HOV lanes were faster than average speeds across the GP lanes for more than 75% of the examined samples in all corridors (except I-210E) in District 7 (Figure 28). Speeds on I-210E were slower for about 50% of samples.

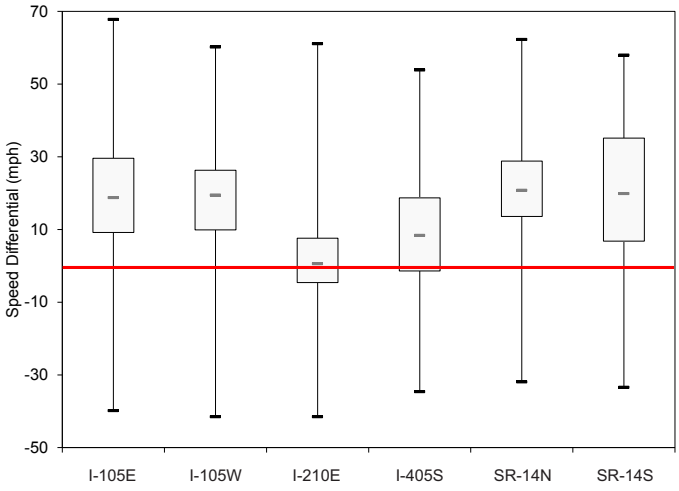

Figure 28. Speed differential (by Corridor, District 7)

- ***VMT Ratio***

At the corridor-level, about 75% of VMT ratios (representing relative level of utilization by vehicles to average across GP lane) in all corridors were below 1, meaning that a HOV lane serves fewer vehicle-miles traveled than a GP lane (Figure 29).

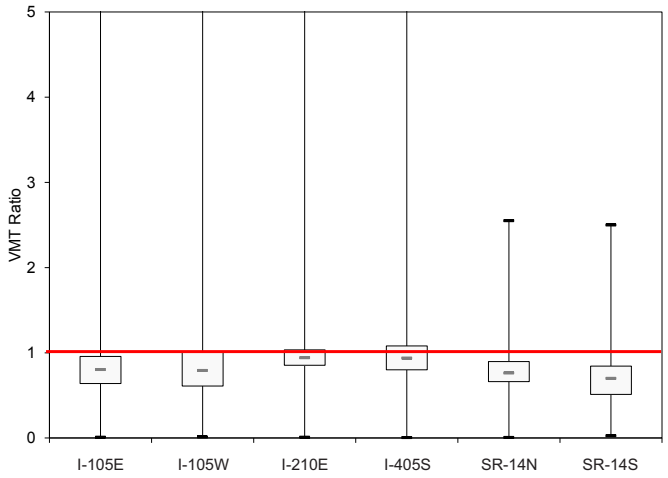

Figure 29. VMT Ratio (by Corridor, District 7)

- ***PMT Ratio***

At the corridor-level, all the corridors exhibit a PMT ratio higher than 1, meaning that a HOV lane serves more person-miles traveled than a GP lane (Figure 30).

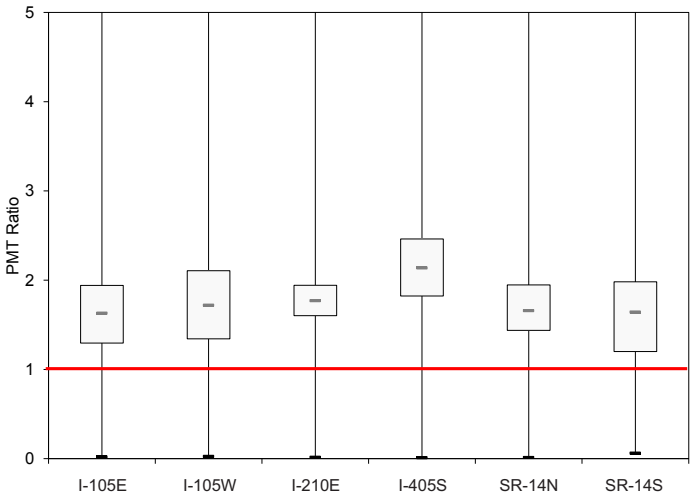

Figure 30. PMT Ratio (by Corridor, District 7)

5.2.3 District 12

- ***Speed***

Median speeds of HOV lanes are over 45 mph in all corridors in District 12 (See Figure 31) while those of the GP lanes are about 30 mph (see Figure 32).

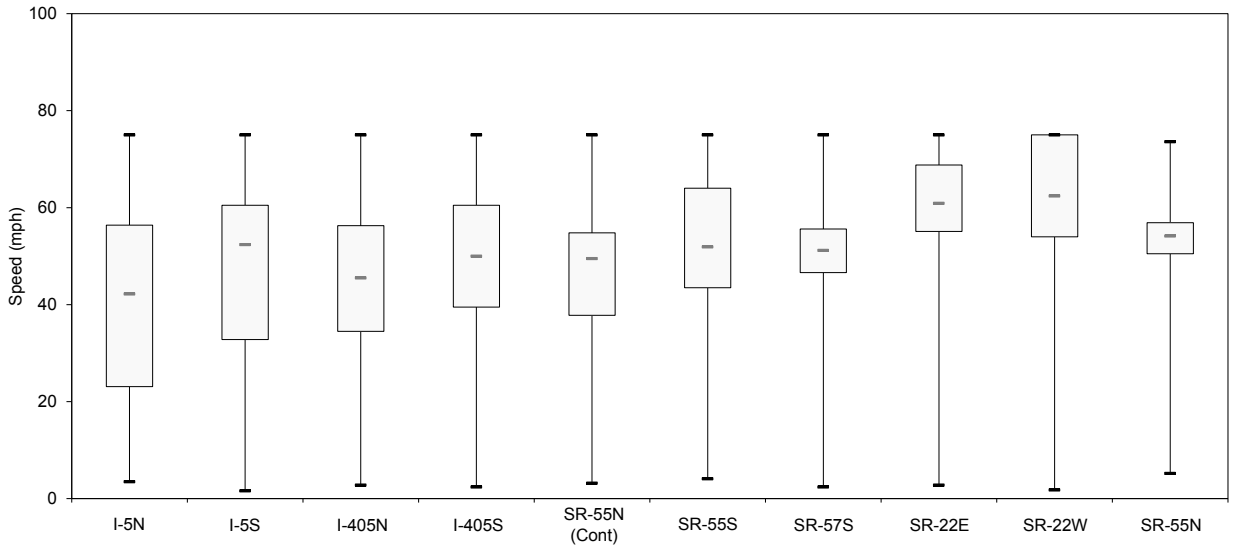

Figure 31. HOV Lane Speed (by Corridor, District 12)

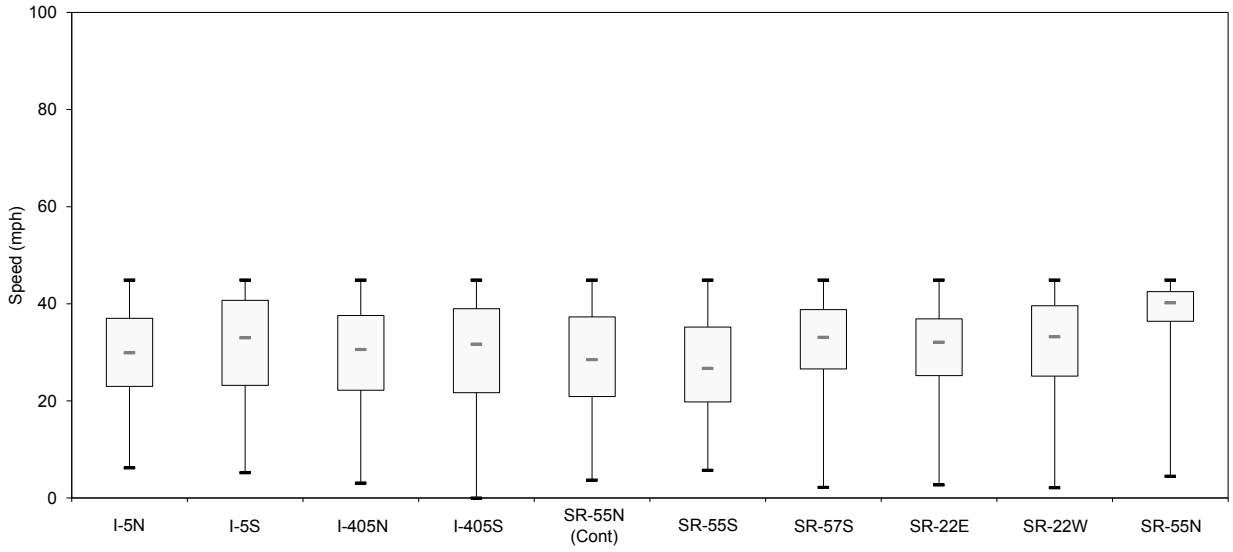

Figure 32. GP Lane Speed (by Corridor, District 12)

- ***Flow***

HOV lane flows are noticeably lower in two of the corridors in District 12, SR-57S and SR-22E, while the values in the GP lanes are relatively consistent at around 1500 vph. (Figure 33 and Figure 34)

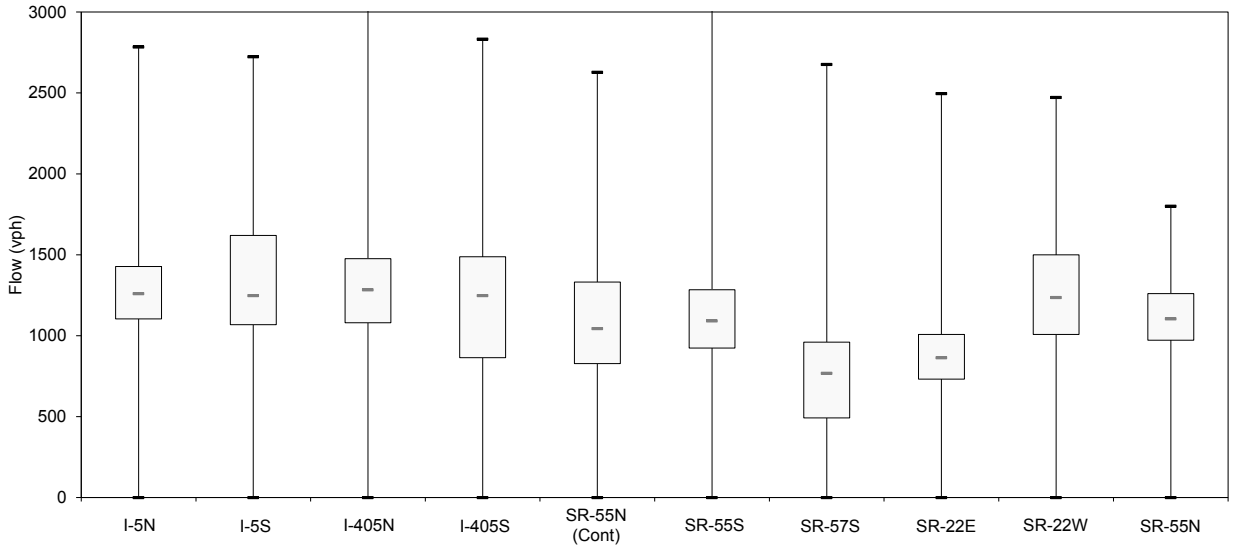

Figure 33. HOV Lane Flow (by Corridor, District 12)

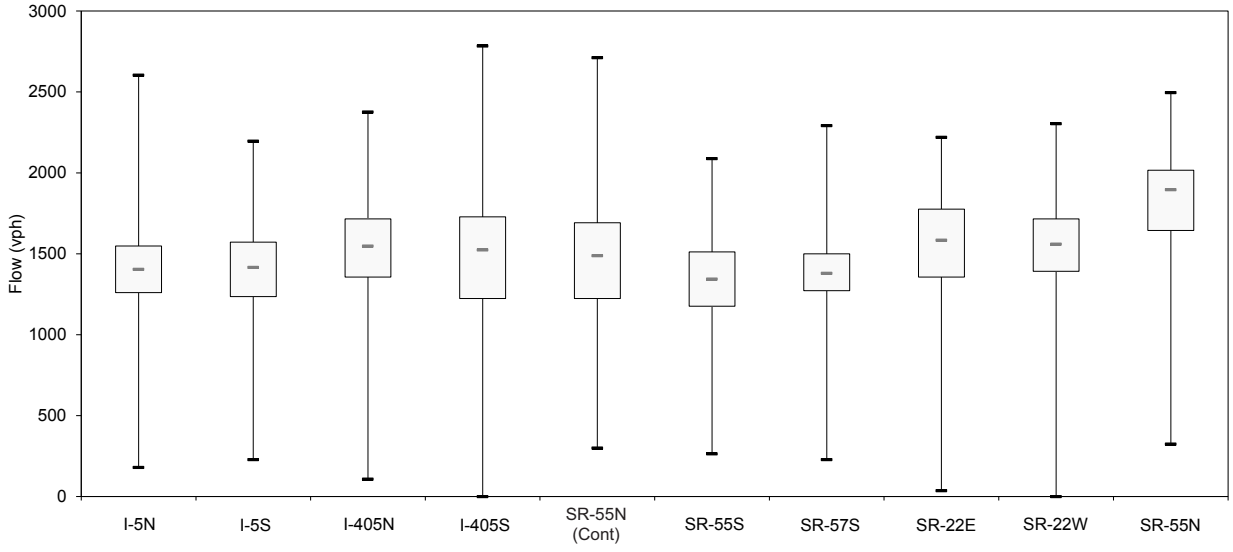

Figure 34. GP Lane Flow (by Corridor, District 12)

- ***Speed Differential***

At the corridor-level, vehicle speeds in the HOV lanes were faster than average speeds across the GP lanes for more than 75% of the examined samples in all corridors in District 12 (Figure 35).

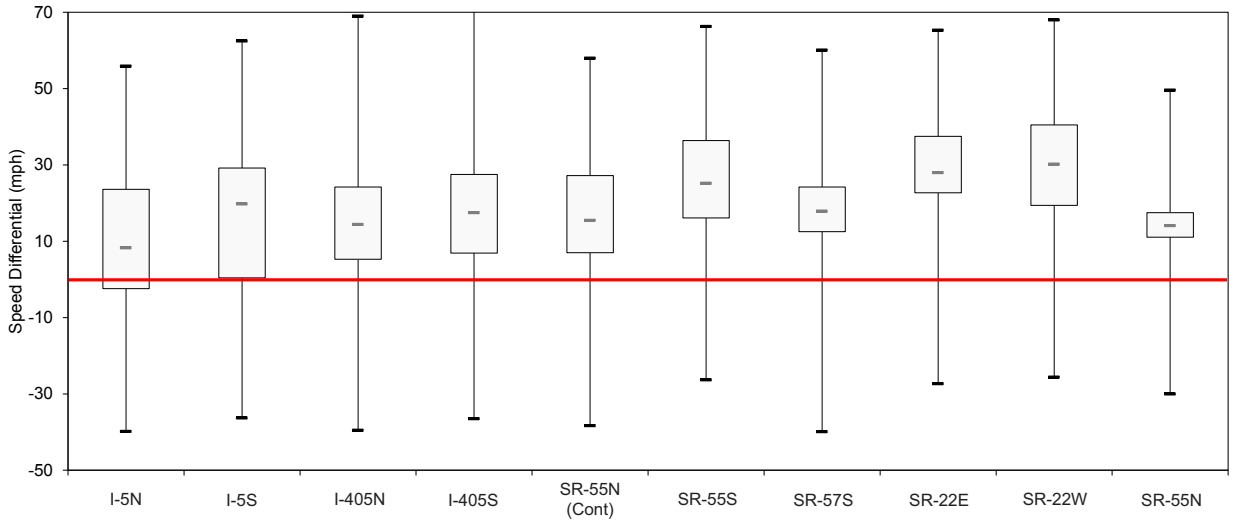

Figure 35. Speed Differential (by Corridor, District 12)

- ***VMT Ratio***

At the corridor-level, about 75% of VMT ratios (representing relative level of utilization by vehicles to average across GP lanes in all corridors were below 1, meaning that a HOV lane serves fewer vehicle-miles traveled than a GP lane (Figure 36).

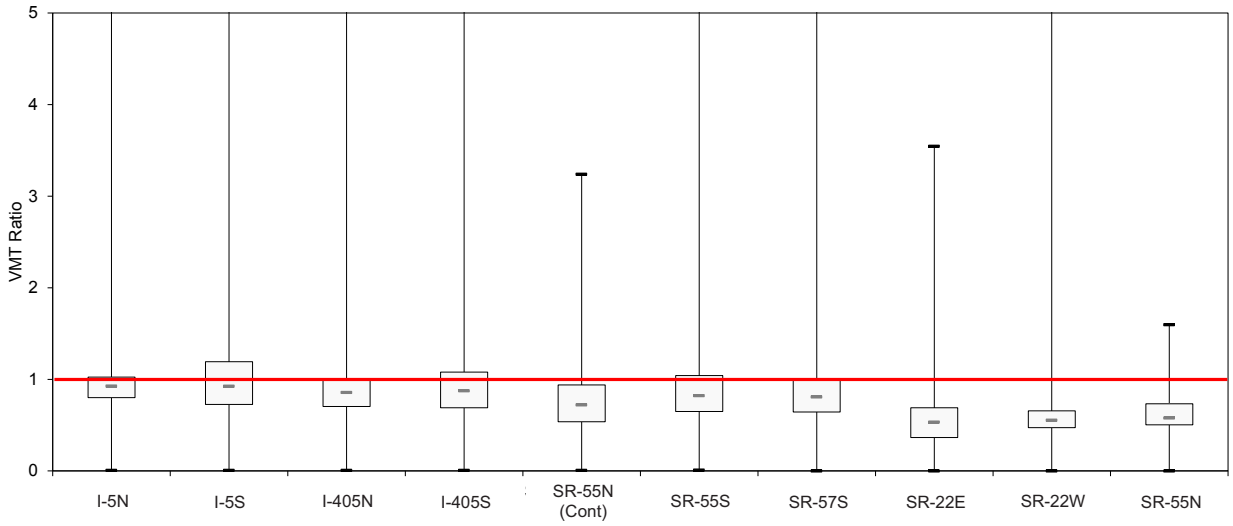

Figure 36. VMT ratio (by Corridor, District 12)

- ***PMT Ratio***

At the corridor-level, about 75% of PMT ratios (representing relative level of utilization by people to average across GP lane) in all corridors (except both directions in SR-22) were above 1, meaning that a HOV lane serves more person-miles traveled than a GP lane (Figure 37).

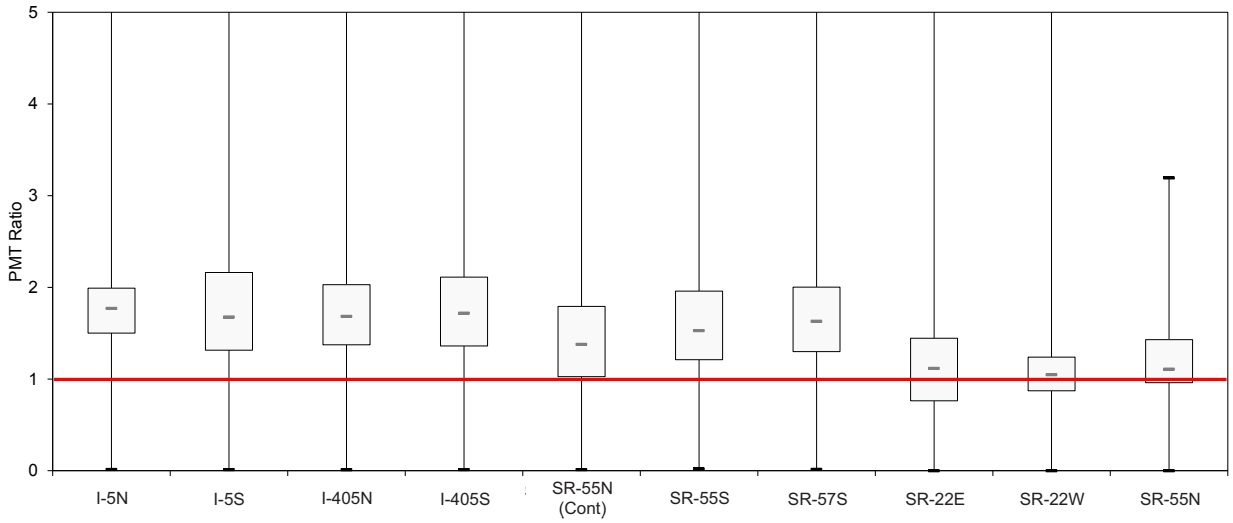

Figure 37. PMT Ratio (by Corridor, District 12)

5.3 Comparison by District and by Access Type

This section regroups samples by district and access type. First, collected samples are aggregated by district and the box plot for each district is displayed in Figure 38, Figure 39, and Figure 40. The "n" under each column in the following charts indicates the number of samples that are included in the analysis. Each sample data point is one 5-minute interval sample from one detector on any corridor.

Speed differentials and VMT ratios from all three districts exhibit similar outcomes. However, we noted that the PMT ratio in District 4 appeared to be higher that the remaining two districts. This is because D4 includes samples from I-80 which imposes an occupancy requirement of 3 or more occupants per vehicle while all other routes require 2 or more occupants.

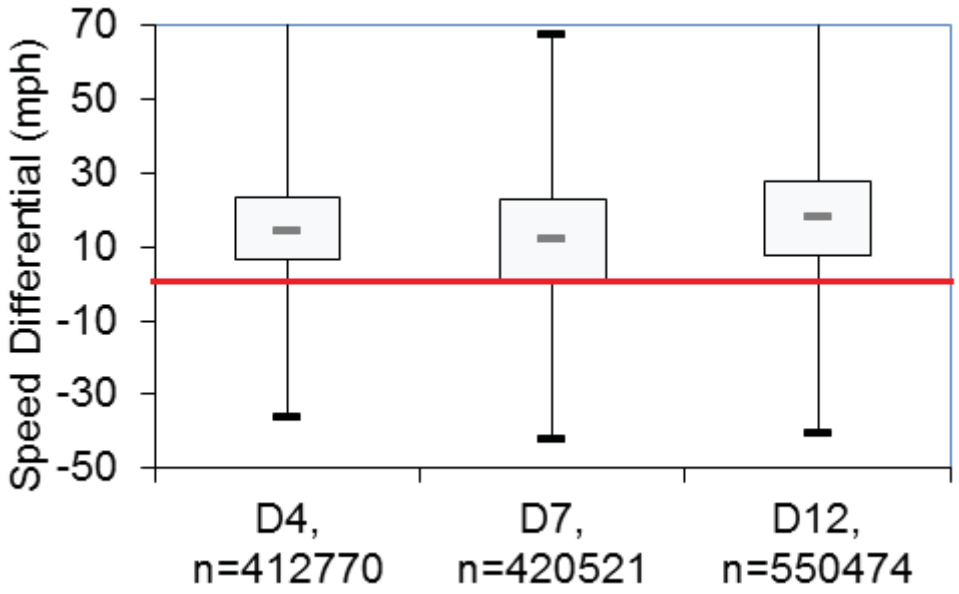

Figure 38. Speed Differential Comparison by District

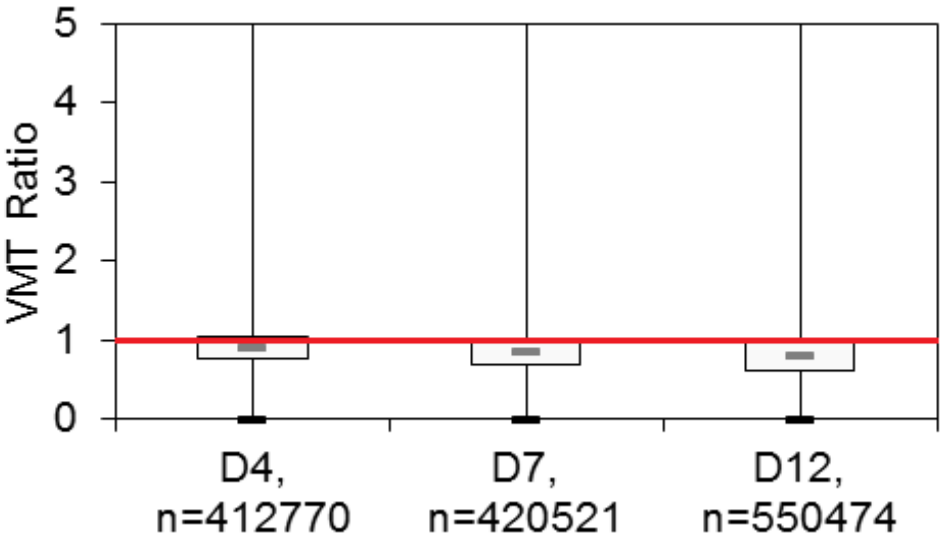

Figure 39. VMT Ratio Comparison by District

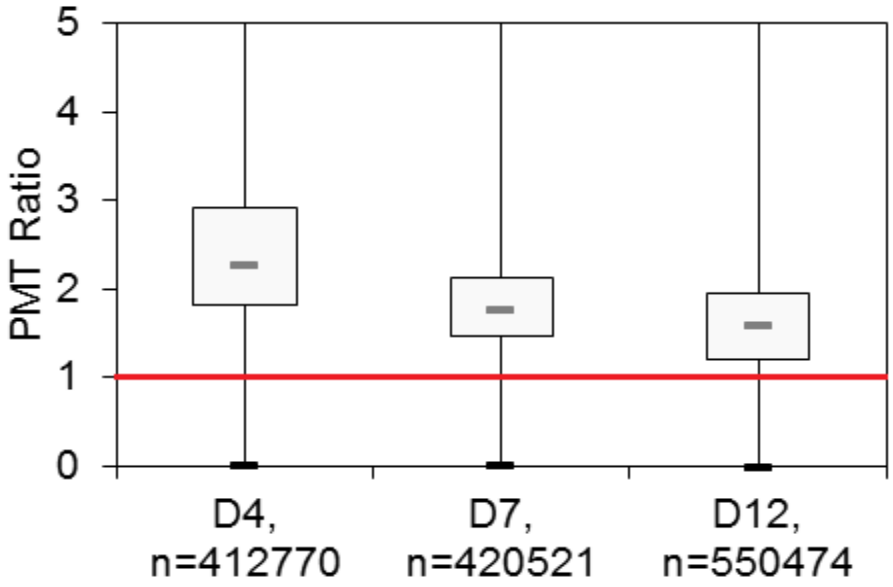

Figure 40. PMT Ratio Comparison by District

As the next step, we regrouped samples into two different categories by access type, continuous and limited. The corridors with continuous access are all the corridors in District 4 (except I-80 in both directions), State Route 22 in both directions, and State Route 55 Northbound, PM 12-18, (continuous section). I-80 corridors are excluded in this comparison because the occupancy requirement for both directions of I-80 in District 4 is 3 or more and thus, may result in bias especially when comparing PMTs between two different access types. State Route 22 and State

Route 55, PM 12-18, are operational for 24 hours. The corridors with limited access are all the corridors in District 7 and 12 except State Route 22 and 55. On State Route 14 both directions are operational part-time. Figure 41, Figure 42, and Figure 43 show that there are differences between performance measures of the two HOV groups (continuous and limited), even though the magnitude of the differences is small.

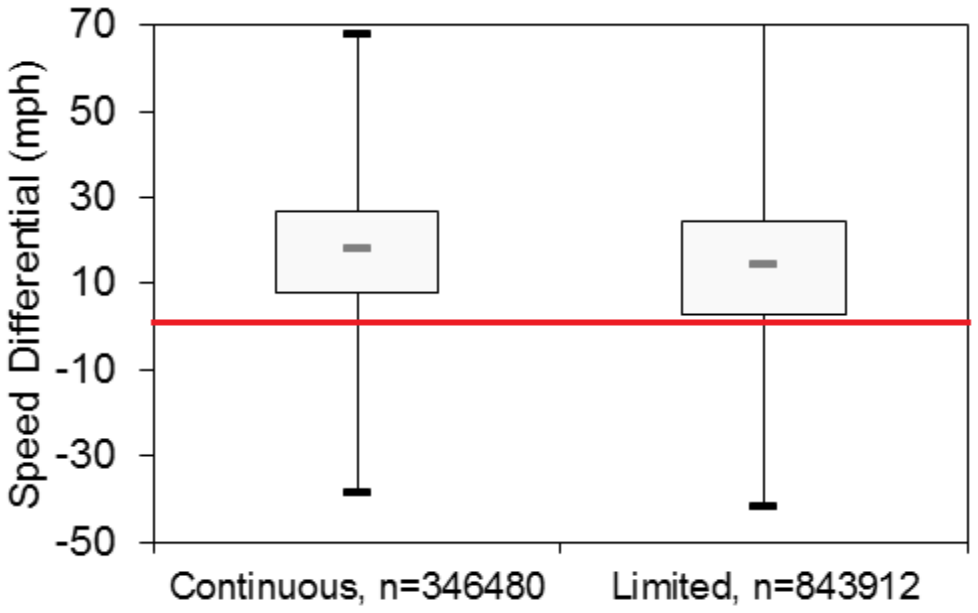

Figure 41. Speed Differential Comparison by Access Type

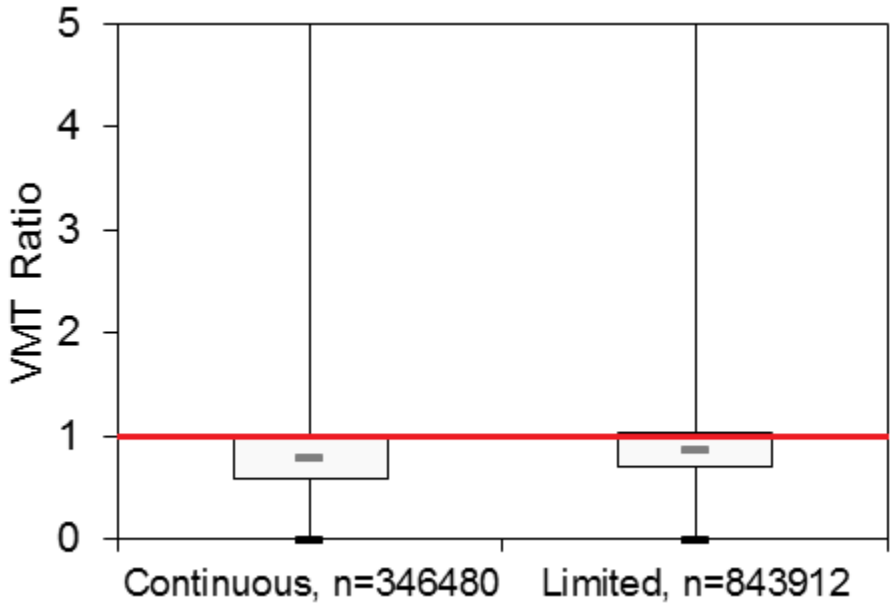

Figure 42. VMT Ratio Comparison by Access Type

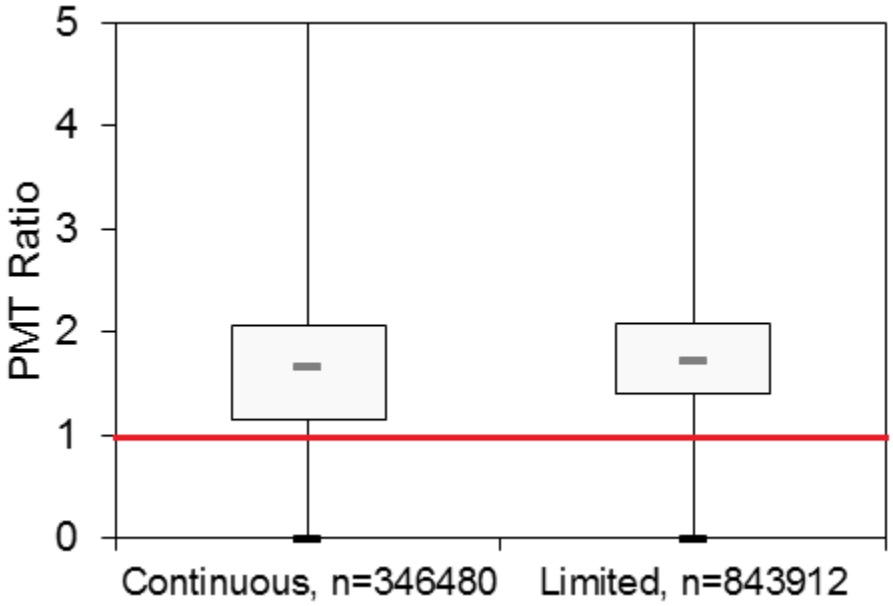

Figure 43. PMT Ratio Comparison by Access Type

5.4 Statistical Test

To determine the differences in speed differential, VMT ratio and PMT ratio between different types of HOV facilities, statistical tests were performed for data samples from all study corridors. A two sample Kolmogorov-Smirnov test was conducted. The null hypothesis, H0, is that the true distribution function continuous-access HOV facilities, is equal to the distribution function of limited- access ones at the 5% significance level.

As is shown in Table 5, the test results reveal that all the null hypotheses should be rejected, which means that there is a statistically meaningful difference between the distributions of performance measures for different access types.

Table 5. Results of K-S Tests for HOV Lane

Test	KS P-Value	KS K-Value	Test result H0: C=L	Access Type	Mean	Median	Sample Variance
Flow_HOV	0	0.0994	rejected	CON	98.1	101	1012.2
				LIM	102.9	105	817.1

Flow_AGP	0	0.0449	rejected	CON	120	121	565.4
				LIM	121.6	124	679.9
Person Flow_HOV	0	0.1053	rejected	CON	217.3	220.8	523
				LIM	229.4	232.7	428.5
Person Flow_AGP	0	0.1028	rejected	CON	130.1	130	698.1
				LIM	134	136.5	867.1
Speed Differential	0	0.1668	rejected	CON	19.1310	19.1079	186.5949
				LIM	13.3293	14.0000	224.1658
VMT Ratio	0	0.0758	rejected	CON	0.8382	0.8613	0.0884
				LIM	0.8626	0.8718	0.0369
PMT Ratio	0	0.0821	rejected	CON	1.7263	1.7727	0.4063
				LIM	1,7424	1.7374	0.1633

5.5 Concluding Remarks on Real-World Data Analysis and Evaluation of Performance Measures

The results as observed from the comparisons between the HOV and GP lanes in all districts can be summarized as follows:

1) HOV lanes generally have a higher traveling speed than GP lanes, as illustrated in Figure 38 and Figure 41.
2) The VMT ratio for HOV lanes is generally below 1, indicating that HOV lanes serve fewer vehicle-miles than GP lanes, as shown in Figure 39 and Figure 42.
3) The PMT ratio for HOV lanes is generally above 1, as shown in Figure 40 and Figure 43, indicating that HOV lanes carry more person-miles than GP lanes.

The results for the comparison between continuous and limited access types are summarized below. Please note that the compilation of results is based on the inclusion of study sites that have been selected for this report. They are representative of operational performance in different districts but they do not encompass all HOV facilities. Thus, the evaluation results should be considered within the scope of data samples from the selected corridors.

1) Continuous- and limited-access HOV lanes offer noticeable levels of speed differentials under a majority of operational conditions. This can be seen in Figure 44, in which the data were sampled for every 5-minute interval from all qualified conditions when the speed of the average general purpose lanes was below 45 mph. The distribution of speed differential is widely dispersed, and the continuous-access type has a higher mean value. The thin lines near the center of the figures represent the placement of the mean values.

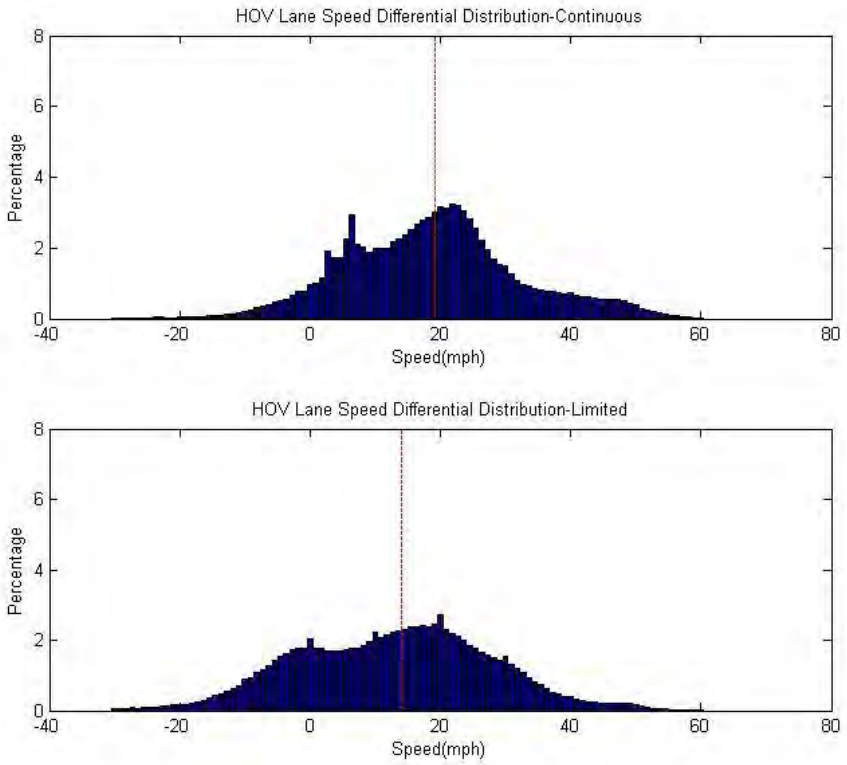

Figure 44. Speed Differential Distribution (by Access Type)

2) In Figure 45 and Figure 46, the 5-minute flow distribution of the two access types are shown. As can be seen in Figure 45(a), the overall shapes of distribution curves are very similar in HOV lane, but the continuous access has a larger tail at the lower end of the curve, which implies that there are slightly more instances of lower flows among the continuous-access corridors.
3) In Figure 46, the 5-minute person-flow distribution of the two access types are shown. As can be seen in Figure 46(a) the overall shapes of distribution curves are very similar in the HOV lane, but the continuous access has a larger tail at the lower end of the curve, which is the result of the same pattern in Figure 44.

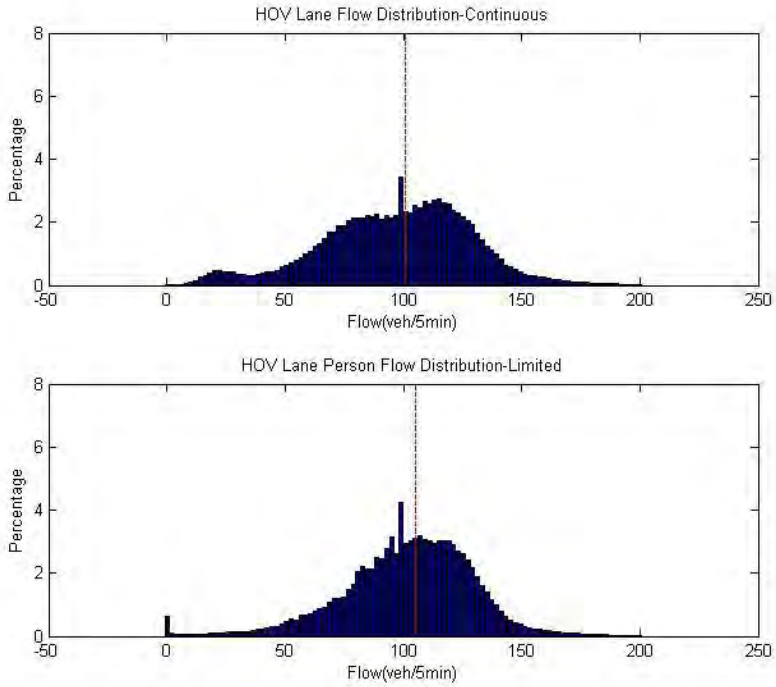

(a) HOV Lane

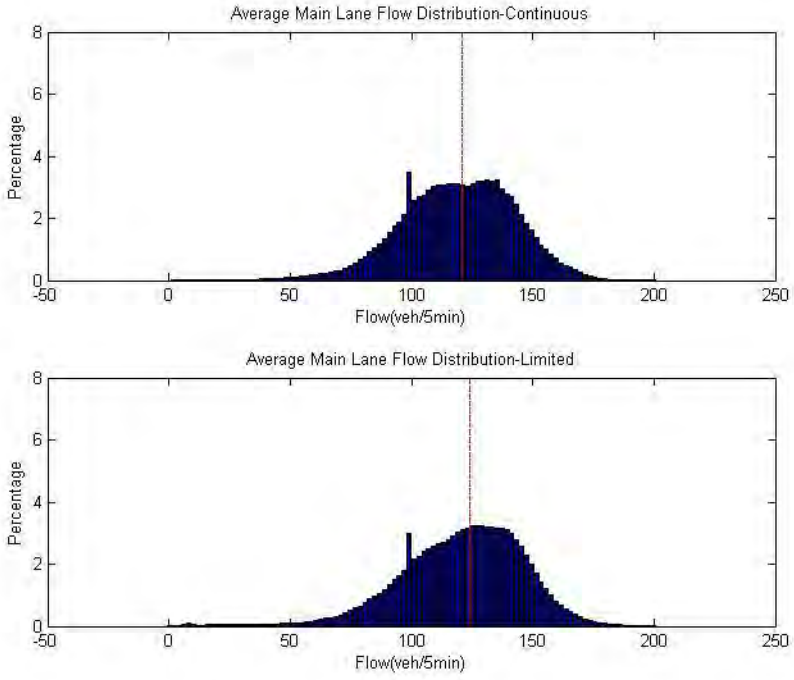

(b) GP Lane

Figure 45. Flow Distribution (a) HOV lane, and (b) GP lane (by Access Type)

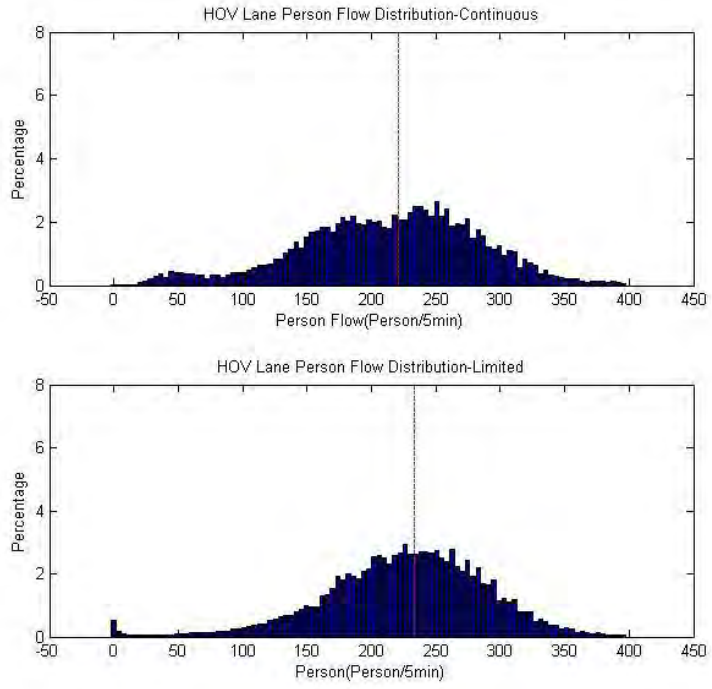

(a) HOV Lane

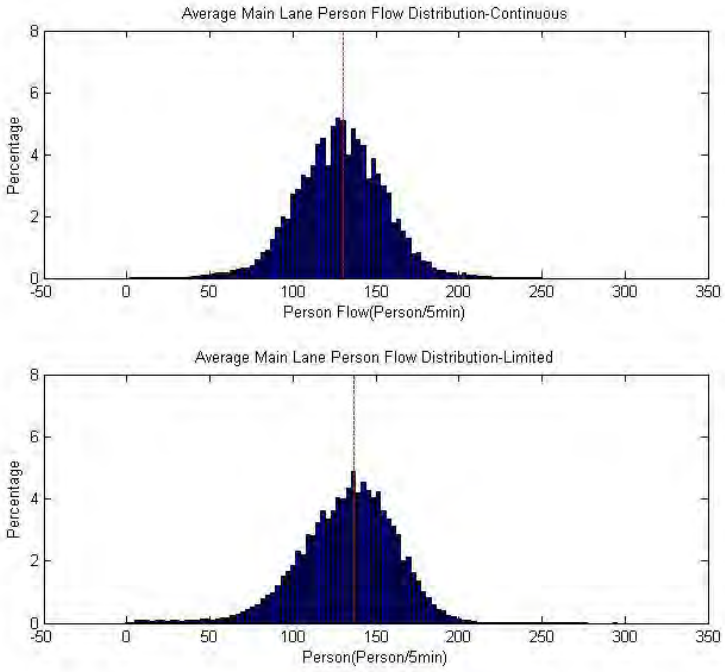

(b) GP Lane

Figure 46. Person Flow Distribution (a) HOV lane, and (b) GP lane (by Access Type)

4) The VMT ratios in both types of HOV access are at comparable levels, which can be observed in Figure 47, with mean values roughly the same. The continuous access has a larger tail at the lower end of the distribution curve.
5) Similarly, the PMT ratios in both types of HOV access are at comparable levels, which can be observed in Figure 48, with mean values close to each other. The continuous access has a larger tail at the lower end of the distribution curve.

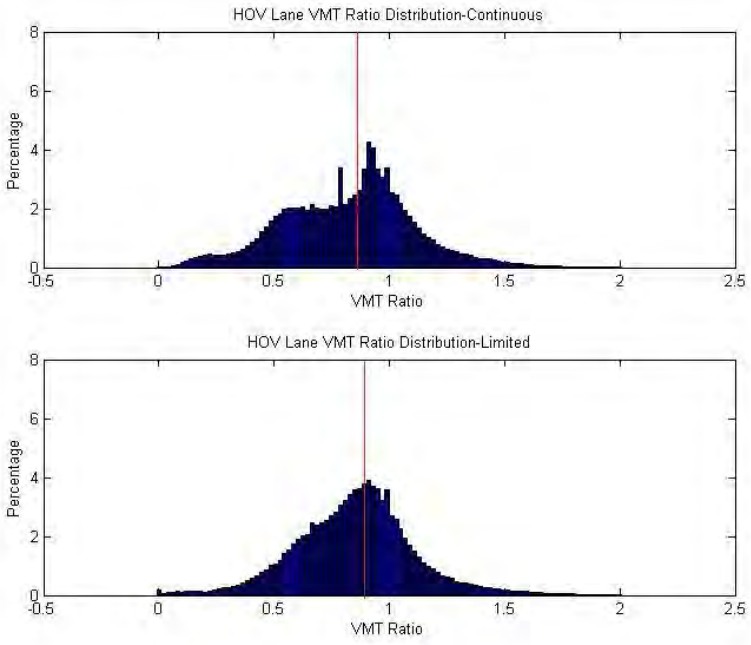

Figure 47. VMT Ratio Distribution (by Access Type)

Continuous-access and limited-access configurations offer different operational advantages. For example, the continuous-access configuration provides flexibility for flow distribution during HOV non-operational hours. The limited-access configuration, on the other hand, provides a clear separation of flows and isolates roadways users from frequent lane-changing maneuvers except at designated access areas. At certain freeway junction locations, limited-access configurations can also prevent or discourage last-second traffic weaving maneuvers so that traffic flows can be safely channelized.

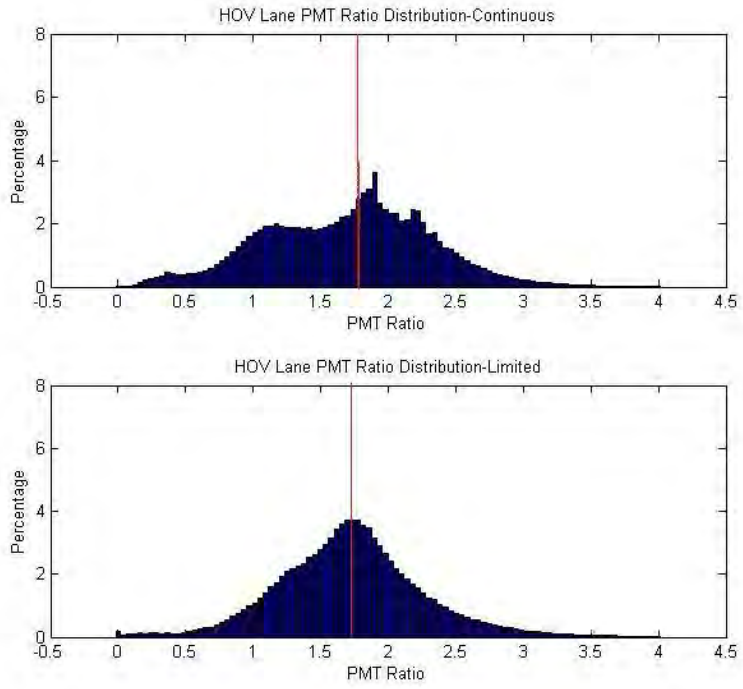

Figure 48. PMT Ratio Distribution (by Access Type)

In the context of enforcement against HOV violations, in Southern California, drivers may get multiple tickets (HOV lane violations, crossing double yellow lines, and evasion of enforcement) for a higher level of total fines when compared to Northern California. This provides a deterrence effect.

This chapter analyzed the detailed performance evaluation for HOV facilities by District, by corridor, and by access type using the real-world data. In the next chapter, the before-and-after performance of several HOV facilities that have recently undergone conversion from limited- to continuous-access operation will be compared using real-world data.

PART II: BEFORE-AND-AFTER PERFORMANCE COMPARISON

6. Real-World Before-and-After Performance Comparison

This section focuses on evaluation of the performance of several California HOV facilities that have recently undergone conversion from limited- to continuous-access operation. This provides an opportunity to gain useful insight into the relative performance of both operational schemes and provides a different perspective by comparing corridors with different access types.

6.1 Methodology

6.1.1 Traditional Before-and-After Comparison

In this section, we describe performance measures that are extracted from real-world traffic data and used in the before-and-after analysis. The performance measures used and presented here include:

- Speed contour
- Speed differential
- VMT ratio
- Demand flows
- HOV lane changing rate
- HOV violation rate

The first three measures are similar to those described in previous sections.

The demand flow is defined as the total flow for GP lanes and HOV lane during the whole AM or PM period that starts from a free-flow condition to another free-flow condition. Because the traffic condition may be different, the AM or PM peak period may be different for different corridors.

HOV lane changing rate is defined as the number of HOV vehicles' lane changes divided by all HOV vehicles' VMT.

The HOV violation rate is defined as the number of vehicle occupancy violators divided by the total HOV volume.

6.1.2 Traffic Flow Fundamental Diagram-Based Approach

Since before-and-after travel demands may not be the same, traditional before-and-after methods may not provide a fair comparison. In this section, we propose an alternative method that compares before-and-after traffic flow fundamental diagrams. The diagram represents the traffic flow characteristics primarily determined by geometry. We hypothesize that when HOV lane configuration changes, drivers may respond with different behavior and thus the traffic flow characteristics or traffic flow fundamental diagram may change. Thus, the operational performance of limited-access versus continuous-access HOV lane facilities can be compared and evaluated through detector flow and detector occupancy diagrams and through parameters derived from the diagrams.

Detector flow and detector occupancy data are direct outputs of a detector. Detector occupancy is defined as *the percentage of time that the detection zone of the instrument is occupied by a vehicle* and is a measure of density. In Chapters 6 and 7 of this report, occupancy is referred to as detector occupancy.

a) Traffic Flow Fundamental Diagram

There are three basic traffic flow parameters: flow, density and speed. Traffic flow fundamental diagrams describe the relationships of these traffic flow parameters, such as volume-density and/or speed-density. Lighthill and Whitham in their classical work described a traffic flow fundamental diagram as one in which "…at any point of the road the flow (vehicle per hour) is a function of the concentration (vehicles per mile)…" (Lighthill & Whitham, 1955). Traffic in the real world is a complex dynamic process; the fundamental diagram is essentially a representation of complex non-linear traffic phenomena. Edie pointed out that traffic behavior appears to be different at high versus low concentrations (Edie, 1961). Hall et al concluded that an inverted "V" shape is a plausible representation of the flow-density relationship (Hall, Allen, & Gunter, 1986).

Although the fundamental diagram was originally used to define the flow-density relationship, the detector flow and detector occupancy diagram is usually analyzed because volume and occupancy data from point detectors are widely available.

As shown in Figure 49, the inverted "V" shape or two-phase piecewise flow-occupancy curve includes two parts, free-flow and congestion flow. Occupancy at the joint point is called critical occupancy, x_0, which is the threshold for distinguishing between free-flow and congested-flow conditions. The flow at the joint point is called critical volume, corresponding to capacity. The slope for the free-flow portion corresponds to the free-flow speed. The negative slope for the congestion flow portion corresponds to the shockwave propagation speed (Newell, 1993).The triangular traffic flow-occupancy fundamental diagram can be represented as a continuous piecewise linear curve:

$$\begin{Bmatrix} y = a \bullet x, & if\,(x \le x_0) \\ y = b \bullet x + c, & if\,(x \ge x_0) \end{Bmatrix}$$

where the first equation represents the free-flow line and the second represents the congested flow line. X_0 is the critical occupancy.

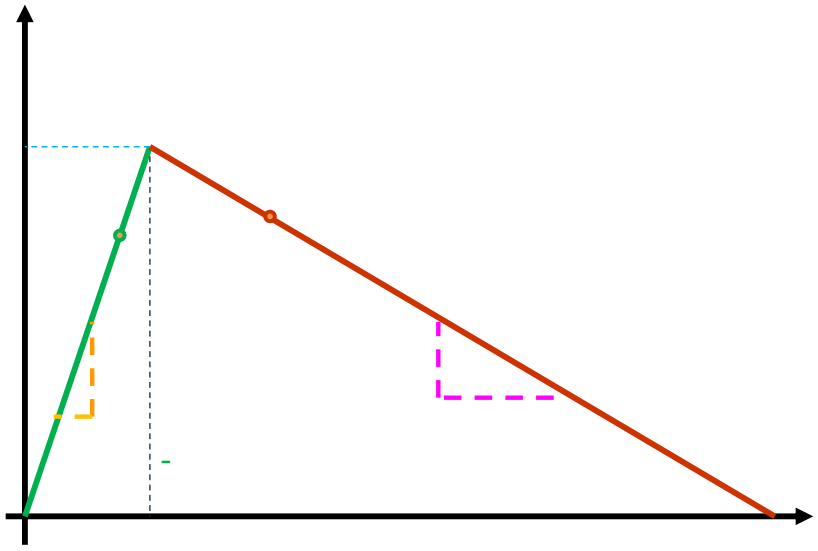

Figure 49. Two-Phase Flow-Occupancy Diagram

The traffic flow fundamental diagram is a reflection of driving behavior, including both car-following and, probably, lane-changing behaviors, at a certain location. It is drawn based on a collection of flow and occupancy values obtained at the location under different demand levels. In other words, the diagram responds to a change in demand. When demand is low, its corresponding data point in the diagram is located in the free-flow portion (Point A in Figure

49). When demand is high, its corresponding data point in the diagram is located in the congested flow portion (Point B in Figure 49).

The traffic flow fundamental diagram is thus a fundamental feature at a location of a roadway facility. It will not change if the factors that influence driver behavior remain the same. These factors include roadway geometry, vehicle type composition, vehicle performance, guidance signs and inclement weather.

The traffic flow fundamental diagram has been widely used in traffic model development and calibration. For example, TOPL (Tools for Operational Planning) is a cell transmission model-based mesoscopic traffic simulator that uses traffic flow fundamental diagrams as model inputs (Chow, Gomes, Kurzhanskiy, & Varaiya, 2010). In addition, the development of microscopic models usually involves the calibration and validation of simulated traffic flow fundamental diagrams (Chu L. , Liu, Recker, & Zhang, 2004).

b) Estimation of Traffic Flow Fundamental Diagram Parameters

Because of the existence of detection errors in the observed detector data, the determination of traffic flow fundamental diagram parameters can be quite subjective and, in practice, is often based on traffic engineers' experience -- experience that often takes a long time to acquire and is generally not governed by quantitative standards.

A recent study uses raw detector data directly and derives its parameters based on data points with the maximum flow for each occupancy level for development of a mesoscopic model (Dervisoglu, Gomes, Kwon, & Muralidharan, 2008). A quartile regression on stable-flow regime and unstable-flow regime is then applied to obtain free-flow and shockwave speeds. However, judging critical flow and critical occupancy with only maximum flow data may generate misleading results because of "noise" from detectors.

Antoniou et. al. compared machine-learning methods for estimating performance parameters (Antoniou & Koutsopoulos, 2006). One of their approaches was to use local weight regression to fit a triangular shape diagram. Since data from detectors can be erroneous if weights are not properly adjusted, the results may yield a saddle-like diagram, which may then lead to misleading results when applied to various detectors. Therefore, we must develop a method to

accommodate detector malfunction and to recognize suspicious data when automatically estimating performance parameters.

Cassidy proposed a method for using detector data under a stationary state in which drivers are able to maintain their headways (Cassidy, 1998). However, identifying data in a stationary state is very challenging. In this study, the ratio of volume versus occupancy was used to determine whether a data point is stationary. If the absolute difference of each timestamp's ratio and its precedent is greater than one standard deviation of the difference array, the timestamp's data will be excluded. This procedure will examine every available study day to estimate the parameters of fundamental diagrams.

c) A Statistical Approach to Determine Traffic Flow Parameters

The focus of this study is to evaluate the average impact on traffic conditions of changes in the traffic flow fundamental diagram.

Empirical data analysis shows that traffic flow performance is different when a queue is built up and when a queue is dissipated. Higher capacity is normally achieved when the queue is built up. Figure 50 shows a volume-occupancy plot based on data collected from a few days. Each data point is shown as a dot with different colors in the plot. The color theme is shown on the right. The figure clearly shows that, at a certain occupancy level, the data points with higher volumes are collected in the early morning when the queue or congestion is forming. The data points with lower volumes are collected in the late morning when the queue or congestion is dissipating.

Thus, for a detailed analysis, we must divide the data from the entire study period into two phases: the formulation phase and the dissipation phase. The formulation phase is defined as the time period from the free-flow condition to traffic congestion. The dissipation phase is defined as the time period from traffic congestion back to the free-flow condition. To divide the data into the formulation and dissipation phases, we must determine a turning point for each day's data; data points earlier than the turning point belong to the formulation phase and data points later than the turning point belong to the dissipation phase. As illustrated in Figure 51, a piecewise linear regression module (called "SiZer" and developed by Derek Sonderegger) in the R package was used to find the best turning point by estimating two pieces of linear regression lines.

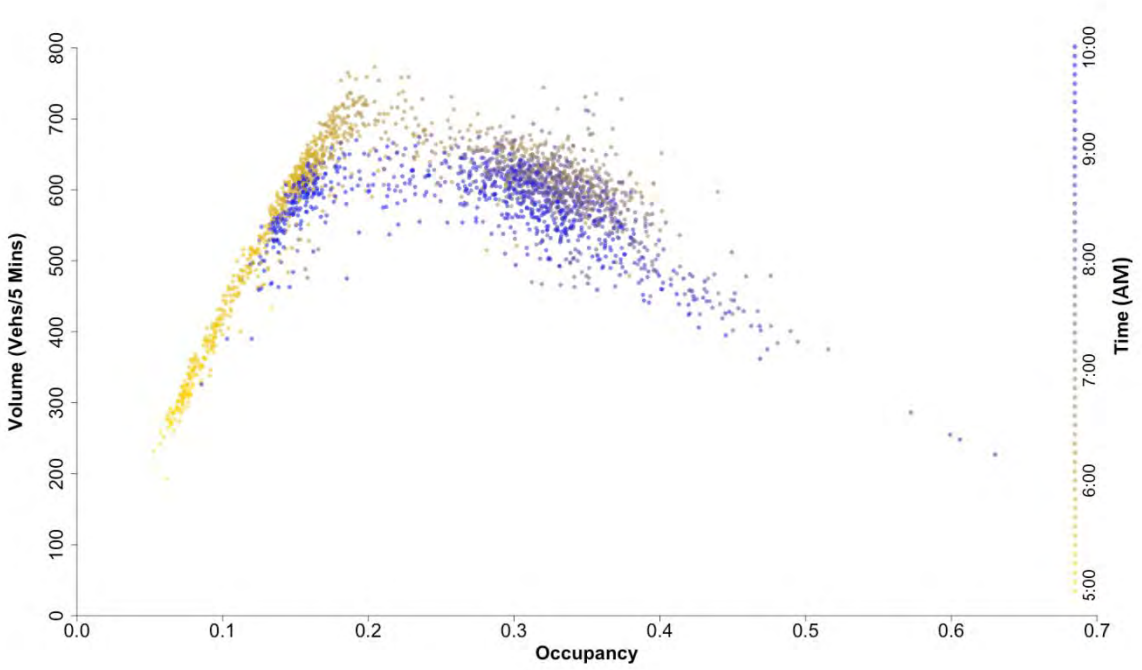

Figure 50. 5-Min Volume-Occupancy Data Plots

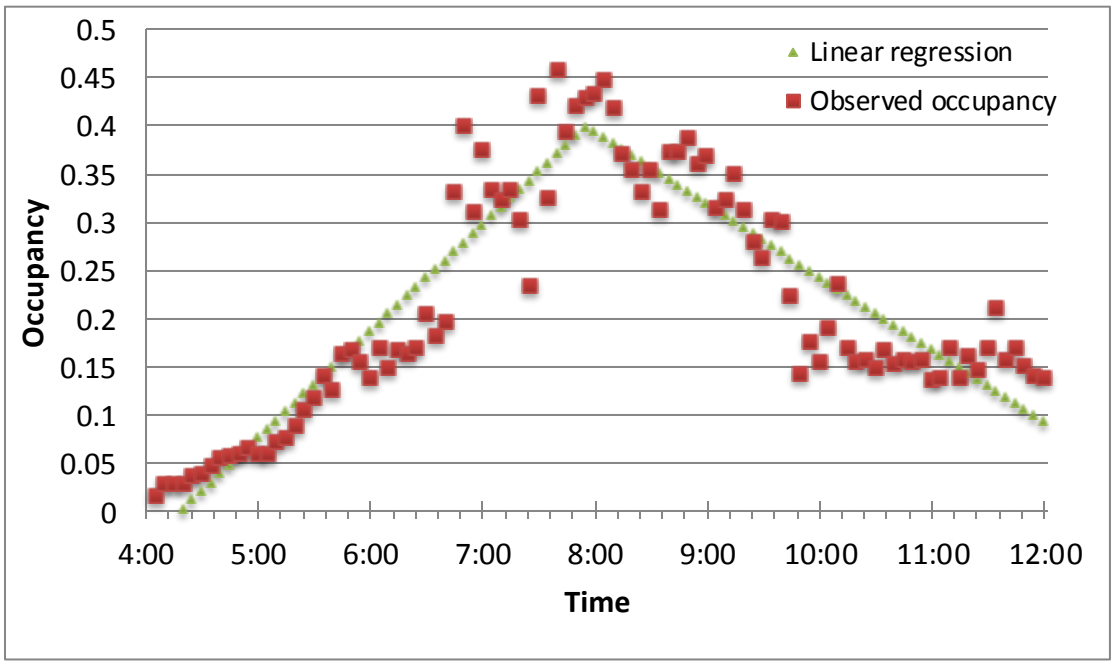

Figure 51. Search for the Best Turning Point

Based on the assumption that the volume-occupancy plots can be represented as a continuous piecewise linear curve, as shown in Figure 49, we will estimate the traffic flow fundamental diagram parameters (including critical occupancy, critical volume, free-flow speed, and

shockwave speed) using the same piecewise linear regression module as in the R package. To provide a comprehensive analysis of before- and after- traffic flow performance, we will perform the estimation using three data sets:

- The entire data set is used to estimate average traffic flow performance, which can be seen from the estimated critical occupancy and critical volume.
- Data from the formulation phase are used to estimate traffic flow performance from free flow conditions to traffic congestion. The estimated critical volume corresponds to the maximum capacity that can be achieved. The estimated shockwave speed provides information on how fast or slow the queue propagates backward.
- Data from the dissipation phase are used to estimate traffic flow performance from traffic congestion back to free flow. This phase's critical volume is usually lower than the average condition. The estimated shockwave speed provides information on how fast or slow the traffic flow can be recovered.

We also proposed a statistical approach to process the detector volume and detector occupancy data to make the piecewise linear regression generate more meaningful and reasonable results. Figure 52 (a) shows volume-occupancy plots based on a few days' worth of data on 5-min volume and occupancy data. We discovered that a certain occupancy value may correspond to a range of volume values. To satisfy the assumption, for each 0.5% occupancy bin, the 50^{th} percentile volume value is obtained as the representative volume of all volumes within the occupancy range. Figure 52(b) illustrates the representative volume-occupancy plot drawn based on representative volume and occupancy data. These representative volumes and their corresponding occupancy values are then used to estimate the traffic flow fundamental diagram parameters.

d) Assumptions

HOV lane facilities are demand management strategies. A key assumption in our analysis is that HOV lane conversion does not alter vehicle composition and modal split between high-occupancy vehicles (HOVs) and single occupancy vehicles (SOVs). Although changes in relative operational performance may, in the long term, influence the mix of vehicles, there is no evidence of the relative attractiveness of continuous-access versus limited-access HOV lanes.

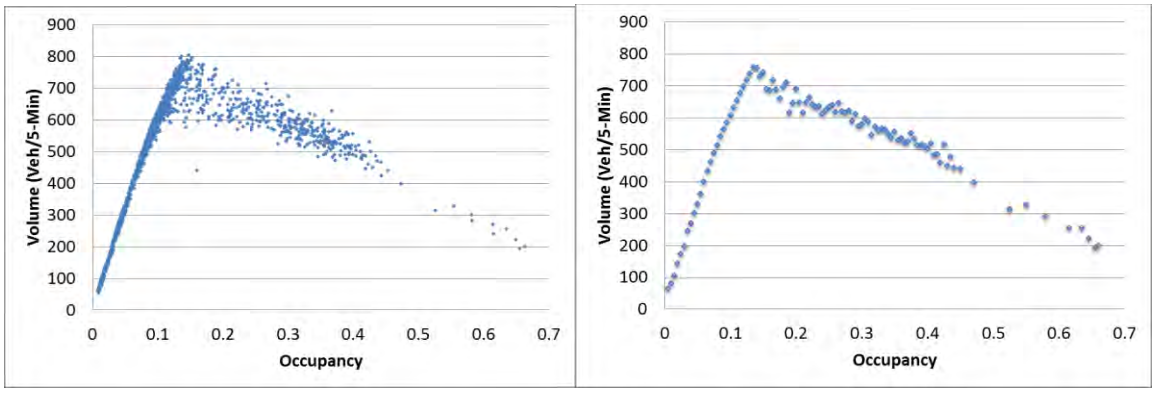

(a) Vol-Occ plots using all data (b) Vol-Occ plots using the representative dataset

Figure 52. Volume-Occupancy Plots

In general, HOV lanes are less congested than GP lanes. An example is shown in Figure 53, which shows GP and HOV lane speed contours for a freeway with limited-access HOV lane. The reason for HOV lane to be less congested is HOV drivers choose whether to use HOV lanes based on real-time traffic condition along GP lanes and the HOV lane access type (limited-access or continuous-access). Because of HOV drivers' lane selection behavior, if the traffic condition in the GP lanes improves, conditions in the HOV lane will more likely improve. As a result, the before-after comparison in this study will primarily focus on a comparison of volume-occupancy diagrams of detector data on the GP lanes.

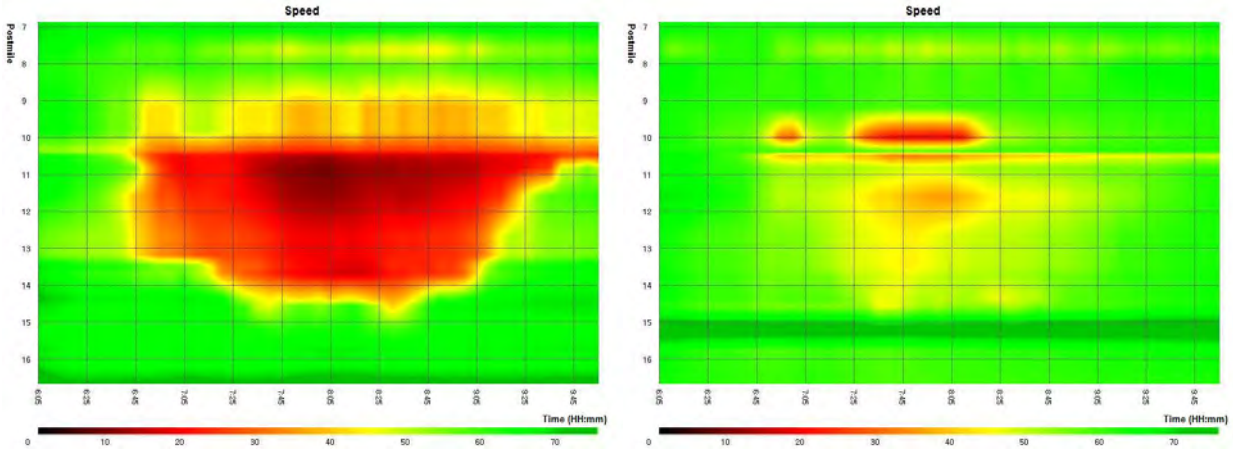

(a) GP lanes (b) HOV lane

Figure 53. Speed Contours for GP and HOV Lanes

Another reason to use data from the GP lanes is because GP lanes are more congested than HOV lanes and thus have more data points in the congestion regime for easier and more accurate estimation of parameters for the traffic flow fundamental diagram.

e) Comparison of Fundamental Diagram Parameters

The proposed method evaluates the performance of HOV lane conversion by comparing the before-and-after traffic flow fundamental diagrams on GP lanes. Among the four traffic flow fundamental diagram parameters (critical occupancy, critical volume, free-flow speed, and shockwave speed), free-flow speed is of the least consequence. For others, their physical meanings are as follows:

- A higher critical volume means improvement of capacity and throughput.
- A higher critical occupancy may mean (1) the roadway facility is less likely to break down easily, or (2) the location becomes congested.
- A faster shockwave speed means that the queue or congestion is built up and/or dissipates at a faster speed.

6.2 Study Sites and Data

In August 2008, Caltrans District 12 in Orange County began to convert some of its HOV lanes from limited-access to continuous-access operation. Figure 54 illustrates the six study sites. They were located on SR-55 and SR-57, which are two north-south facilities, connecting Orange County with Riverside County and Los Angeles County, respectively. Both freeways have similar traffic patterns and are heavily congested. The peak direction of flow is southbound (SB) in the morning and northbound (NB) in the afternoon.

These study sites have four or five GP lanes and one HOV lane and are well covered by detector stations. Figure 55 shows each site's geometry before the conversion. The amber lines between GP lanes and HOV lanes correspond to sections of freeway with HOV lane conversion. The figure also shows the vehicle detector locations using ellipses, inside of which is the location's absolute postmile (ABS-Postmile). The color of the circle represents the usability of the data, which we explain later in this report. A vehicle detection location usually has one Vehicle

Detector Station (VDS) on GP lanes and one VDS on the HOV lane. The VDS IDs are shown on the right side of each detector location in the figure.

Table 6 shows the HOV lane conversion date, before-and-after data collection time periods, and the study period for each study site. We considered the following factors in selecting the data collection periods:

- The "before" data collection period should be a time shortly before the HOV lane conversion.
- "Before" and "after" data should be collected in the same season.
- Detector data should be in a "healthy condition", which means that the majority of data are actual field observations and the data are sufficiently accurate.
- "After" data should not be collected during the transition period when people are familiarizing themselves to the new striping configuration. We allowed at least a period of three months after the conversion to take samples of the "after" data.

Each data collection period includes only weekdays (from Tuesday to Thursday, excluding holidays). Detector data (including 5-min volume and occupancy data) were collected through either PeMS or the Front End Processor (FEP) data source from Caltrans District 12.

Detector data quality, observation rates, and data consistency were checked to ensure its usability. We found communication problems on some days that kept detectors' flow or occupancy values the same for a long period. When this occurred, we removed data from that day.

Our final data set includes a limited number of detector stations for these study sites. As shown in Figure 55, those detector stations designated by a green ellipse had good data during both the "before" and "after" data collection periods. Those designated by a red ellipse did not have good data during these periods. Those without a color are outside of the study area.

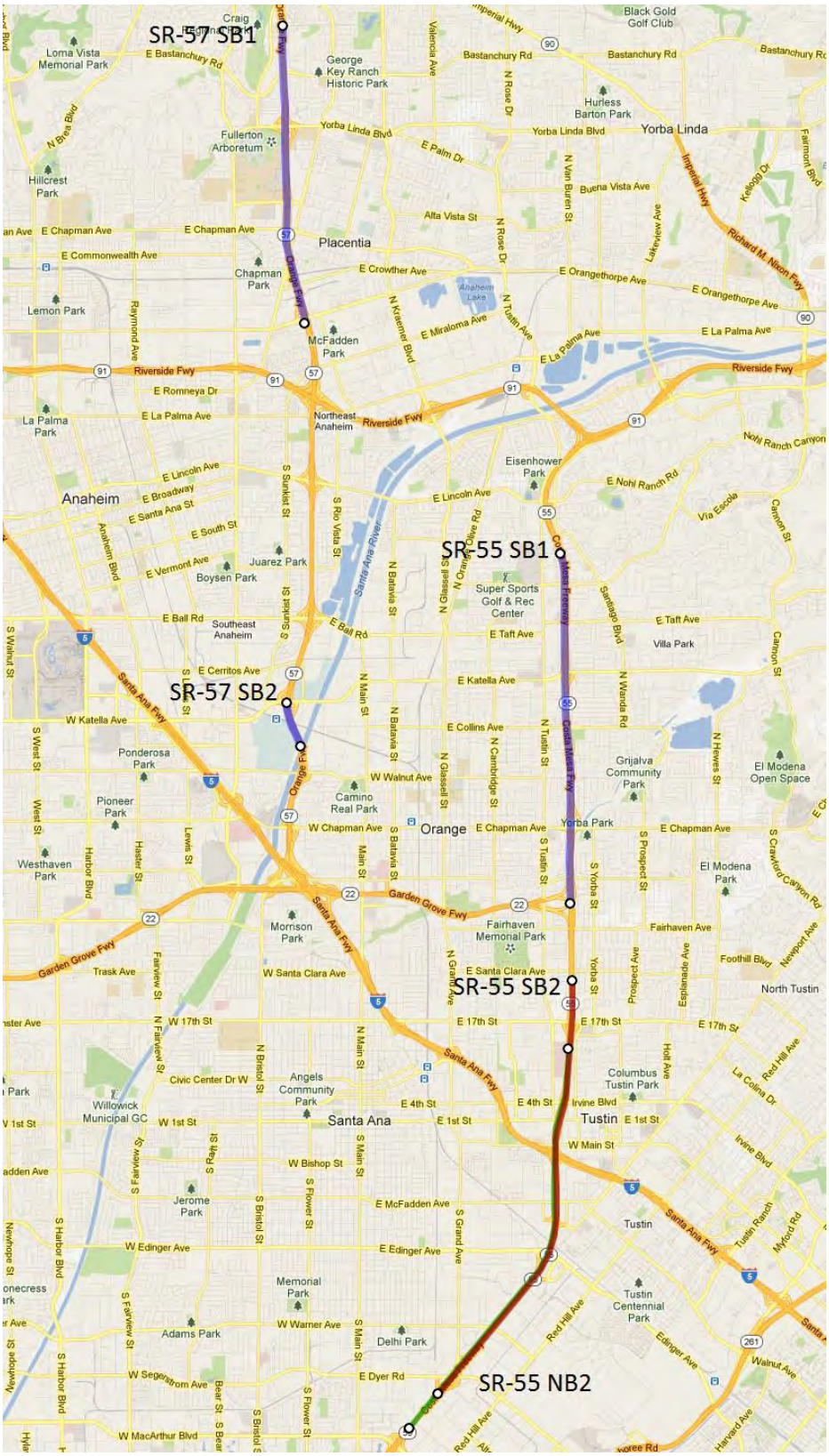

Figure 54. Study Sites

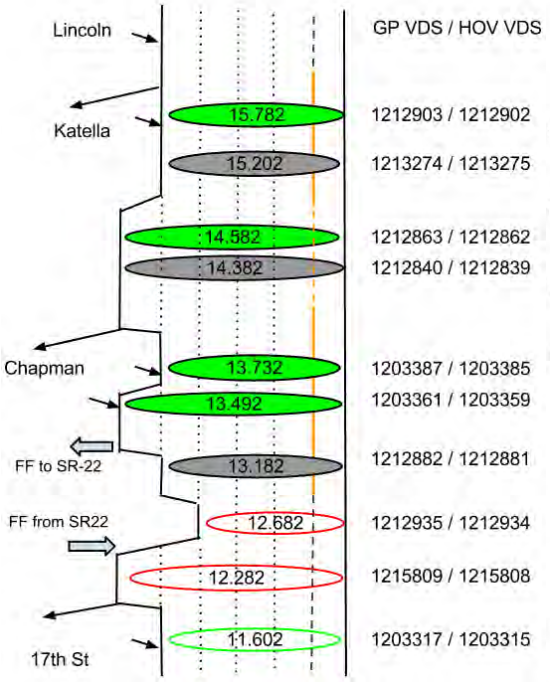

(a) SR-55 SB1 Site

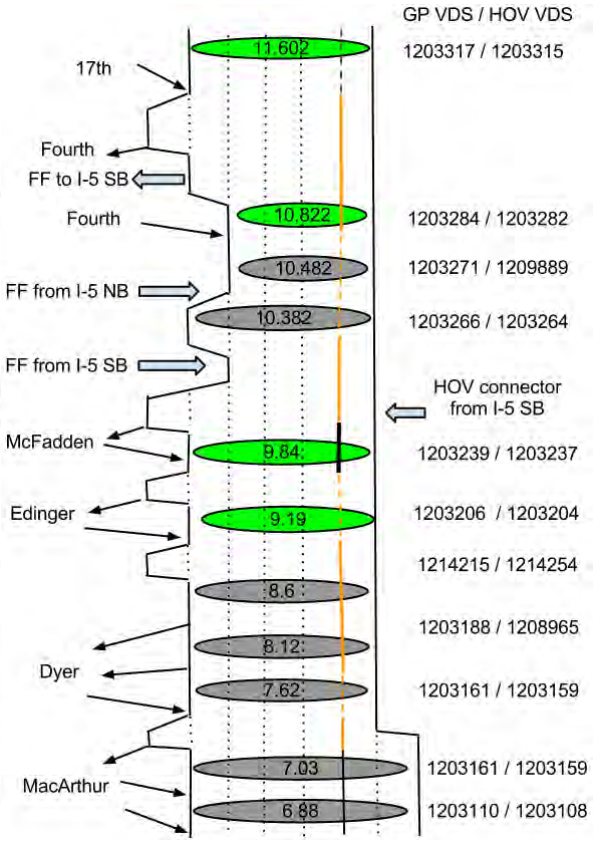

(b) SR-55 SB2 Site

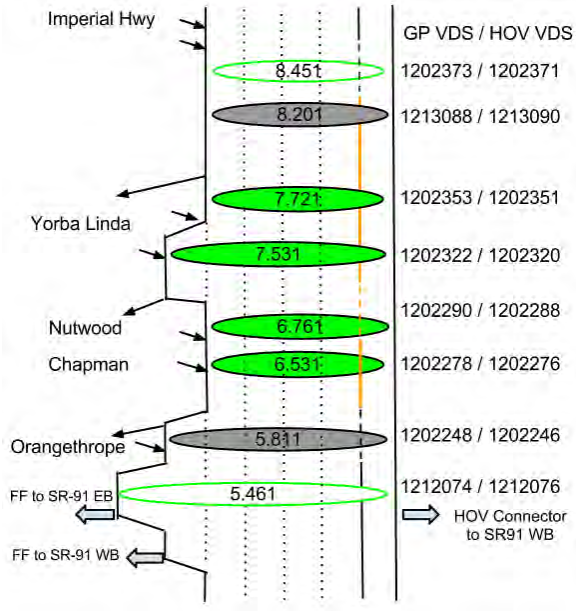

(c) SR-57 SB1 Site

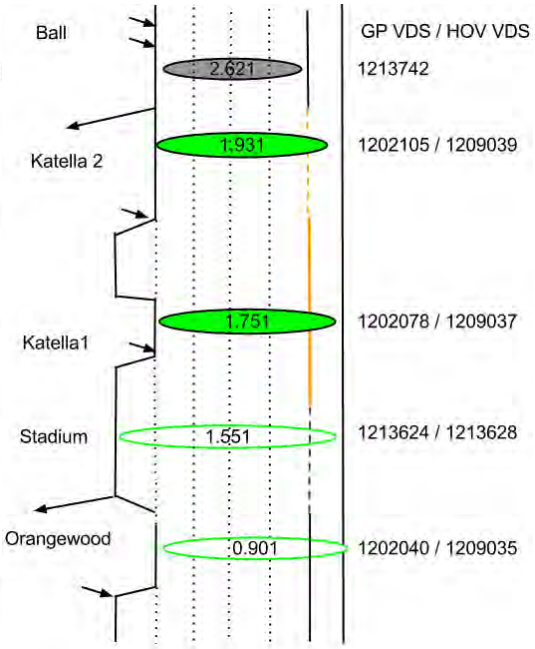

(d) SR-57 SB2 Site

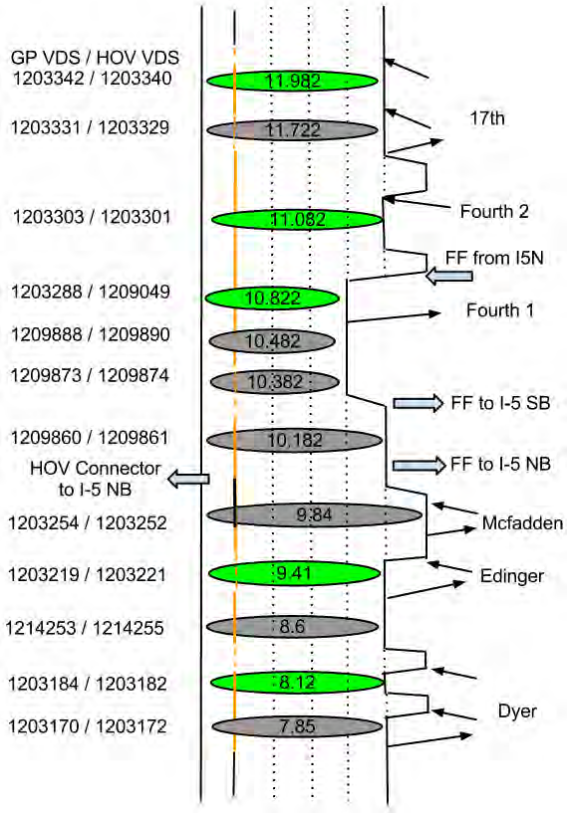

(e) SR-55 NB2 Site

Figure 55. Geometry and Detectors along the Study Sites (Green: Good Detector Data; Grey: Incomplete or Bad Detector Data)

Table 6. Before-and-After Data Collection Periods

Location (ABS-postmile range)	Conversion Date	"Before" Dataset	"After" Dataset	Study Period
SR-55 SB1: Lincoln to SR-22 (15.8 - 13.2)	Aug 2008	Jan 2, 2008 - Apr 1, 2008	Jan 6, 2009 - Apr 22, 2009	AM
SR55 SB2: 17th St to MacArthur (11.6 - 7)	4/1/2011	2010 Q3	2011 Q3	AM
SR-57 SB1: downstream of Imperial to Orangethrope (8.5 - 5.8)	Sep 2009	Jan 6, 2009 - Apr 22, 2009	Jan 5, 2010 - Apr 13, 2010	AM
SR 57 SB2: Katella to Orangewood (1.93 – 1.4)	12/1/2010	2010 Q2	2011 Q2	AM
SR55 NB2: Dyer to 17th St. (7.8 - 12)	4/1/2011	2010 Q4	2011 Q4	PM

6.3 Performance Comparison

The following operational performances were utilized to measure the before and after conditions on the five study sites as a result of the HOV lane conversion:

- Speed contour
- Speed differential
- VMT ratio
- Demand flow
- Traffic flow fundamental diagram parameters

Full analysis results are given for the SR-55 SB1 and SR-57 SB1 sites first, followed by a summary of the performance of all study sites.

6.3.1 Analysis

A. SR-55 SB1 Site

a) Speed Contour

The speed contour map illustrates the traffic congestion patterns of the study site. This helps to identify bottleneck locations, congested areas, queue lengths and congestion time periods. Figure 56 presents the 50th percentile speed contours for both GP lanes and HOV lane for the site, drawn based on 5-min speed data obtained from PeMS. The X-coordinate represents time-of-day; the y-coordinate represents freeway absolute postmile. The traffic direction is from bottom to top. The color theme is shown on the bottom of each picture. Green means free-flow; red means congestion.

The geographic range of the site is from absolute postmile 16.8 to 13.2. However, the speed contours in the figures cover a longer segment from the Lincoln interchange (postmile 16.7) to the MacArthur interchange (postmile 7.03) to provide an overview of traffic conditions downstream of the study site segment. The study site has a major bottleneck around postmile 9 to 10 at the I-5 interchange, located three miles downstream of the site. The diagram shows that traffic after the HOV lane conversion appears to be less congested.

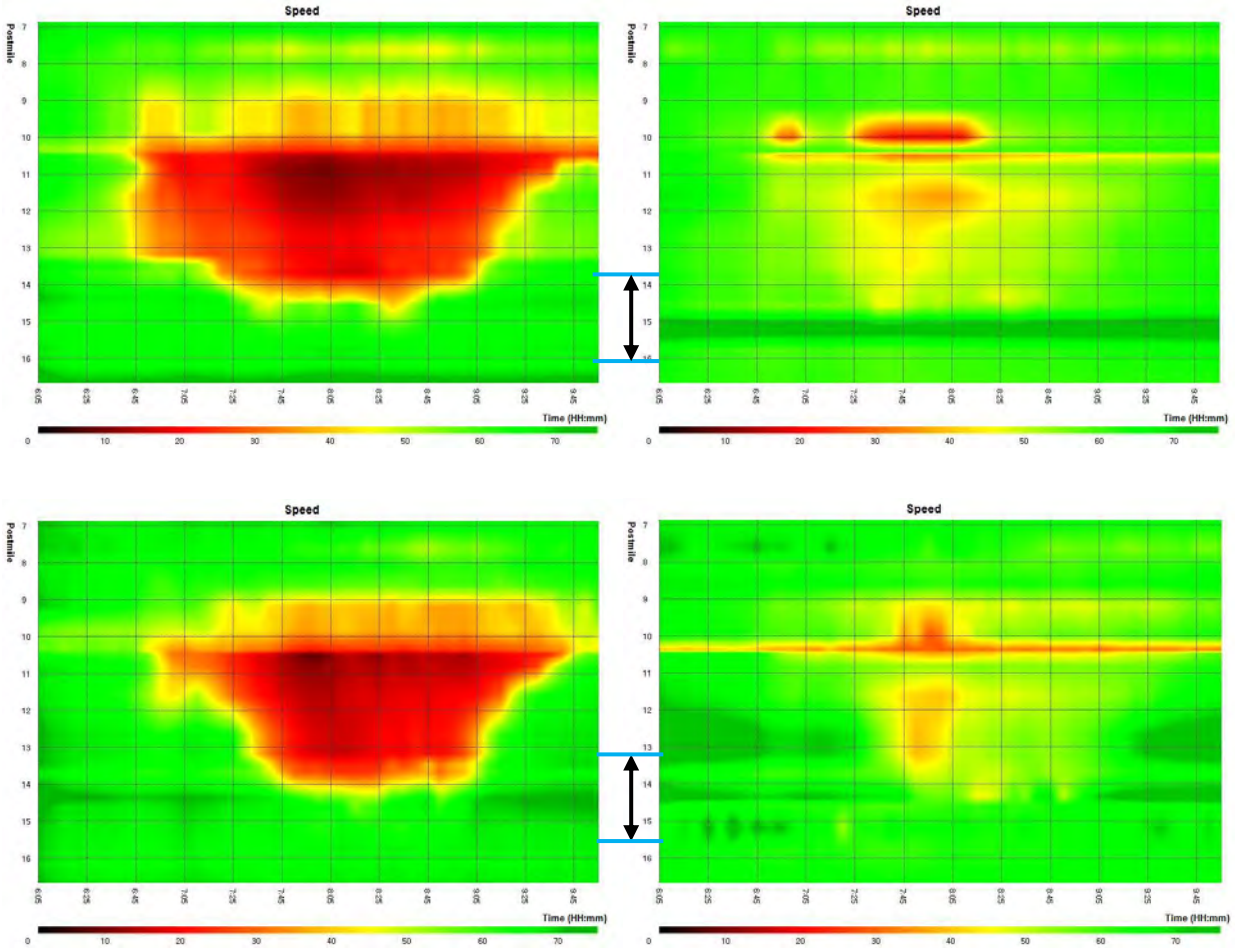

(a) before (top) and after GP Lanes (b) before (top) and after HOV Lanes

Figure 56. SR-55 SB1 Speed Contours Before and After the HOV Lane Conversion

b) Speed Differential

In Figure 57, we present the speed differential distribution between the HOV lane and the GP lane average for the SR-55 SB1 site. In each subplot, we show data for the before-and-after periods. Our analysis also distinguishes congestion on the GP lanes using a GP lane average speed of below 45 mph as the boundary of congestion. The data, only selected from those with high data health, for all traffic conditions during the study period are shown in the upper charts (a and b), while those filtered for congested situations with GP below 45 mph are shown in the lower two subplots (c and d).

All plots show a positive speed differential, which implies that speed in the HOV lanes was higher than average speed across GP lanes for a great majority of the situations. Note that the

median value of the speed differential during the after-study period increased when compared with the before-study period.

Subplots of (c) and (d) show that, when the GP lanes were congested, the HOV lane appeared to benefit more in speed differential from the conversion. Specifically, the median value of the speed differential increased from 19 mph to 23 mph, and the distribution was more centralized.

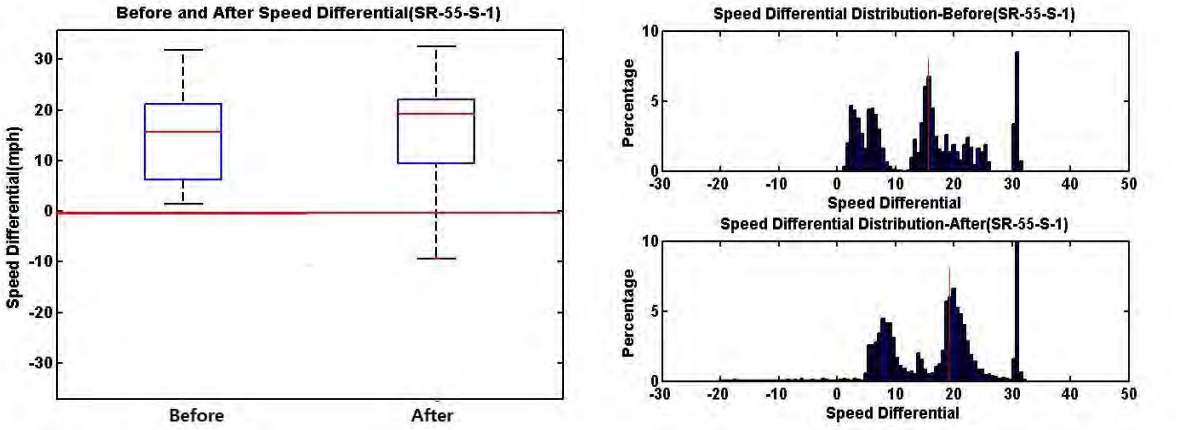

(a) Speed Differential Boxplot (all periods) (b) Speed Differential Distribution (all periods)

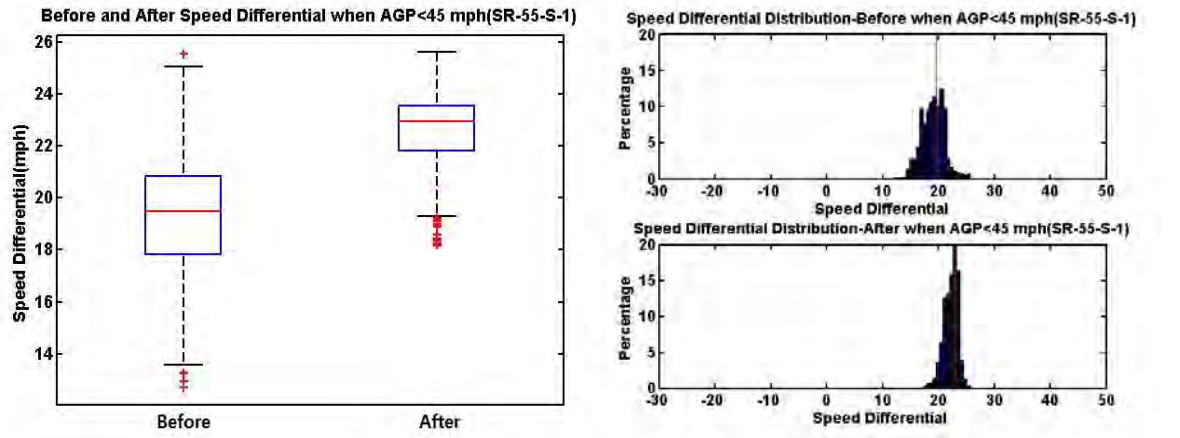

(c) Speed Differential Boxplot (congestion) (d) Speed Differential Distribution (congestion)

Figure 57. Speed Differential for SR-55 SB1

c) VMT Ratio

The VMT ratio provides an indication of the relative levels of vehicle flow volume between the HOV lanes and the average across the GP lanes in the before-and-after study period. If the ratio is below 1, it implies that the VMT in the HOV lanes is lower than that in the GP lanes. From Figure 58, we can see that the overall distribution of the VMT ratio is slightly lower after

conversion. This result is mainly because the traffic condition was less congested and fewer vehicles used the HOV lane after the conversion.

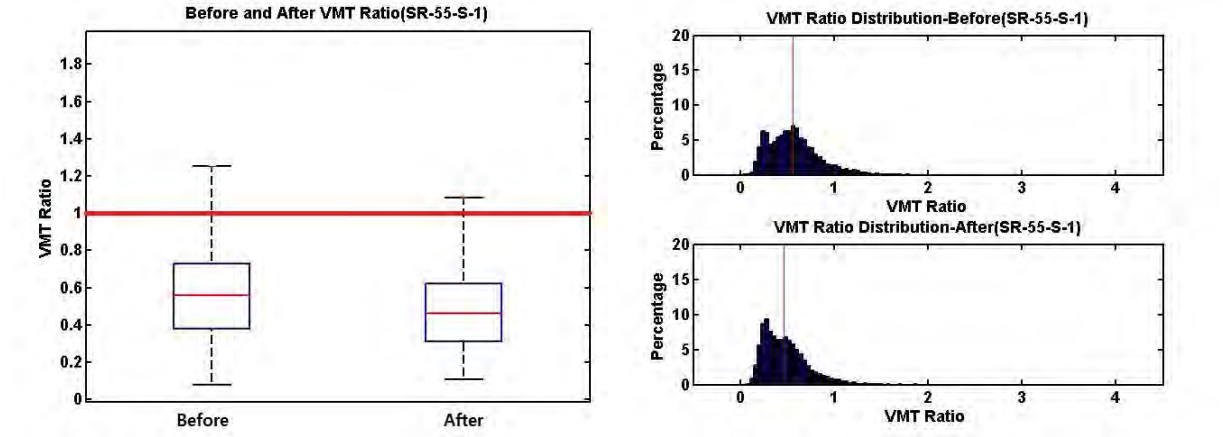

(a) VMT Ratio Boxplot (all periods) (b) VMT Ratio Distribution (all periods)

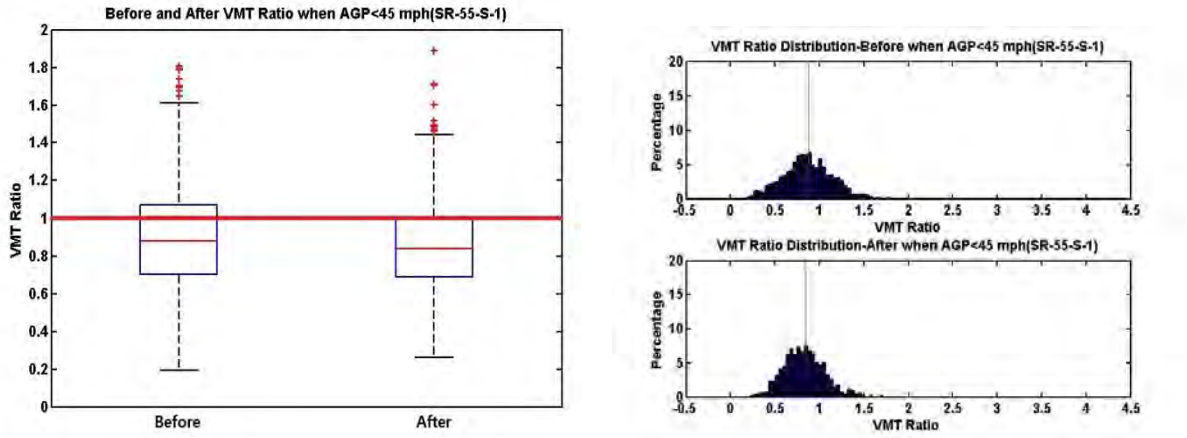

(c) VMT Ratio Boxplot (congestion) (d) VMT Ratio Distribution (congestion)

Figure 58. VMT Ratio for SR-55 SB1

d) Demand Flow

Demand flow is defined as total vehicular throughput on GP and HOV lanes for the entire peak period, which begins at a time with free-flow conditions and ends at another time with free-flow conditions. For the SR-55 SB1 site, the entire a.m. peak period is from 6:00 a.m. to 10:00 a.m. Table 7 shows that the site has higher flows on GP lanes and lower flows on the HOV lane. In total, the site had higher demand flows after HOV lane conversion. (Note that the detector station at postmile 11.602 was added to the table for information only since it is outside the study area).

Table 7. Demand flows for SR-55 SB1

	GP Lanes			HOV Lane			Total			
PostMile	Before	After	Change	Before	After	Change	Before	After	Change	Change %
15.782	25885	26430	545	3319	2936	-383	29204	29366	162	0.6%
14.582	27933	29415	1482	3562	3099	-463	31495	32514	1019	3.2%
13.732	23908	25763	1855	3605	3230	-375	27513	28993	1480	5.4%
13.492	27244	30078	2835	3582	3248	-334	30826	33326	2501	8.1%
11.602	22527	23906	1379	3894	3443	-451	26421	27349	928	3.5%

e) Traffic Flow Fundamental Diagram Parameters

The speed contours show that the site has less congestion after HOV lane conversion, although the demand flow is higher. Thus, one could conclude that the site performs better with the continuous-access HOV configuration. For more certainty, we will use the proposed traffic flow fundamental diagram- based approach to analyze the operational performance of the site before and after conversion to verify this result and explain the result from the traffic flow theory perspective.

Table 8 and Table 9 compare the key traffic flow fundamental diagram parameters at all mainline VDS locations for the formulation phase and dissipation phase, respectively. The key parameters in the formulation phase include critical occupancy, critical volume, and shockwave speed. The key parameters in the dissipation phase include critical volume, and shockwave speed. If the differences between before-and-after values are less than 2%, they are considered negligible (or, not significant). Among all mainline detector stations, the key station is located at the Chapman interchange (postmile 13.732), which appears to be a hidden bottleneck of the study site before the conversion. Its representative volume-occupancy plots and the estimation results are shown in Figure 59. Detector station ID, location and postmile are shown at the top of each plot.

Based on the analysis of the traffic flow diagram parameters, we found:

- Most mainline detector stations have equivalent or higher critical occupancy in the formulation phase, which means the freeway is less likely to break down after the conversion of HOV lane to continuous-access.

- Higher critical volumes are achieved for mainline detector stations in the formulation phase and the dissipation phase, which means higher capacity and better performance after the conversion.
- Higher shockwave speed is achieved for both phases after the HOV conversion, which means that the queue is built up and/or dissipates at a faster speed under traffic congestion. A queue may build up faster, reducing operating benefits, due to higher levels of lane changing. One reason for the queue to dissipate faster, which is operationally beneficial, is the flexibility provided to drivers by continuous-access to the HOV facility.

To summarize, the HOV lane conversion to continuous-access operation makes the SR-55 SB1 site perform better.

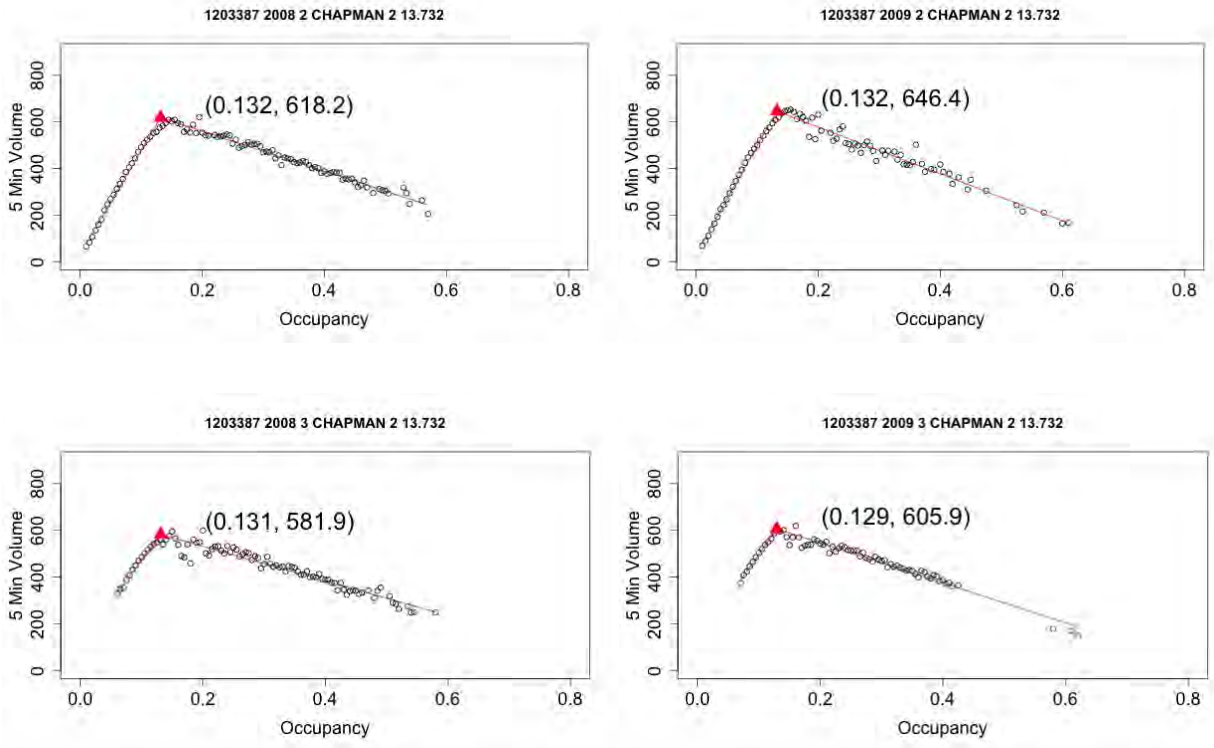

Figure 59. SR-55 SB1: Estimated Traffic Flow Diagram Parameters using Data in Formulation Phase (Top) and Dissipation Phase (Bottom) at Postmile 13.732

Table 8. SR-55 SB1: Traffic Flow Diagram Parameters in the Formulation Phase

	Postmile	Ingress/ Egress before conversion?	Before	After	Diff	% Diff	Before v.s. After
Critical Occupancy	15.782	no	0.128	0.127	-0.001	-0.8%	Equivalent
	14.582	yes	0.117	0.119	0.002	1.7%	Equivalent
	13.732	no	0.132	0.132	0	0.0%	Equivalent
	13.492	no	0.114	0.128	0.014	12.3%	After: Higher
Critical Volume	15.782	no	625.8	641.7	15.9	2.5%	After: Higher
	14.582	yes	683.6	708.3	24.7	3.6%	After: Higher
	13.732	no	618.2	646.4	28.2	4.6%	After: Higher
	13.492	no	714	768.5	54.5	7.6%	After: Higher
Shockwave Speed	15.782	no	-16.8	-19.8	-3	17.9%	After: Higher
	14.582	yes	-8.9	-9.4	-0.5	5.6%	After: Higher
	13.732	no	-13.4	-15.7	-2.3	17.2%	After: Higher
	13.492	no	-10.3	-12.8	-2.5	24.3%	After: Higher

Table 9. SR-55 SB1: Traffic Flow Diagram Parameters in the Dissipation Phase

	Postmile	Ingress/ Egress before conversion?	Before	After	Diff	% Diff	Before v.s. After
Critical Volume	15.782	no	605.5	612.5	7	1.2%	Equivalent
	14.582	yes	654.9	698.4	43.5	6.6%	After: Higher
	13.732	no	581.9	605.9	24	4.1%	After: Higher
	13.492	no	651	720	69	10.6%	After: Higher
Shockwave Speed	15.782	no	-15.7	-20.5	-4.8	30.6%	After: Higher
	14.582	yes	-9.2	-11.5	-2.3	25.0%	After: Higher
	13.732	no	-14	-15.9	-1.9	13.6%	After: Higher
	13.492	no	-10.5	-13.2	-2.7	25.7%	After: Higher

B. SR-57 SB1 Site

a) Speed Contour

Figure 60 shows the speed contours for both GP lanes and HOV lane before and after the HOV lane conversion. The study limit of the site is from postmile 8.5 to 5.8. However, the speed contours in the figures show the segment from the Lambert interchange (postmile 10.0) to the I-5/SR-22 interchange (postmile 0) to provide a better overview of traffic conditions beyond the

study site. The diagram shows that the SR-57 SB1 site has a major bottleneck at postmile 6.5, the Chapman interchange, located within the study area. The freeway mainline traffic condition after the HOV lane conversion appears to be more congested.

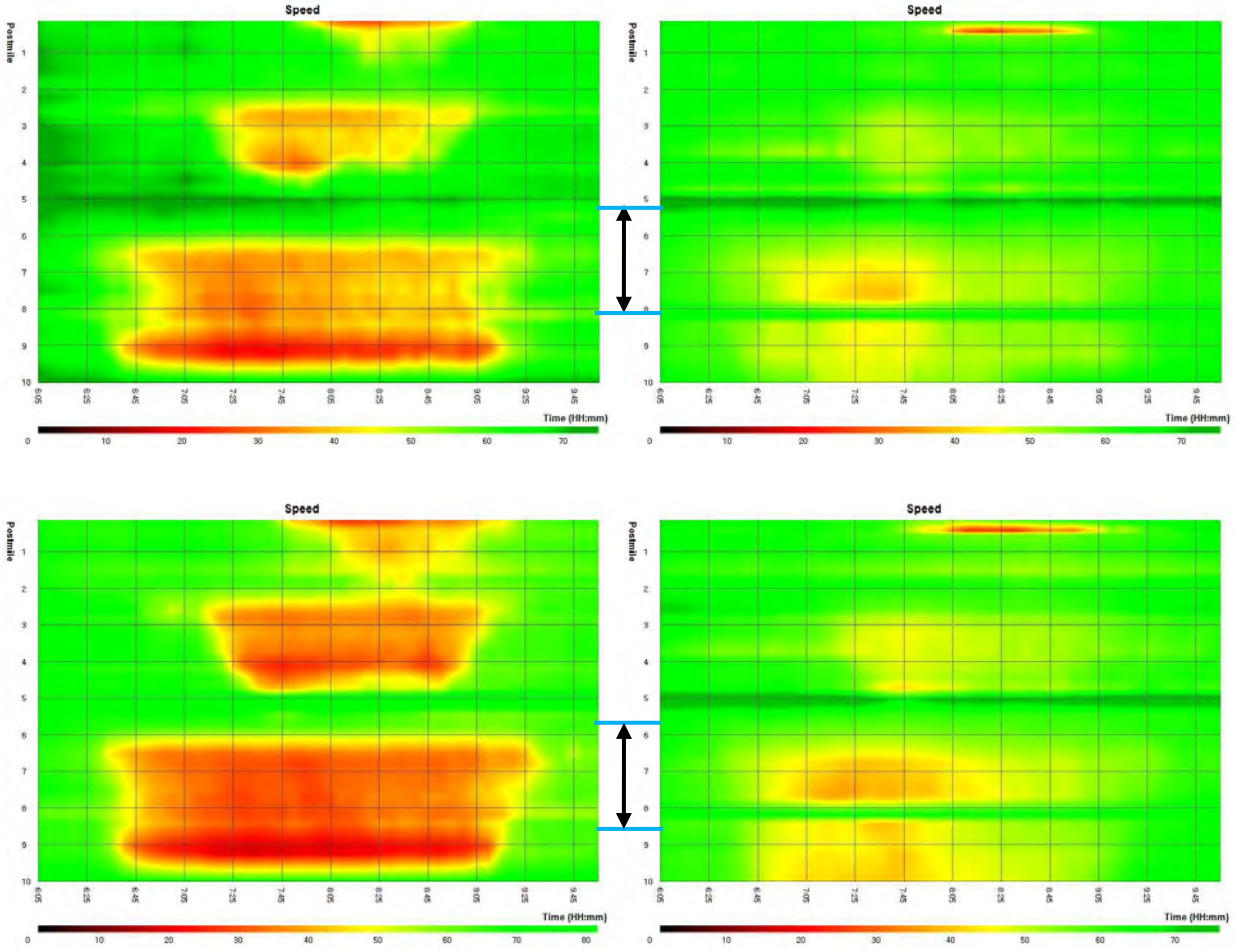

(a) before (top) and after GP Lanes (b) before (top) and after HOV Lanes

Figure 60. SR-57 SB1: Speed Contours Before and After HOV Lane Conversion

b) Speed Differential

The distribution of speed differential between the HOV lane and the GP lane average for the SR-57 SB1 site is presented in Figure 61. Each subplot shows data for both the before and the after periods. All plots show a positive speed differential, which implies that the speed in the HOV lanes was higher than the average speeds across GP lanes for the majority of the data samples examined. We found that the before-and-after speed differential distribution was almost the same.

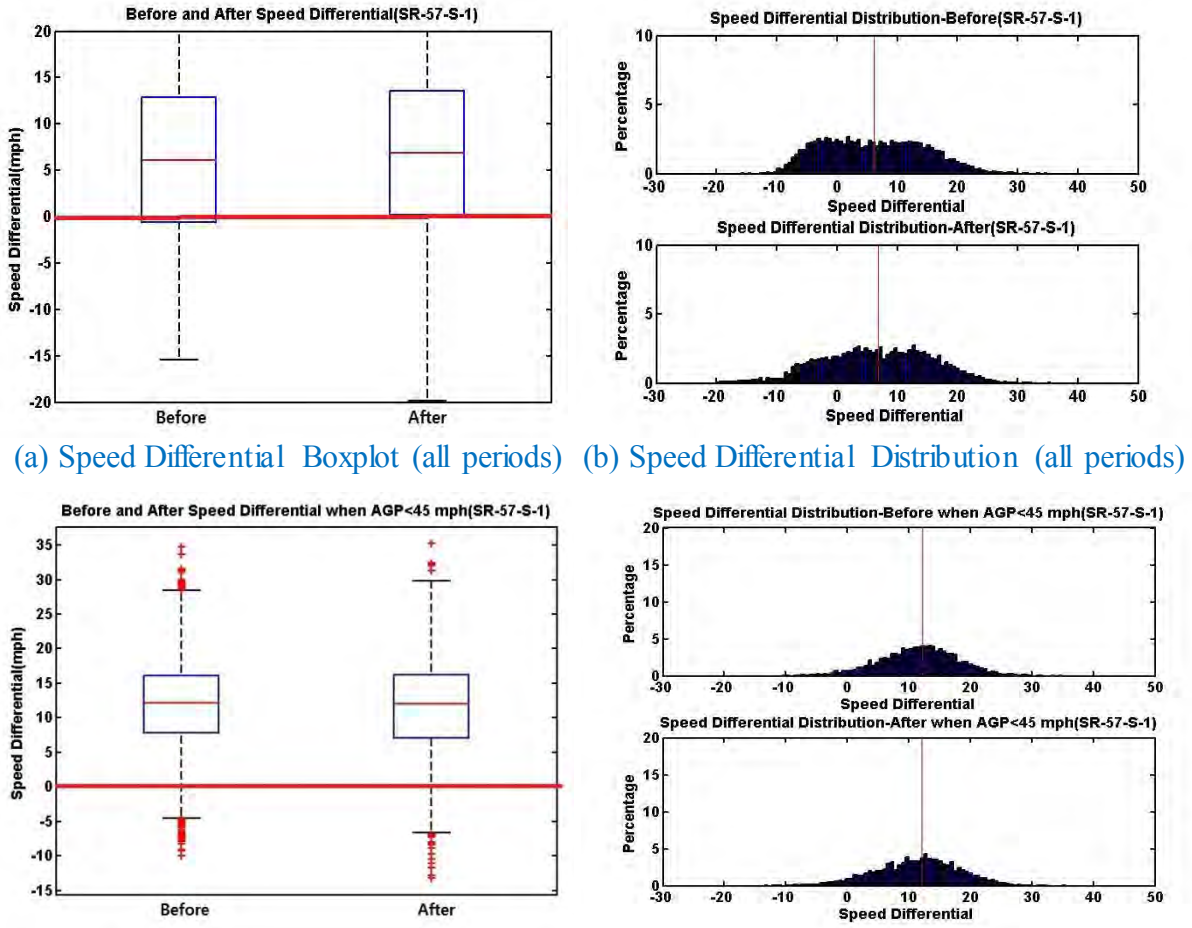

(a) Speed Differential Boxplot (all periods) (b) Speed Differential Distribution (all periods)

(c) Speed Differential Boxplot (congestion) (d) Speed Differential Distribution (congestion)

Figure 61. Speed Differential for SR-57 SB1

c) VMT Ratio

As illustrated in Figure 62, the distribution of VMT ratio slightly shifts to a higher value for all periods and congestion periods. This is mainly due to more congestion on the GP lanes and thus more vehicles switching to the HOV lane.

d) Demand Flow

For the SR-57 SB1 site, demand flows at all detector locations were analyzed for the a.m. peak period (from 6:00 a.m. to 10:00 a.m.). Table 10 shows that the site has lower flow for GP lanes and equivalent flow for HOV lanes after the conversion. In total, the demand flows, which are equal to the total GP lane flow plus the total HOV lane flow, are 2%-4% lower after conversion.

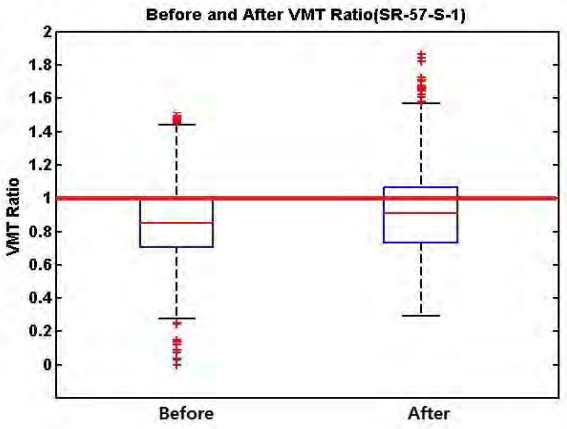

(a) VMT Ratio Boxplot (all periods)

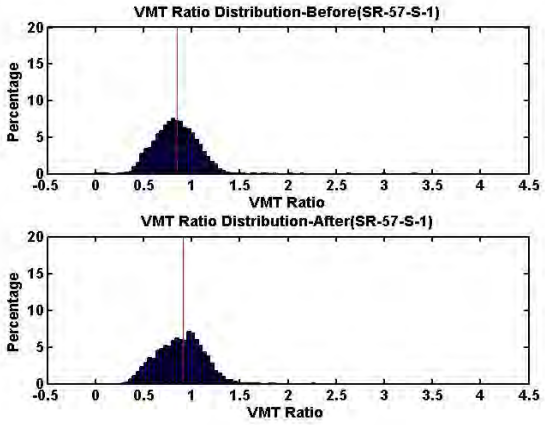

(b) VMT Ratio Distribution (all periods)

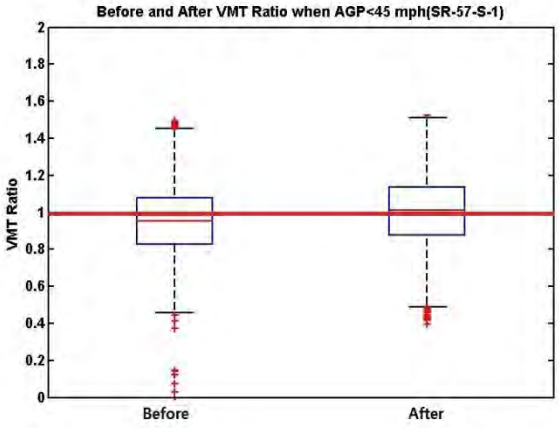

(c) VMT Ratio Boxplot (congestion)

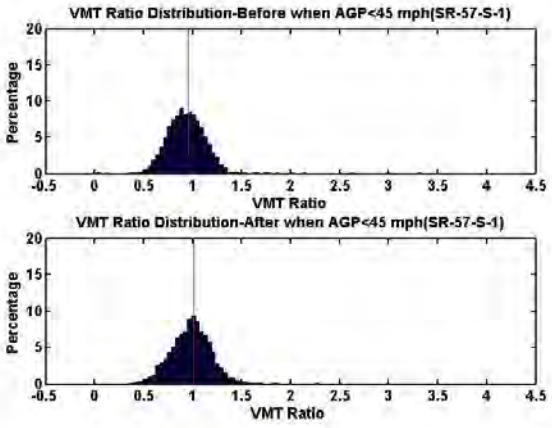

(d) VMT Ratio Distribution (congestion)

Figure 62. VMT Ratio for SR-57 SB1

Table 10. Demand Flows for SR-57 SB1

	GP Lanes			HOV Lane			Total			
PostMile	Before	After	Change	Before	After	Change	Before	After	Change	Change %
7.721	25812	24696	-1116	5323	5225	-98	31135	29921	-1214	-3.9%
6.761	27317	26441	-876	5595	5614.5	20	32912	32056	-856	-2.6%
6.531	29929	28927	-1002	5554.5	5560.5	6	35484	34488	-996	-2.8%

e) Traffic Flow Fundamental Diagram Parameters

Because the demand flows are lower (as presented in Table 10) and traffic congestion is more severe (as illustrated in Figure 60) after the conversion, it may indicate that the continuous-access HOV configuration makes the site perform worse. The traffic flow fundamental diagram-based approach was employed to further analyze the operational performance of the site before

and after the conversion, to verify the above result, and to explain the result from the perspective of traffic flow theory.

Table 11 and Table 12 compare the key traffic flow fundamental diagram parameters at all mainline VDS locations for the formulation phase and dissipation phase, respectively. Among all mainline detector stations, the key station is located at the Chapman interchange (postmile 6.531), which is the bottleneck of the study site. Its representative volume-occupancy plots and estimation results are shown in Figure 63.

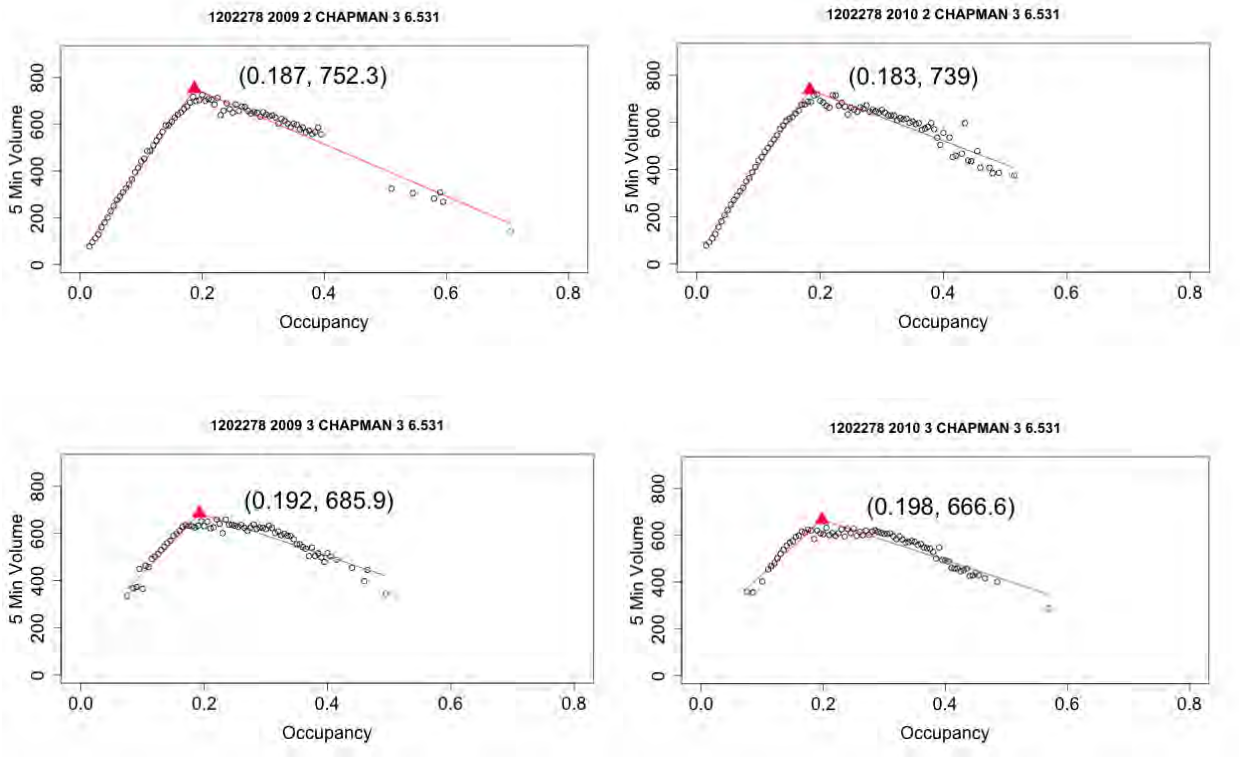

Figure 63. SR-57 SB1: Estimated Traffic Flow Diagram Parameters using Data in Formulation Phase (Top) and Dissipation Phase (Bottom)

Based on the traffic flow diagram parameters shown in Table 11 and Table 12, we found:

- All mainline stations have similar critical volumes in the formulation phase. The actual critical volumes are slightly lower after the conversion, although not significant.
- After the conversion, lower critical occupancy is obtained at the two downstream detector stations, which are located at the bottleneck of the site and determine the performance of the site. Lower critical occupancy means that the freeway is easier to break down.

- Lower shockwave speed is achieved in the formulation phase, which means congestion takes longer to build up.
- Lower throughputs are achieved in the dissipation phase, which means worse performance after the conversion.
- After the HOV conversion, higher shockwave speed is achieved in the dissipation phase at the two downstream detector stations. Thus, the queue is dissipated at a faster speed under traffic congestion.

Table 11. SR-57 SB1: Traffic Flow Diagram Parameters in the Formulation Phase

	Postmile	Ingress /Egress	Before	After	Diff	% Diff	Before v.s. After
Critical Occupancy	7.721	No	0.157	0.157	0	0.0%	Equivalent
	7.531	No	0.127	0.126	-0.001	-0.8%	Equivalent
	6.761	Yes	0.146	0.143	-0.003	-2.1%	After: Lower
	6.531	No	0.187	0.183	-0.004	-2.1%	After: Lower
Critical Volume	7.721	No	641.7	640.9	-0.8	-0.1%	Equivalent
	7.531	No	693.1	685.6	-7.5	-1.1%	Equivalent
	6.761	Yes	680.4	674.7	-5.7	-0.8%	Equivalent
	6.531	No	752.3	739	-13.3	-1.8%	Equivalent
Shockwave Speed	7.721	No	-14.8	-14.5	0.3	-2.0%	After: Lower
	7.531	No	-12.4	-11.3	1.1	-8.9%	After: Lower
	6.761	Yes	-16.5	-15.6	0.9	-5.5%	After: Lower
	6.531	No	-17.3	-15.4	1.9	-11.0%	After: Lower

Table 12. SR-57 SB1: Traffic Flow Diagram Parameters in the Dissipation Phase

	Postmile	Ingress /Egress	Before	After	Diff	% Diff	Before v.s. After
Critical Volume	7.721	No	596.4	569.6	-26.8	-4.5%	After: Lower
	7.531	No	624.6	607.6	-38.3	-5.9%	After: Lower
	6.761	Yes	618.1	602.2	-15.9	-2.6%	After: Lower
	6.531	No	685.9	666.6	-19.3	-2.8%	After: Lower
Shockwave Speed	7.721	No	-14.2	-12.1	2.1	-14.8%	After: Lower
	7.531	No	-13.9	-10.3	3.6	-25.9%	After: Lower
	6.761	Yes	-13.2	-15.1	-1.9	14.4%	After: Higher
	6.531	No	-16.7	-17.8	-1.1	6.6%	After: Higher

To summarize, the SR-57 SB1 site performs worse after HOV lane conversion, mainly due to lower critical volume and lower critical occupancy at the two downstream detector stations, which are the bottleneck locations of the site.

6.3.2 Summary of Performance

Appendix I provides the performance comparison results for the rest three study sites. We found that the SR-57 SB2 site does not have an active bottleneck within the study area and may also be influenced by the downstream bottleneck. We exclude the site from the summary shown below.

Table 13 summarizes the performance after the conversion in terms of speed contours, demand flows, and speed differentials and VMT ratios during congestion. We found that

- Traffic congestion is higher for GP lanes and HOV lane for most study sites after conversion.
- Demand flows vary for different study sites.
- The speed differential is similar or higher after the conversion, which means the HOV lane continues to provide the same or more travel time saving after the conversion to continuous-access operation.
- The VMT ratio is similar after the conversion. For the two sites that have different VMT ratios, the differences are minor. This means the HOV lane volume remains almost the same after the conversion to continuous-access operation.

Table 13. Performance after the Conversion

Site	Speed Contour (GP Lanes/ HOV Lanes)	Demand Flows	Speed Differential	VMT Ratio
SR-55 SB1	Less / Less congested	Higher	Higher	Slightly Lower
SR-57 SB1	More / More congested	Lower	Similar	Slightly Higher
SR-55 SB2	More / More congested	Higher	Similar	Similar
SR55 NB2	More / More congested	Similar	Slightly Higher	Similar

Although different demand flows were present in the before- and after- conditions, the proposed traffic flow fundamental diagram approach showed its capability to provide an objective and detailed comparison of two different HOV lane access configurations from the traffic flow theory perspective. Table 14 and Table 15 summarize the traffic flow performance at detector stations located within a limited-access area and within a continuous-access area before the

conversion, respectively. The ratings, such as slower, higher, lower, similar, etc., in these two tables were determined based on a 2% threshold. If the difference was within 2%, the performance was rated as similar. The text colors of these ratings represent whether the after value is larger than the before value. Green means the after value is larger; red means the after value is smaller; black means the difference between before and after values is rated as similar.

Based on the analysis of Table 14 and Table 15, we found:

- The HOV lane performance after the conversion from limited-access to continuous-access operation is site-specific. Among the four study sites, one (SR-55SB1) performs better, one (SR-57SB1) performs worse, and two (SR-55SB2 and SR-55NB2) remain the same.
- For the key traffic flow parameter, the critical volume or vehicle throughput's performance after the conversion is mixed. Except for the SR-55 SB1 site that has higher throughput, all other locations have similar or lower critical volume in the formulation phase and dissipation phase.
- The conversion of a HOV lane from limited-access to continuous-access leads to a faster shockwave speed on GP lanes during the dissipation phase, which means that the queue is able to dissipate at a faster speed at the end of the traffic congestion. In other words, a freeway with continuous-access would see congestion clear up faster.

Table 14. Summary of Traffic Flow Performance after the Conversion at a Mainline Detector Station Located within a Limited-access Area before Conversion

Site (VDS ABS-postmile)	Formulation			Dissipation	
	Critical Occupancy	Critical Volume	Shockwave Speed	Critical Volume	Shockwave Speed
SR-55 SB1 (13.732)	Similar	Higher	Faster	Higher	Faster
SR-57 SB1 (6.531)	Lower	Similar	Slower	Lower	Faster
SR-55 SB2 (10.822)	Similar	Similar	Slower	Similar	Faster
SR55 NB2 (11.982)	Similar	Similar	Similar	Similar	Similar

Table 15. Summary of Traffic Flow Performance after the Conversion at a Mainline Detector Station Located within an Ingress/Egress Area before Conversion

	Formulation			Dissipation	
Site (VDS postmile)	Critical Occupancy	Critical Volume	Shockwave Speed	Critical Volume	Shockwave Speed
SR-55 SB1 (14.582)	Similar	Higher	Faster	Higher	Faster
SR-57 SB1 (6.671)	Lower	Similar	Slower	Lower	Faster
SR-55 SB2 (9.19)	Similar	Similar	Faster	Similar	Faster
SR55 NB2 (9.41)	Similar	Similar	Similar	Similar	Faster

6.4 Site Specific Analysis

A major finding of this analysis is that conversion of HOV lanes to continuous-access operation yields site-specific operational outcomes. As described earlier, the two sites, SR-55 SB1 and SR-57 SB1, have completely different performance profiles after HOV lane conversion. Here, we further analyze the reasons of different performance from the site-specific perspectives.

6.4.1 Geometry and Traffic Flow Pattern

For SR-55 SB1, HOV lane conversion to continuous-access operation improved freeway performance, largely because of higher critical volume post- conversion.

The critical occupancy and volume for VDS at postmile 13.492 increased significantly, as shown in Table 8 and Table 9. The increase of critical occupancy implies higher density at the location. In other words, HOV lane conversion shifts the high-density downstream. This shift is understandable since the continuous-access HOV lane facility provides more flexibility for HOV drivers. This can be further analyzed from the perspective of roadway geometry. Figure 64 illustrates the HOV lane configuration before and after the conversion. Before the conversion, all HOV vehicles going to SR-22 (Garden Grove freeway) were required to exit the HOV lane within the ingress/egress area. After HOV lane conversion to continuous-access, HOV vehicles can now utilize the available space for their lane changes. The increase of the critical occupancy and volume at postmile 13.492 may be caused by last-minute lane-changes of some HOV vehicles at this location.

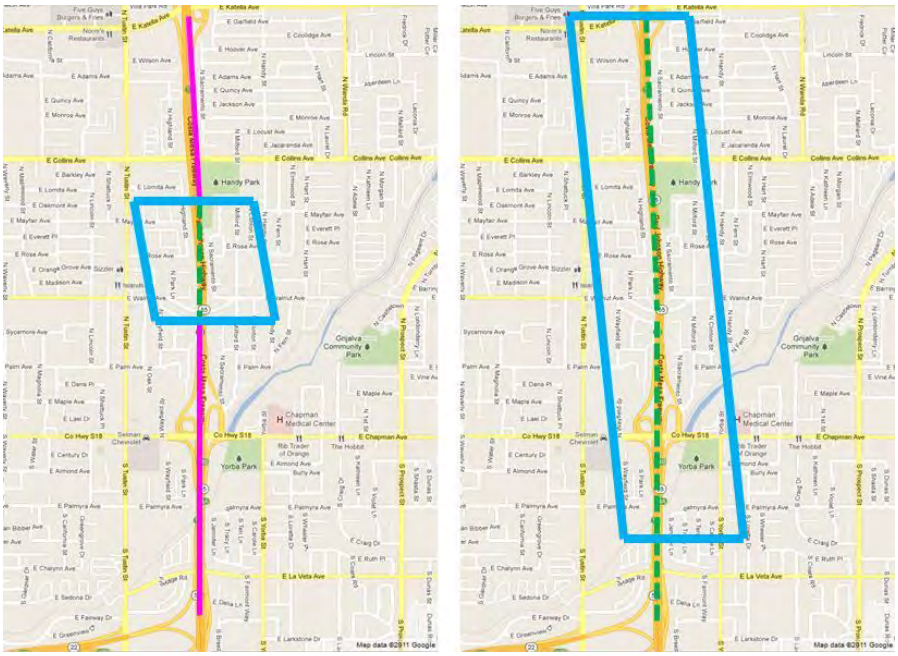

Figure 64. SR-55 SB1: HOV Lane Configuration before (Left) and after (Right) the Conversion

For SR-57 SB1, conversion of the HOV lane to continuous-access operation worsened freeway performance, primarily because of lower critical volume and critical occupancy post- conversion.

We further analyzed the roadway geometry of the SR-57 site. We noted that VDS at postmile 6.531 as the key location within the merging area of the Nutwood on-ramp and downstream at the Chapman on-ramp. The merging flows from these two on-ramps are approximately 1250 vehicles per hour. There is a guide sign located downstream of the VDS, as shown in Figure 65. The HOV lane conversion to continuous-access, as shown in Figure 66, might have made this location more vulnerable to congestion because of the potential increase of lane-changing activities.

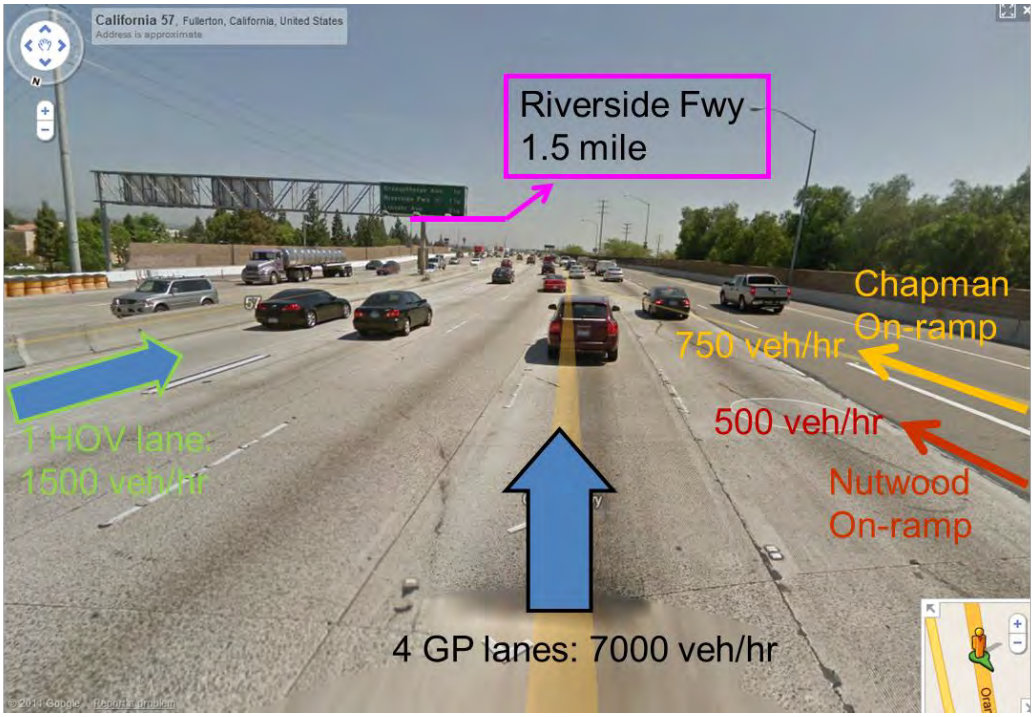

Figure 65. Geometry, Sign, and Traffic Flows around Postmile 6.531 of the SR-57 SB1 Site

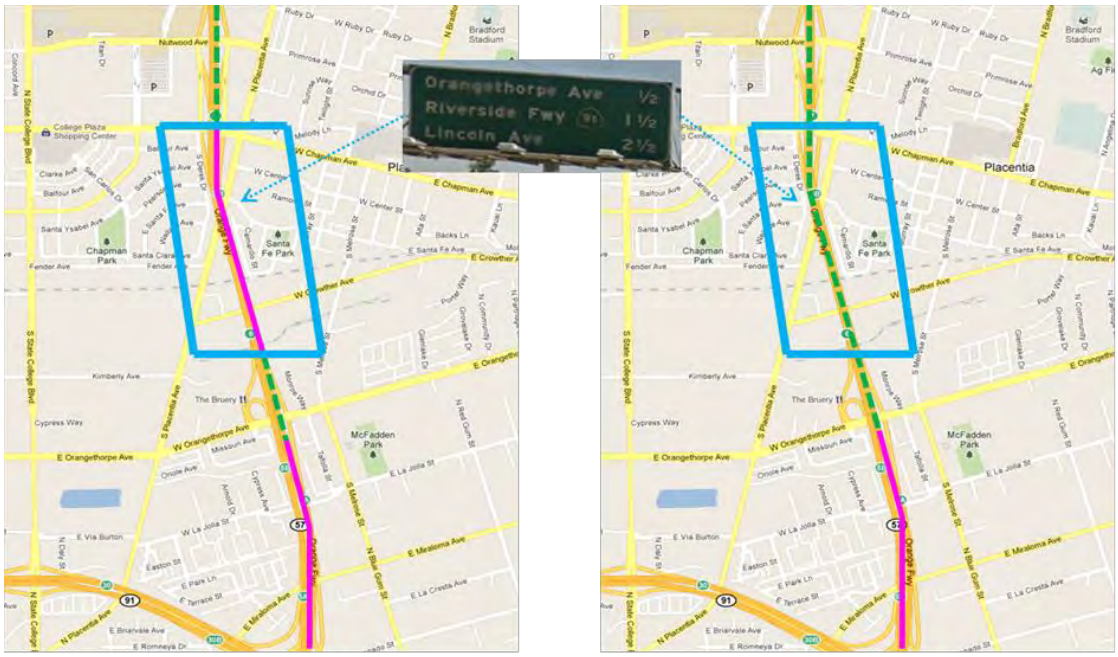

Figure 66. SR-57 SB1: Geometry around the Key Location of the Site (Postmile 6.531)

6.4.2 Interchange Spacing

The evaluation results show that the conversion of HOV lane from limited-access to continuous-access improves the performance along the SR-55 SB1 site but does not improve the performance along the SR-57 SB1 site. A further analysis of freeway geometry found that the SR-55 SB1 site has longer interchange spacing and thus more available space for traffic merging and diverging than the SR-57 SB1 site, as shown in Table 16.

Table 16. Interchange Spacing for SR-55 SB1 and SR-57 SB1 Sites

	SR-55 SB1 Site		**SR-57 SB1 Site**	
Section	Lincoln on - Katella Off	Katella On - Chapman Off	Yorba Linda On - Nutwood Off	Nutwood / Chapman On - Orangewood Off
Length (mile)	1.11	1.09	0.57	0.72

6.4.3 HOV Violation

The continuous-access HOV facility has a higher vehicle occupancy violation rate than the limited-access HOV facility. Caltrans District 12 has collected data on vehicle occupancy violations in the SR-55 SB1 site. Table 17 compares the average number of HOV violators and average violation rates at Walnut St. (postmile 14.382) along SR-55 before and after HOV lane conversion. The "before" HOV violation data were collected on May 16, 2007 and April 9, 2008. The "after" HOV violation data were collected on five days: October 29, 2008, November 5, 2008, December 12, 2008, February 12, 2009, and May 12, 2009. We found that the "after" HOV violations had a great deal of variance. Thus, we excluded those days with the highest and lowest violators and used the remaining three days' worth of data in the analysis. We found that HOV lane violation rates increased after conversion to continuous-access.

Table 17. Comparison of Violation Rates Before and After the HOV Lane Conversion

	Before: Limited-access			**After: Continuous-access**		
	# of Violators	Total HOV vehicles	Violation Rate	# of Violators	Total HOV vehicles	Violation Rate
SB AM	28.0	2530.5	1.11%	55.3	3089.3	1.79%
NB PM	1.5	2597.0	0.06%	55.0	2957.0	1.86%

6.5 HOV Lane Changing Rates

We collected aerial data for one site with limited-access HOV configuration and one site with continuous-access HOV configuration. The site with limited-access HOV configuration is a 1.13-mile long section along SR-57 northbound, starting from the South St. overpass (located south of the Lincoln interchange) to the SR-91 westbound off-ramp, as shown in Figure 67. The site with continuous-access HOV configuration is a 1-mile long section along SR-55 northbound, starting from the Main St. interchange to the 17th St. off-ramp, as shown in Figure 67. Data for the SR-57 site were collected from 4:10 p.m. to 4:35 p.m. on May 11, 2011. The data for the SR-55 site were collected from 4:00 p.m. to 4:20 p.m. on May 22, 2012.

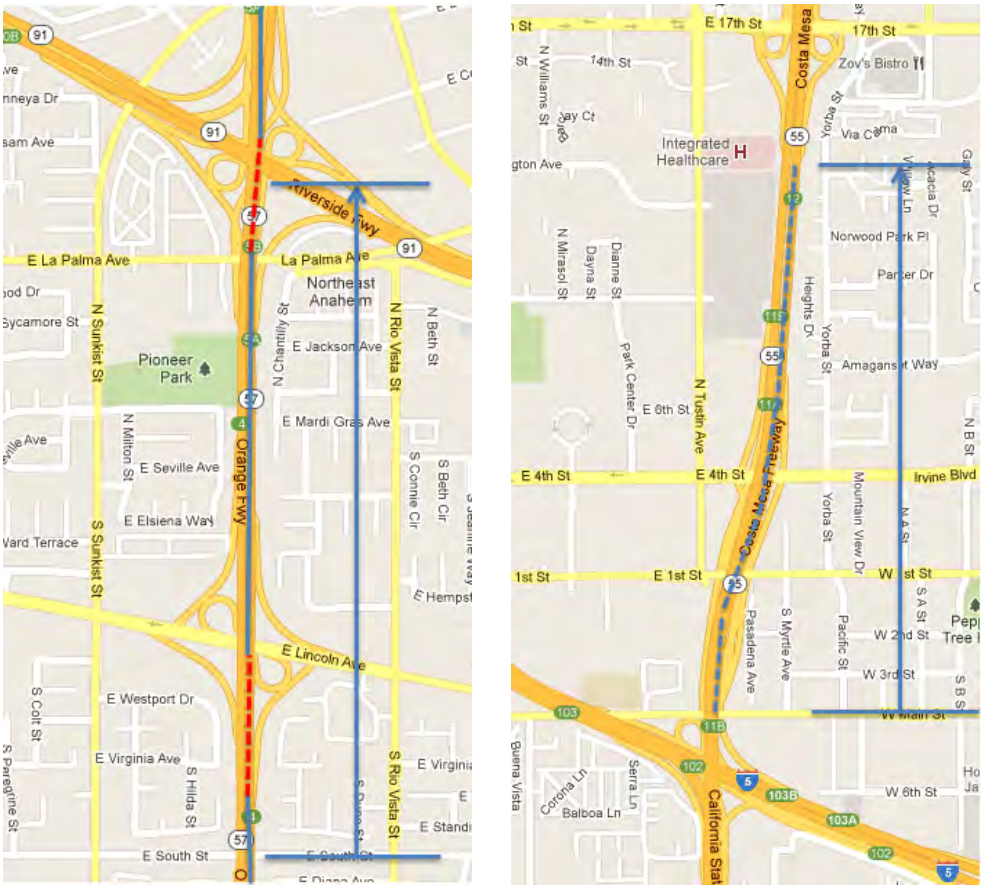

Figure 67. SR-57 (Left) and SR-55 (Right) Aerial Data Collection Sites

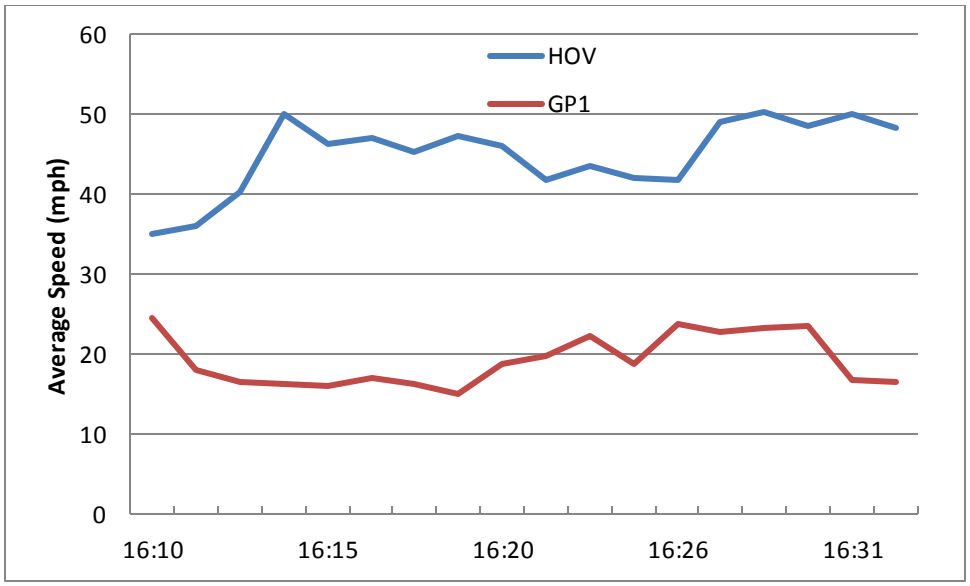

(a) SR-57 Site

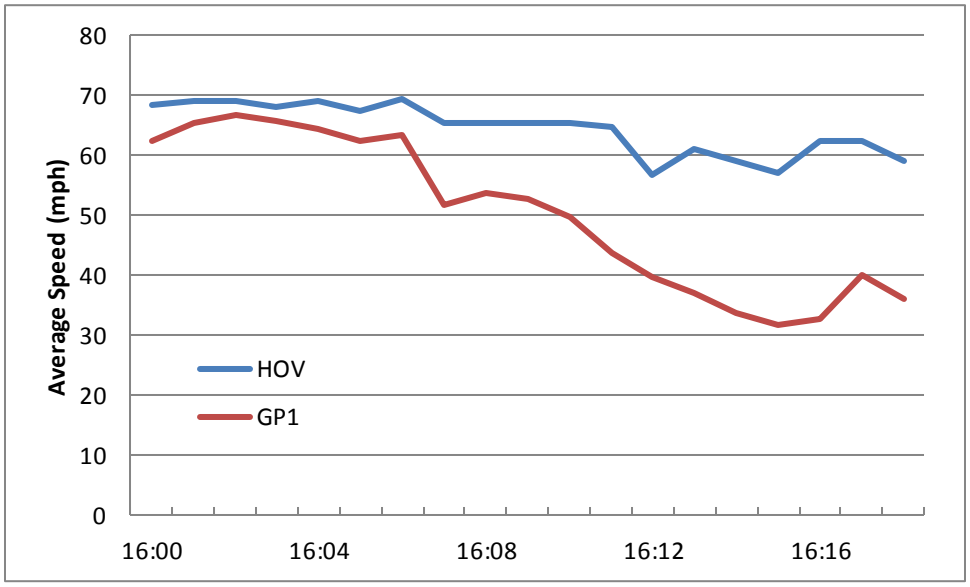

(b) SR-55 Site

Figure 68. Comparison of Speeds on HOV Lane and the Adjacent GP Lane

Both sites had different traffic conditions during the data collection periods. SR-57 was more congested than SR-55. Figure 68 shows the average speeds on the HOV lane and the adjacent GP lane for SR-57 and SR-55. Figure 69 shows the speed box plots on lanes 1 to 5 on both sites.

We tracked all vehicles in both sites during the study period. There were 21 and 18 minutes of fully processed data for SR-57 and SR55 sites, respectively. Because the operating speeds were

different on both sites, we compared the HOV lane changing rate in terms of speed differential bins (HOV lane speed – GP lane speed). Here, HOV lane changing rate is defined as follows:

HOV lane changing rate = number of lane changes of HOV vehicles / HOV vehicles' VMT

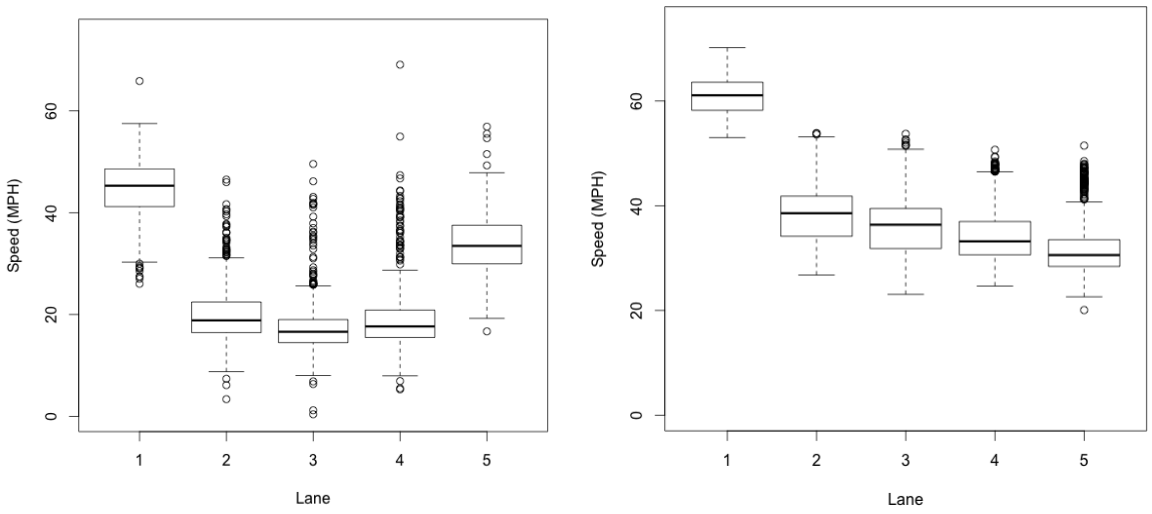

Figure 69. Speed Box Plots on Different Lanes for SR-57 (Left) and SR-55 (Right)

The HOV vehicles refer to those vehicles that use the HOV lane for at least 1 second within the entire study period (21 minutes for SR-57 and 18 minutes for SR-55). When calculating the number of lane changes, a lane change from one to another was recorded as one lane change. Here are some different situations:

- A vehicle from an on-ramp needs to change lanes four times (from lane 5 to lane 4, 4 to 3, 3 to 2, and 2 to 1) to enter the HOV lane of a freeway with four GP lanes and one HOV lane.
- Similarly, a vehicle on an HOV lane needs to change lanes four times in order to exit on the off-ramp located on the rightmost side of the freeway with four GP lanes and one HOV lane.
- Also, some HOV vehicles may change lanes back and forth. For example, a HOV vehicle may change from lane 1 to lane 2 and then back to lane 1. In this situation, two lane changes were recorded.

The meaning of the HOV lane changing rate is the average number of lane changes for a vehicle traveling on the HOV lane. Figure 70 compares the HOV lane changing rate various speed differential categories for both SR-57 (limited-access) and SR-55 (continuous-access) sites.

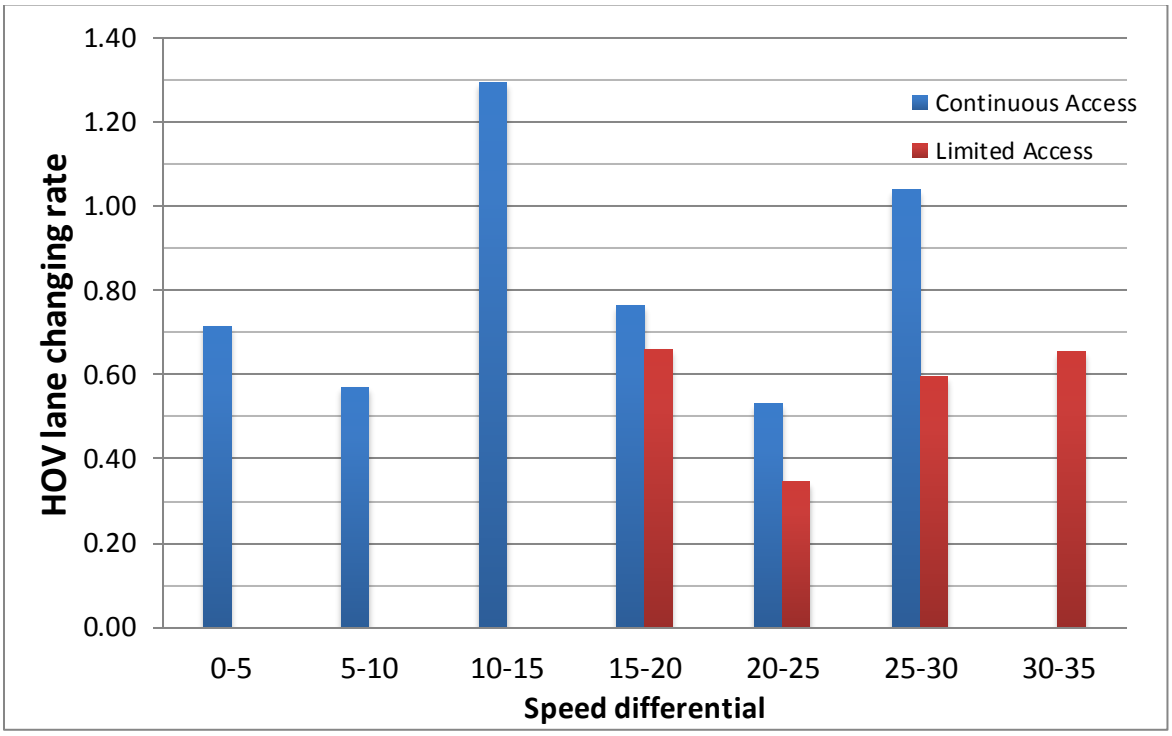

Figure 70. Comparison of Lane Changes to HOV Lane for Different Speed Differential

Since the SR-57 site was congested from the beginning of data collection, we could not obtain data points with speed differentials smaller than 15 mph. Because the SR-55 site was free-flow at the beginning and then began to become congested; hence we were able to obtain data points with various speed differentials except for the 30-35 mph category. The continuous-access HOV facility showed a higher HOV lane changing rate than the limited-access HOV facility. The SR-55 (continuous-access) site has 15%, 54% and 74% more lane changes than the SR-57 site under the 15-20, 20-25, and 25-30 speed differential bins, respectively. In total, SR-55 has 48% more HOV related lane changes.

Although the HOV lane changing rate along the SR-57 freeway is lower, most lane changes occurred within the 430-ft long ingress/egress area and thus the intensity of lane changes is much higher. While, the HOV lane changing rate along the SR-55 freeway is higher, these lane changes are spread out along the whole stretch of the study freeway.

6.6 Summary of Performance Comparison

Based on the performance evaluation of five sites in Orange County, where HOV lanes have been converted from limited-access to continuous-access operation, we found:

- The performance after the conversion of HOV lanes from limited-access to continuous-access operation is site-specific and influenced by local geometric attributes and associated traffic patterns.
- Except for the SR-55 SB1 site, the continuous-access HOV facility has slightly lower throughputs at most detector stations in every other study sites.
- The conversion of a HOV lane from limited-access to continuous-access leads to a faster shockwave speed on GP lanes during the dissipation phase, which means the queue can be dissipated at a faster speed at the end of traffic congestion. In other words, a freeway with continuous-access would see congestion clear up faster.
- Continuous-access HOV facility is more susceptible to higher violation rate than limited-access, as observed on SR-55.
- The continuous-access HOV facility has a higher HOV lane changing rate. The limited-access HOV facility has a higher HOV lane changing intensity within the ingress/egress areas.

For future research, we feel that the analysis of geometry and traffic flow performance at bottleneck locations may help determine which type of HOV lane facility is more appropriate for a freeway corridor. A combination of both HOV lane access types in a freeway corridor may help improve the freeway performance. More research to clarify the relationship between merging and diverging intensity and its effect on freeway performance is needed.

In the next chapter, we will focus on the evaluation of limited- and continuous-access HOV facilities based on microsimulation.

7. Micro-simulation Evaluation

7.1 Introduction

7.1.1 Travel Demand Forecasting and Traffic Simulation

Travel demand modeling is a four-step method widely used by Metropolitan Planning Organizations (MPOs) for various planning studies, such as travel demand forecasting, traffic impact assessment, transit ridership estimation, and roadway improvements. The approach is not appropriate for traffic operation analysis because the static assignments in travel demand modeling typically use Bureau of Public Roads (BPR) type link performance functions. These functions assume a monotonic relationship between traffic flow and travel time. As traffic flow approaches roadway capacity, speed asymptotically drops to zero. Although the assumption greatly eases problem solving, it falls short in reflecting true traffic dynamics, especially under congested traffic conditions.

Compared to the traditional travel demand modeling approach, traffic simulation attempts to improve the accuracy of mathematical models by modeling traffic flow dynamics. Traffic simulation models can be classified into three types: macroscopic, mesoscopic, and microscopic.

- *Macroscopic simulation* is able to handle relatively large networks with less details and fast simulation speed. Macroscopic simulation uses an analytical traffic flow model that may describe the relationship between volume and delay or between volume and speed. Most popular macrosimulation models have been developed for specific applications. For example, FREQ has been employed to evaluate ramp metering, priority lane, and operational improvement strategies along freeways. Transyt and Synchro have been used for optimizing signal timing along arterials.

- *Mesoscopic simulation* can model with more detail than macro-simulation models but with slower simulation speed. Mesoscopic models simulate traffic flow as groups of vehicles called *traffic cells* and *streams*. The traffic flow model in mesoscopic simulations is either a speed-density, volume-density, volume-occupancy curve or cell transmission model. Individual vehicles are modeled for their route choices. Existing

mesoscopic models, such as DYNASMART, DYNAMIT, Dynameq, and VISTA, were originally developed by university researchers and are still in their early stages.

- *Microscopic simulation* is able to model most aspects of a traffic system, including individual drivers, vehicles, and various roadway facilities. However, the size of the network with which microscopic simulation can deal with is relatively small and simulation speed is slow. Microscopic simulation relies on car-following logic, lane changing and gap acceptance rules to model the behavior of individual vehicles in a traffic network. Interactions between vehicles at intersections are modeled by right-of-way, gap-acceptance, and traffic control logic. In microscopic simulation, vehicles are modeled with varying characteristics and multiple classes. Variability in driver behavior is explicitly modeled. In addition, microscopic simulation usually has 3-D animation capabilities, which can make public presentations more attractive. Examples of microscopic simulation models are AIMSUN, Paramics, TransModeler, and VISSIM.

Among these three types of traffic simulation models, microscopic simulation models are more mature and more commercially available. With the advancement of computer technologies and traffic modeling capabilities, microscopic simulation has become an increasingly popular and effective tool for analyzing a wide variety of dynamic problems not amenable to study by other means. Microscopic traffic simulation emulates traffic systems at a level that includes detailed specification of roads, individual drivers and vehicles. Microscopic simulation has many applications, including ITS evaluation (Chu, Liu, & Recker, 2004), TMC operator training (Chu, Gerfen, & Recker, TMC Simulator for Operator Training Using Micro-Simulation, 2008), construction management (Chu, Kim, Liu, & Recker, 2005), operational improvement for emission reduction (K.S.Nesamani, Chu, Mike, & Jayakrishan, 2007), corridor management planning (Ban, Chu, & Benouar, 2008), traffic control studies (Chu L. , Liu, Recker, & Zhang, 2004) (Liu H., 2001), and policy investigations (Breiland, Chu, & Benouar, 2006). Similar to planning studies, microscopic simulation can guarantee that the same demand pattern is applied both before and after the deployment of a policy in order to provide an objective evaluation. However, the limitation of the approach is that evaluation results may be influenced by theoretical limitations of the base traffic models.

For this specific study, the use of of microscopic simulation to evaluate different HOV lane configurations is more appropriate because it more effectively captures traffic flow dynamics and provides more details of vehicle-to-vehicle interactions than both mesoscopic and macroscopic traffic simulation models.

7.1.2 HOV Modeling in Microscopic Simulation Models

The top three micro-simulation models currently available are Paramics, TransModeler, and Vissim. Table 18 summarizes and compares the HOV modeling capabilities of these three microscopic simulation packages. This evaluation draws upon information from user manuals, discussions with software developers, and our previous knowledge and experience with these software packages.

Table 18. Comparison of HOV lane and HOV driver modeling capabilities

	Paramics	**TransModeler**	**Vissim**
HOV Vehicles / Demand	• Defines particular vehicle types as HOV vehicles. • User can have a demand matrix to include both SOV and HOV vehicles, or have a demand matrix for HOV.	TransModeler has a "vehicle occupant" parameter for each vehicle, as a way to simulate HOV eligibility. There are two methods to model HOV vehicles. • User can associate a matrix with HOV 2+ or 3+. • If a matrix is not associated with HOV 2+ or 3+, the occupancy of a vehicle is determined randomly based on the corresponding vehicle type, which has three occupancy related parameters: mean, variance, and max.	• Defines particular vehicle types as HOV vehicles; or • Creates multiple matrices for Vissim simulation
HOV Facility	• Applies a "HOV restriction" that permits only HOV vehicles on HOV lanes or HOV links • HOV lanes can be coded as part of lanes of a multiple-lane link or a separate link if there is a hard barrier between HOV	• Defines certain lanes' lane use to be HOV 2+ or 3+. • HOV lanes are usually coded together with general purpose (GP) lanes. User needs to define the lane changing rule between HOV lanes and GP lanes: (1) a barrier between them; (2) allow or prohibit traffic from HOV to GP lanes, or (3) allow or prohibit traffic from GP to HOV	• Uses "lane closure" on a certain lane to restrict certain vehicle types • Creates an "independent" link to represent HOV lane and access

	and GP lanes. The lane changing rule from or to HOV lanes can't be modeled directly. • HOV lanes can be modeled to be part time by defining time-dependent links.	lanes. • HOV lanes can be set up as part-time HOV lanes through adding an access management rule, which allows user to associate a time-of-day schedule of HOV lane operation. • User can add a HOV sign but it is just used for visualization.	
HOV Behavior	• No exclusive HOV behavior is provided by Paramics. HOV vehicles just have more lanes to use than other types of vehicles. There is no incentive for HOV vehicles to use HOV lanes. • One plugin from Quadstone to force HOV drivers to use HOV lanes. It doesn't model HOV drivers' lane selection behavior but simply forces HOV drivers to use HOV lanes. • If HOV lane is modeled as a separate link, corresponding to the buffer-separate HOV facility, HOV lane selection can be realized through HOV drivers' route choice decision.	• There are two levels of HOV driver behaviors, route choice and lane choice level. (1) From the route choice level, HOV vehicles tend to select a path with HOV lanes. The path-size logit probabilistic route choice model is used in the process. (2) The default model is recommended and it considers many factors in the lane choice process. For HOV vehicles, the use of HOV lanes depends on whether or not HOV lanes are connected with the prospective lane with respect to its path;higher speeds on HOV lanes have positive impacts on HOV lane selection. A multinomial logit model is used to calculate the probability of selecting HOV lanes. • Like the reaworld, a single occupancy vehicle may violate the HOV lane use rule, which has a compliance rate. It can be set up as a global or a local parameter.	• No exclusive HOV behavior is provided by Vissim •HOV vehicles have fixed paths, which can be generated from Vissim. • For "independent" link, the access point controls the interaction of general vehicle and HOV vehicles.

We found that TransModeler is more sensitive to HOV driver behavior than Paramics or Vissim. However, a key issue with TransModeler is that it is unable to replicate the realistic volume-occupancy curve along the freeway based on TransModeler version 2.5 Build 980, which was the

software version when we performed this software comparison. This issue led us to reject the use of TransModeler for our analysis.

Paramics (Paramics 6.7) and Vissim (Vissim 5.1) have similar HOV lane modeling capabilities. Both allow each individual vehicle type to have its own driver behavior parameters. Paramics is superior to Vissim in five ways:

- Driver behavior in Paramics is more realistic since its volume-occupancy curve looks more similar to those found in real-world data.
- Paramics is designed to do Origin Destination (OD) based simulation and have full information about each individual vehicle. Vissim was originally used to do path-based simulation and does not give users the origin and destination of any vehicle in the simulation.
- Vehicles in Paramics can change their travel paths (either HOV lane or GP lanes) enroute, similar to driver behavior in the real world. While, Vissim locks in the vehicles' paths when vehicles are released to the network. A HOV vehicle that is assigned to the HOV route will not change its path even though there are benefits to switching to the GP lane.
- Paramics (after version 6.9) allows lane-based driver behavior, which is useful for modeling a freeway with both GP lanes and a continuous-access HOV lane.
- Vissim must remove stuck vehicles to make the model perform; this is not the case for a calibrated Paramics model.
- Paramics has strong Application Program Interface (API) capabilities enabling users to implement better HOV driver behavior through their own codes.

Both Paramics and Vissim have limitations on modeling continuous-access HOV lane facilities. Paramics requires a HOV plugin to push HOV vehicles to use HOV lanes whether or not there is traffic congestion along the GP lanes. This is not realistic. Vissim seems to suffer from similar issues but the research team could not confirm this because of lack of continuous-access HOV modeling experience with the software.

Based on this review, we chose the Paramics for our analysis.

7.2 Study Site and the Existing Model

7.2.1 Study Site

The study site, SR-57, is a major north-south corridor connecting Orange County and Los Angeles County and is one of the most congested freeways in California. The corridor has four to five GP lanes and one full-time HOV lane. The freeway corridor serves most daily commuters traveling southbound to Orange County during the morning and returning to LA County during the afternoon. The study portion of the SR-57 corridor extends from the Orange County line in the north through the end of SR-22 in the south (including the SR-22/I-5 interchange). The total length is about 12 miles.

7.2.2 Existing Simulation Model

Figure 71 shows the SR-57 corridor in Google Map alongside the SR-57 Paramics model. The SR-57 model was developed under Paramics version 6.6.1 and well-calibrated through the SR-57 Orange County Corridor System Management Plan (CSMP) project.

The SR-57 Paramics model covers the entire extent of freeway mainline, ramps, freeway-to-freeway connectors, ramp terminal intersections, as well as adjacent arterial intersections along the service interchanges. Inclusion of freeway connectors with SR-91, I-5 and SR-22 enables the consideration of traffic queuing effects from connecting freeways. The model includes a total of 63 signalized intersections and 38 ramp meters emulated using the Semi-Actuated Traffic Metering System (SATMS) plug-in.

SR-57's HOV lane was a full-time limited-access facility in the model base year (2007). HOV vehicles can only enter or exit the HOV lane within ingress/egress areas, typically set apart every one to two miles. In the model, the HOV lane is modeled as a separate link parallel to the GP link. The ingress/egress area is modeled as a link with both GP lanes and an HOV lane. For HOV vehicles, HOV lane selection in the model is a route choice problem instead of a lane choice problem. Model assumptions include:

(1) Some HOV drivers prefer the use of HOV lanes, which is controlled through a stochastic assignment route choice model. The HOV lane is set to have lower cost factor as a way to attract HOV vehicles.

(2) Other HOV drivers choose whether or not to use the HOV lane based on traffic conditions. This is controlled through the dynamic feedback assignment route choice model. The parameter for dynamic feedback assignment is familiarity. Only familiar drivers are able to select either the HOV lane or GP lanes based on traffic conditions.

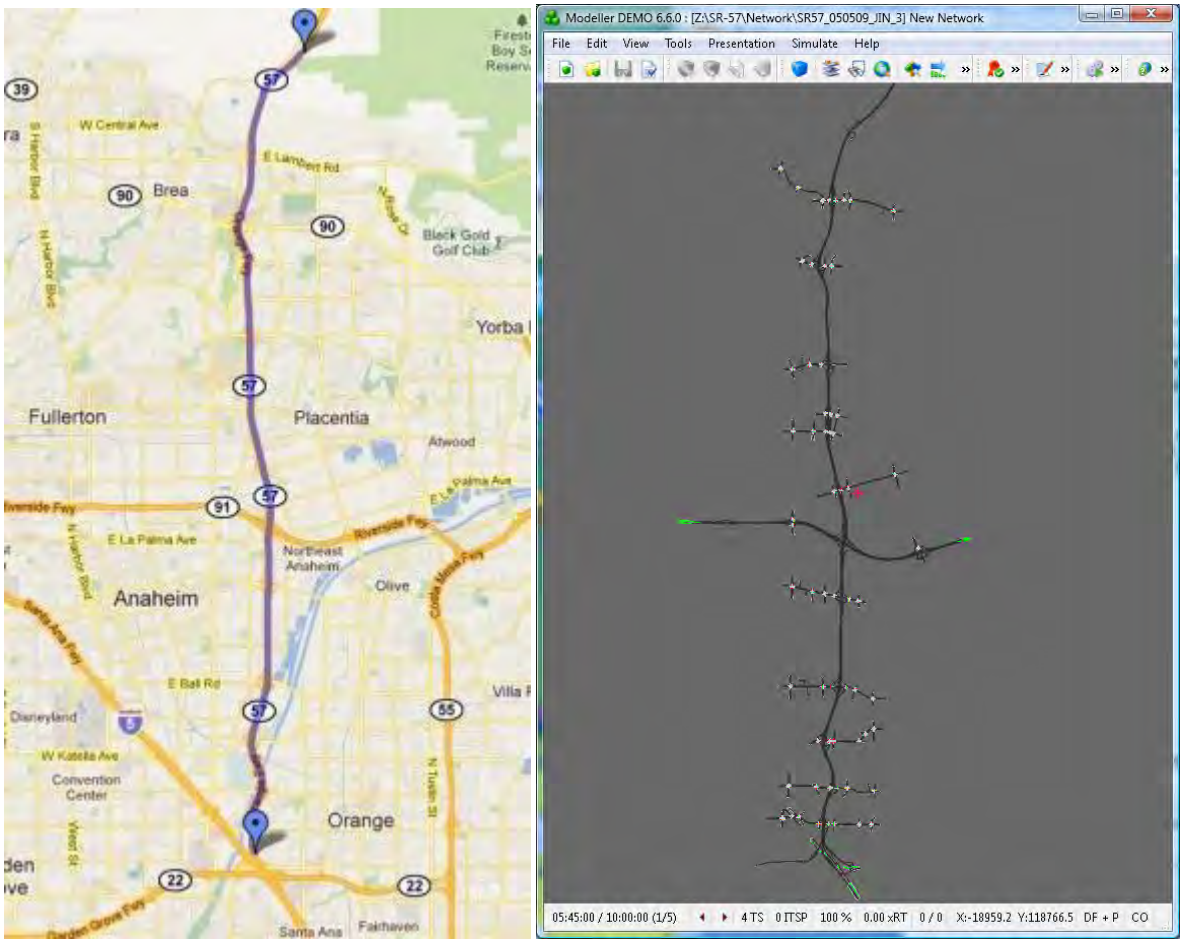

Figure 71. The SR-57 corridor (Source: Google Map) and its Paramics model

Paramics has three route choice models. These are: all-or-nothing assignment, stochastic assignment and dynamic feedback assignment.

- *All-or-nothing assignment* assumes that there is only one path from an origin to a destination and that this path has the lowest cost. The familiarity settings for each type of vehicle are indirect parameters of the method. The definition of generalized cost function is the key to the method.

- *Stochastic assignment* in Paramics assumes that different drivers perceive different costs from a decision node to the destination. The perceived cost is calculated based on the given perturbation factor with a random number assigned to the vehicle, and the shortest perceived route is chosen at the decision node. The parameter of the method includes perturbation of each vehicle type. The familiarity settings for each type of vehicle are indirect parameters of the method.

- The dynamic feedback assignment routing method assumes that travelers select a route based on instantaneous traffic information. It has two parameters—feedback period and compliance rate or the familiarity parameter. The dynamic feedback routing method updates link costs at a certain feedback period. Then, a certain percentage of travelers determined by the compliance rate are regarded as familiar drivers and can change paths en-route.

The SR-57 model uses all three route choices in order to properly model the route choice behaviors of various vehicle/driver types.

- Trucks: All-or-nothing
- Unfamiliar HOV: Stochastic assignment
- Familiar HOV: Dynamic assignment
- Unfamiliar SOV: Stochastic assignment
- Familiar SOV: Dynamic assignment

The model covers the morning period from 6:00 a.m. to 10:00 a.m. and the afternoon/evening period from 2:00 p.m. to 8:00 p.m. in order to cover all periods of congested travel. The model has a total of 122 zones. Each simulation hour has one demand file, which includes one SOV demand matrix and one HOV demand matrix. Some demand profiles are used to dynamically load the demands during simulation.

The model was calibrated against volume, speed and travel time data collected in Year 2007/2008 based on FHWA microsimulation model calibration guidelines. Freeway traffic data were collected from September 4, 2007 – November 15, 2007 through PeMS and arterial turning data were collected in late October and early November of 2008. The calibrated model is able to

capture how and when each bottleneck occurs, the length and severity of freeway queues associated with each bottleneck, and the time it takes for each queue to dissipate.

7.2.3 Limitations on Modeling Limited-access and Continuous-access HOV Lanes

The SR-57 model was calibrated under Paramics version 6.6.1. Further analysis found that the version of the software has the following issues for continuous-access HOV lane modeling:

- There is a nextlane bug (Quadstone reference number 1419), which causes some vehicles to get stuck at the rightmost lane if the rightmost lane is a lane dedicated to the off-ramp and the leftmost lane is an HOV lane. The temporary solution is to use a plug-in to remove the vehicles when they are stuck for a few seconds, typically 10 sec.
- Paramics has two major driver behavior parameters, headway and reaction time. These two parameters are link-based (After Paramics version 6.7, they are both vehicle-type and link-based parameters). The way to calibrate a model in Paramics is to adjust these two driver behavior parameters in order to match the observed capacities along GP lanes and HOV lanes. Since HOV lanes are observed to have lower capacity than GP lanes, GP lanes' driver behavior parameters are different than those of the HOV lanes. For a Paramics network with limited-access HOV configuration, such as the SR-57 network, the GP lane links have lower headway and reaction time settings than the HOV lane links in order to achieve higher capacity. However, when the calibrated model was modified to represent the continuous-access HOV configuration, both GP lanes and HOV lanes have to share the same headway and reaction time settings. Thus, the SR-57 Paramics network with continuous-access HOV configuration has higher capacity.

Both issues were solved under Paramics V6.7 and later. However, based on a few simulation runs, we found that that the use of Paramics version 6.7 to run the model makes it perform in a totally different manner. Since updating the model would be costly and is out of the scope of this project, we decided to use Paramics 6.6.1 for the study.

7.3 Comparison of Limited-access and Continuous-access HOV Lane Configurations

This study uses the SR-57 AM model to compare the performance of the limited-access HOV lane configuration (existing scenario) versus the continuous-access HOV lane configuration (alternative scenario). The comparison was only applied to the southbound lanes because their morning congestion levels warrant that HOV commuters will benefit from using the HOV lane. The northbound lanes did not show much congestion in the morning peak periods under the existing scenario and thus was not considered in the analysis.

Our study focused on a comparison of the following performance measures related to vehicle dynamics:

- Speed difference on GP lanes versus HOV lane
- Density difference on GP lanes versus HOV lane
- Flow difference on GP lanes versus HOV lane
- Total number of lane changes

These performance measures were collected from a plug-in developed using Paramics' Application Programming Interface (API). The plug-in collects these performance measures by segments that can be defined by users. For this study, a segment was defined based on the start and end points of the ingress/egress areas. A segment can be a buffer-separated segment or an ingress/egress segment. As shown below, there are a total of 21 segments, 11 of which are buffer-separated segments and 10 are ingress/egress segments. The naming convention of the segment is Direction_StartLocation_EndLocation for a buffer-separated segment and Direction_Location_gress for an ingress/egress area.

1. SB_Start_Tonner
2. SB_Tonner_gress
3. SB_Tonner_Lambert
4. SB_Lambert_gress
5. SB_Lambert_Imperial
6. SB_Imperial_gress
7. SB_Imperial_south

8. SB_Imperial_south_gress
9. SB_Imperial_Nutwood
10. SB_Nutwood_gress
11. SB_Nutwood_Orangethorpe
12. SB_Orangethorpe_gress
13. SB_Orangethorpe_91
14. SB_91_gress
15. SB_91_Lincoln
16. SB_Lincoln_gress
17. SB_Lincoln_Katella
18. SB_Katella_gress
19. SB_Katella_Orangewood
20. SB_Orangewood_gress
21. SB_Orangewood_57

After collecting performance data from simulations, hourly and average performance of the existing and alternative scenarios were compared with respect to all buffer-separated areas and all ingress/egress areas.

Figure 72 shows the simulated speed contour maps along the GP lanes and HOV lanes under the two scenarios. A speed contour map was used to show the simulated congestion pattern based on speed data from point detectors placed in the simulation model. In the speed contour map, the X-coordinate represents the time from 6 a.m. to 10 a.m.; the y-coordinate represents the post mile of the freeway (The traffic direction is from bottom to top). The color theme is shown on the bottom of each picture. Green indicates free-flow conditions; red indicates congestion.

We found that congestion along the HOV lane disappeared and congestion along the GP lanes eased under the alternative scenario. As explained earlier, the version of the Paramics simulation software used in our study (version 6.6.1) is not capable of modeling different driver behaviors on GP lanes and the HOV lane under the continuous-access HOV lane case. We found the Paramics model overestimates the throughput for the continuous-access HOV lane facility and thus the simulation results for the alternative scenario are too optimistic to be realistic. As a

result, the speed, flow and density, and their differences between GP lanes and HOV lanes under the continuous-access HOV scenario, as shown in Appendix J, are less trustworthy.

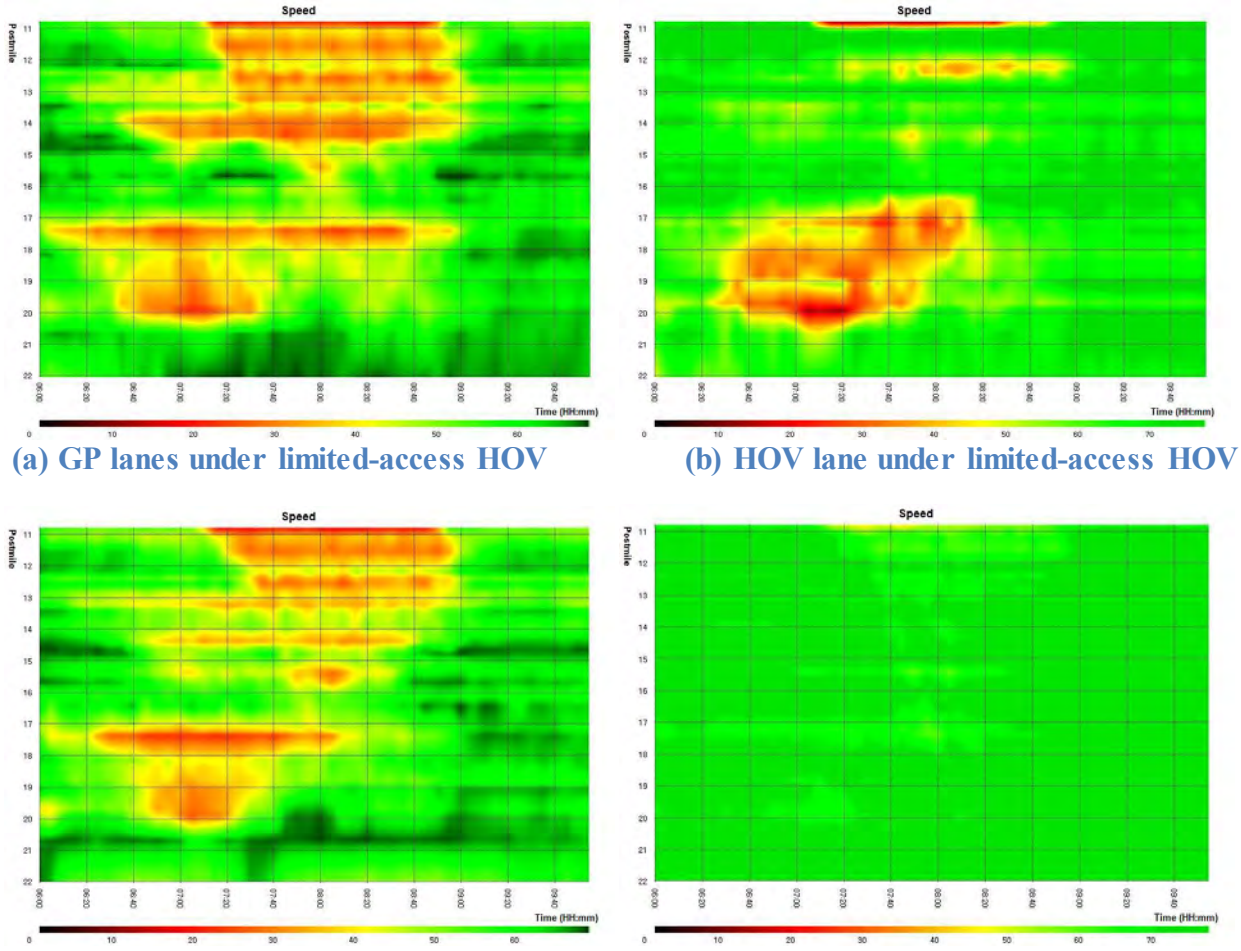

(a) GP lanes under limited-access HOV (b) HOV lane under limited-access HOV

(c) GP lanes under continuous-access HOV (d) HOV lane under continuous-access HOV

Figure 72. Simulated speed contours before and after HOV lane conversion

Although the simulation result of the alternative scenario is optimistic, its total number of lane changes may be meaningful since these types of data are very hard to obtain in the real world. Table 19 compares detailed lane changing data for the existing and alternative scenarios. The lane change data include not only the total number of lane changes, but also the lane changes from a GP lane to another GP lane, from a GP lane to an HOV lane, and from an HOV lane to a GP lane. We found that after the conversion, locations that were previously buffer-separated areas experience an average of 25% increase in lane changes and the ingress/egress areas experience an average of 65% decrease in lane changes. Regarding the total number of lane changes, the continuous-access scenario has about 8% more lane changes, as shown in Table 20.

Table 19. Comparison of number of lane changes for existing and alternative scenarios

Time	Segment Type	Existing (Limited-access)				Alternative (Continuous-access)				Comparison	
		total	GP-GP	GP-HV	HV-GP	total	GP-GP	GP-HV	HV-GP	Total increase	% Increase
6-7 am	Buffer-separated areas	4545	4545	0	0	5814	5242	275	297	1269	28%
	Ingress/egress areas	1097	759	140	199	366	264	52	50	-731	-67%
7-8 am	Buffer-separated areas	5222	5222	0	0	6549	5958	297	294	1327	25%
	Ingress/egress areas	1245	888	159	197	404	286	68	50	-841	-68%
8-9 am	Buffer-separated areas	5132	5132	0	0	6237	5669	275	293	1105	22%
	Ingress/egress areas	1140	825	127	188	415	317	54	44	-726	-64%
9-10 am	Buffer-separated areas	4183	4183	0	0	5335	4845	239	251	1152	28%
	Ingress/egress areas	930	653	118	159	348	253	40	54	-583	-63%
Average	Buffer-separated areas	4770	4770	0	0	5984	5428	271	284	1213	25%
	Ingress/egress areas	1103	781	136	186	383	280	54	49	-720	-65%

Table 20. Comparison of total lane changes for existing and alternative scenarios

	Existing (Limited-access)	Alternative (Continuous-access)	Increase	%Increase
6-7 am	5642	6180	538	10%
7-8 am	6467	6953	486	8%
8-9 am	6272	6651	379	6%
9-10 am	5113	5683	570	11%
Total	23493	25466	1973	8%

7.4 HOV Lane Re-stripe at a Freeway-Freeway Interchange with a HOV-to-HOV Direct Connector

Caltrans District 12 is in the process of converting some HOV lanes from limited-access to continuous-access and needs guidance about HOV lane re-striping around a freeway-freeway interchange where there is a HOV-to-HOV direct connector.

As an example, Figure 73 shows the SR-57/SR-91 interchange in Orange County. There is a HOV-to-HOV direct connector from eastbound SR-91 to northbound SR-57. The HOV connector merges onto the northbound SR-57 HOV lane and then one HOV lane is dropped. Based on detector data in the last quarter of 2007 and 2008, northbound SR-57 is very congested in both the GP lanes and the HOV lane, as illustrated in Figure 74. A major reason for the HOV lane congestion around the CA postmile 16.0 is the extra traffic flow from eastbound SR-91.

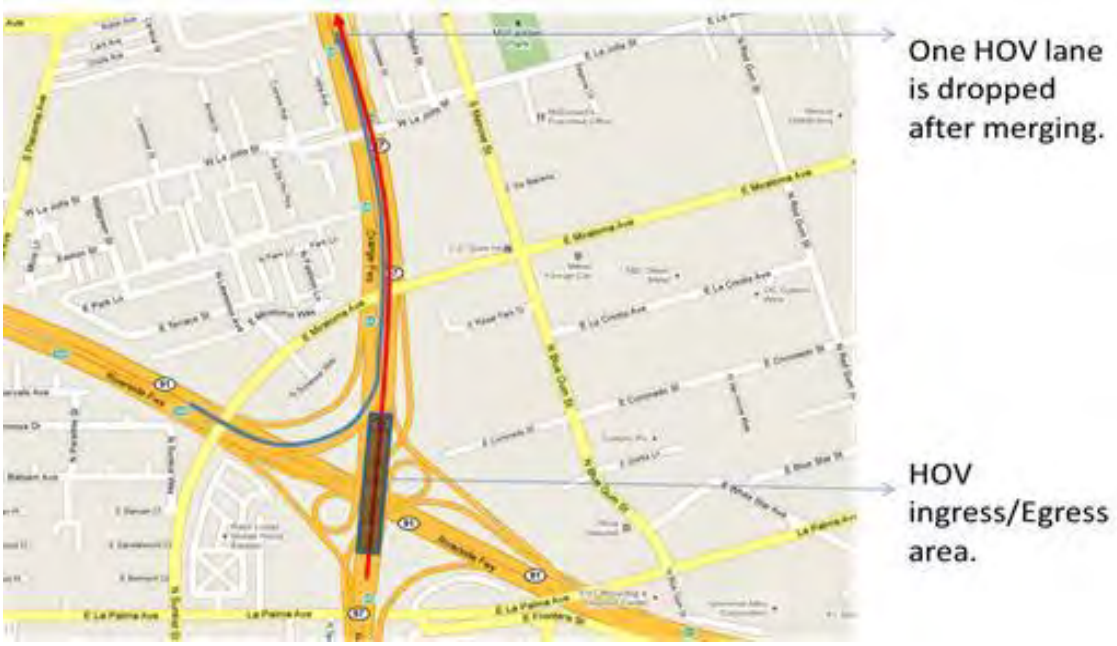

Figure 73. The HOV direct connector and HOV lane stripping at SR-57/SR-91 interchange

Caltrans proposed the following re-stripe guideline, which is graphically explained in Figure 75:

- The HOV lane is re-striped to be continuous-access until 300 ft before the HOV connector.
- The HOV lane remains buffer-separated until the next off-ramp (or 1000 ft downstream from the merging point of the HOV connector)

The question is whether or not the proposed HOV lane re-stripe guideline is operationally appropriate and efficient. We used the calibrated SR-57 PM model to analyze this. There are two simulation scenarios: the existing scenario as shown in Figure 75(a), and the proposed scenario as shown in Figure 75(b).

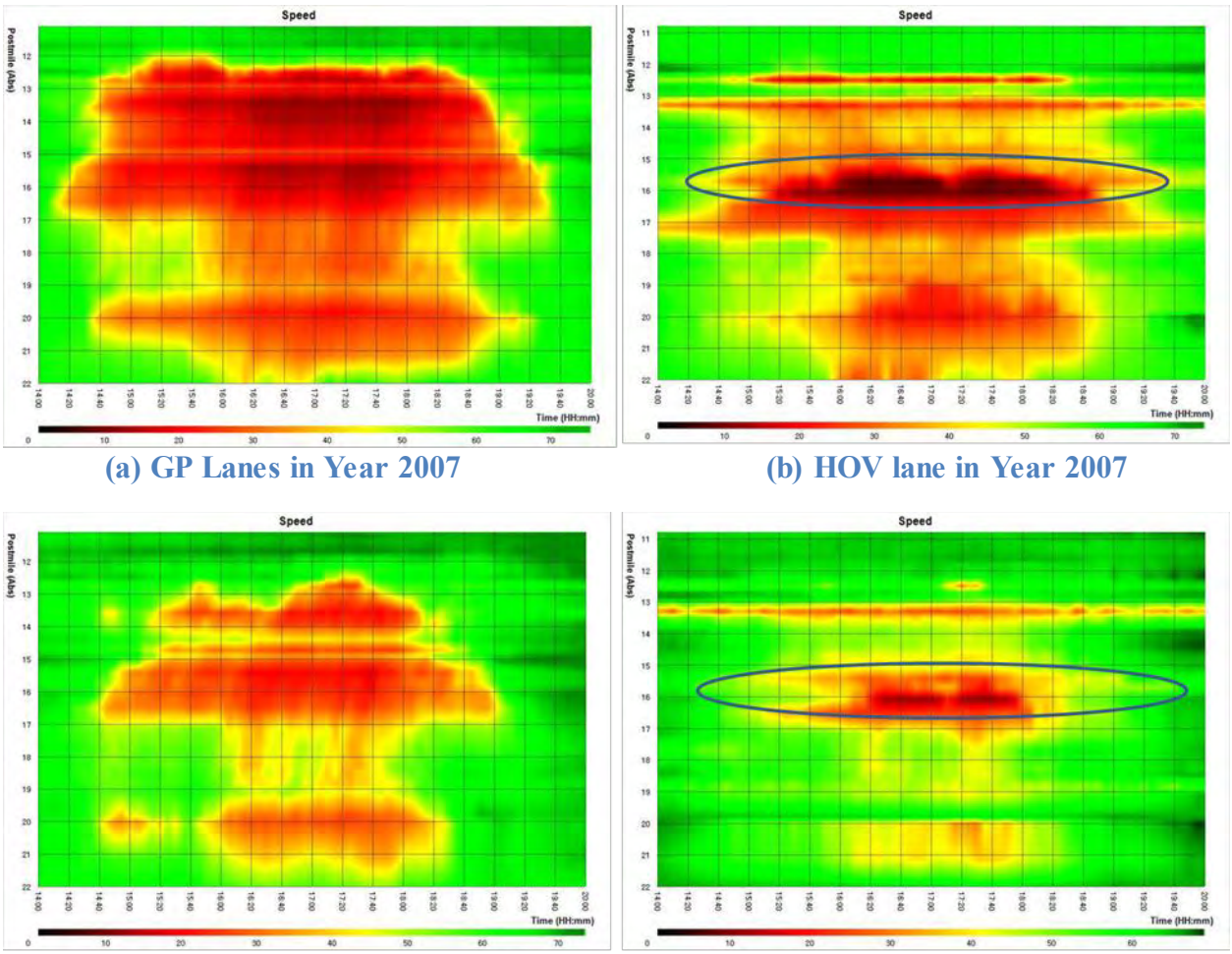

(a) GP Lanes in Year 2007

(b) HOV lane in Year 2007

(c) GP Lanes in Year 2008

(d) HOV lane in Year 2008

Figure 74. Typical traffic congestion pattern for northbound SR-57 in Year 2007 and 2008

Figure 76 compares the simulated speed contour maps on the GP lanes and HOV lane under both scenarios. We found that the proposed scenario has:

- Less congestion at the beginning of the congestion period partially due to the more-utilized HOV lane, as shown in the blue circles.
- More congestion and longer queue during the peak hour, as shown in the black circles.
- A longer congestion period since the queue needs time to dissipate, as shown in the red circles.

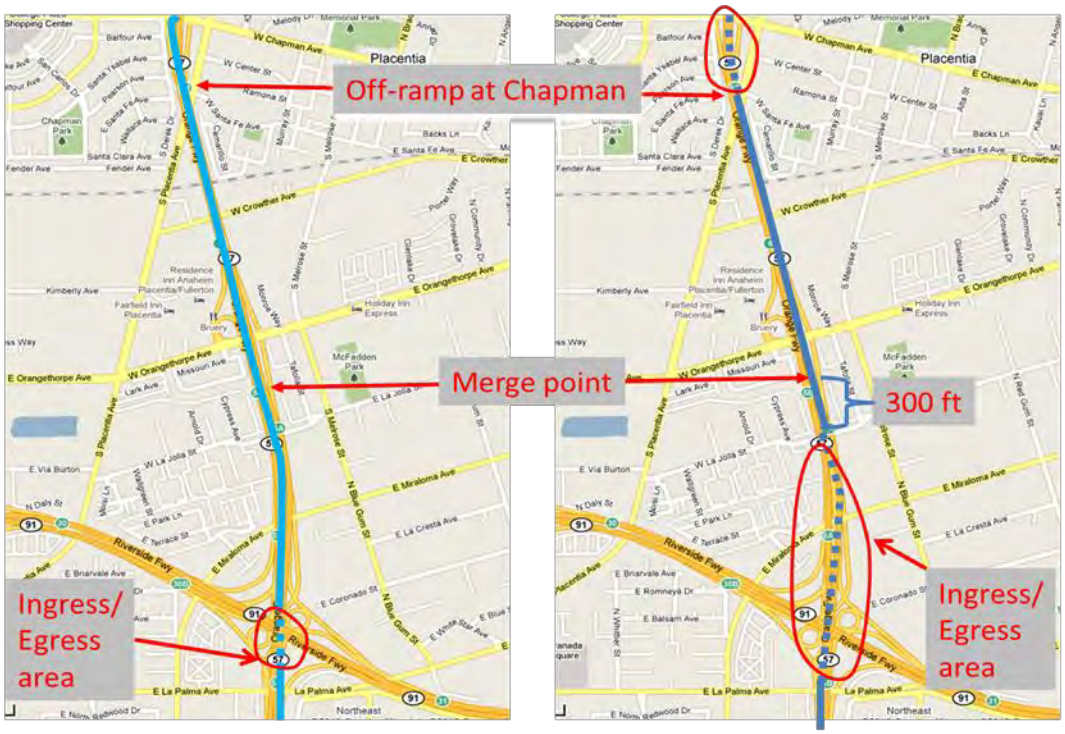

(a) Existing condition (b) Proposed guideline

Figure 75. Proposed HOV lane re-stripe for the interchange with HOV connector

Figure 77 illustrates the average speed contour maps based on five simulation runs. We found that the results of single and multiple runs maintain the same pattern.

Figure 78 compares the total delay from the northbound starting point (SR-22/I-5 interchange) to the Orangethorpe interchange. Consistent with the comparison result of speed contour maps, the total delay for the proposed scenario is lower than the existing scenario at the beginning two hours from 2:00 p.m.to 4:00 p.m., and higher than the existing scenario in later hours from 4:00 p.m. to 8:00 p.m. The total delay during the simulation period is 5188 vehicle-hours for the existing scenario and 5844 vehicle-hours for the proposed scenario, which means that the proposed scenario is not operationally efficient.

The conclusion from this study is that the proposed scenario does not perform as well as the exiting scenario. The 300 ft distance from the starting point of buffer-separated HOV lane to the HOV-to-HOV merging point seems to be too short. The suggestion is to keep the existing HOV lane striping (operating the HOV lane as a limited-access facility) if HOV demands are high enough to cause the HOV lane to be congested.

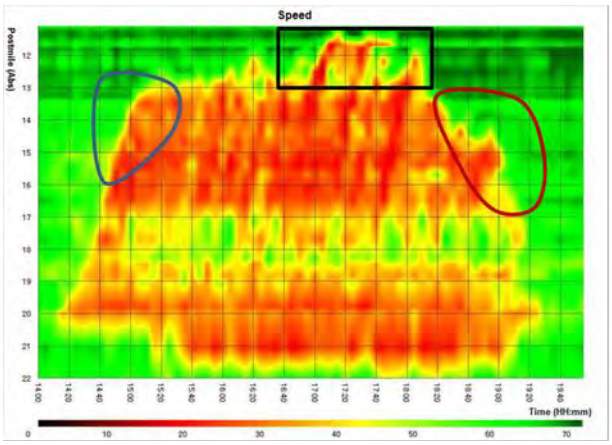

(a) Existing scenario: Simulated GP lanes

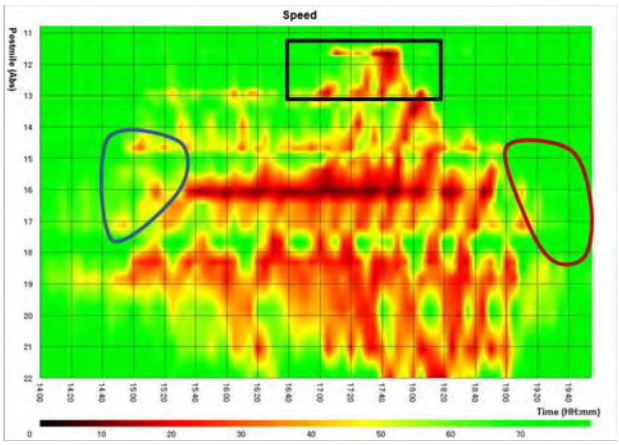

(b) Existing scenario: Simulated HOV lanes

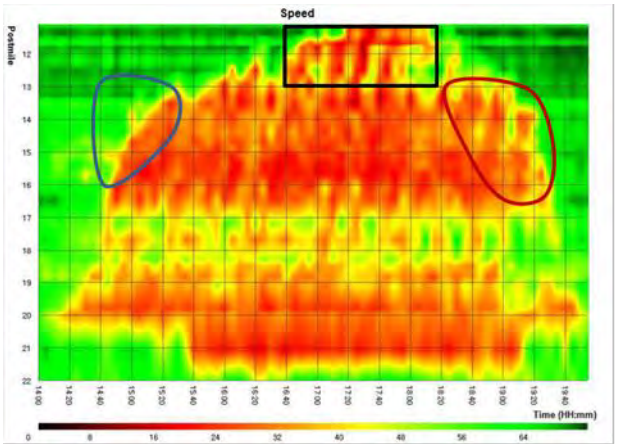

(c) Proposed scenario: Simulated GP lanes

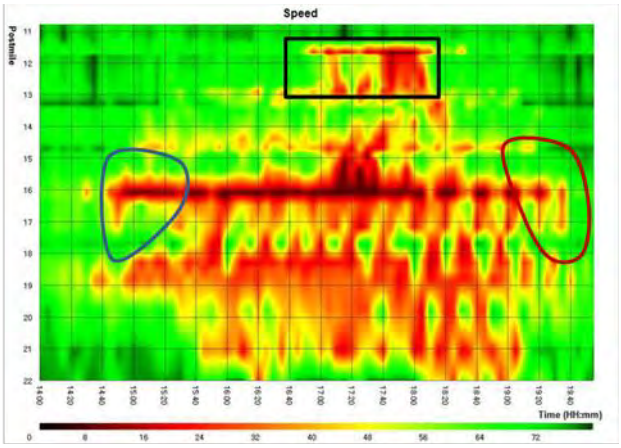

(b) Proposed scenario: Simulated HOV lanes

Figure 76. Comparison of simulated speed contours for existing and proposed scenarios

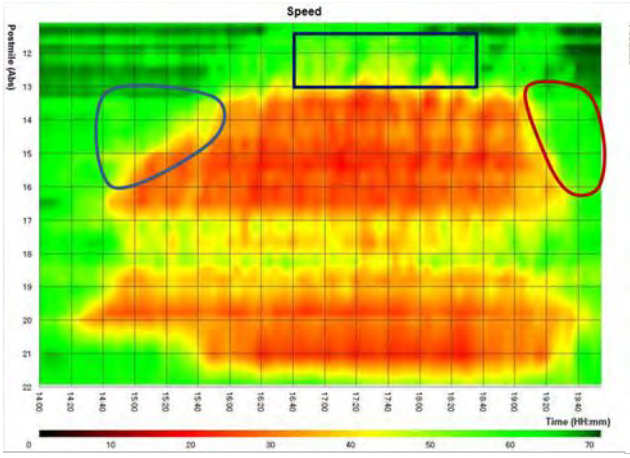

(a) Existing scenario: Simulated GP lanes

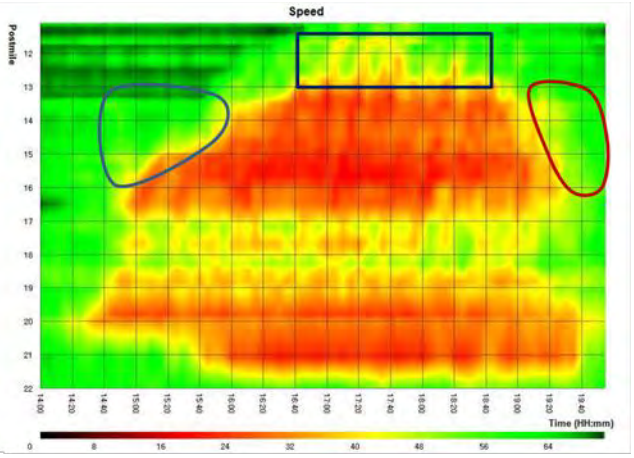

(b) Proposed scenario: Simulated GP lanes

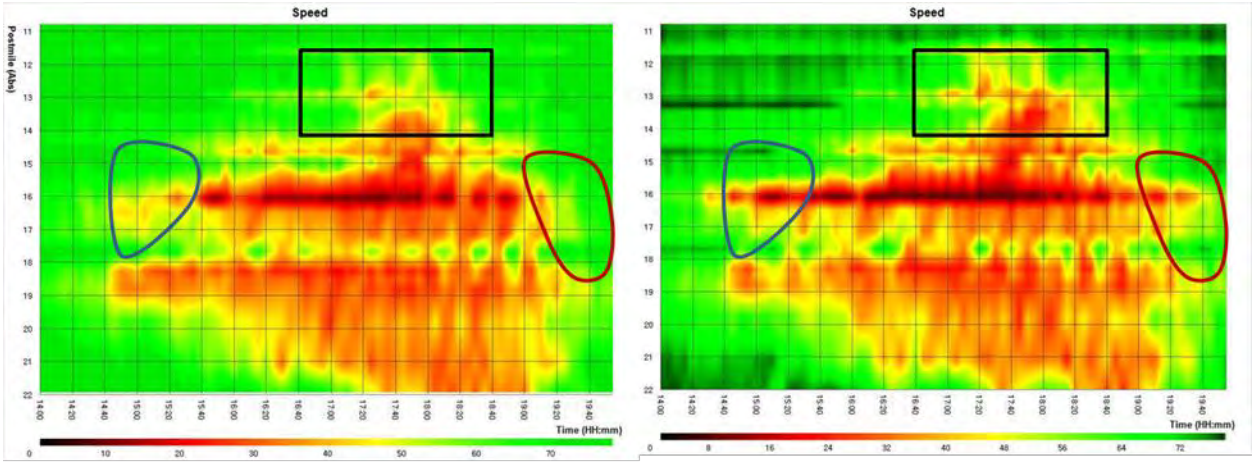

(c) Existing scenario: Simulated HOV lanes (b) Proposed scenario: Simulated HOV lanes

Figure 77. Comparison of average simulated speed contours for existing and proposed scenarios

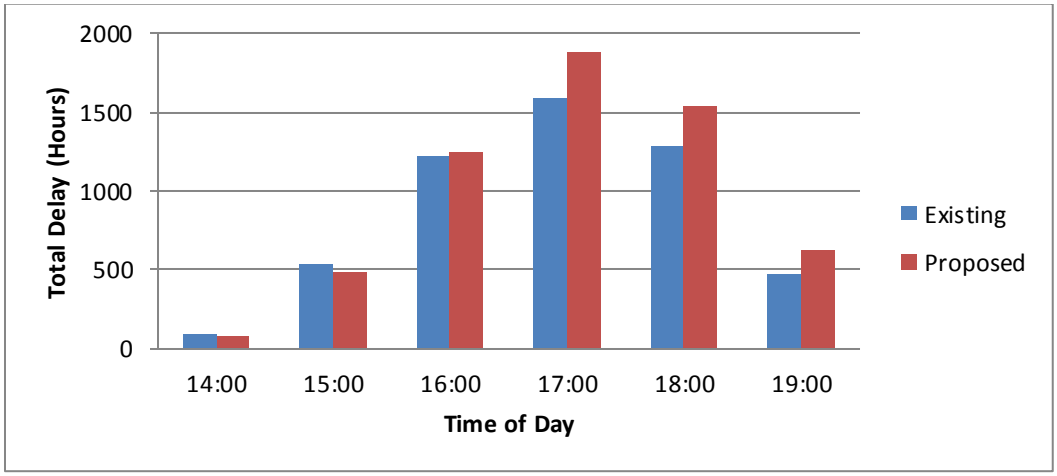

Figure 78. Comparison of total delay for existing and proposed scenarios

7.5 Summary of Simulation Results

There are two conclusions from the simulation studies:

- There are more lane change and weaving activities after converting the HOV lane from limited-access to continuous-access.
- For the location with a HOV-to-HOV direct connector, it is better to operate the HOV lane as a limited-access facility if HOV demands are high enough to cause congestion on the HOV lane.

8. References

Antoniou, C., & Koutsopoulos, H. (2006). Estimation of Traffic Dynamics Models with Machine-Learning Methods. *Transportation Research Record, 1965*, 103-111.

Ban, J. X., Chu, L., & Benouar, H. (2008). Bottleneck Identification and Calibration for Corridor Management Planning. *Transportation Research Record: Journal of the Transportation Research Board, 1999*, 40-53.

Breiland, C., Chu, L., & Benouar, H. (2006). Operational Effect of Allowing Single Occupant Hybrid Vehicles into High Occupancy Vehicle Lanes. *1959*, 151-158.

Cassidy, M. J. (1998). Bivariate relations in nearly stationary highway traffic. *Transportation Research Part B: Methodological, 32*(1), 49-59.

Chow, A., Gomes, G., Kurzhanskiy, A., & Varaiya, P. (2010). Aurora RNM--A Macroscopic Simulation Tool for Arterial Traffic Modeling and Control. *Transportation Research Board 89th Annual Meeting*. Wanshington, D.C.

Chu, L., Gerfen, J., & Recker, W. W. (2008). TMC Simulator for Operator Training Using Micro-Simulation. Washington D.C.: Transportation Research Board 87th Annual Meeting.

Chu, L., Kim, H. K., Liu, H. X., & Recker, W. W. (2005). Evaluation of Traffic Delay Reduction from Automatic Workzone Information Systems using Micro-simulation.

Chu, L., Liu, H. X., & Recker, W. W. (2004). Using Microscopic Simulation to Evaluate Potential Intelligent Transportation System Strategies under Nonrecurrent Congestion. *1886*, 76-84.

Chu, L., Liu, H. X., Recker, W. W., & Zhang, M. H. (2004). Performance Evaluating of Adaptive Ramp Metering Algorithms Using Microscopic Traffic Simulation Model. *130*(3), 330-338.

Dervisoglu, G., Gomes, G., Kwon, J., & Muralidharan, A. (2008). Automatic calibration of the fundamental diagram and empirical observations on capacity.

Edie, L. (1961). Car-following and steady-state theory for noncongested traffic. *Operations Research*, 66-76.

Hall, F. L., Allen, B. L., & Gunter, M. A. (1986). Empirical analysis of freeway flow-density relationships. *Transportation Research Part A: General Theory*, 197-210.

Jang, K. a. (2009). Safety Performance of High-Occupancy-Vehicle Facilities. *Transportation Research Record: Journal of the Transportation Research Board*, 132-140.

K.S.Nesamani, Chu, L., Mike, M., & Jayakrishan, R. (2007). Estimation of Vehicle Emissions by Capturing Dynamic Traffic Variations. *41*, 2996-3008.

Kwon, J., McCullough, B., Petty, K., & and Varaiya, P. (2007). *Evaluation of PeMS to Improve the Congestion Monitoring Program*. Berkeley: California PATH Research Report UCB-ITS-PRR-2007-6.

Lighthill, M. J., & Whitham, G. B. (1955). On kinematic waves. II. A theory of traffic flow on long crowded roads. *Proceedings of the Royal Society of London. Series A. Mathematical and Physical Sciences*, 317.

Liu H., O. J. (2001). Adaptive Signal Control with On-line Performance Measure. *1811*, 131-138.

Newell, G. F. (1993). A simplified theory of kinematic waves in highway traffic, part I: general theory. *Transportation Research Part B: Methodological*, 281-287.

Appendix A Speed Contour Plots of Study Corridors

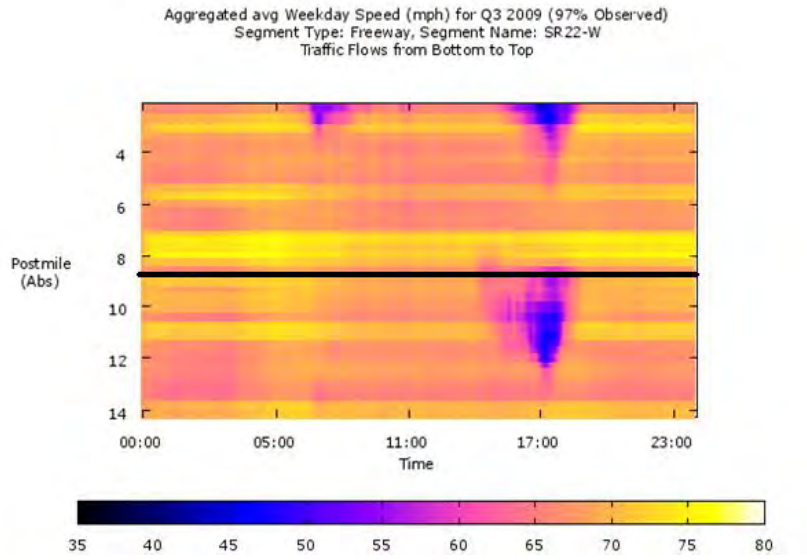

Figure A1. Speed contour plot, SR-22W, Orange County, District 12

Major Bottleneck
D12, Orange County, Garden Grove, PM R7.93 (Abs9.39), Harbor Blvd.
Afternoon bottleneck

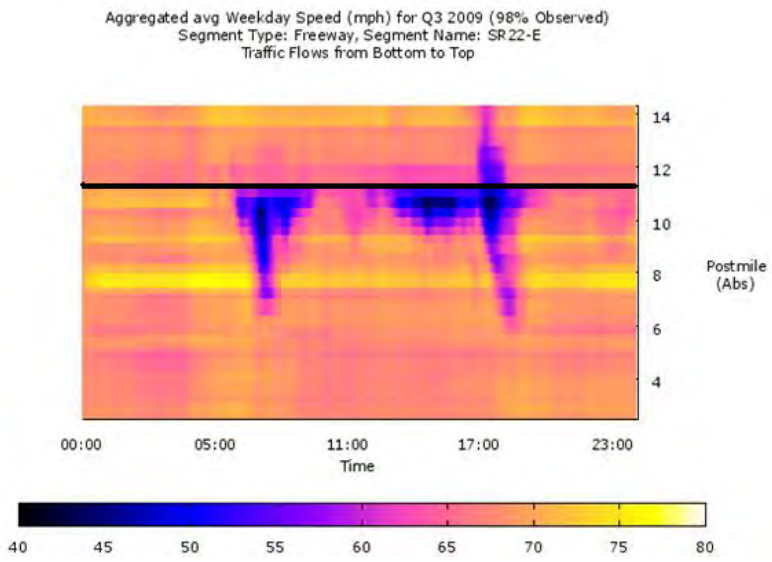

Figure A2. Speed contour plot, SR-22E, Orange County, District 12

Major Bottleneck
D12, Orange County, Orange, PM R9.7 (Abs11.36), The City Drive Ave
Both morning and afternoon bottlenecks.

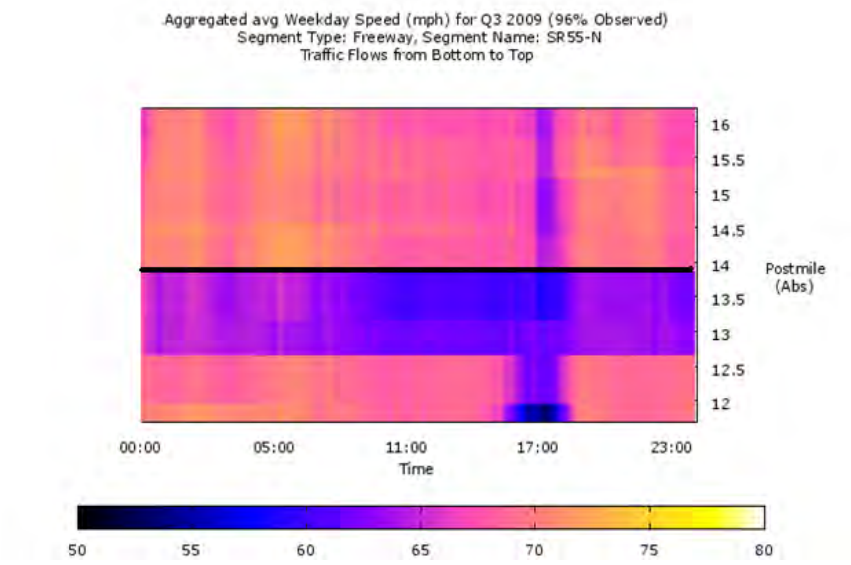

Figure A3. Speed contour plot, SR-55N, Orange County, District 12

No bottleneck (All detector data indicate average speeds were greater than 50 mph)

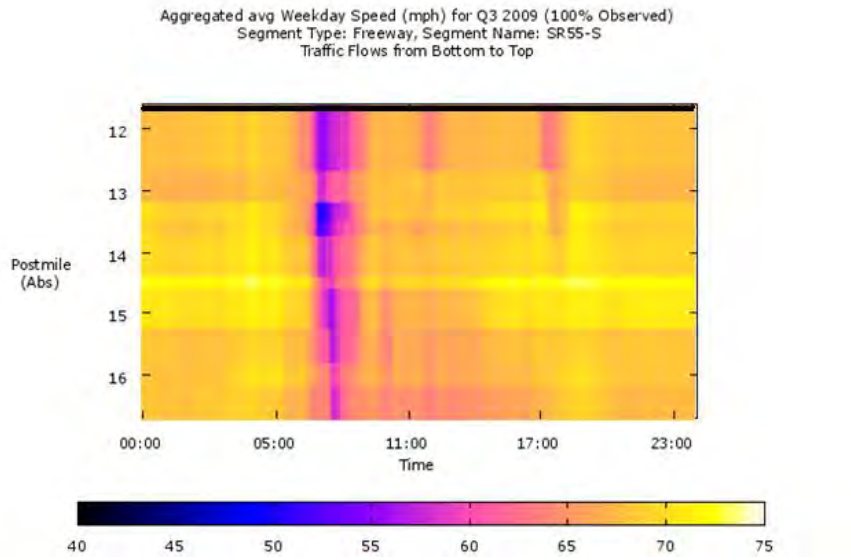

Figure A4. Speed contour plot, SR-55N, Orange County, District 12

Major Bottleneck
D12, Orange County, Santa Ana, PM 11.62 (Abs11.6), 17th Ave
Morning bottleneck

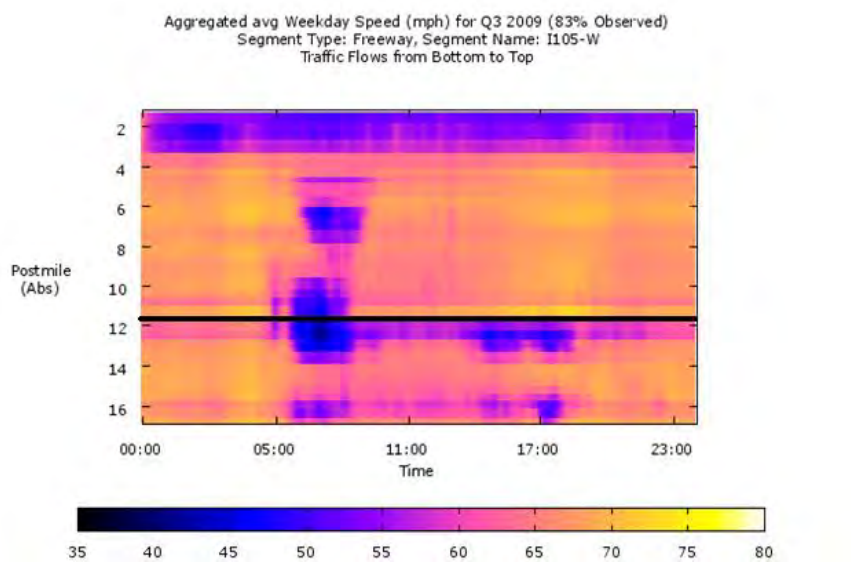

Figure A5. Speed contour plot, I-105E, Los Angeles County, District 7

Major Bottleneck
D7, Los Angeles, Lynwood, PM R12.1(Abs 12.10), Bullis Ave
- Multiple bottlenecks
- Morning bottlenecks were pronounced

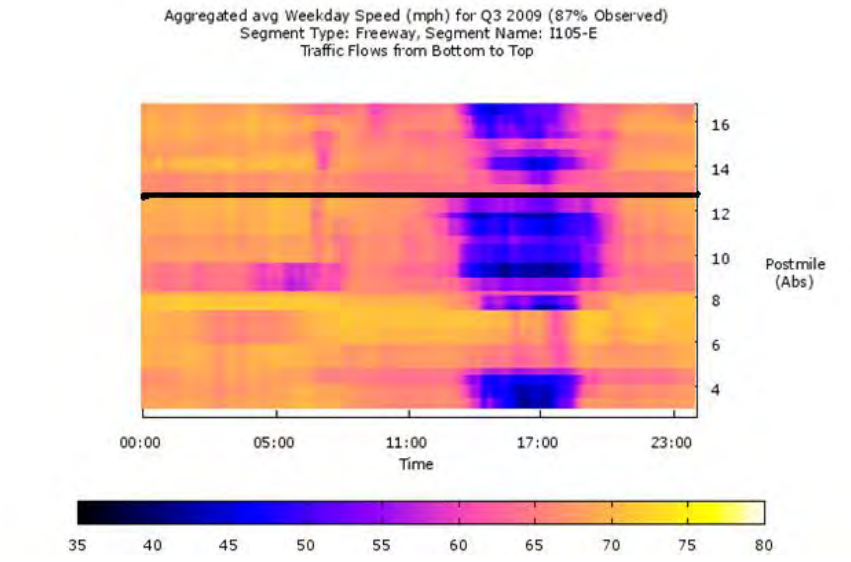

Figure A6. Speed contour plot, I-105W, Los Angeles County, District 7

Major Bottleneck
D7, Los Angeles, Lynwood, PM R12.6 (Abs 12.6), Harris Ave
- Multiple bottlenecks
- Afternoon bottlenecks were pronounced

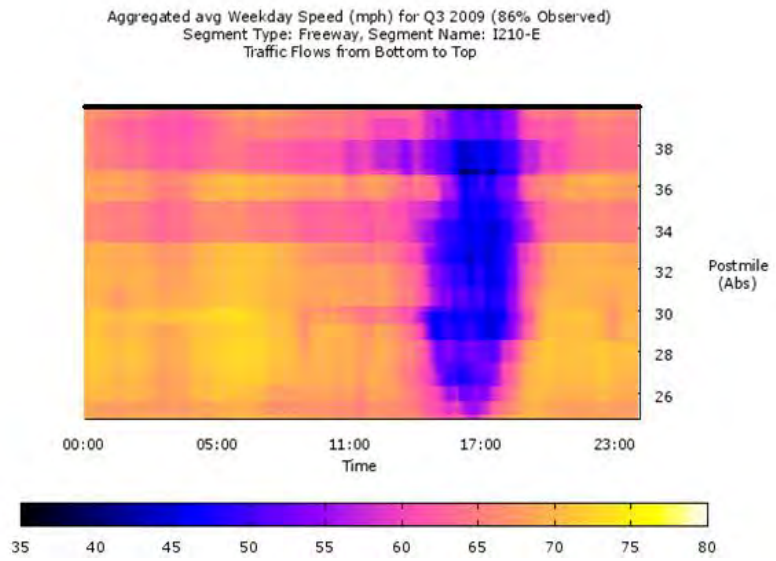

Figure A7. Speed contour plot, I-210E, Los Angeles County, District 7

Major Bottleneck
D7, La Angeles County, Azusa, PM 39.64 (Abs39.93), Azusa Rd
-Afternoon bottlenecks were pronounced.

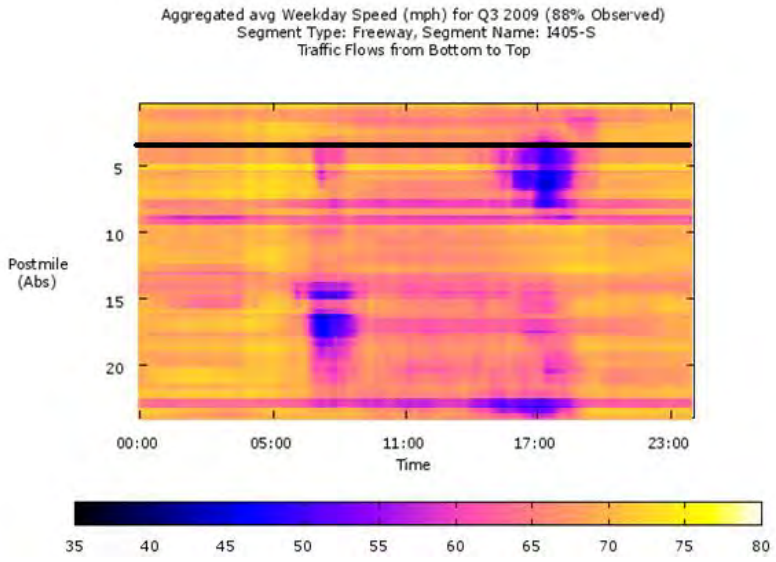

Figure A8. Speed contour plot, I-405S, Orange County, District 12

Major Bottleneck
D12, Orange County, Irvine, PM 3.84(Abs3.61), Jeffrey Rd

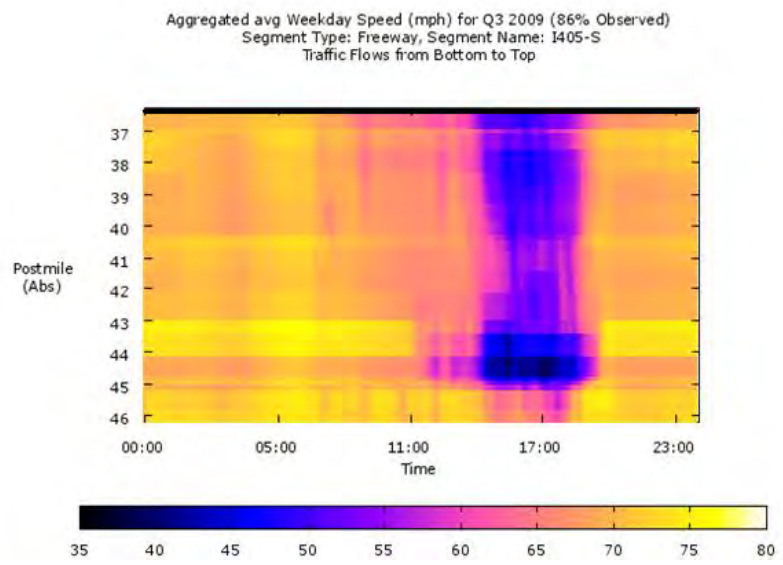

Figure A9. Speed contour plot, I-405S, Los Angeles County, District 7

Major Bottleneck
D7, Los Angeles County,Carson , PM 11.32(Abs35.09), Avalon Rd
Afternoon bottleneck

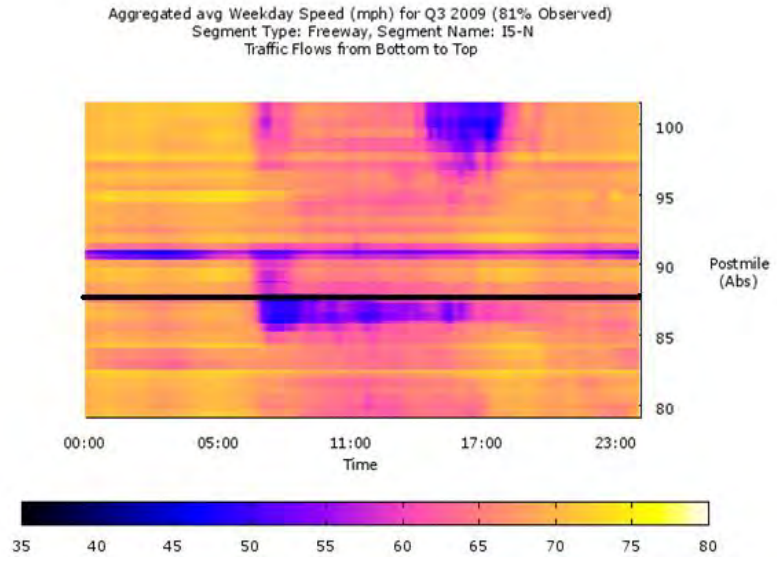

Figure A10. Speed contour plot, I-5N, Orange County, District 12

Major Bottleneck
D12, Orange County, Mission Viejo, PM 14.46 (Abs 86.72), Faircourt Ave

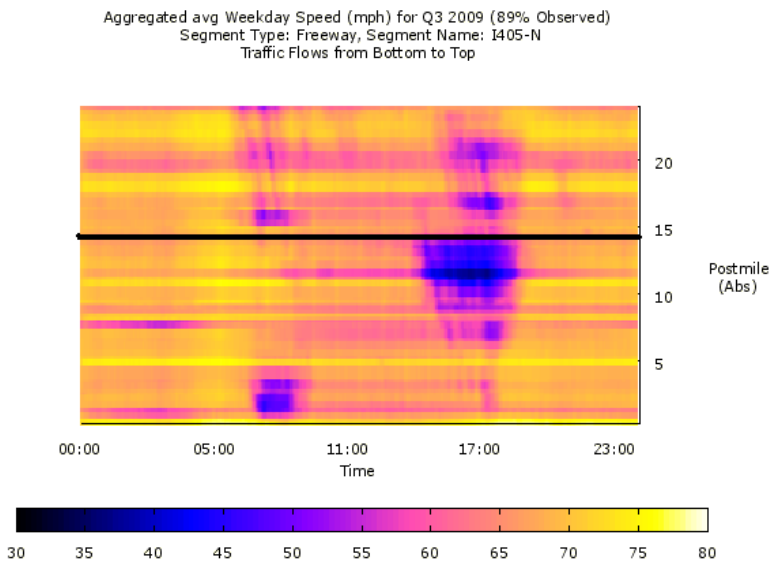

Figure A11. Speed contour plot, I-405N, Orange County, District 12

Major Bottleneck
D12, Orange County, Fountain Valley, PM 14.54(Abs14.31), Bushard Ave

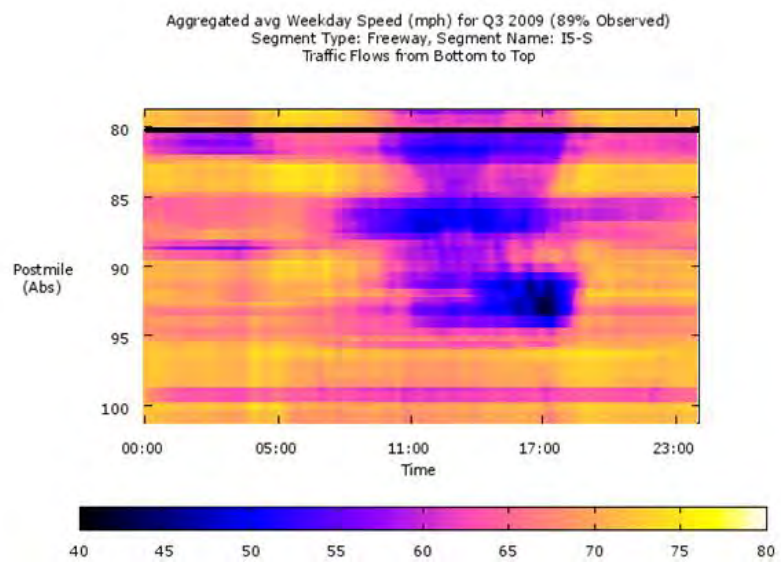

Figure A12. Speed contour plot, I-5S, Orange County, District 12

Major Bottleneck
D12, Orange County, San Juan Capistrano, PM 7.99(Abs80.19), Aeropuerto Ave
- Multiple bottlenecks
- No specific peak periods

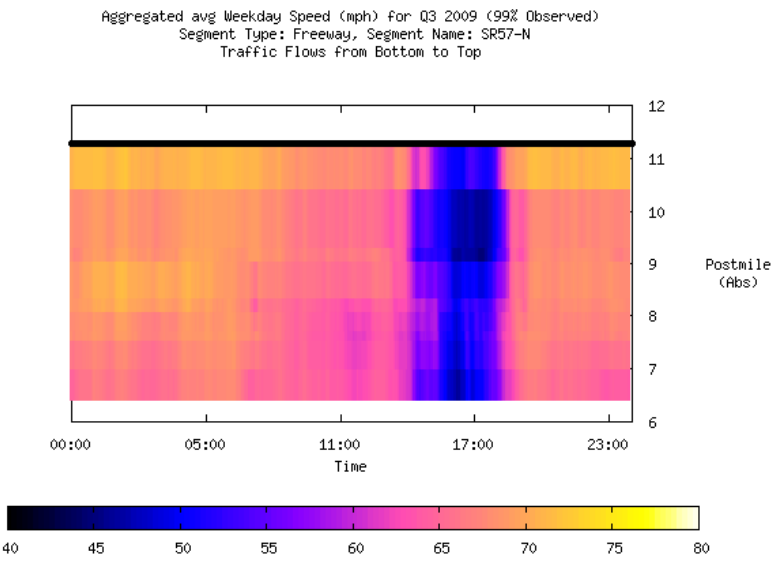

Figure A13. Speed contour plot, SR-57N, OrangeCounty, District 12

Major Bottleneck
D12, Orange County, Orange, PM R1.263 (Abs13.08), Brea canyon Ave
Afternoon bottleneck

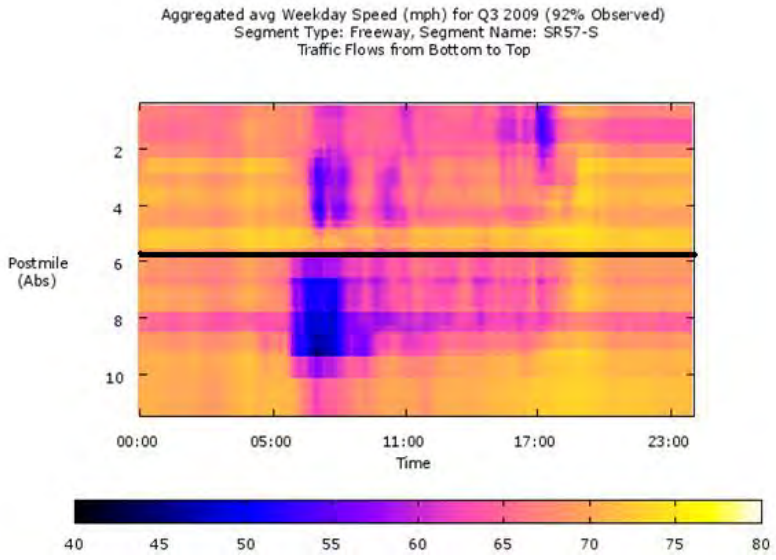

Figure A14. Speed contour plot, SR-57S, Orange County, District 12

Major Bottleneck
D12, Orange County, Orange, PM 16.46 (Abs5.81), Orangethorpe Ave
Morning bottleneck

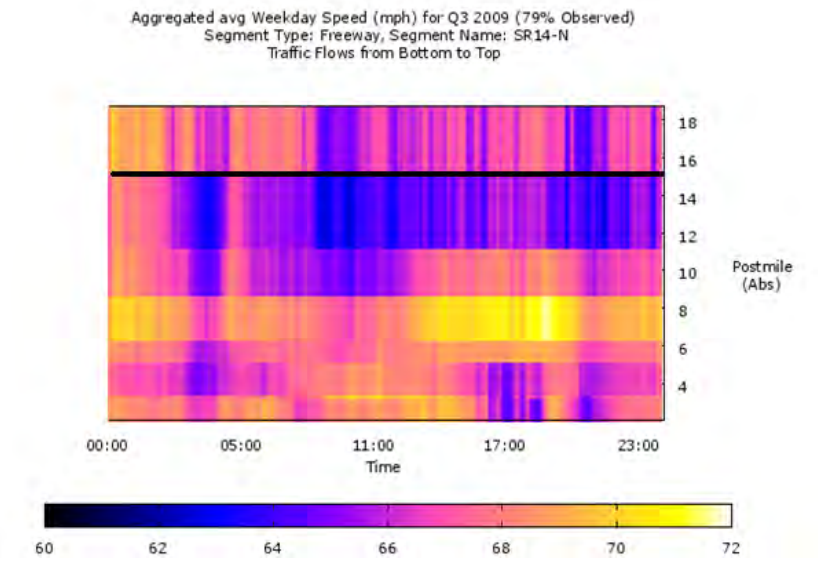

Figure A15. Speed contour plot, SR-14N, Los Angeles County, District 7

No Bottleneck

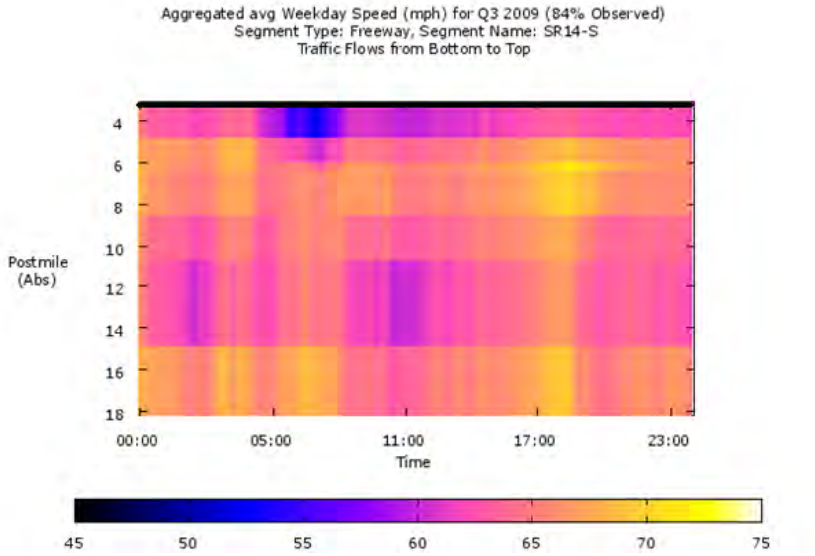

Figure A16. Speed contour plot, SR-14S, Los Angeles County, District 7

No Bottleneck

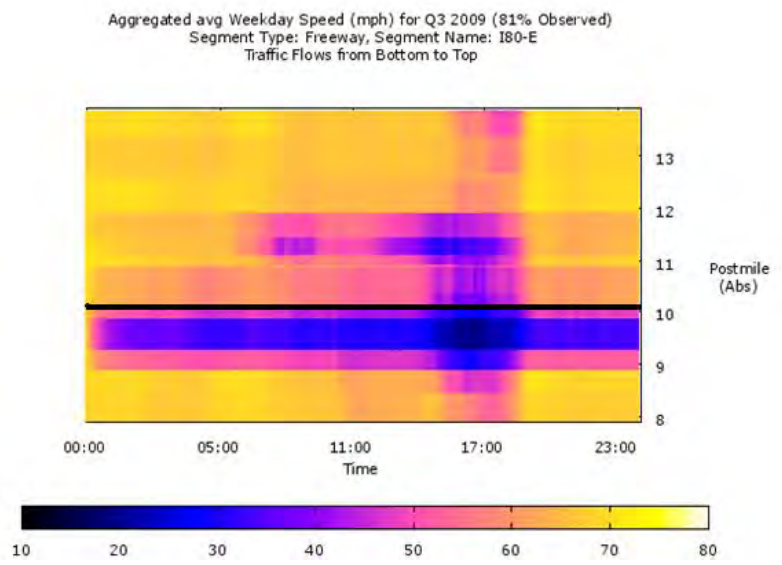

Figure A17. Speed contour plot, I-80E, Alameda County, District 4

Major Bottleneck

D4, Alameda, PM 4.6 (Abs 9.91), Ashby Ave. (Possibly detector malfunctioning)

- There is another bottleneck downstream (around PM 11.5)
- Multiple bottlenecks

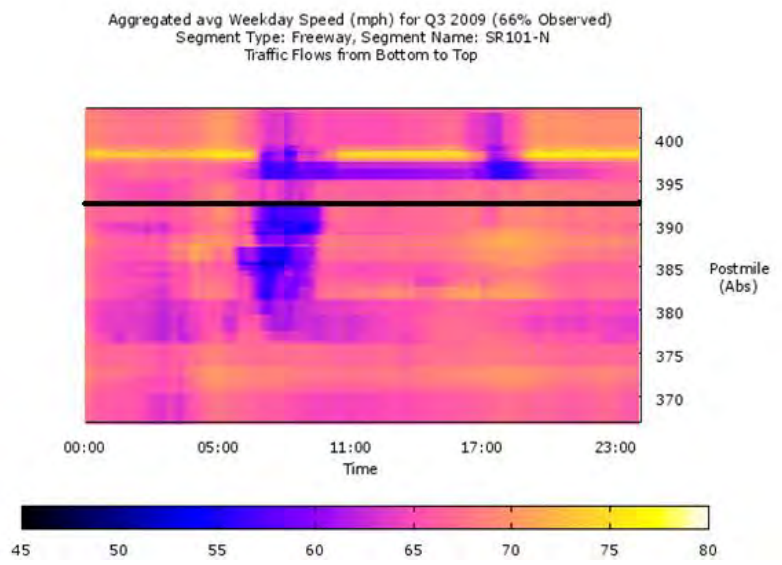

Figure A18. Speed contour plot, SR-101N, Santa Clara County, District 4

Major Bottleneck

D4, Santa Clara County, Santa Clarea, PM 43.3 (Abs392.94), Wildwood Ave

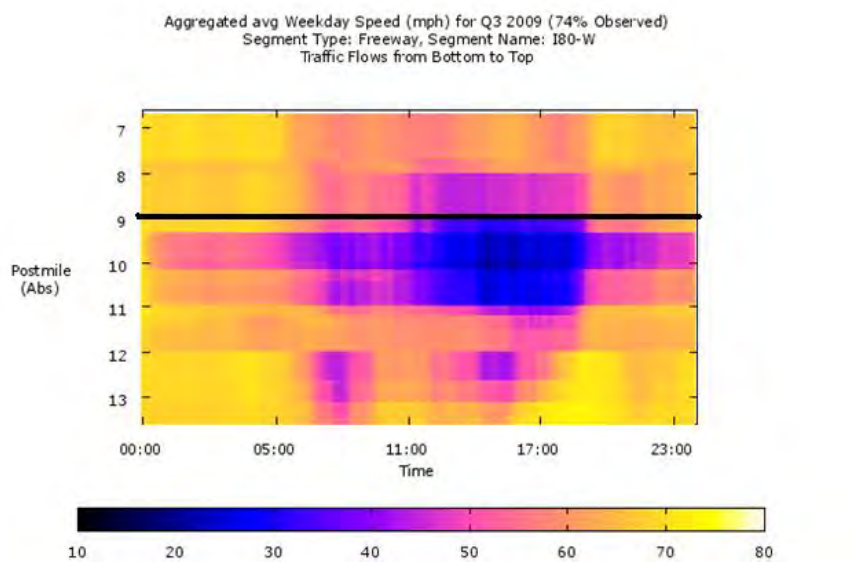

Figure A19. Speed contour plot, I-80W, Alameda County, District 4

Major Bottleneck
D4, Alameda,Berkeley, PM 3.64 (Abs 8.95), Powell St.

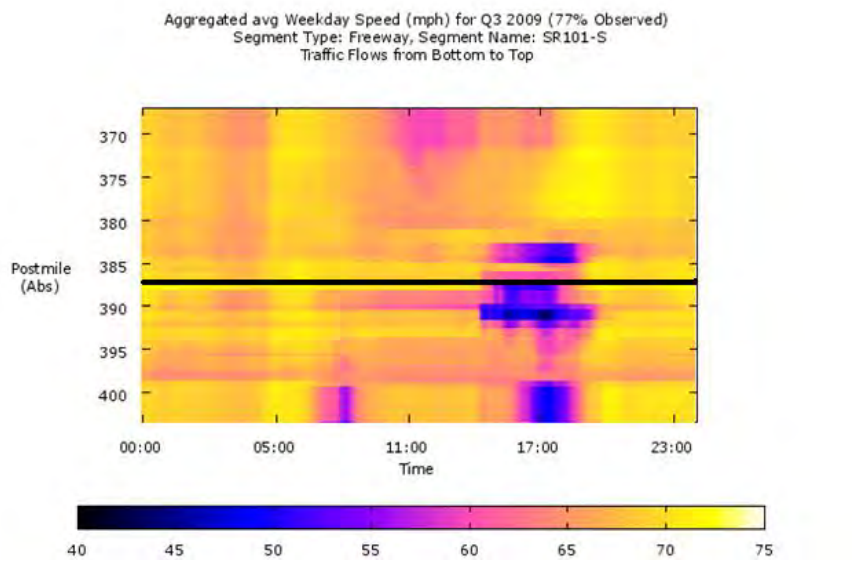

Figure A20. Speed contour plot, SR-101S, Santa Clara County, District 4

Major Bottleneck
D4, Santa Clara County, Santa Jose, PM 36.6 (Abs386.27), Mabury Rd

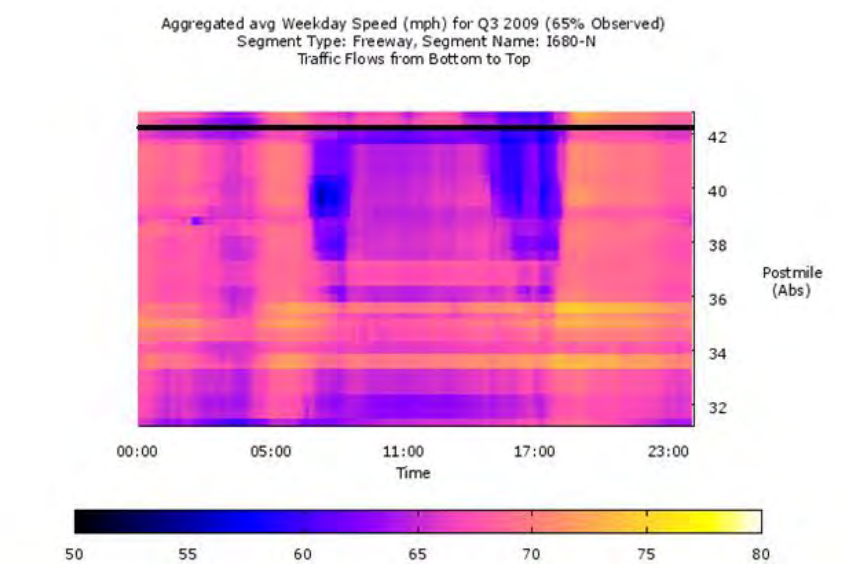

Figure A21. Speed contour plot, I-680N, Contra Costa County, District 4

No Bottleneck

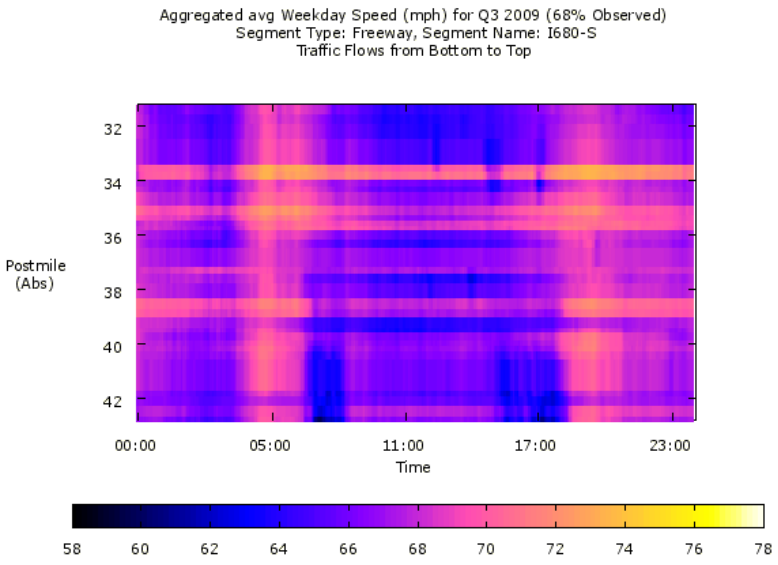

Figure A22. Speed contour plot, I-680S, Contra Costa County, District 4

No bottleneck

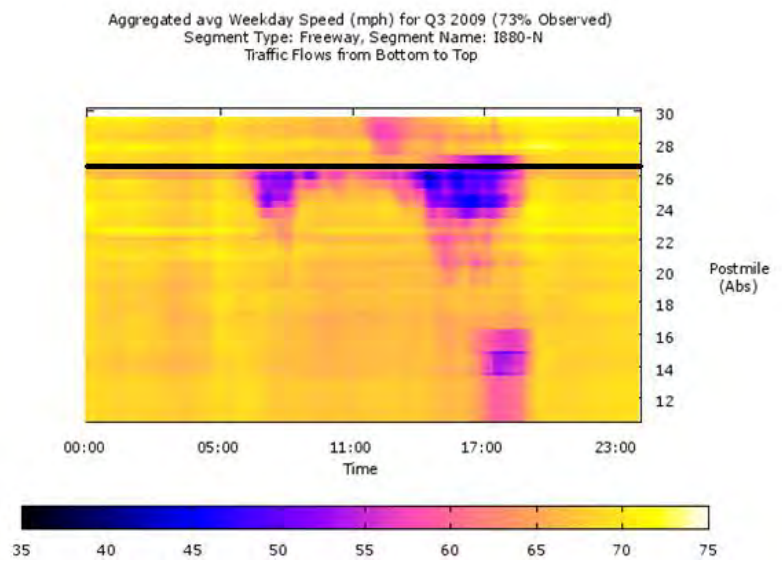

Figure A23. Speed contour plot, I-880N, Alameda County, District 4

Major Bottleneck
D4, Alameda County, Hayward, PM 15.8 (Abs26.03), Tennyson Rd.

Appendix B Speed-Flow Histogram of Study Sites by Corridor, District 4

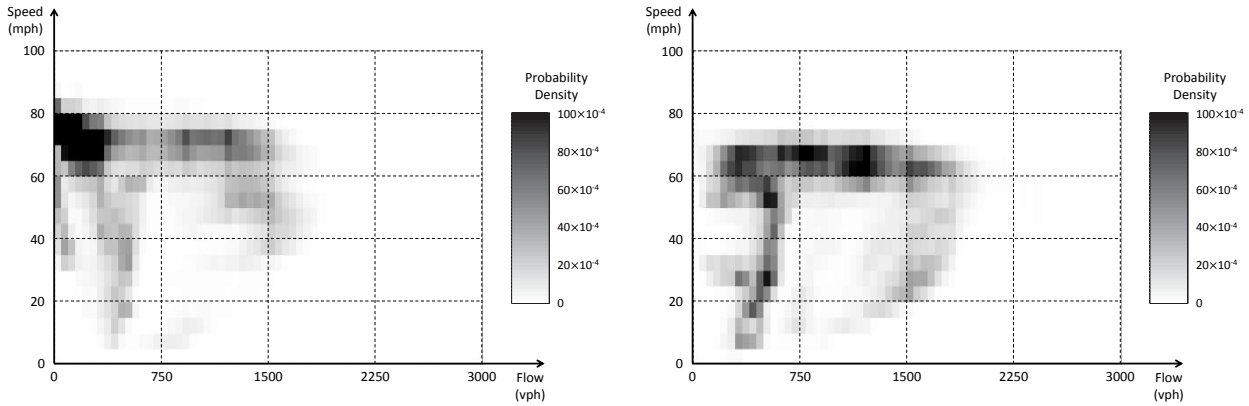

(a) HOV Lane (b) GP lane

Figure B1. Probability density of speed-flow: (a) HOV lane, and (b) GP lane (Interstate 80 Eastbound, District 4)

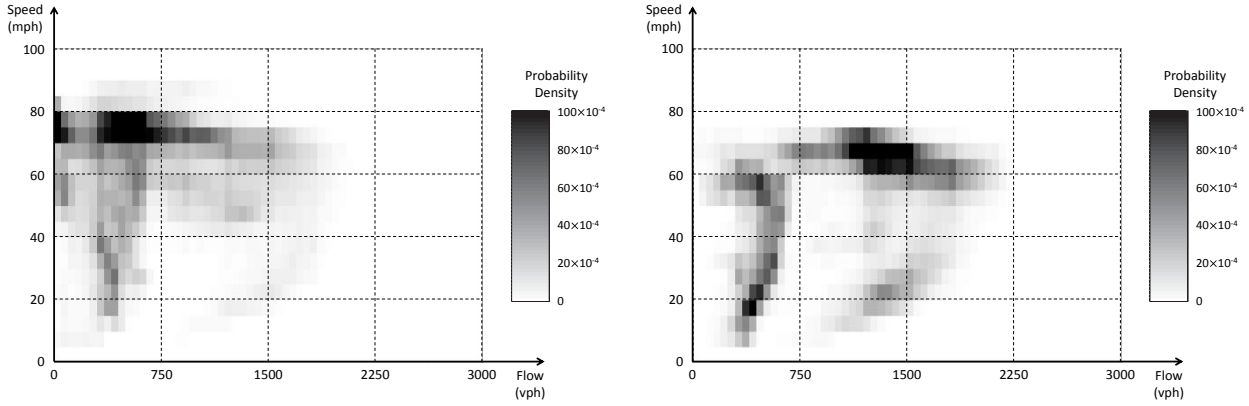

(a) HOV Lane (b) GP lane

Figure B2. Probability density of speed-flow: (a) HOV lane, and (b) GP lane (Interstate 80 Westbound, District 4)

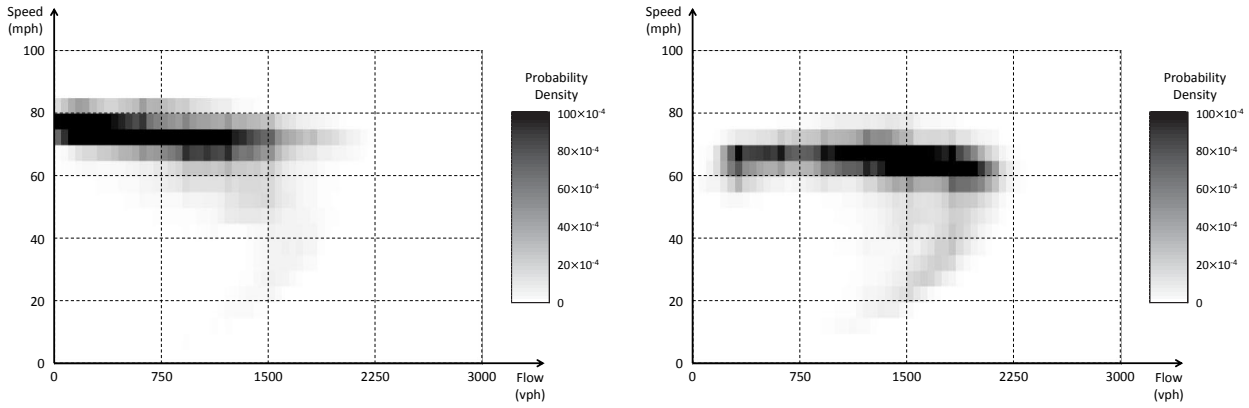

(a) HOV Lane (b) GP lane

Figure B3. Probability density of speed-flow: (a) HOV lane, and (b) GP lane (Interstate 680 Northbound, District 4)

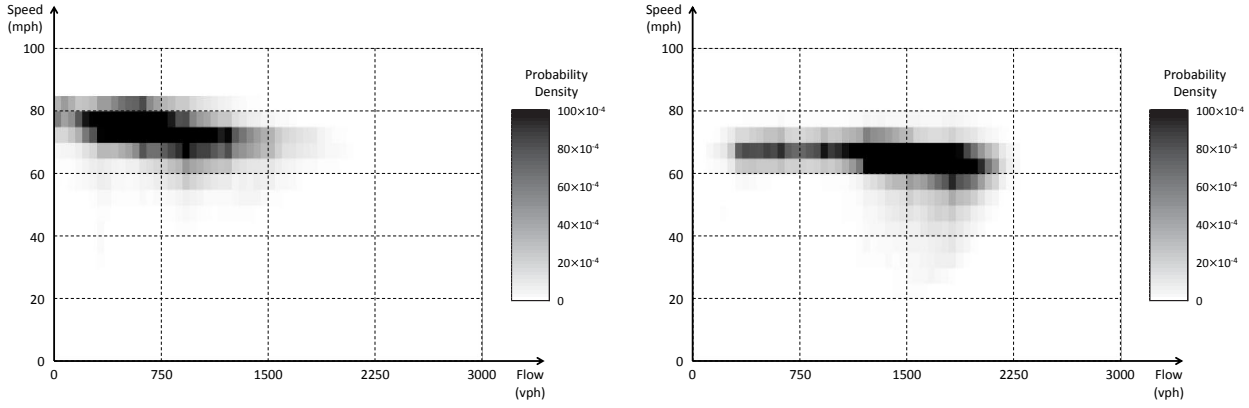

(a) HOV Lane (b) GP lane

Figure B4. Probability density of speed-flow: (a) HOV lane, and (b) GP lane (Interstate 680 Southbound, District 4)

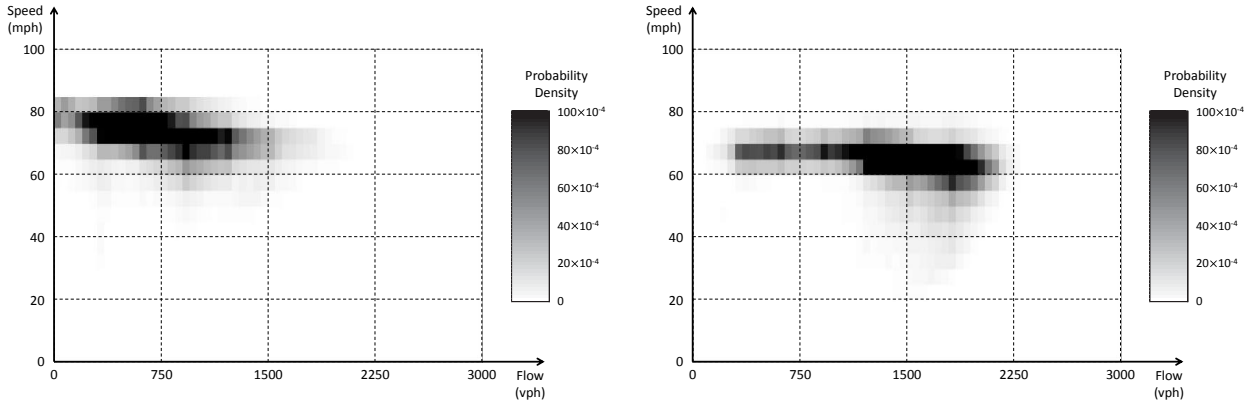

(a) HOV Lane (b) GP lane

Figure B5. Probability density of speed-flow: (a) HOV lane, and (b) GP lane (Interstate 880 Northbound, District 4)

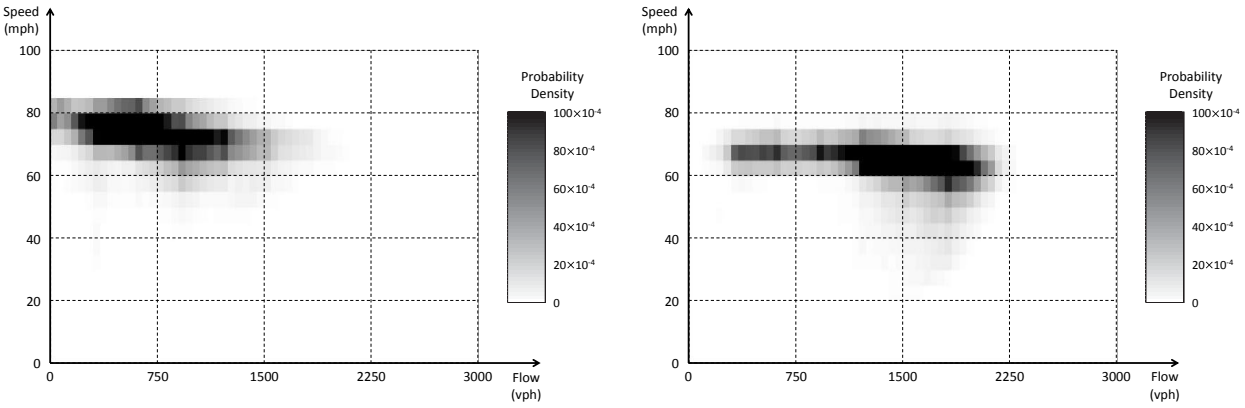

(a) HOV Lane (b) GP lane

Figure B6. Probability density of speed-flow: (a) HOV lane, and (b) GP lane (State Route 101 Northbound, District 4)

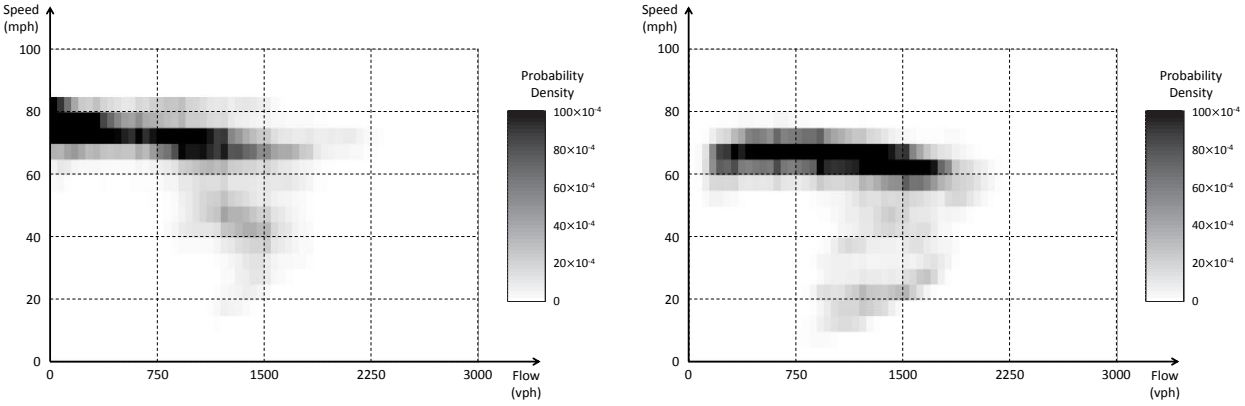

(a) HOV Lane (b) GP lane

Figure B7. Probability density of speed-flow: (a) HOV lane, and (b) GP lane (State Route 101 Southbound, District 4)

Appendix C Speed-Flow Histogram of Study Sites by Corridor, District 7

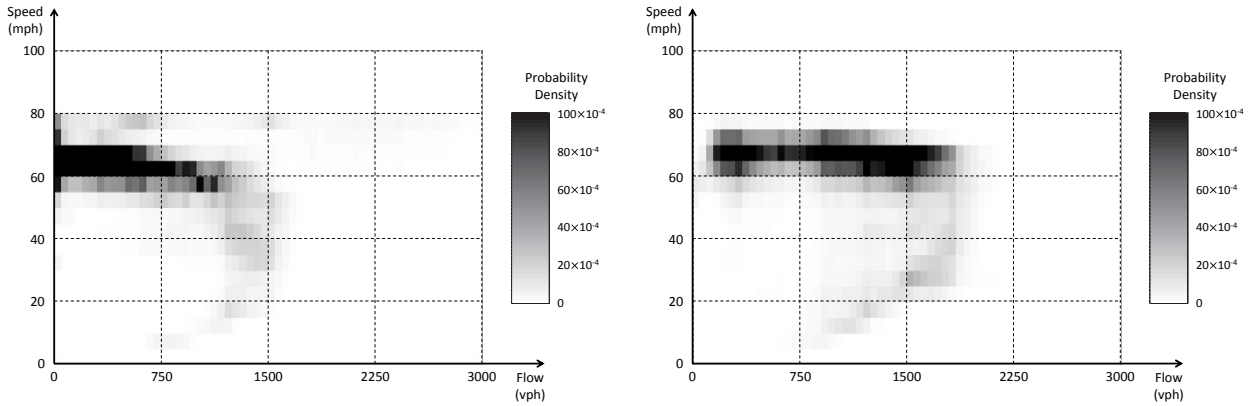

(a) HOV Lane (b) GP lane

Figure C1. Probability density of speed-flow: (a) HOV lane, and (b) GP lane (Interstate 105 Eastbound, District 7)

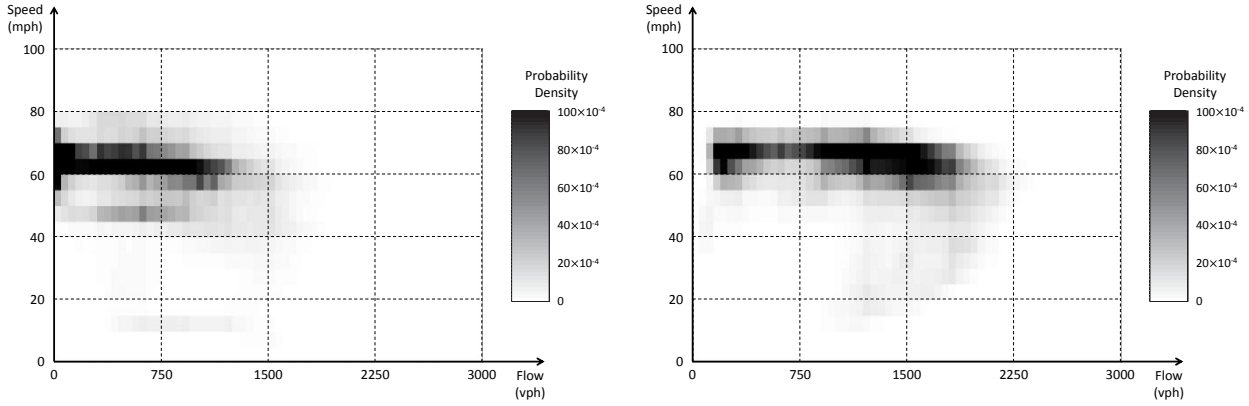

(a) HOV Lane (b) GP lane

Figure C2. Probability density of speed-flow: (a) HOV lane, and (b) GP lane (Interstate 210 Eastbound, District 7)

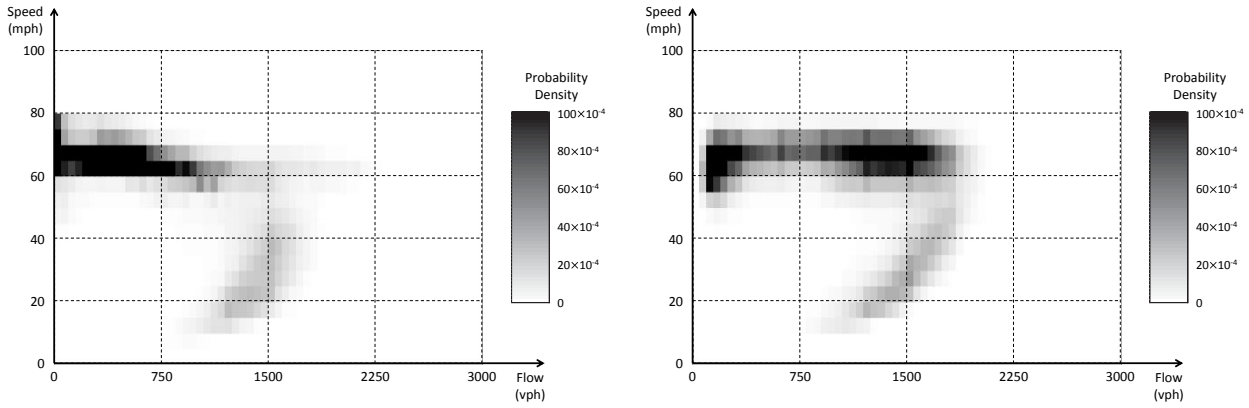

(a) HOV Lane (b) GP lane

Figure C3. Probability density of speed-flow: (a) HOV lane, and (b) GP lane (Interstate 105 Westbound, District 7)

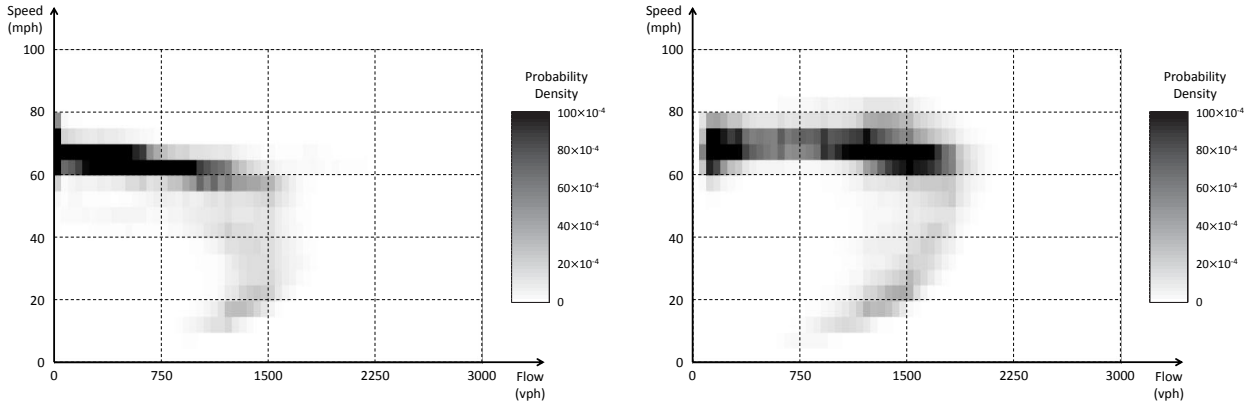

(a) HOV Lane (b) GP lane

Figure C4. Probability density of speed-flow: (a) HOV lane, and (b) GP lane (Interstate 405 Southbound, District 7)

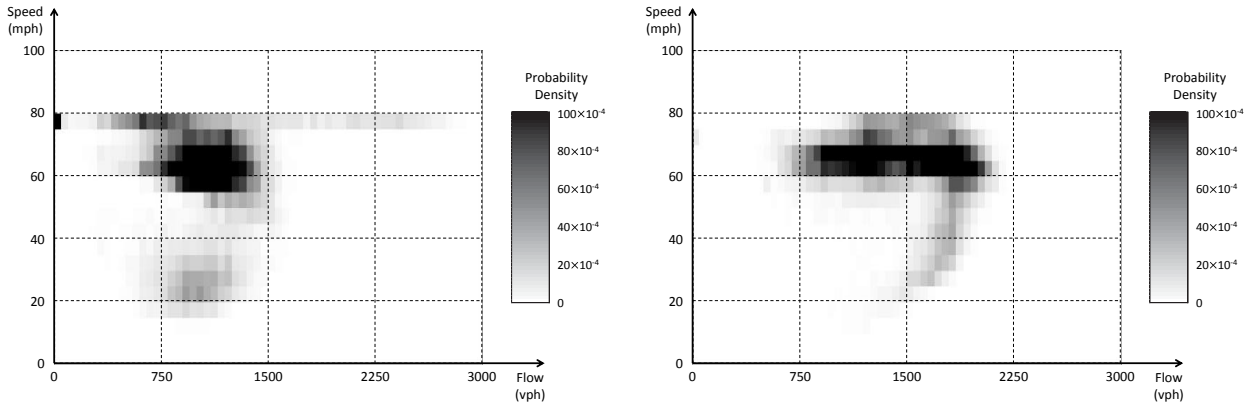

(a) HOV Lane (b) GP lane

Figure C5. Probability density of speed-flow: (a) HOV lane, and (b) GP lane (State Route 14 Northbound, District 7)

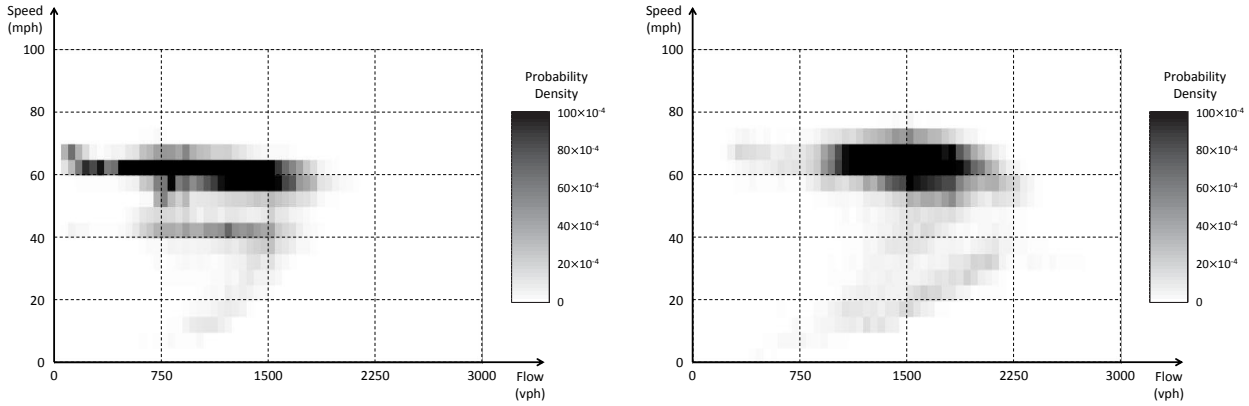

(a) HOV Lane (b) GP lane

Figure C6. Probability density of speed-flow: (a) HOV lane, and (b) GP lane (State Route 14 Southbound, District 7)

Appendix D Speed-Flow Histogram of Study Sites by Corridor, District 12

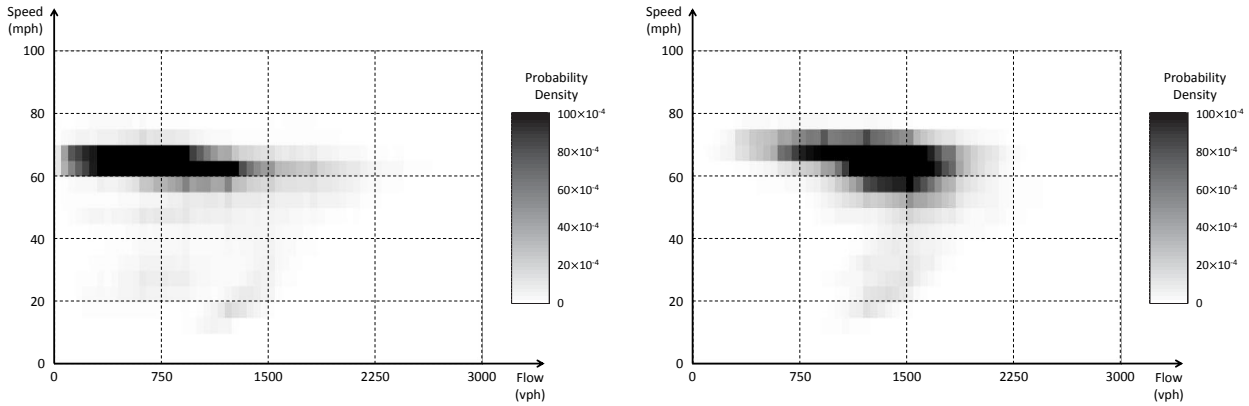

(a) HOV Lane (b) GP lane

Figure D1. Probability density of speed-flow: (a) HOV lane, and (b) GP lane (Interstate 5 Northbound, District 12)

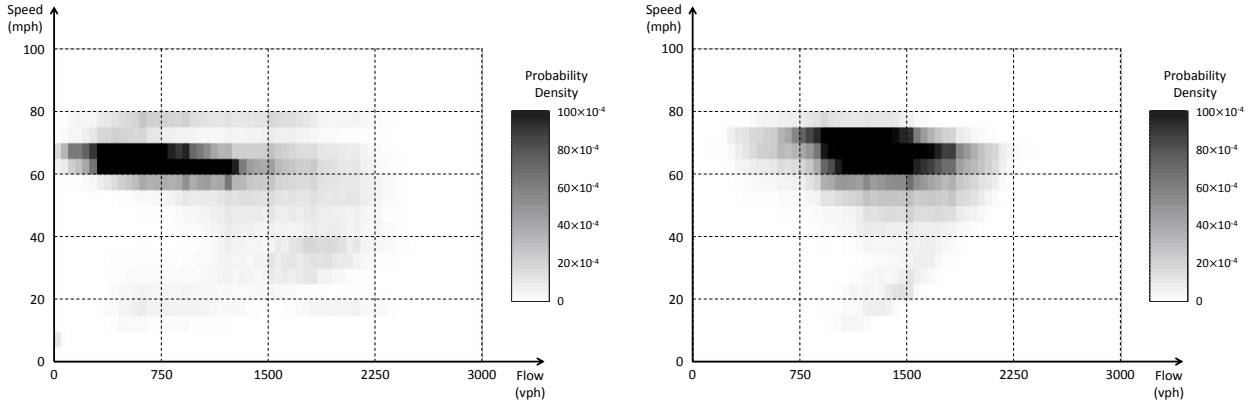

(a) HOV Lane (b) GP lane

Figure D2. Probability density of speed-flow: (a) HOV lane, and (b) GP lane (Interstate 5 Southbound, District 12)

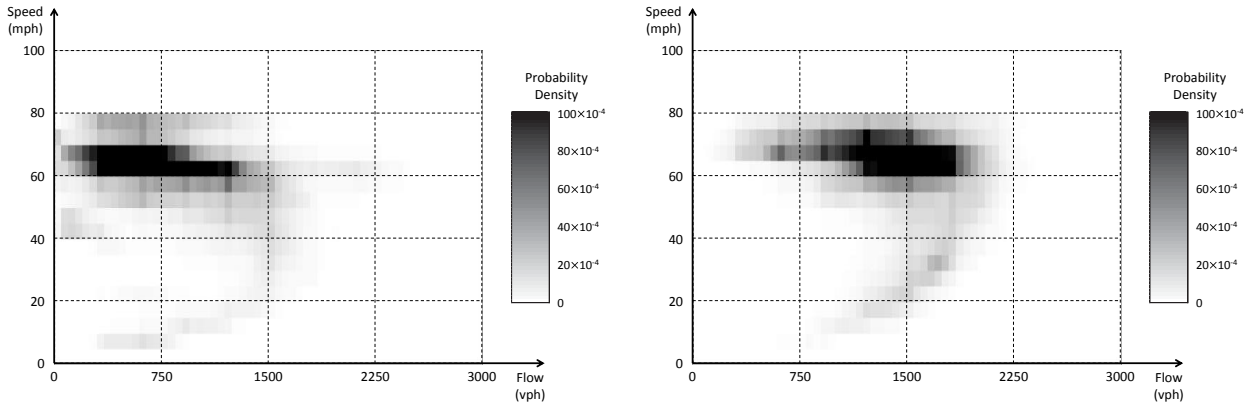

(a) HOV Lane (b) GP lane

Figure D3. Probability density of speed-flow: (a) HOV lane, and (b) GP lane (Interstate 405 Northbound, District 12)

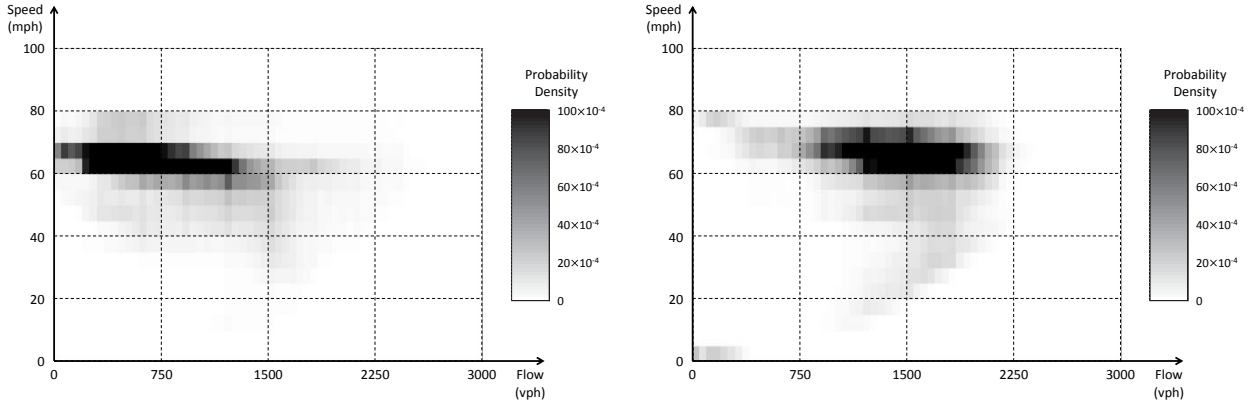

(a) HOV Lane (b) GP lane

Figure D4. Probability density of speed-flow: (a) HOV lane, and (b) GP lane (Interstate 405 Southbound, District 12)

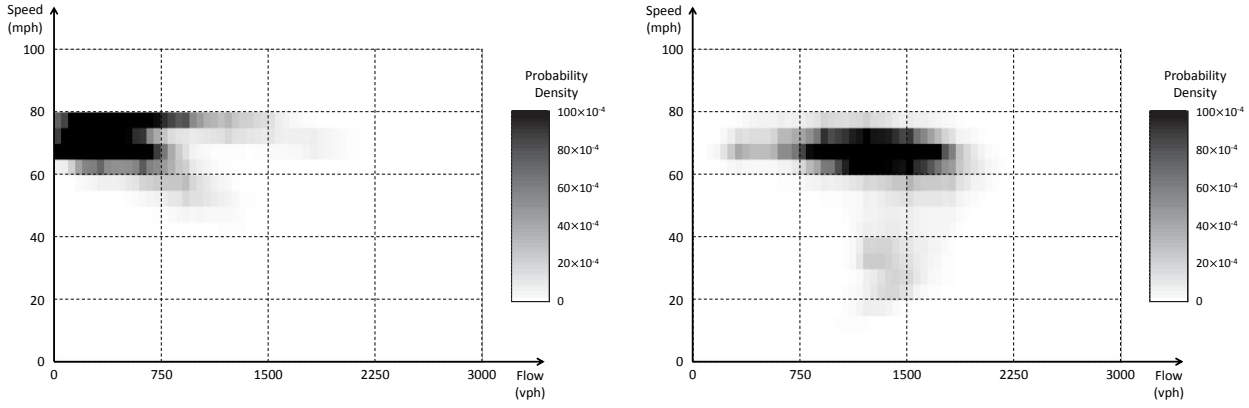

(a) HOV Lane (b) GP lane

Figure D5. Probability density of speed-flow: (a) HOV lane, and (b) GP lane (State Route 22 Eastbound, District 12)

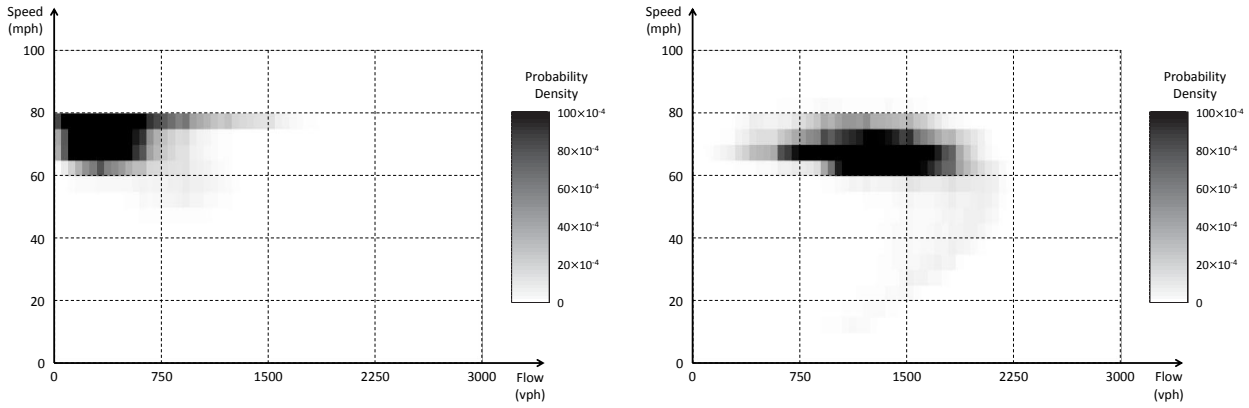

(a) HOV Lane (b) GP lane

Figure D6. Probability density of speed-flow: (a) HOV lane, and (b) GP lane (State Route 22 Westbound, District 12)

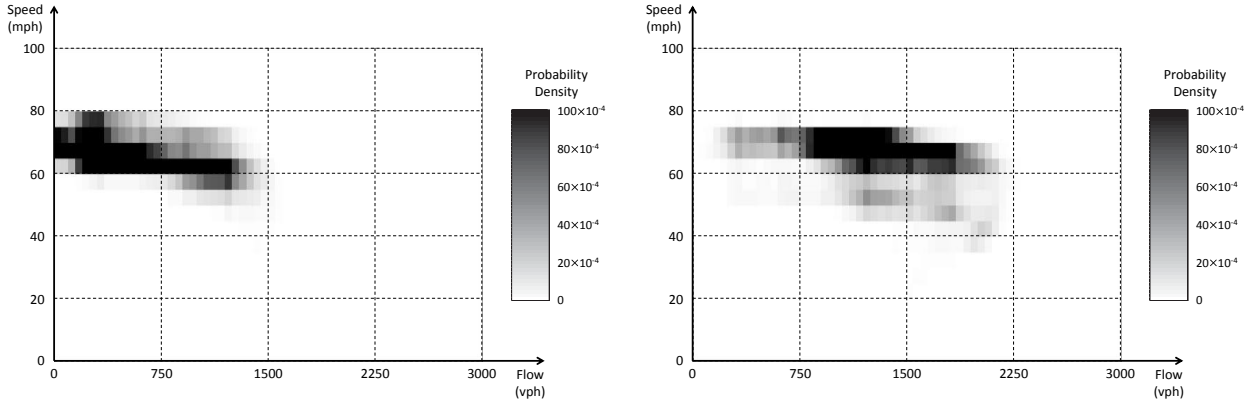

(a) HOV Lane (b) GP lane

Figure D7. Probability density of speed-flow: (a) HOV lane, and (b) GP lane (State Route 55 Northbound, District 12)

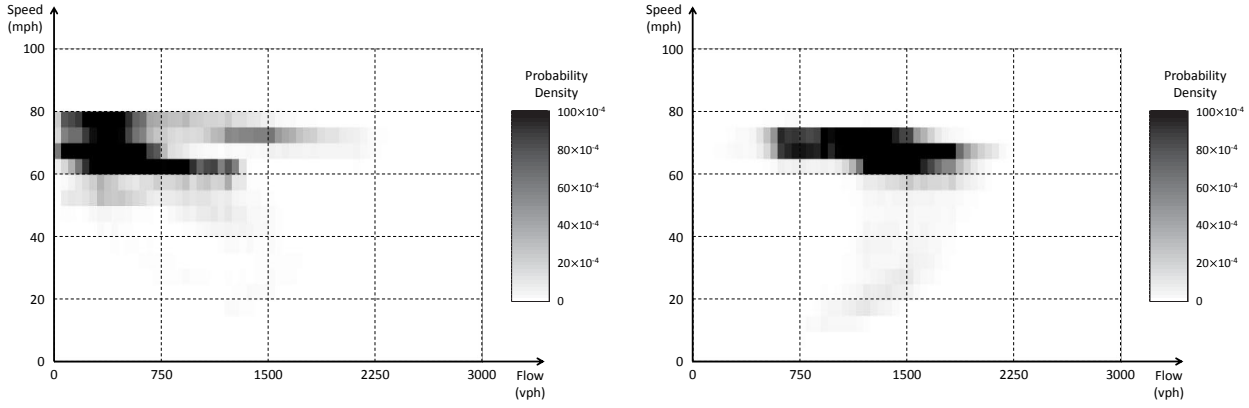

(a) HOV Lane (b) GP lane

Figure D8. Probability density of speed-flow: (a) HOV lane, and (b) GP lane (State Route 55 Southbound, District 12)

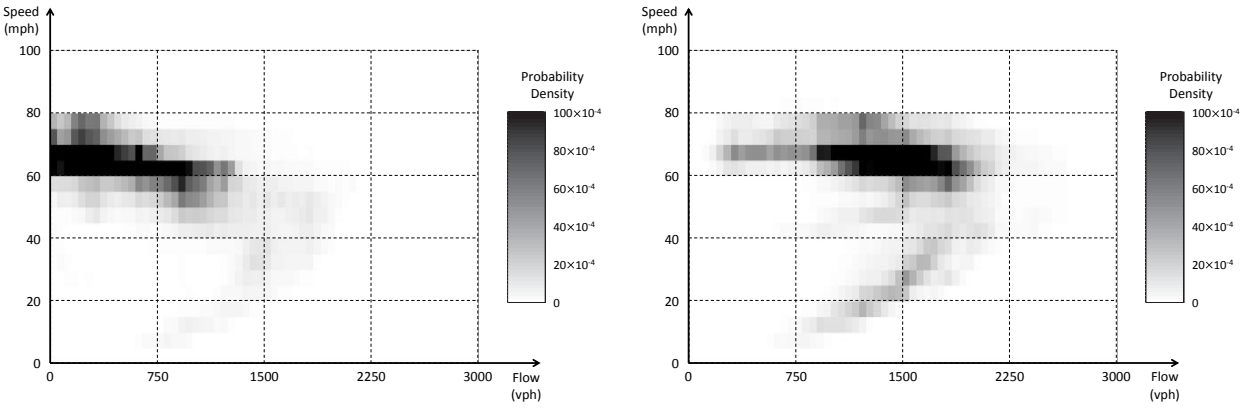

(a) HOV Lane (b) GP lane

Figure D9. Probability density of speed-flow: (a) HOV lane, and (b) GP lane (State Route 55 Continuous Northbound, District 12)

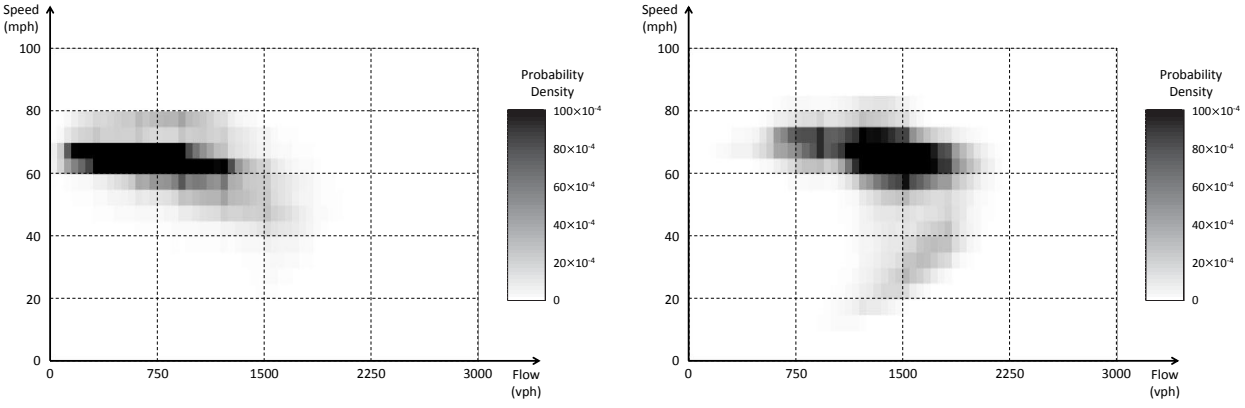

(a) HOV Lane (b) GP lane

Figure D10. Probability density of speed-flow: (a) HOV lane, and (b) GP lane (State Route 57 Southbound, District 12)

Appendix E Detailed Results of Performance Measures, District 4

In District 4, we examined 7 study corridors with part-time continuous access. For each segment or each detector, we computed three performance measures – speed differential, VMT ratio and PMT ratio. Statistics of flow and speed are not furnished because they deliver the same information as speed differential and VMT ratio. As shown in larger scale analysis (district-level or corridor-level), we could not find any sections where HOV facilities exhibit degraded performance compared with a GP lane. There are some noticeable findings for some routes.

- Higher PMT ratios in I-80 Eastbound and Westbound due to: i) occupancy requirement of 3 or more occupants; and ii) higher utilization by vehicles (higher VMT ratio).
- Lower PMT ratio in I-680 Southbound due to lower utilization by vehicles (lower VMT ratio).
- Though some sporadic locations exhibit degraded performance, the segments in the vicinity performs well, meaning that the degraded locations may have been plagued by statistical fluctuations and some detector malfunctioning.

E1) I-80 Eastbound

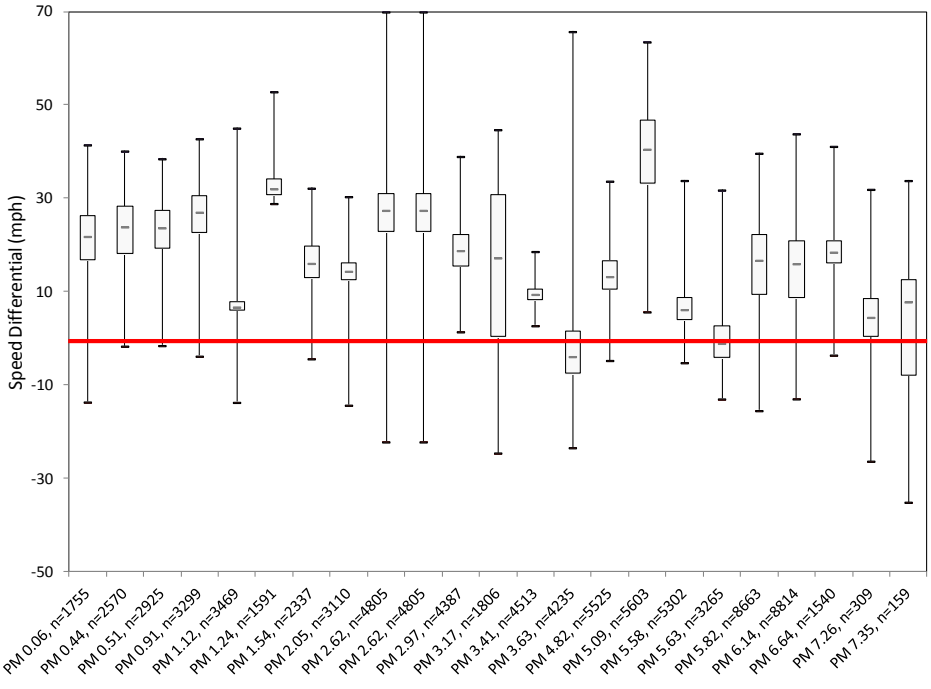

Figure E1. Speed differential (by segment, I-80 Eastbound)

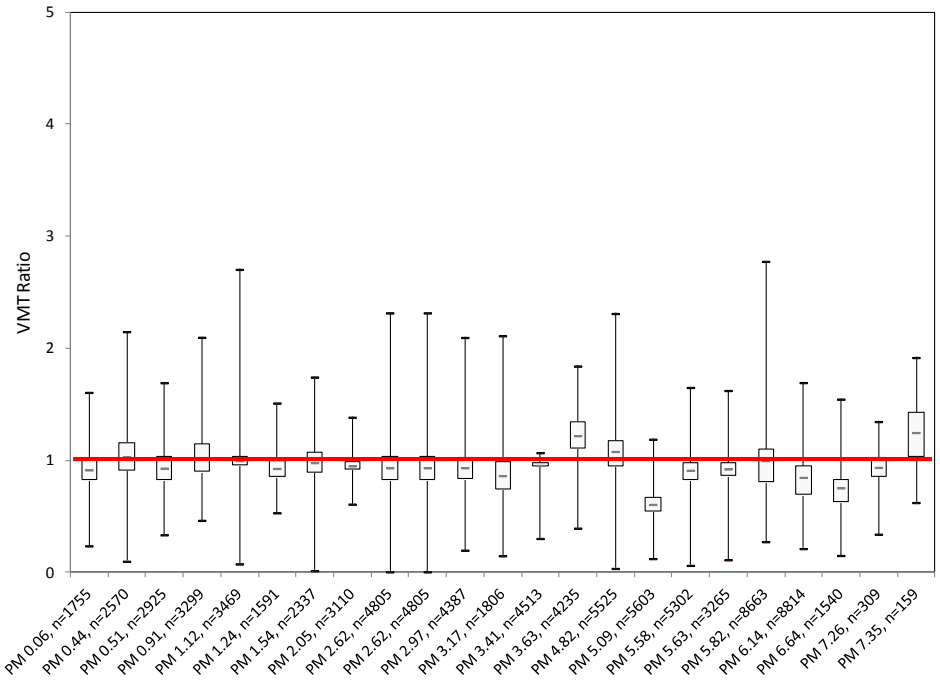

Figure E2. VMT Ratio (by segment, I-80 Eastbound)

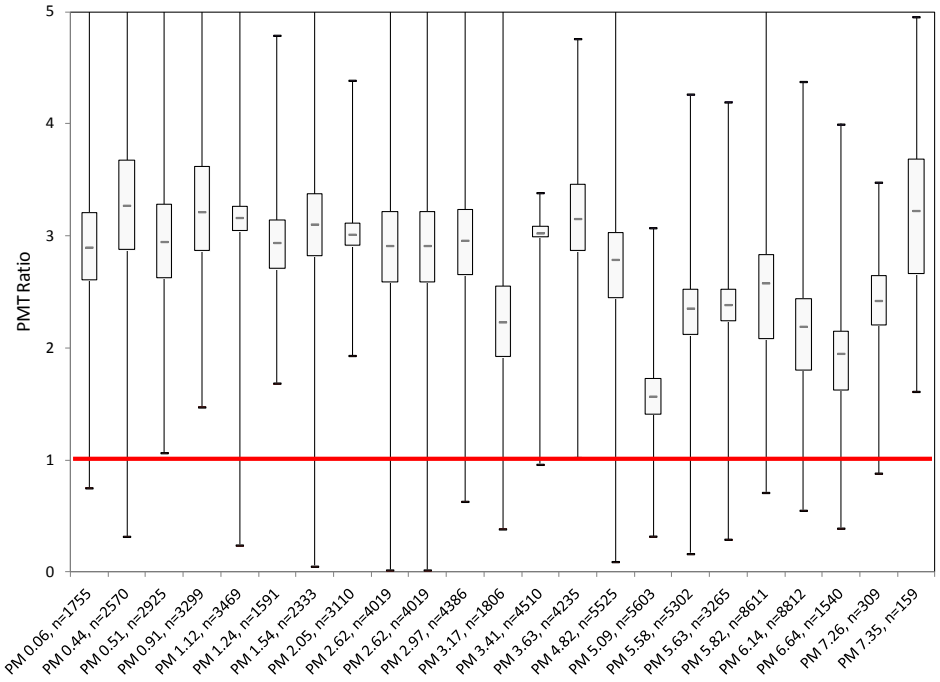

Figure E3. PMT Ratio (by segment, I-80 Eastbound)

E2) I-80 Westbound

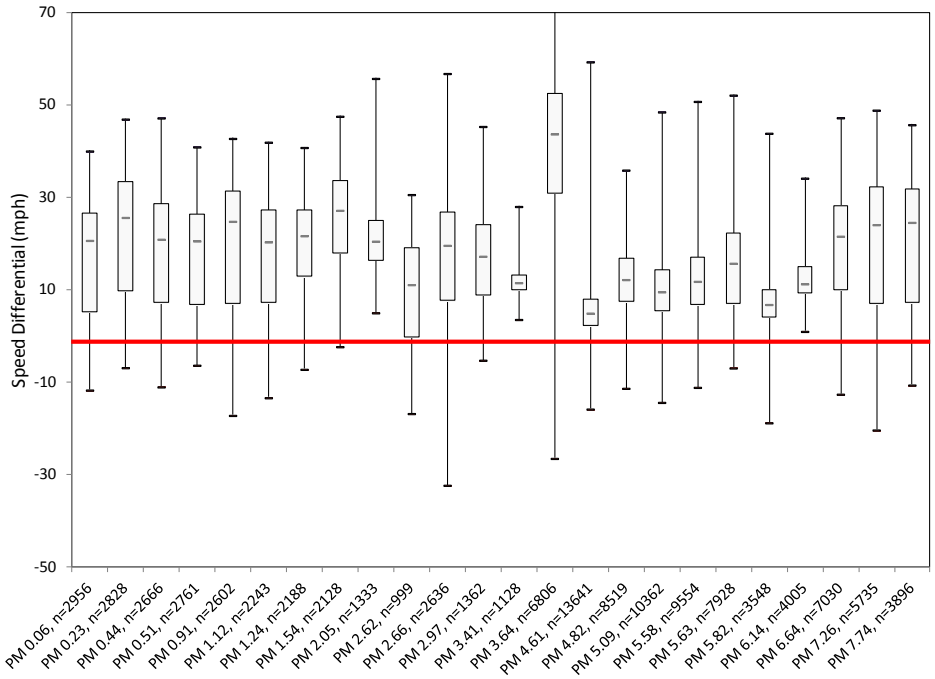

Figure E4. Speed differential (by segment, I-80 Westbound)

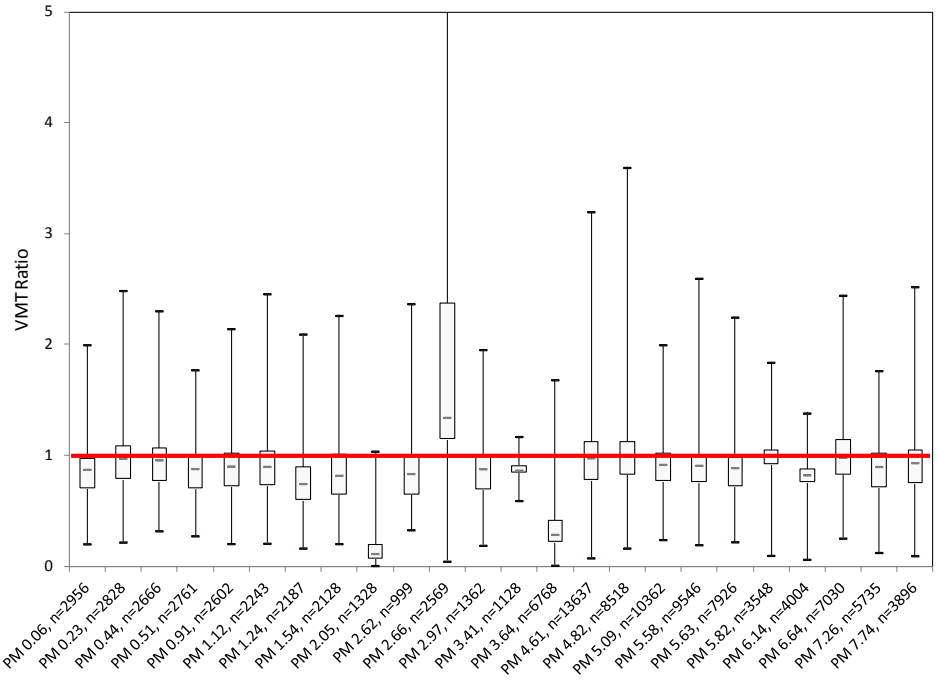

Figure E5. VMT Ratio (by segment, I-80 Westbound)

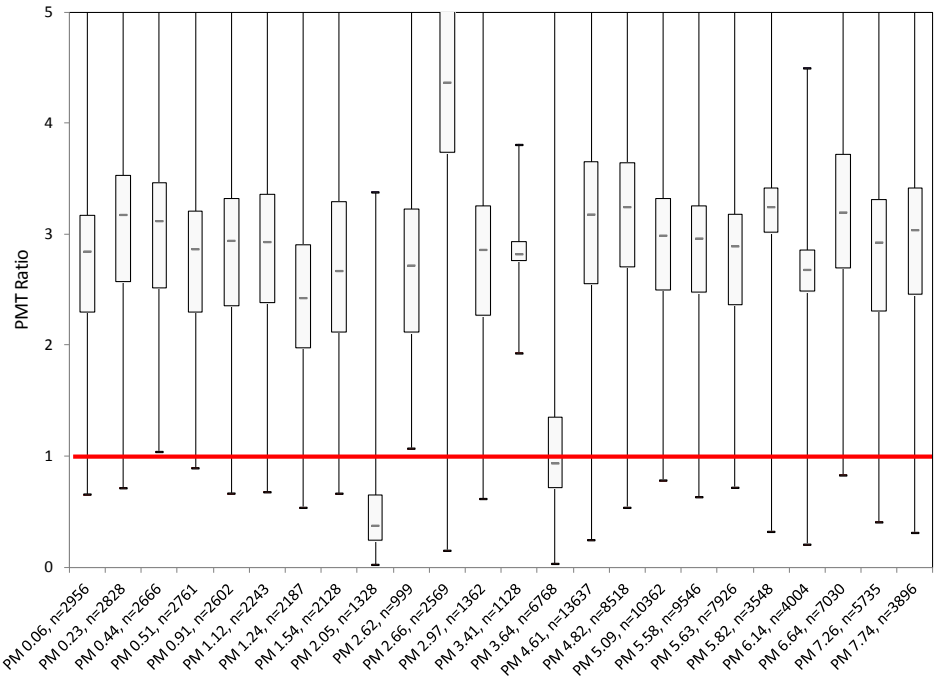

Figure E6. PMT Ratio (by segment, I-80 Westbound)

E3) I-680 Northbound

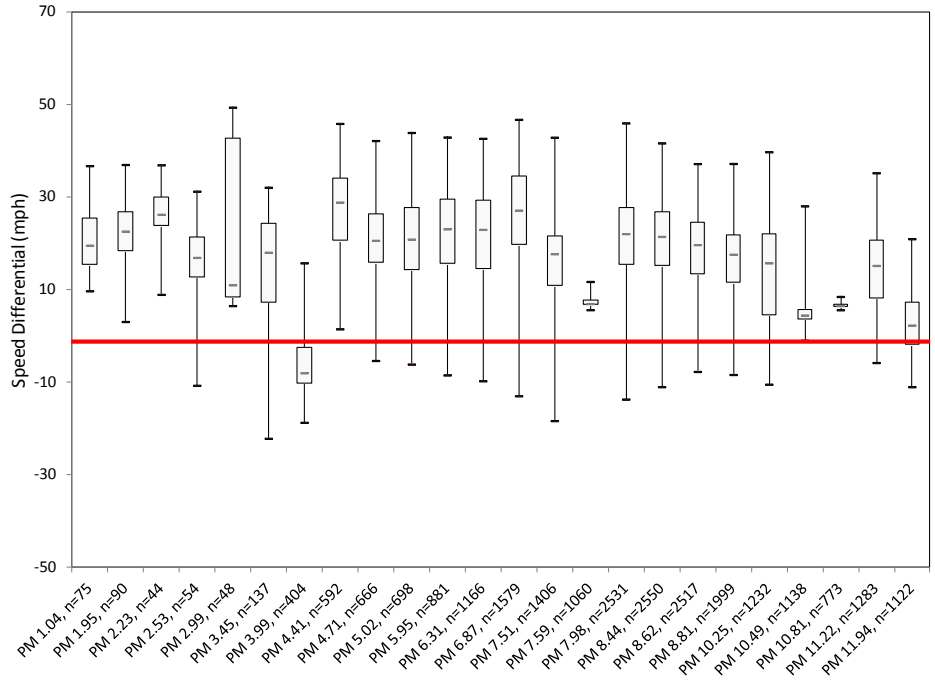

Figure E7. Speed differential (by segment, I-680 Northbound)

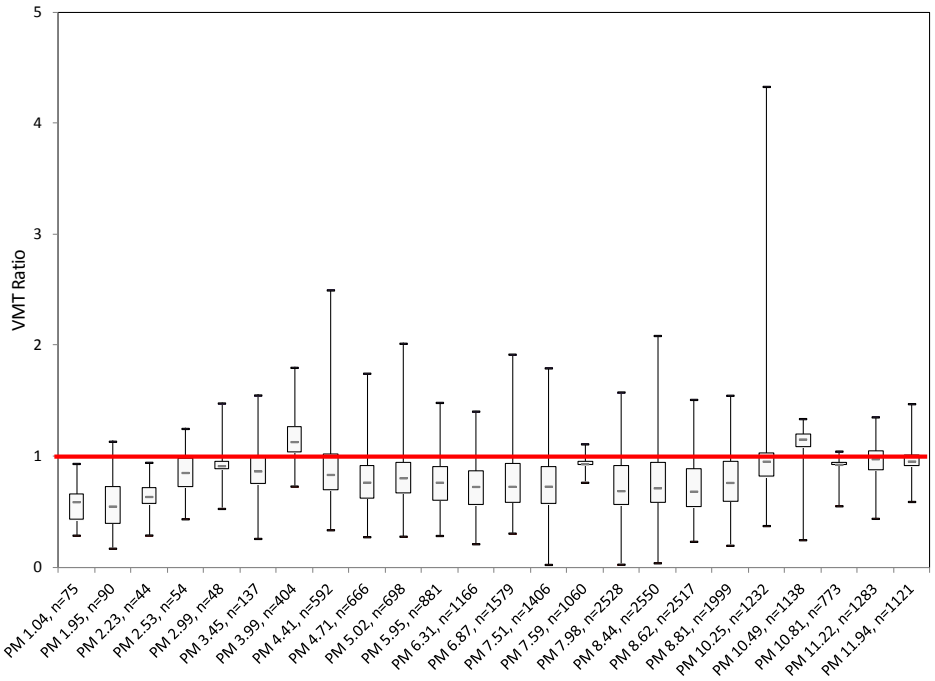

Figure E8. VMT Ratio (by segment, I-680 Northbound)

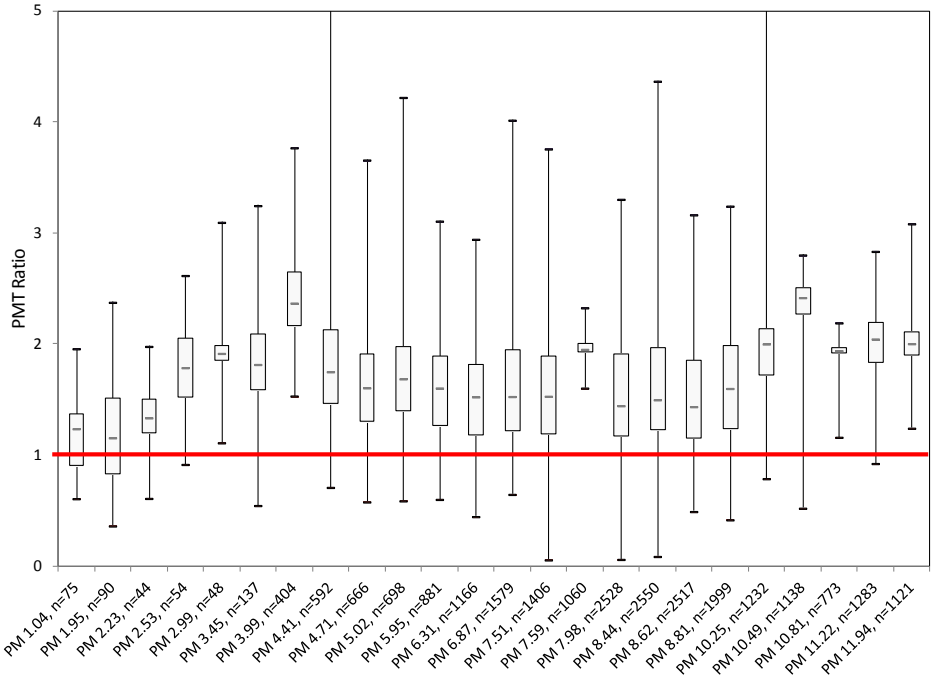

Figure E9. PMT Ratio (by segment, I-680 Northbound)

E4) I-680 Southbound

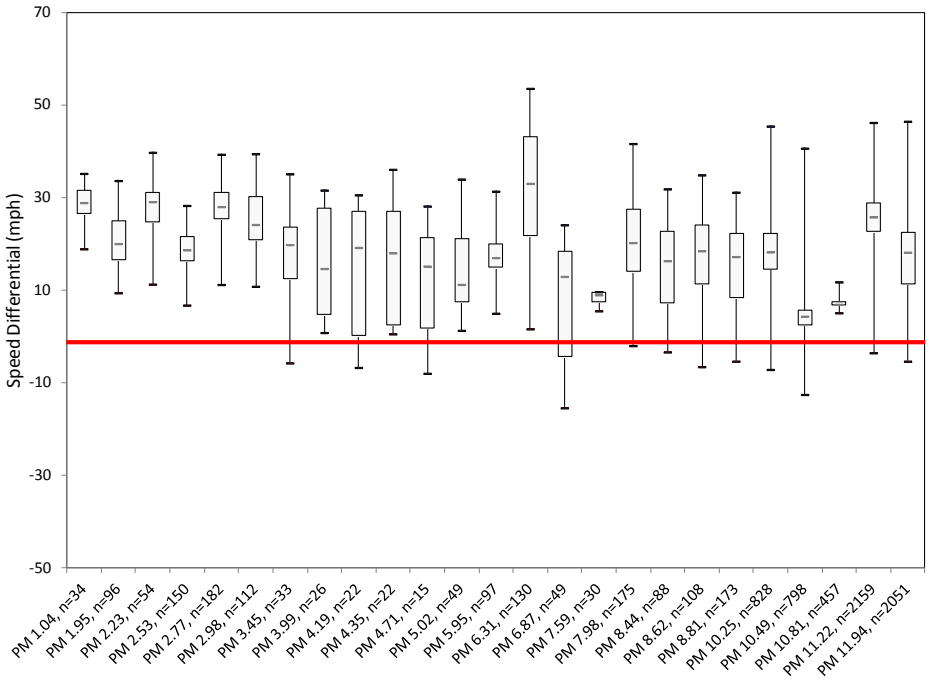

Figure E10. Speed differential (by segment, I-680 Southbound)

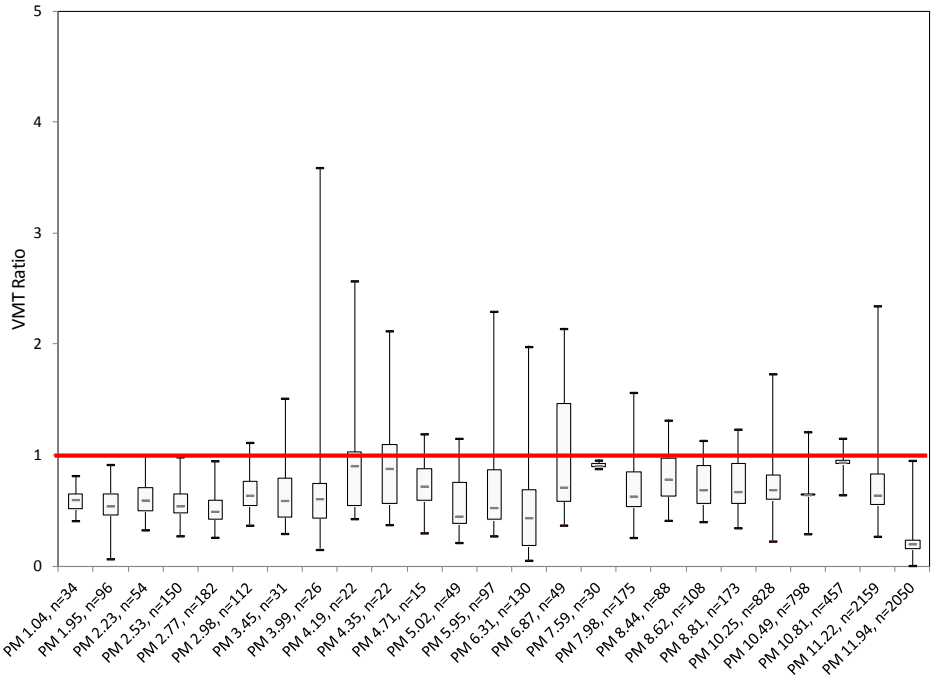

Figure E11. VMT Ratio (by segment, I-680 Southbound)

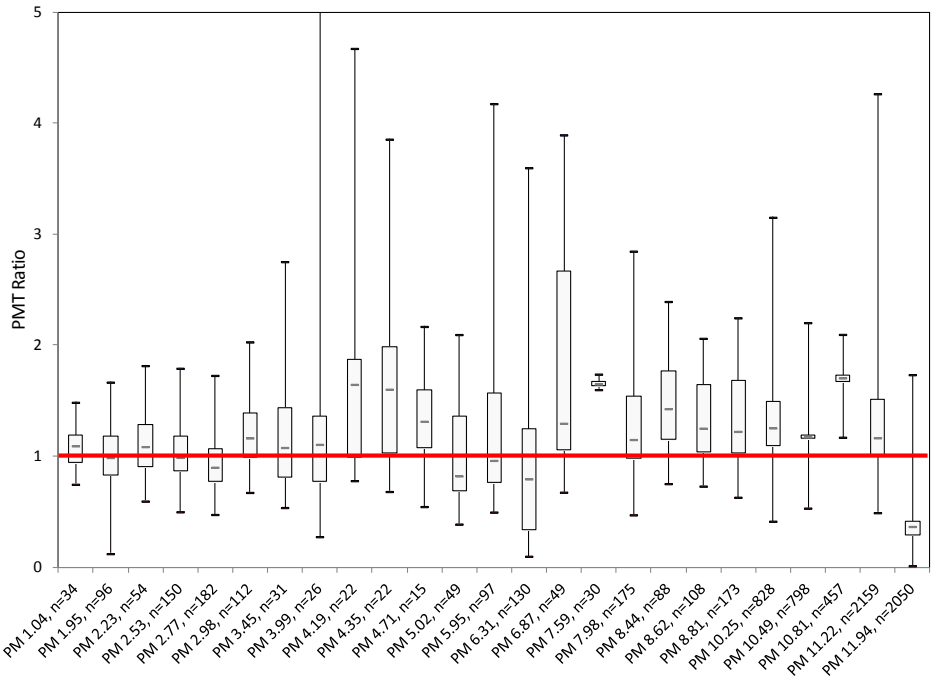

Figure E12. PMT Ratio (by segment, I-680 Southbound)

E5) I-880 Northbound

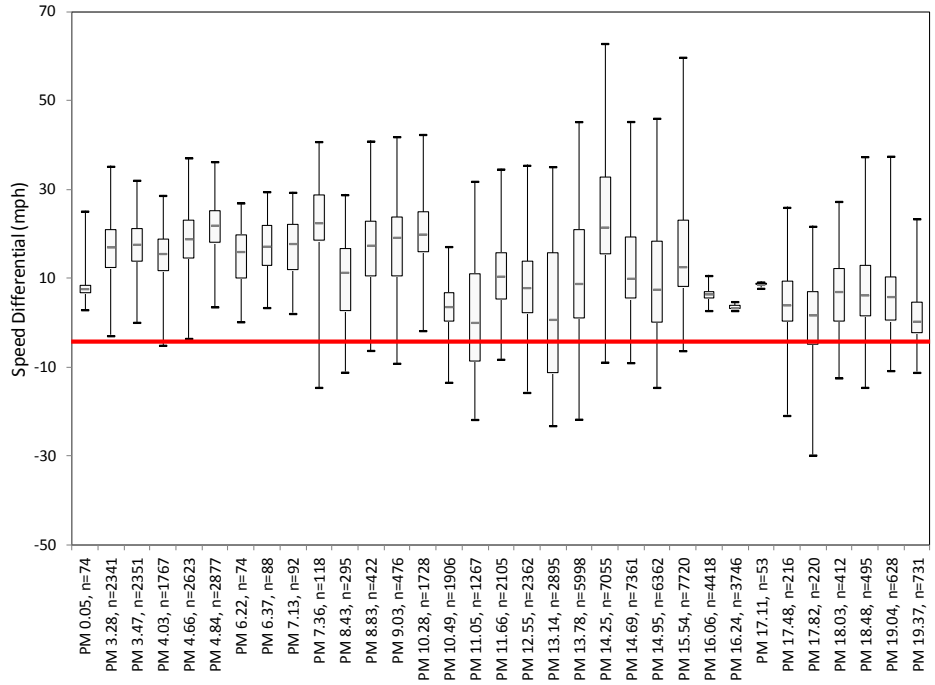

Figure E13. Speed differential (by segment, I-880 Northbound)

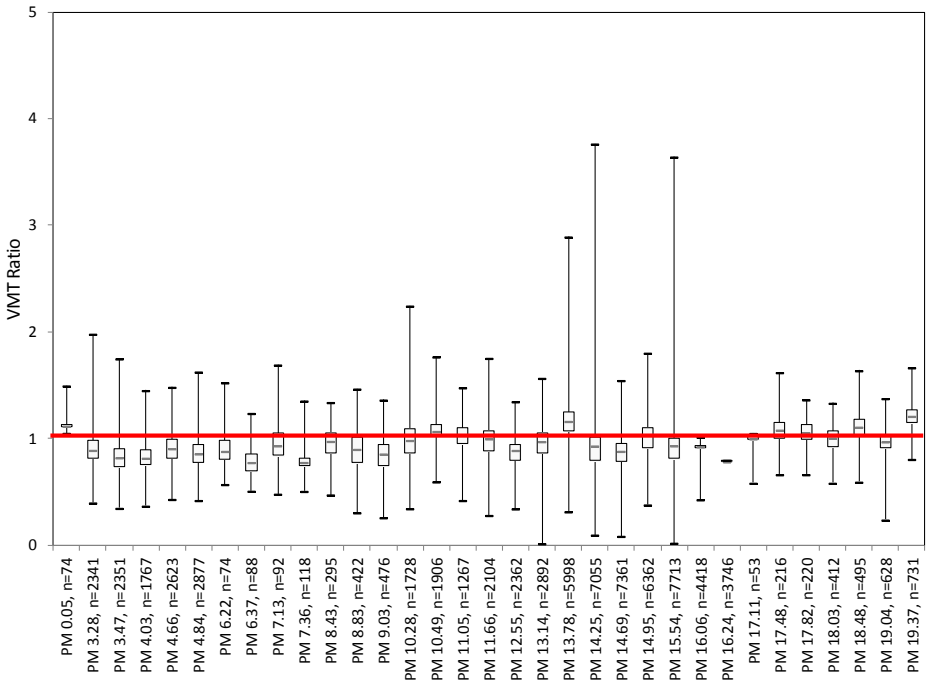

Figure E14. VMT Ratio (by segment, I-880 Northbound)

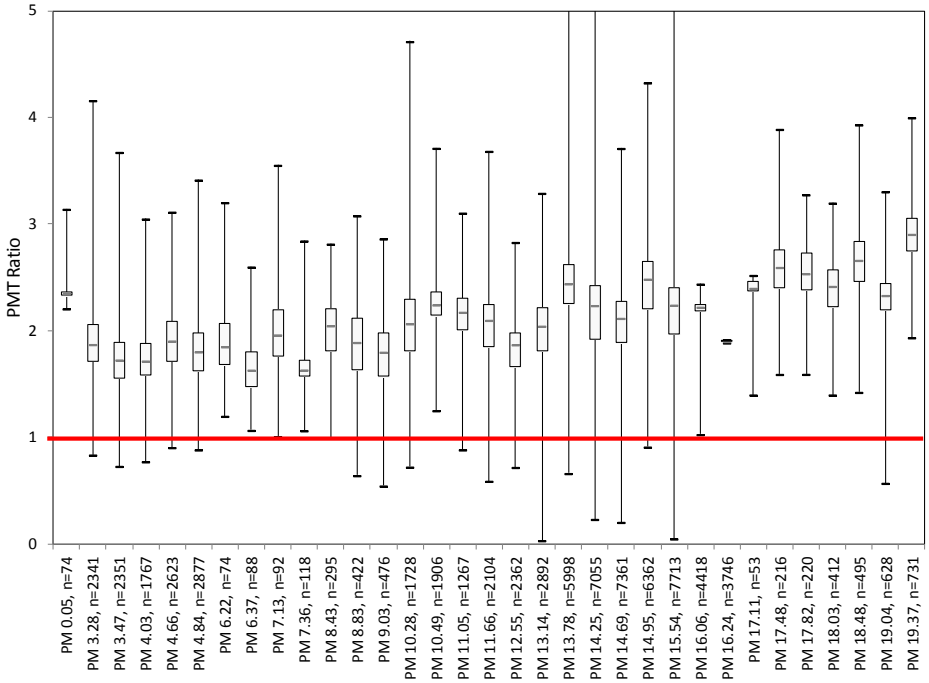

Figure E15. PMT Ratio (by segment, I-880 Northbound)

E6) SR-101 Northbound

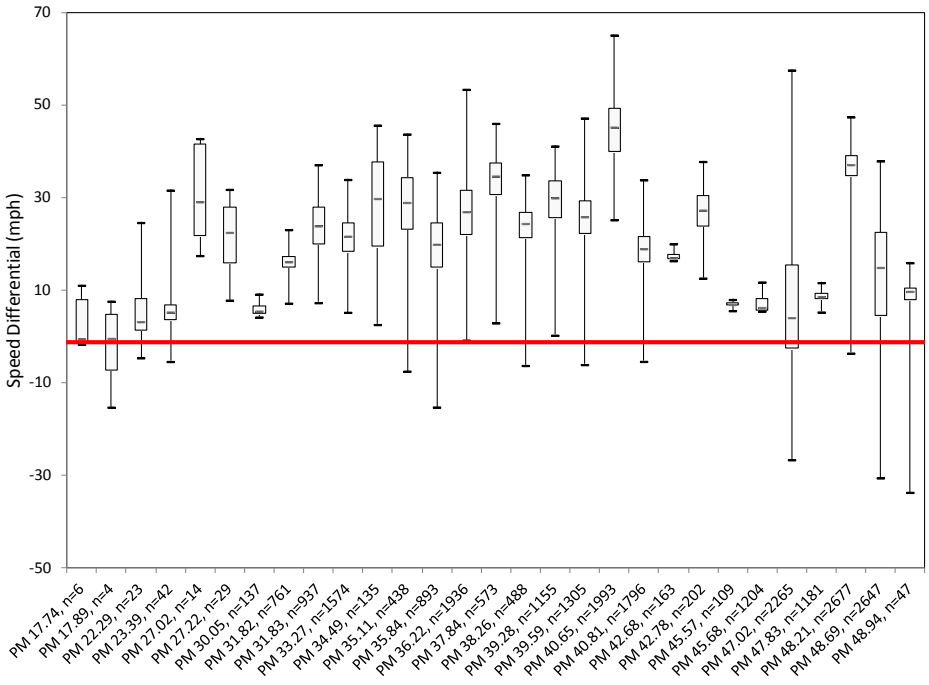

Figure E16. Speed differential (by segment, SR-101 Northbound)

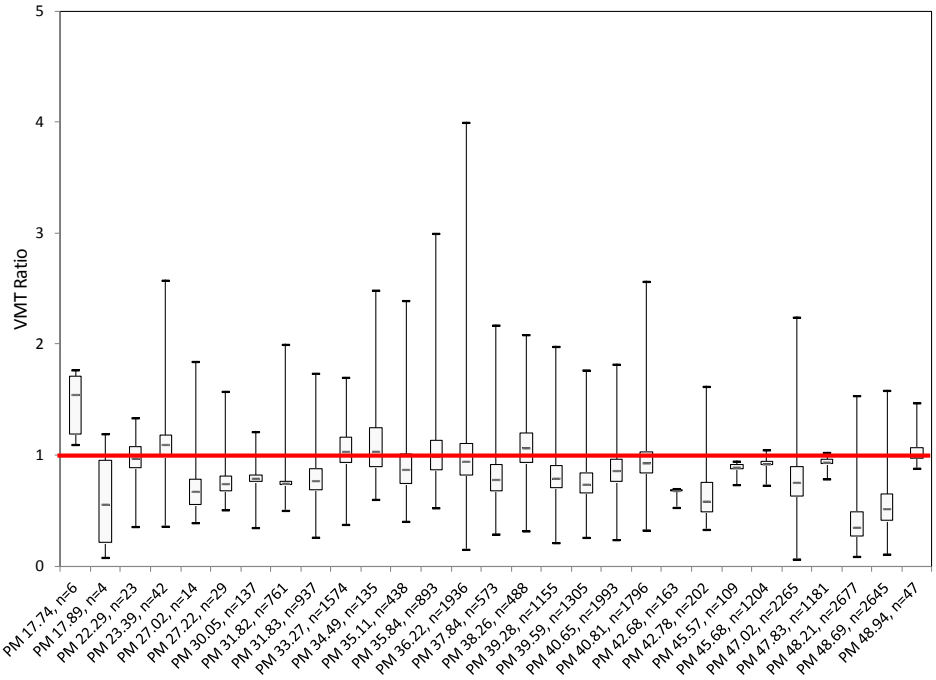

Figure E17. VMT Ratio (by segment, SR-101 Northbound)

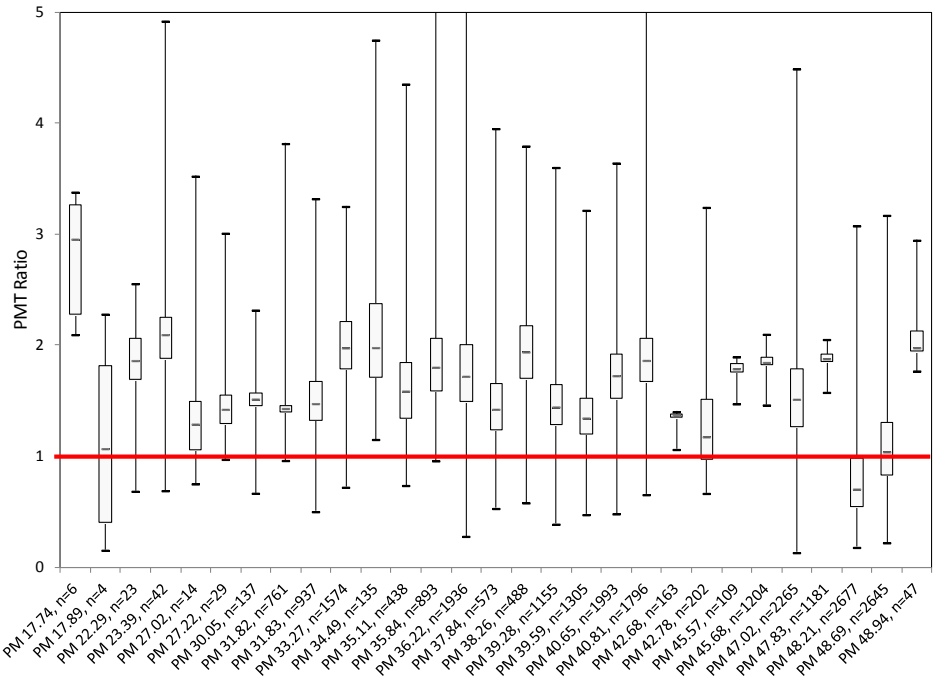

Figure E18. PMT Ratio (by segment, SR-101 Northbound)

E7) SR-101 Southbound

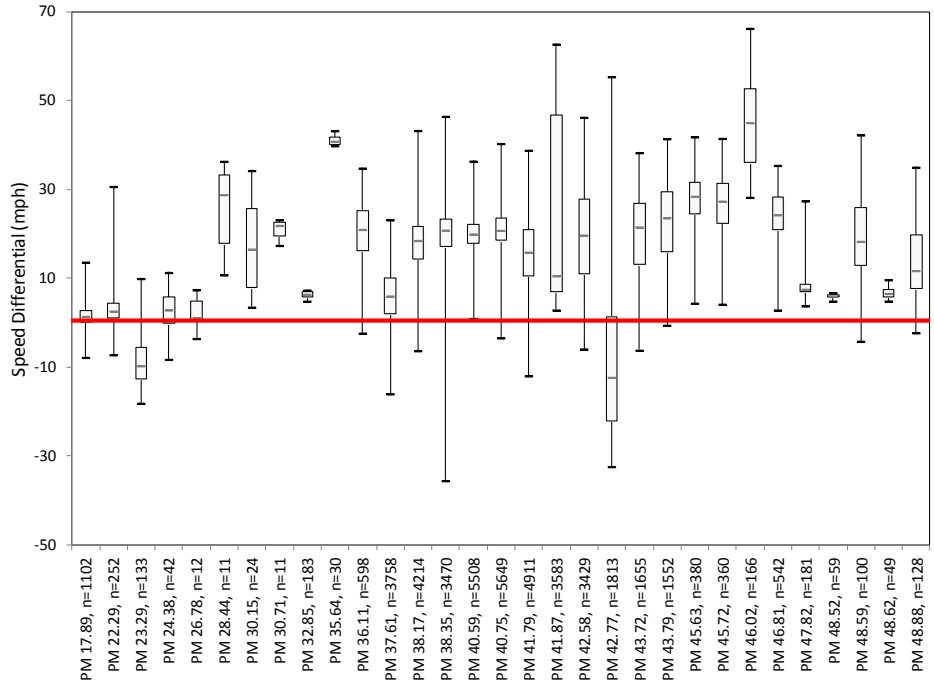

Figure E19. Speed differential (by segment, SR-101 Southbound)

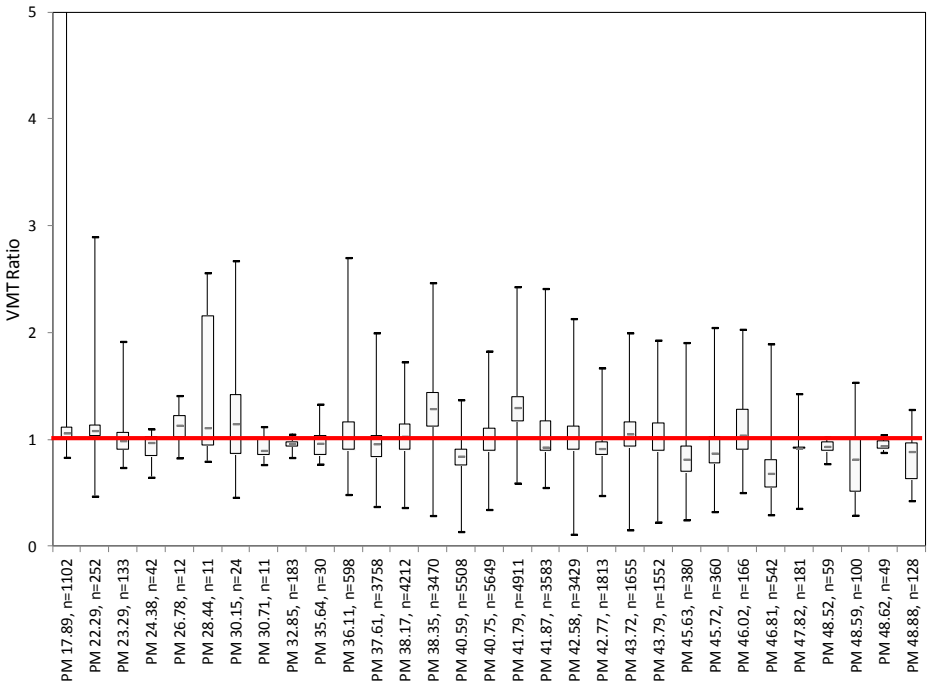

Figure E20. VMT Ratio (by segment, SR-101 Southbound)

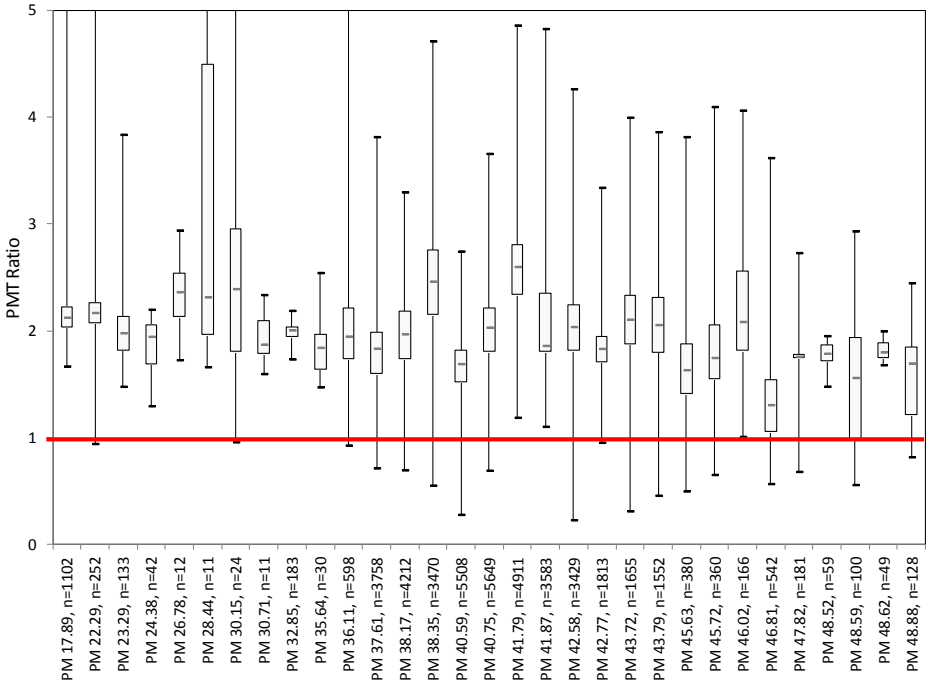

Figure E21. PMT Ratio (by segment, SR-101 Southbound)

Appendix F Detailed Results of Performance Measures, District 7

In District 7, we examined 6 study corridors: four with full-time buffer-separated access and two with part-time limited access. For each segment or each detector, we computed three performance measures – speed differential, VMT ratio and PMT ratio. There are some sections where HOV facilities exhibit degraded performance compared with a GP lane on average. Some noticeable findings are summarized below.

- In the section from PM R4.6 to PM R7.56 of I-105E, negative speed differentials were observed while the level of utilization is not indicated as degraded.
- In almost all sections of I-210 Eastbound, speed differentials between HOV and GP lanes are not shown to be significant due to high utilization by vehicles (VMT ratio is close to 1). But PMT ratio is below 2 for most of the time (not very high).
- In almost all sections of I-405 Southbound, speed differentials between HOV and GP lanes are not shown to be significant due to high utilization by vehicles (VMT ratio is close to 1).
- SR-14 Northbound and Southbound do not have enough samples (not much congested during HOV operation hours) to draw reasonable interpretations for HOV performance.

F1) I-105 Eastbound

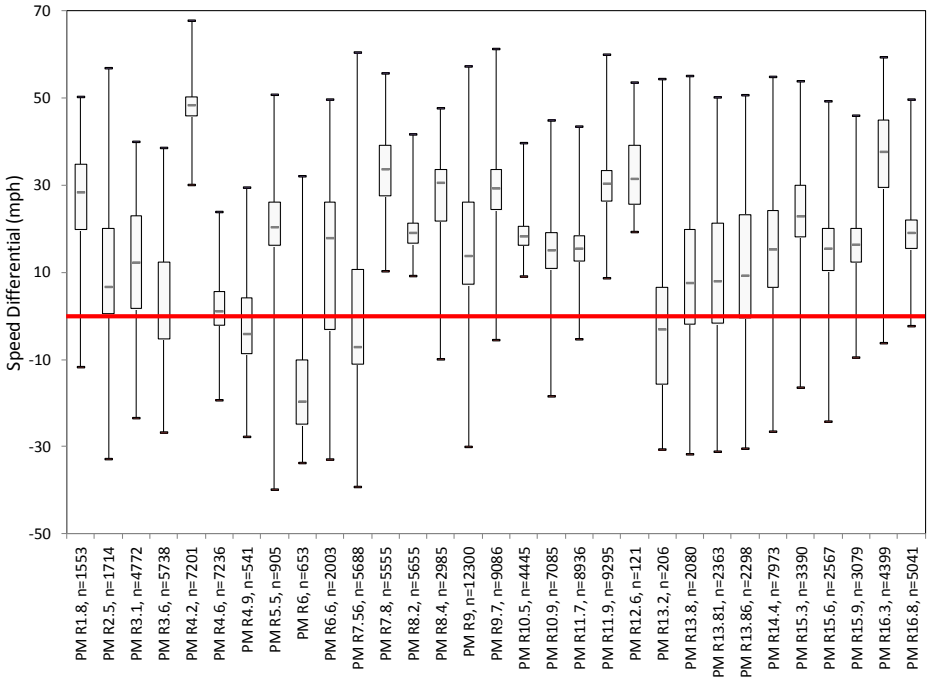

Figure F1. Speed differential (by segment, I-105 Eastbound)

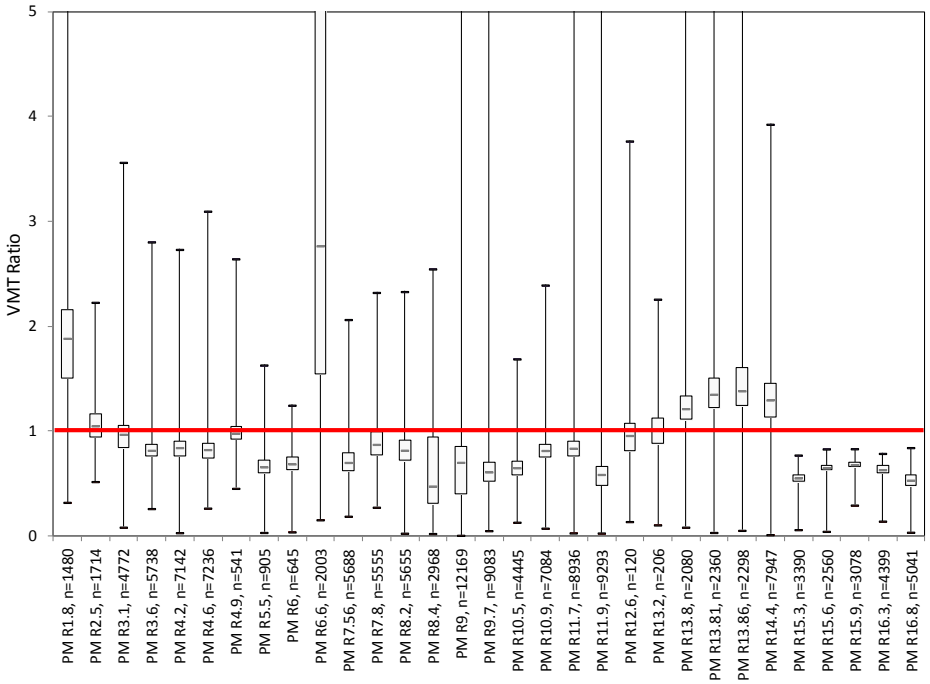

Figure F2. VMT Ratio (by segment, I-105 Eastbound)

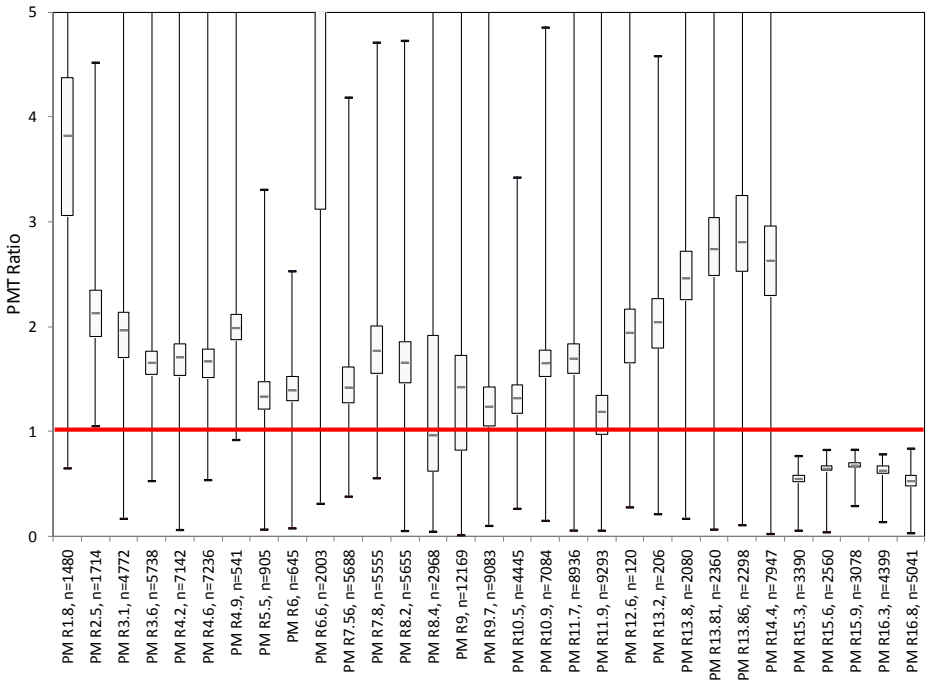

Figure F3. PMT Ratio (by segment, I-105 Eastbound)

F2) I-105 Westbound

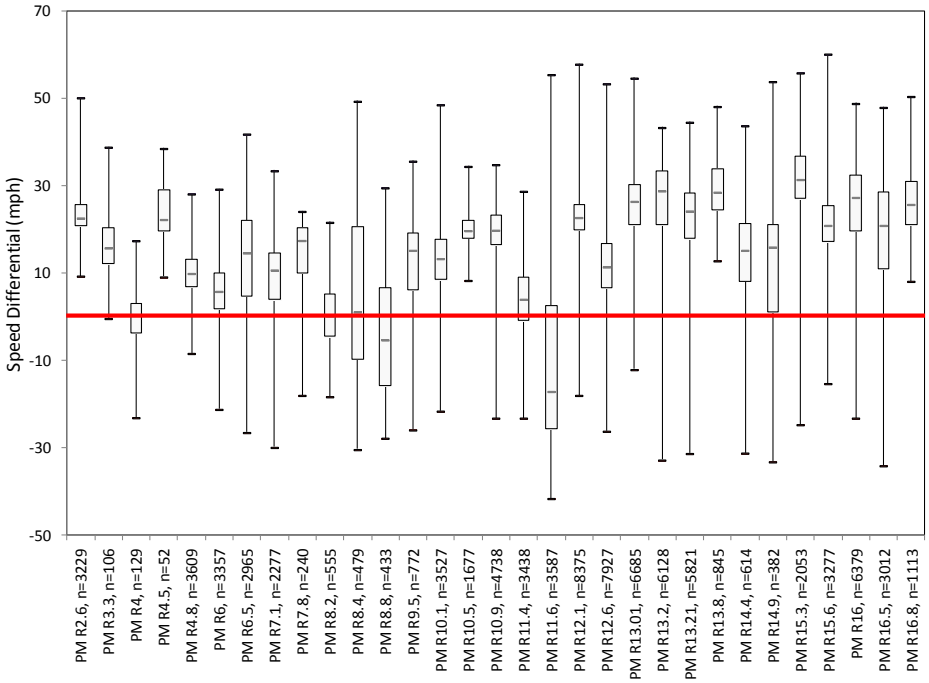

Figure F4. Speed differential (by segment, I-105 Westbound)

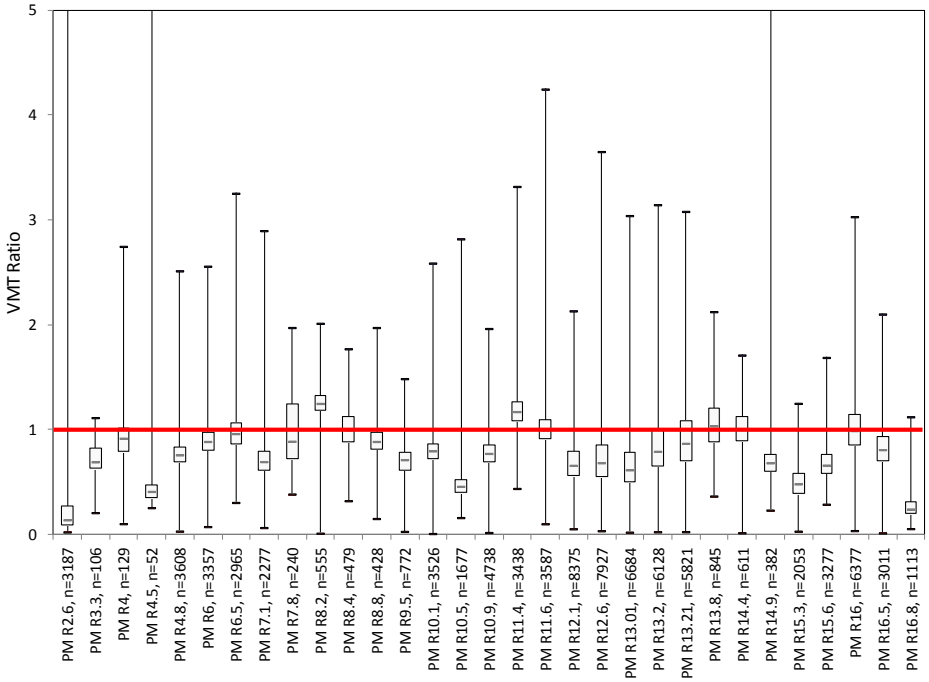

Figure F5. VMT Ratio (by segment, I-105 Westbound)

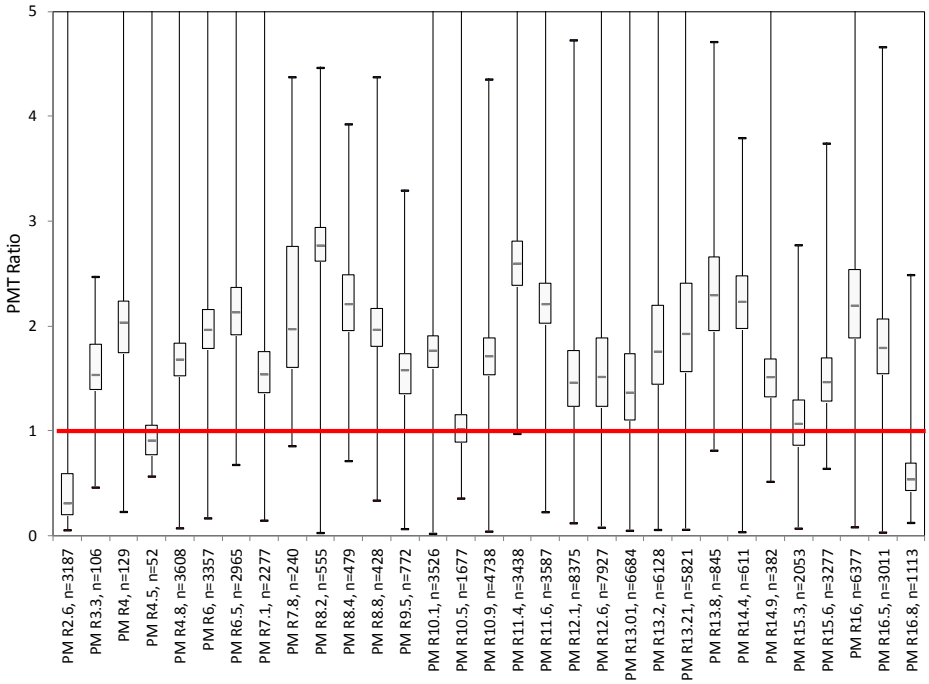

Figure F6. PMT Ratio (by segment, I-105 Westbound)

F3) I-210 Eastbound

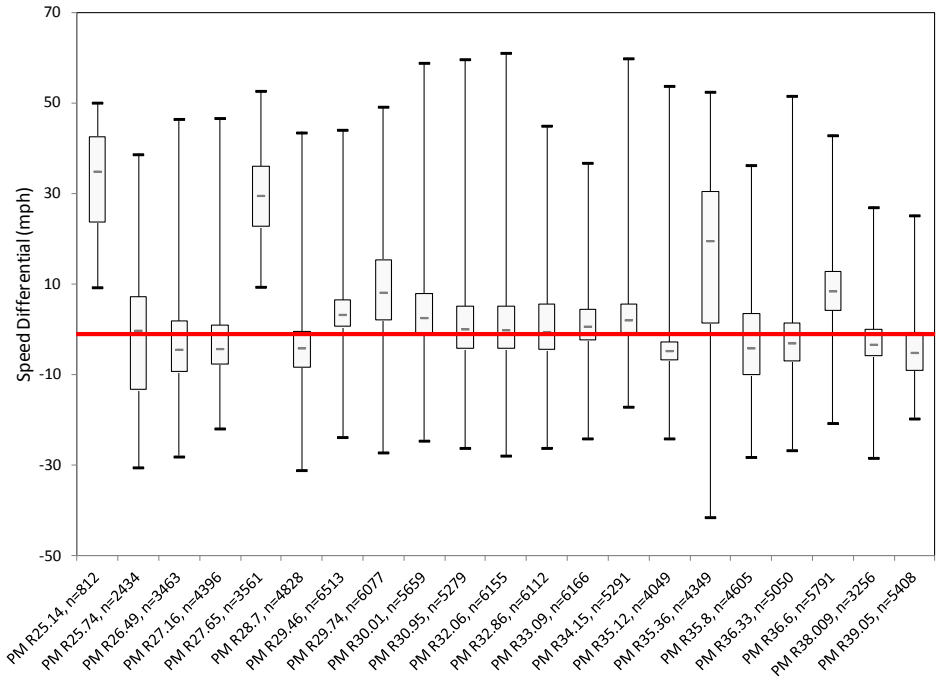

Figure F7. Speed differential (by segment, I-210 Eastbound)

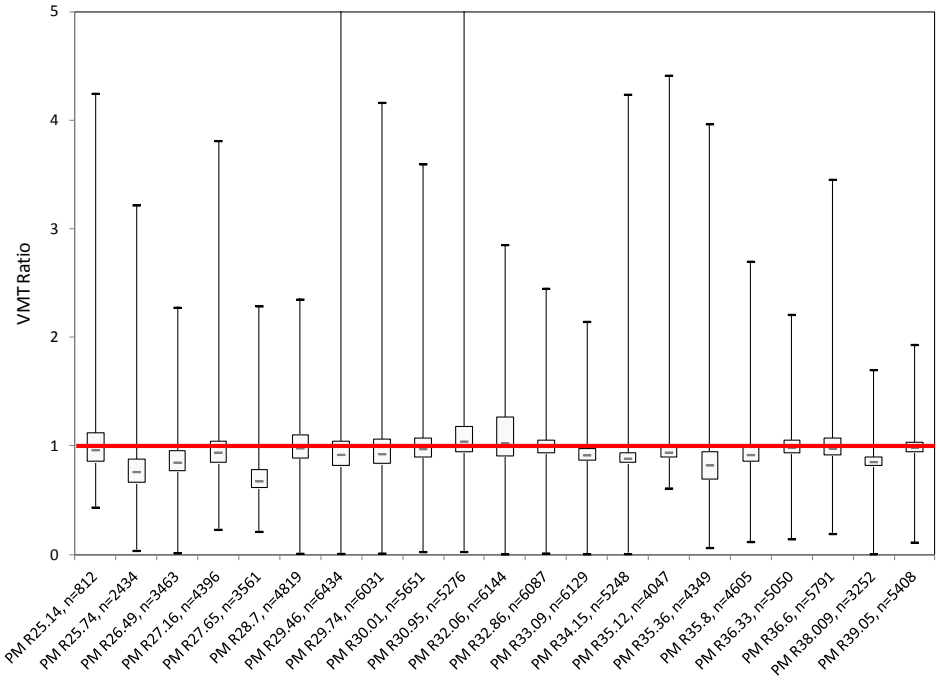

Figure F8. VMT Ratio (by segment, I-210 Eastbound)

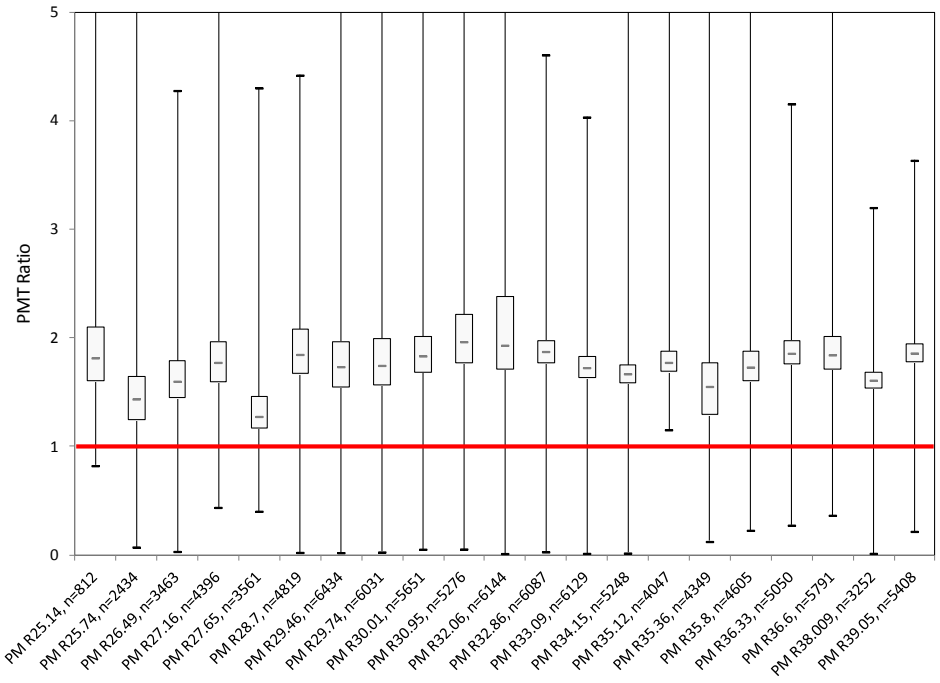

Figure F9. PMT Ratio (by segment, I-210 Eastbound)

F4) I-405 Southbound

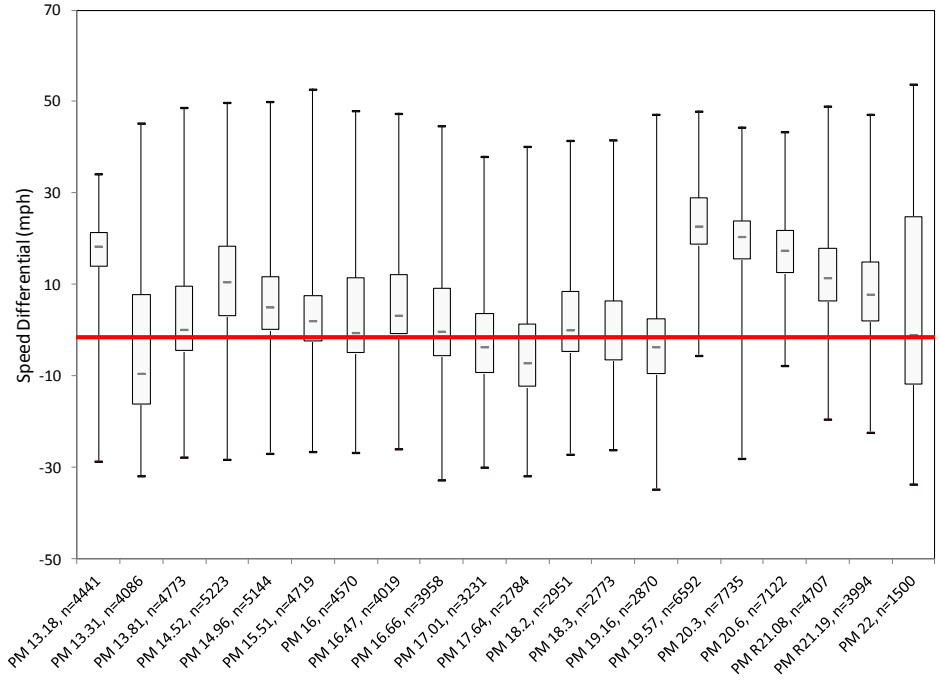

Figure F10. Speed differential (by segment, I-405 Southbound)

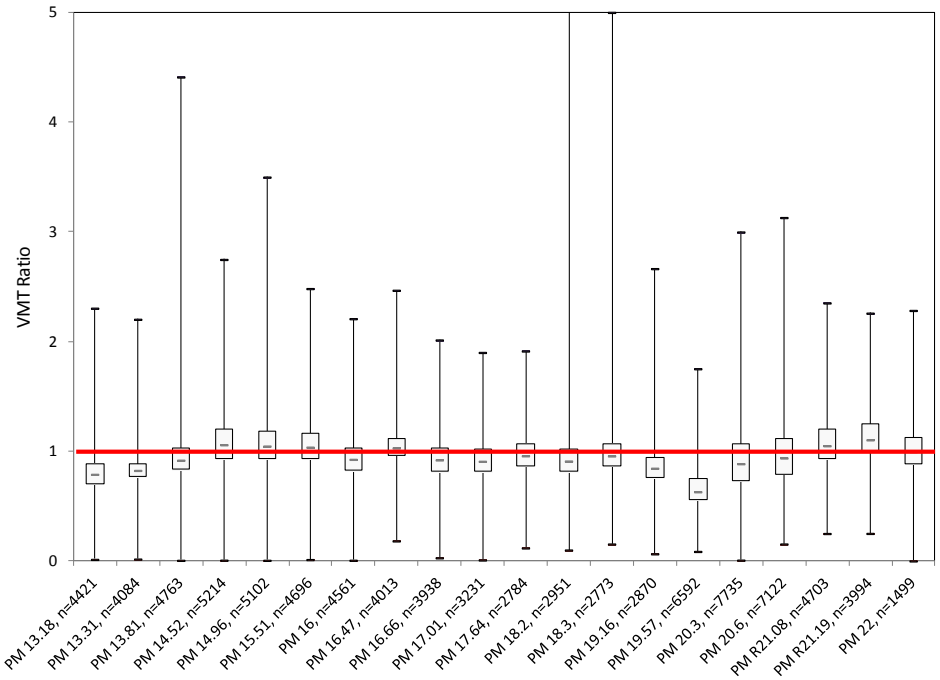

Figure F11. VMT Ratio (by segment, I-405 Southbound)

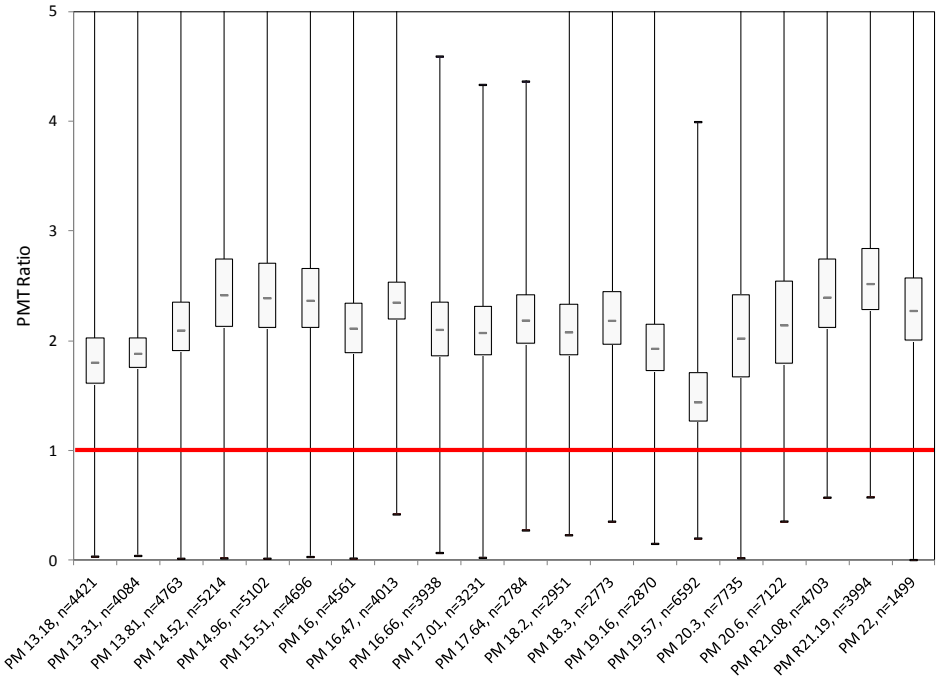

Figure F12. PMT Ratio (by segment, I-405 Southbound)

F5) SR-14 Northbound

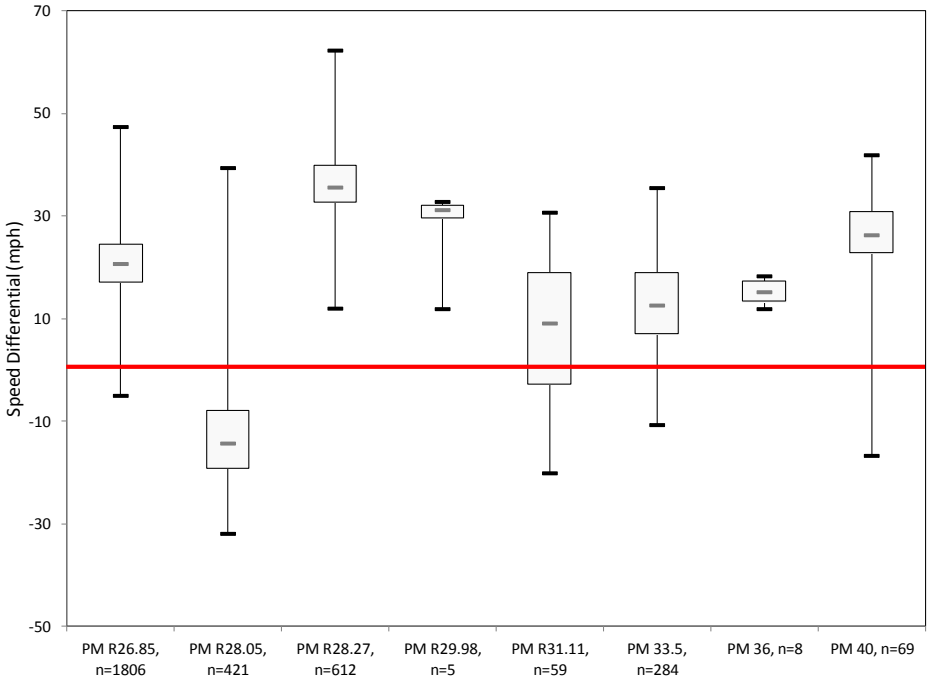

Figure F13. Speed differential (by segment, SR-14 Northbound)

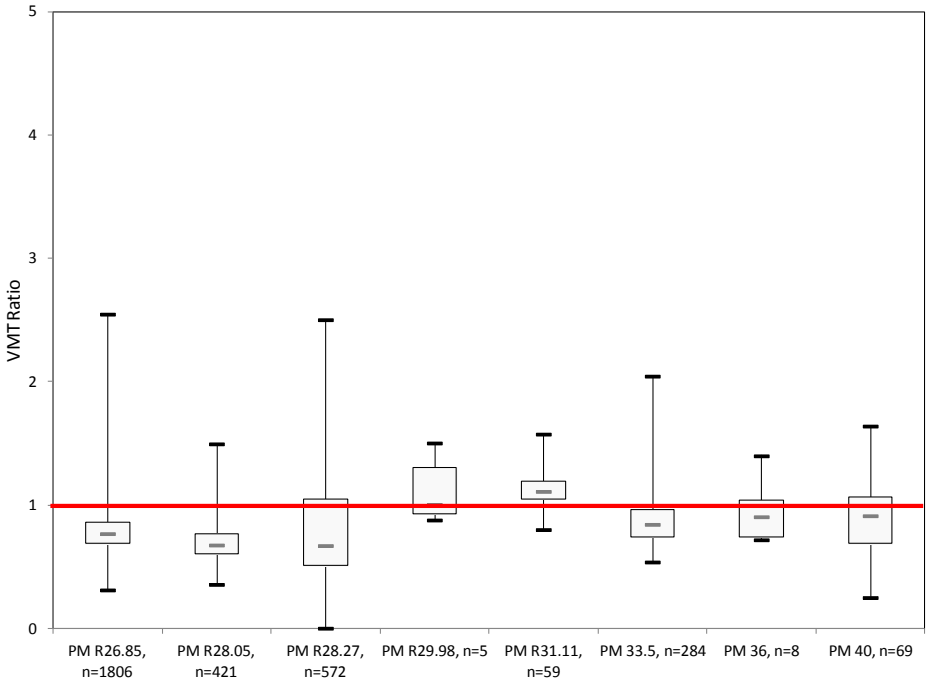

Figure F14. VMT Ratio (by segment, SR-14 Northbound)

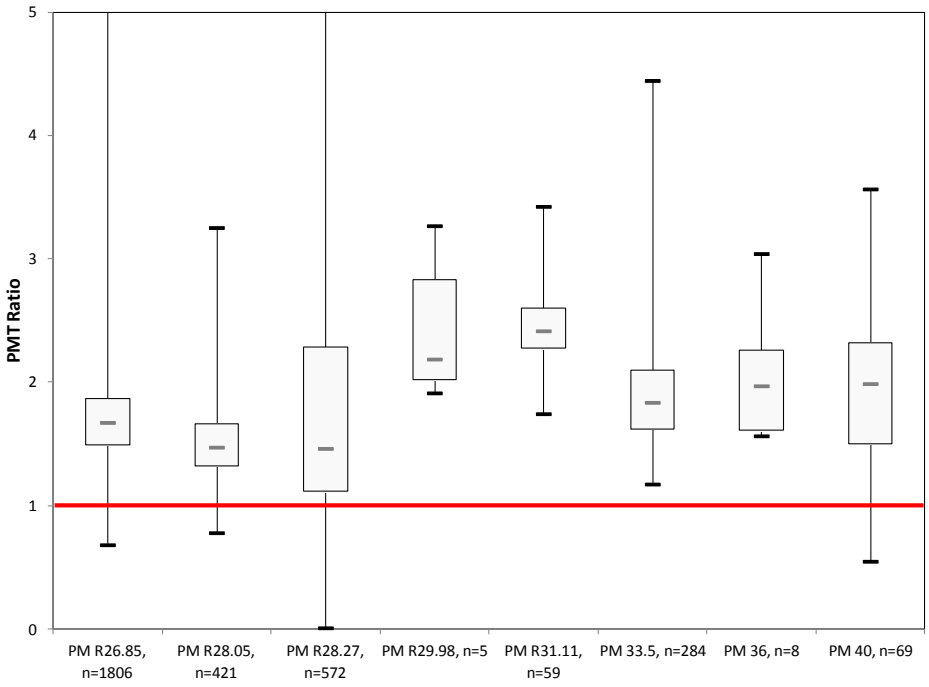

Figure F15. PMT Ratio (by segment, SR-14 Northbound)

F6) SR-14 Southbound

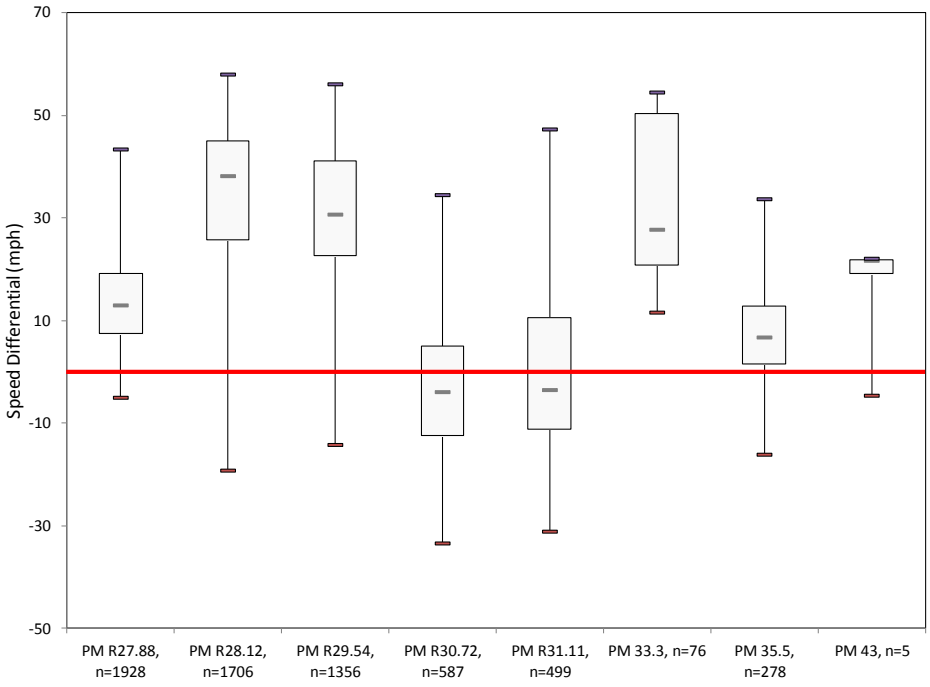

Figure F16. Speed differential (by segment, SR-14 Southbound)

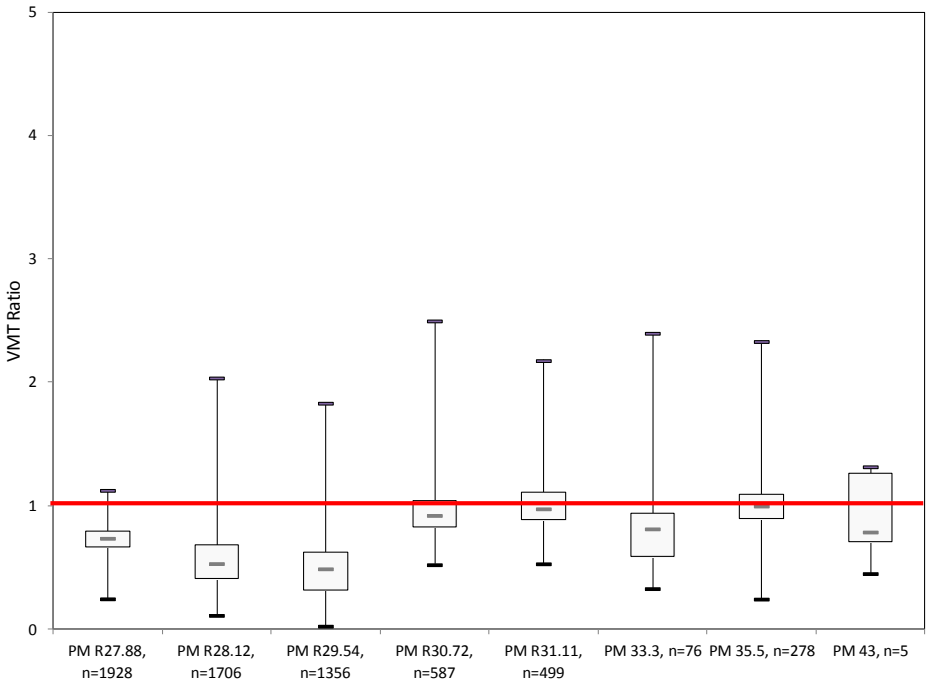

Figure F17. VMT Ratio (by segment, SR-14 Southbound)

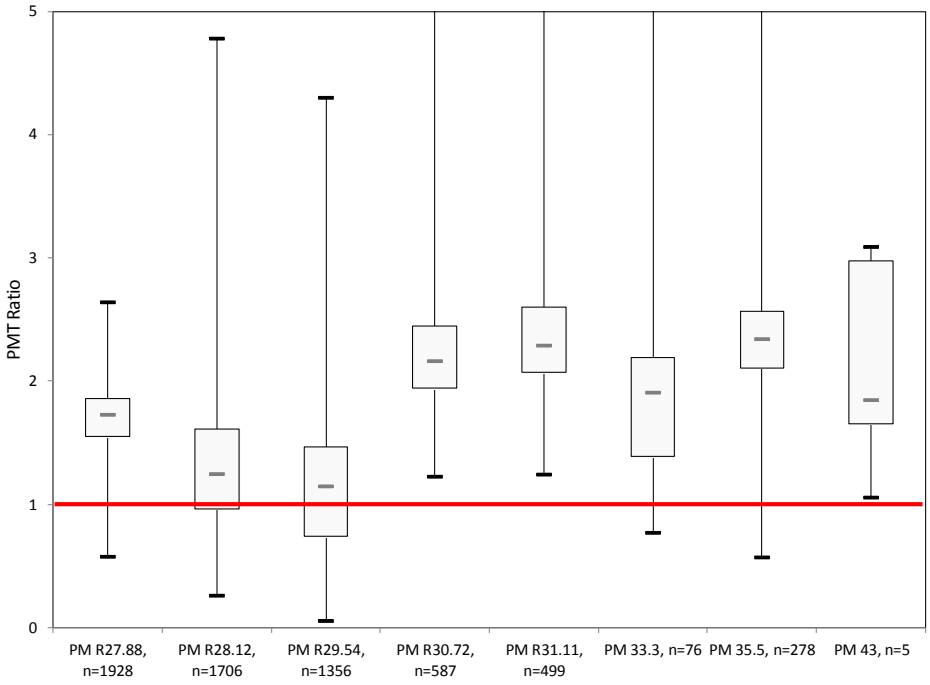

Figure F18. PMT Ratio (by segment, SR-14 Southbound)

Appendix G Detailed Results of Performance Measures, District 12

In District 12, we examined 10 study corridors: four with full-time continuous access and six with full-time limited access. For each segment or each detector, we computed three performance measures – speed differential, VMT ratio and PMT ratio. There are some sections where HOV facilities exhibit degraded performance compared with a GP lane on average. Some noticeable findings are summarized below.

- In the section from PM R23.5 to PM R26.81 in I-5 Northbound, negative speed differentials were observed while the level of utilization is not indicated as degraded.
- In the section from PM 9.4 to PM 14.46 in I-5 Southbound, negative speed differentials were observed while the level of utilization is not indicated as degraded.
- In both directions of SR-22, the level of utilizations by both vehicles and people are shown to be low (VMT ratio is lower than 0.5 and PMT ratio is below 1).

G1) I-5 Northbound

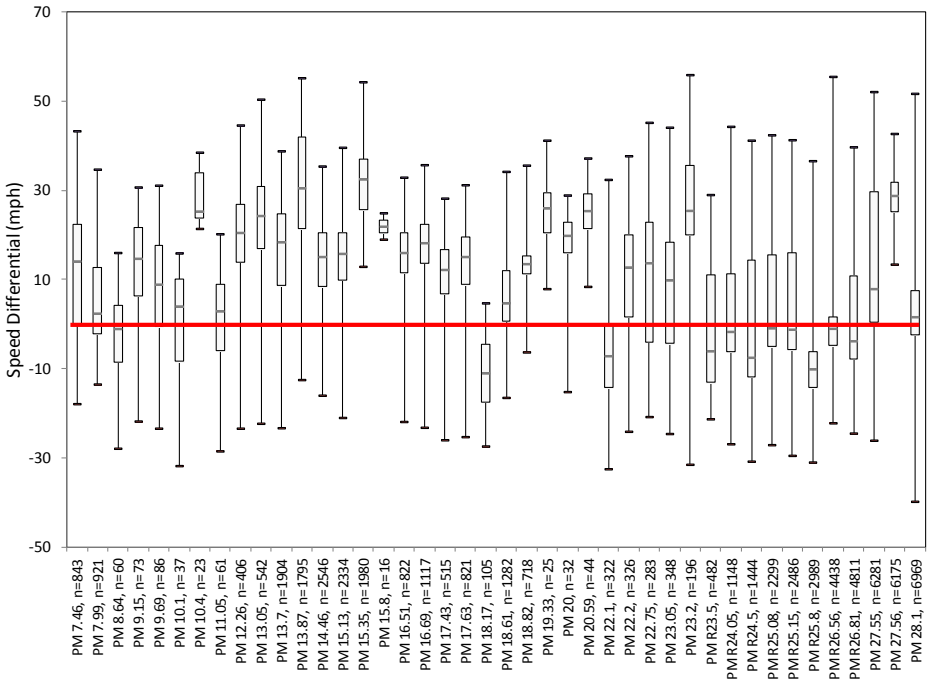

Figure G1. Speed differential (by segment, I-5 Northbound)

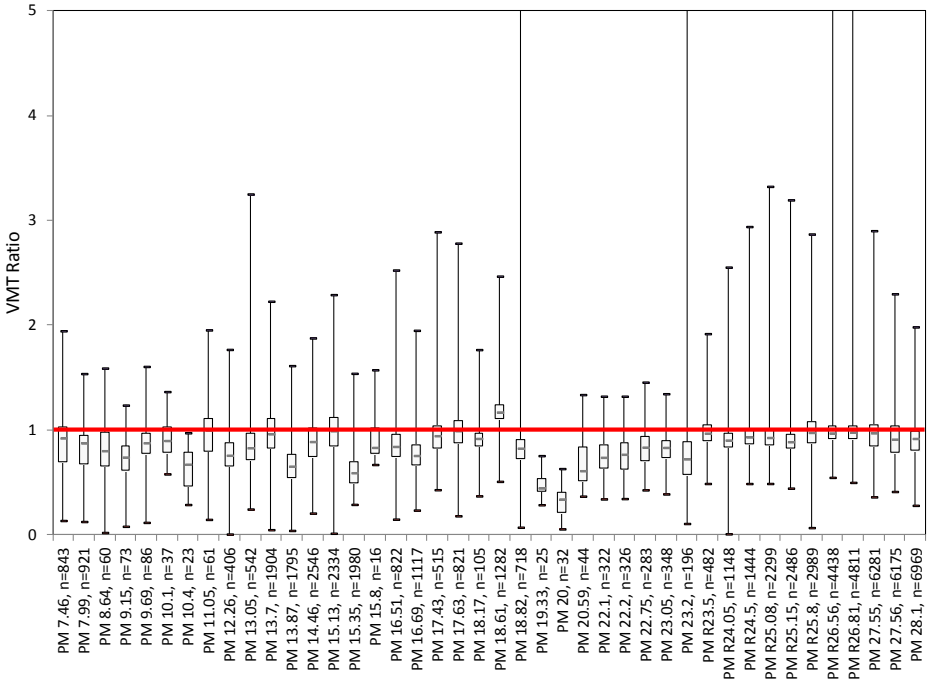

Figure G2. VMT Ratio (by segment, I-5 Northbound)

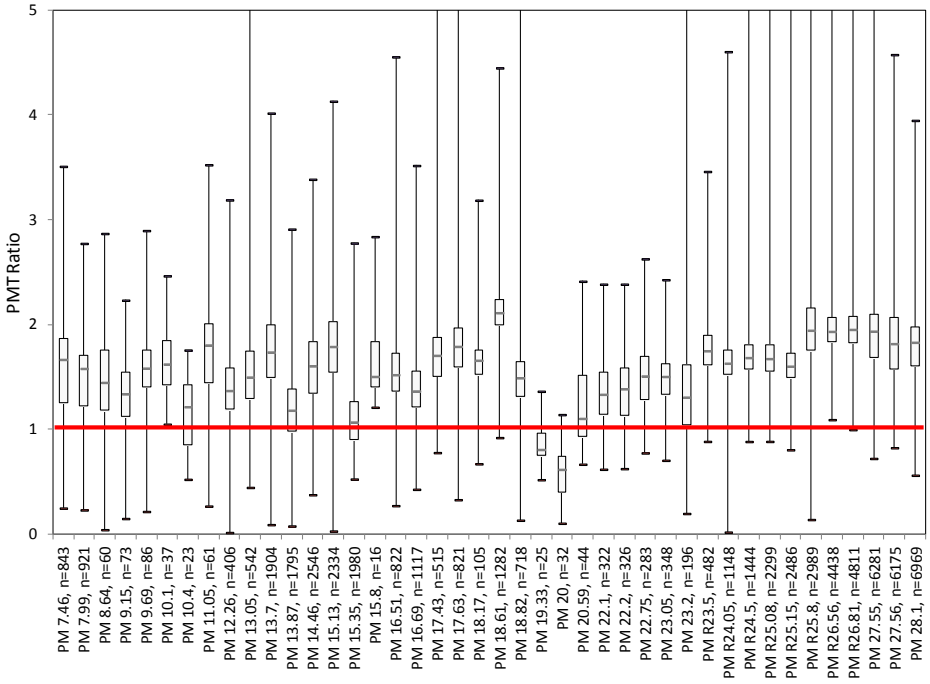

Figure G3. PMT Ratio (by segment, I-5 Northbound)

G2) I-5 Southbound

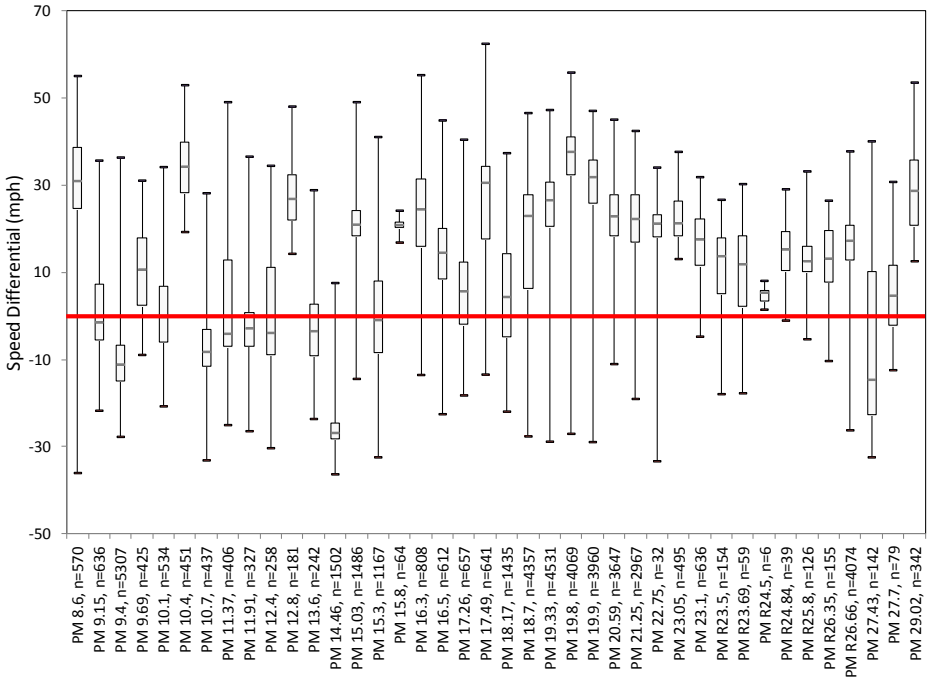

Figure G4. Speed differential (by segment, I-5 Southbound)

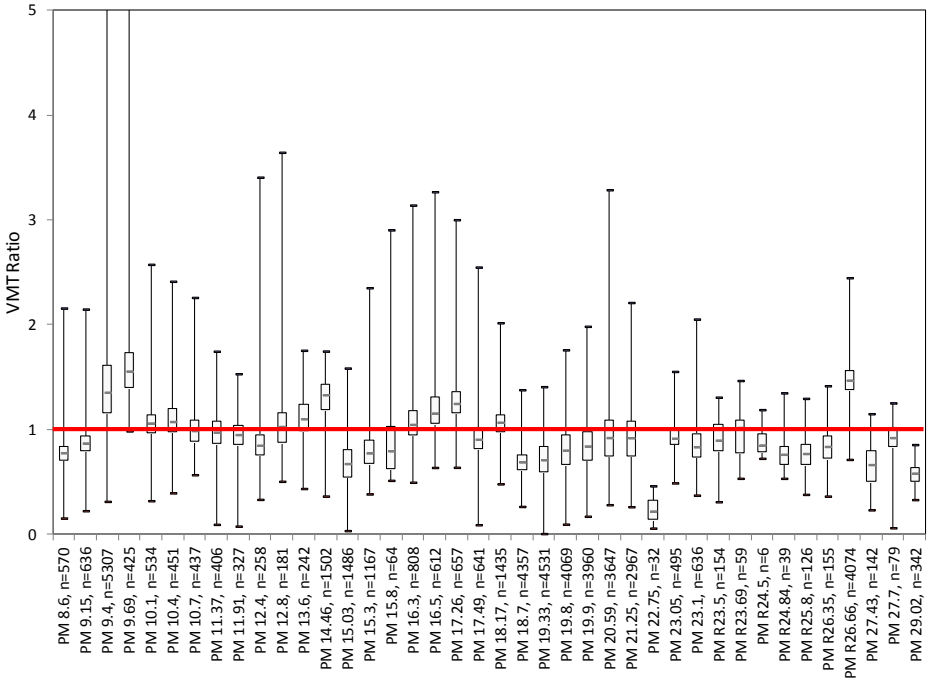

Figure G5. VMT Ratio (by segment, I-5 Southbound)

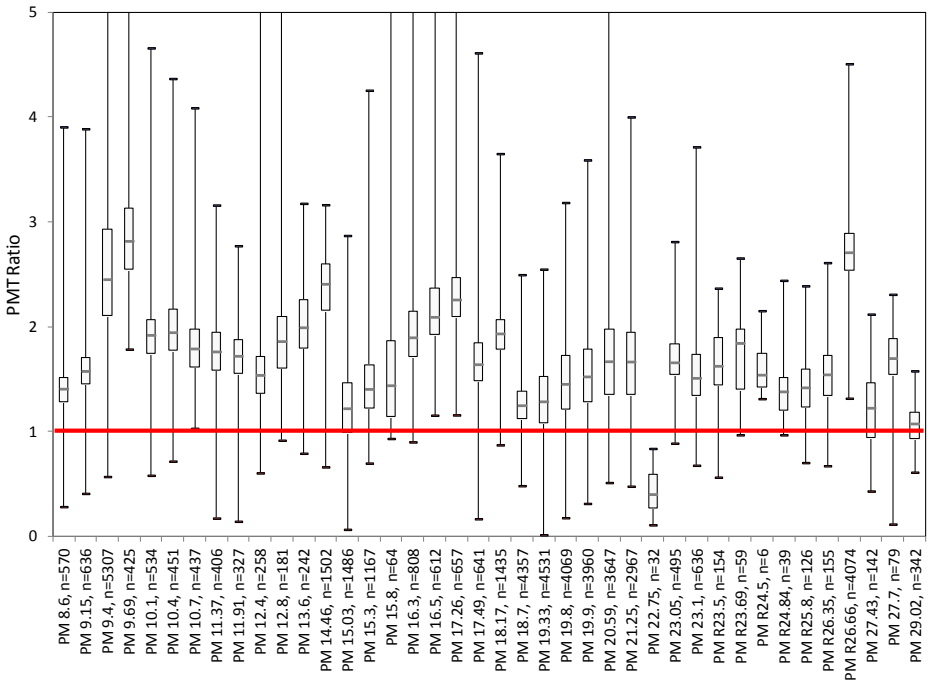

Figure G6. PMT Ratio (by segment, I-5 Southbound)

G3) I-405 Northbound

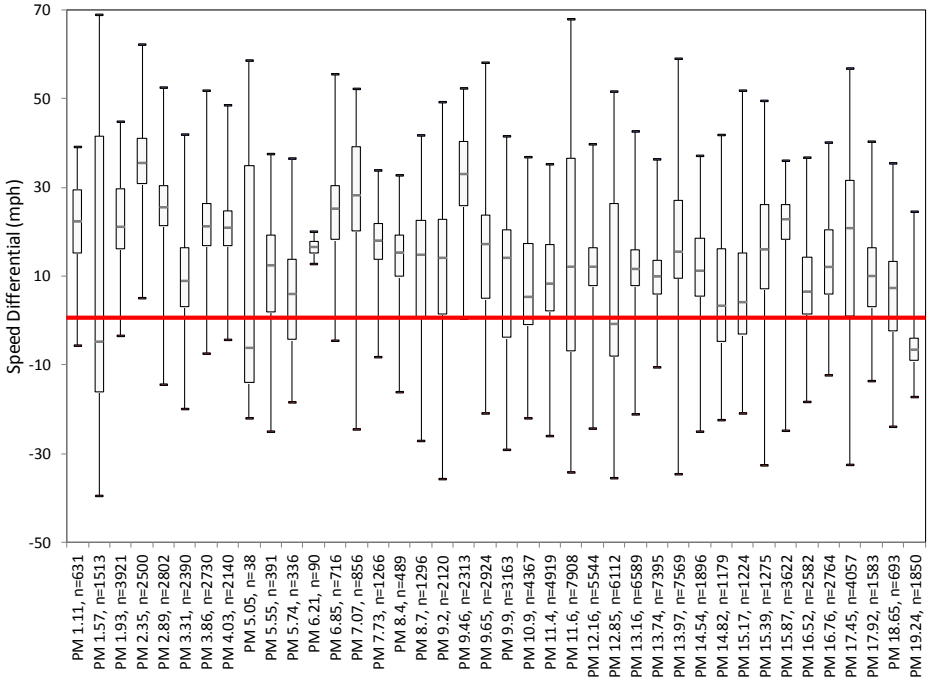

Figure G7. Speed differential (by segment, I-405 Northbound)

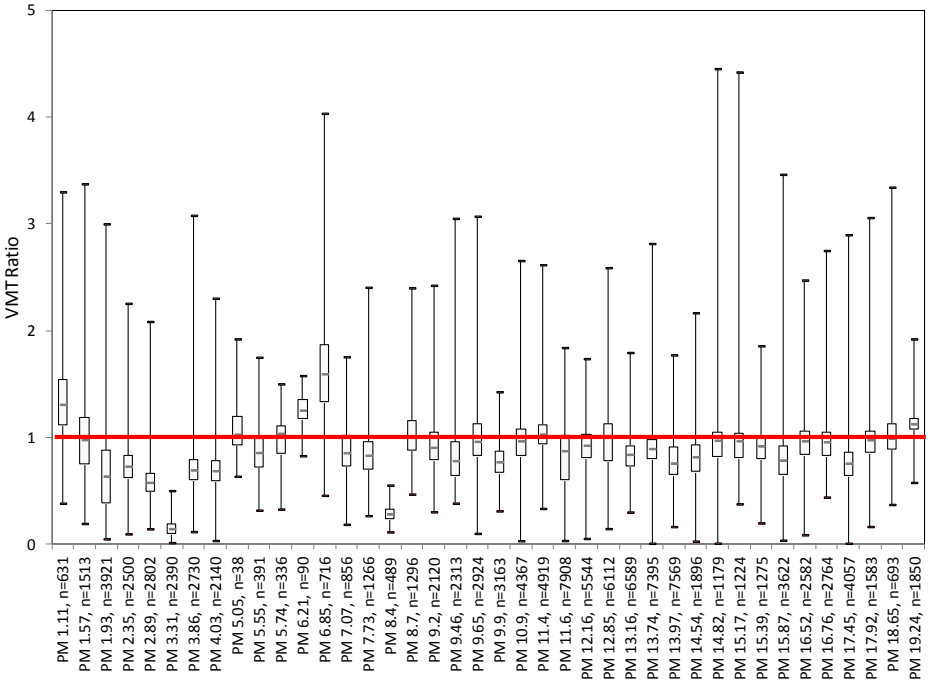

Figure G8. VMT Ratio (by segment, I-405 Northbound)

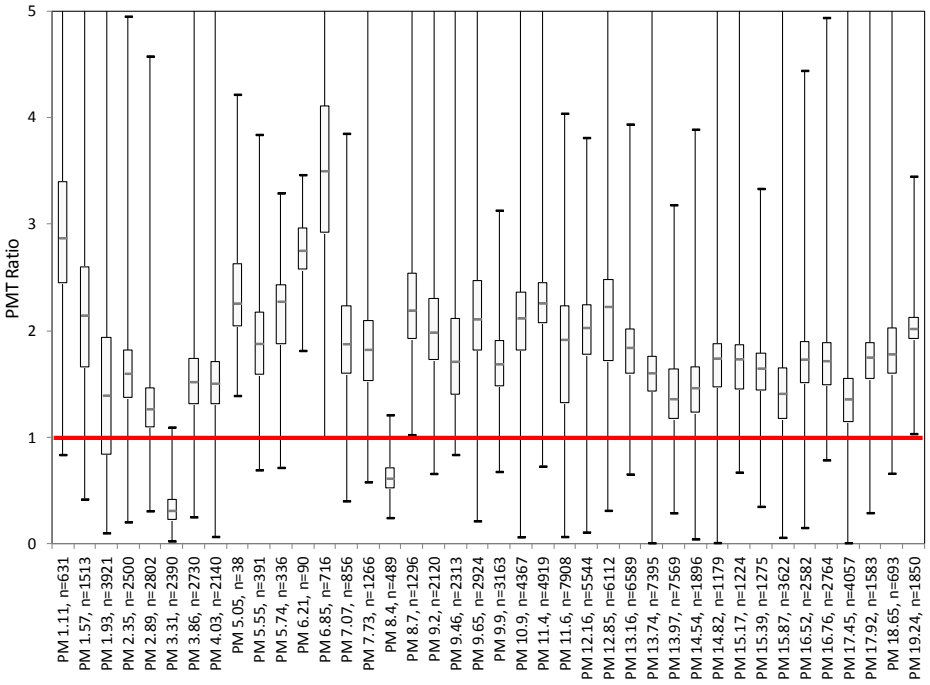

Figure G9. PMT Ratio (by segment, I-405 Northbound)

G4) I-405 Southbound

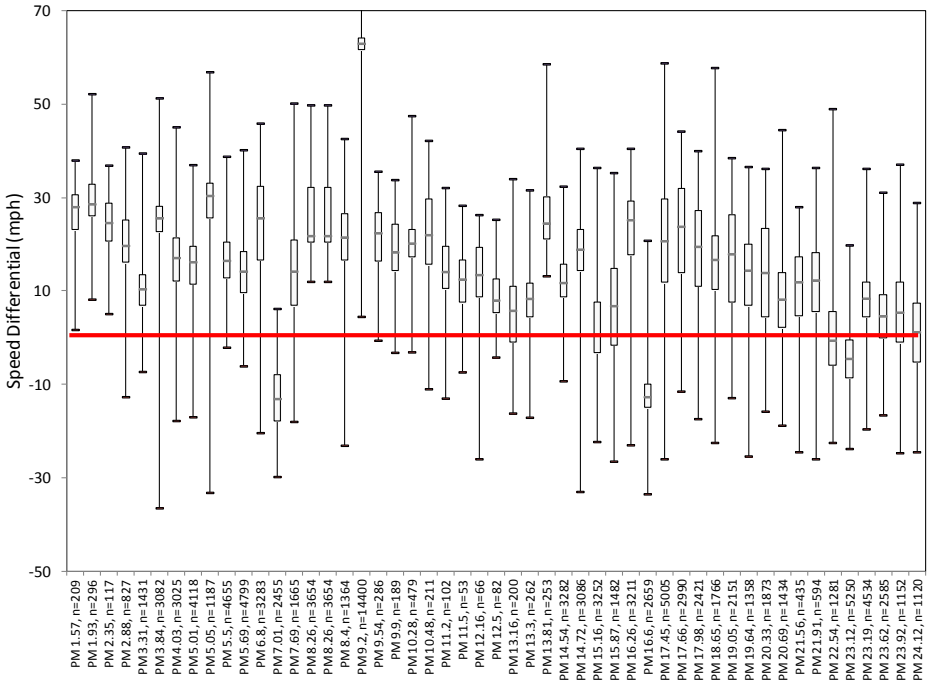

Figure G10. Speed differential (by segment, I-405 Southbound)

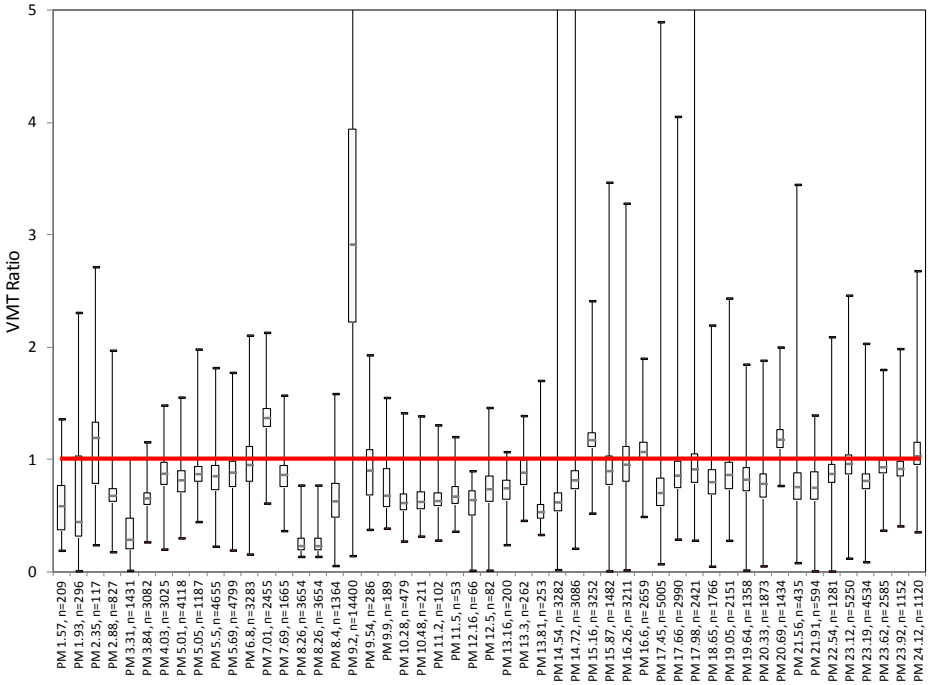

Figure G11. VMT Ratio (by segment, I-405 Southbound)

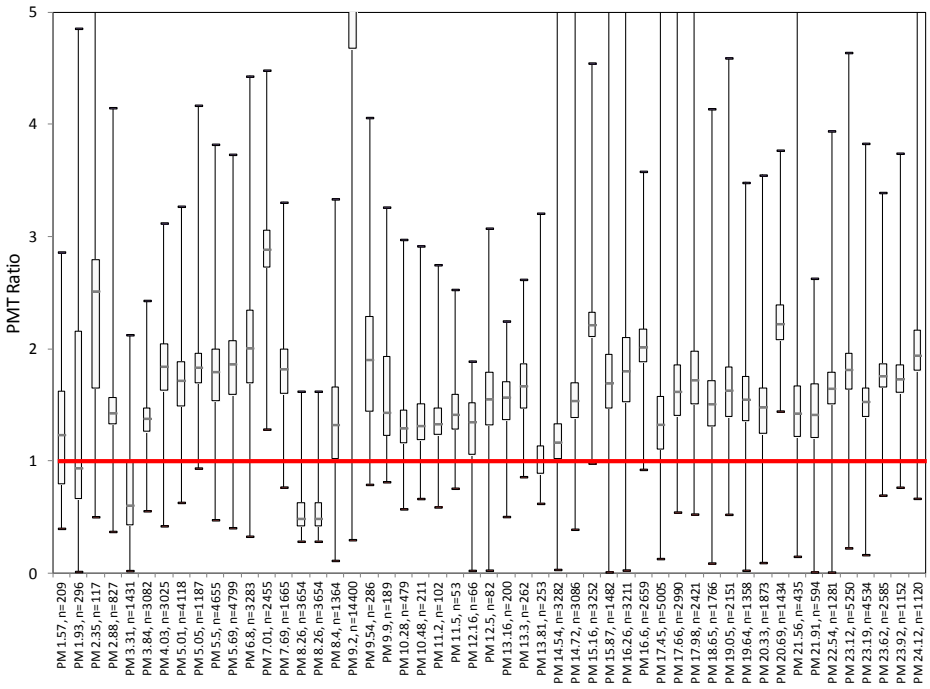

Figure G12. PMT Ratio (by segment, I-405 Southbound)

G5) SR-55 Northbound, Continuous

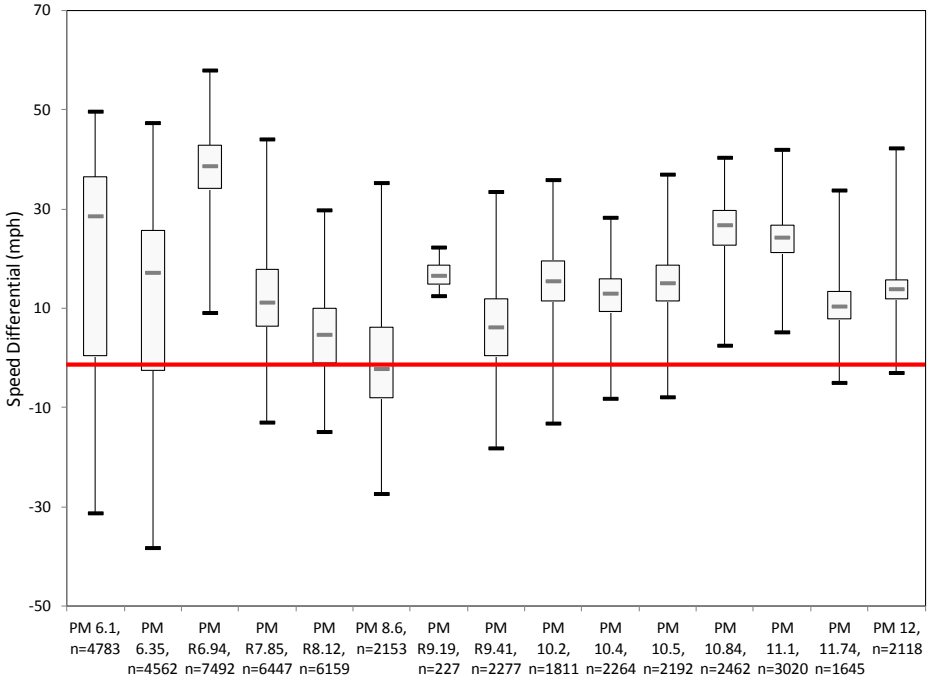

Figure G13. Speed differential (by segment, SR-55 Northbound, Continuous)

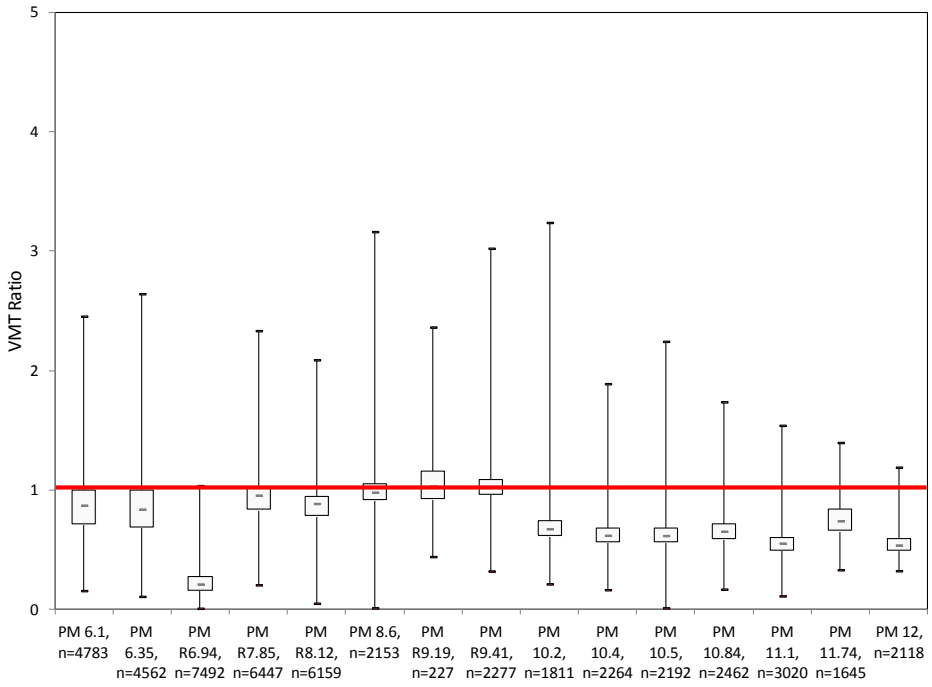

Figure G14. VMT Ratio (by segment, SR-55 Northbound, Continuous)

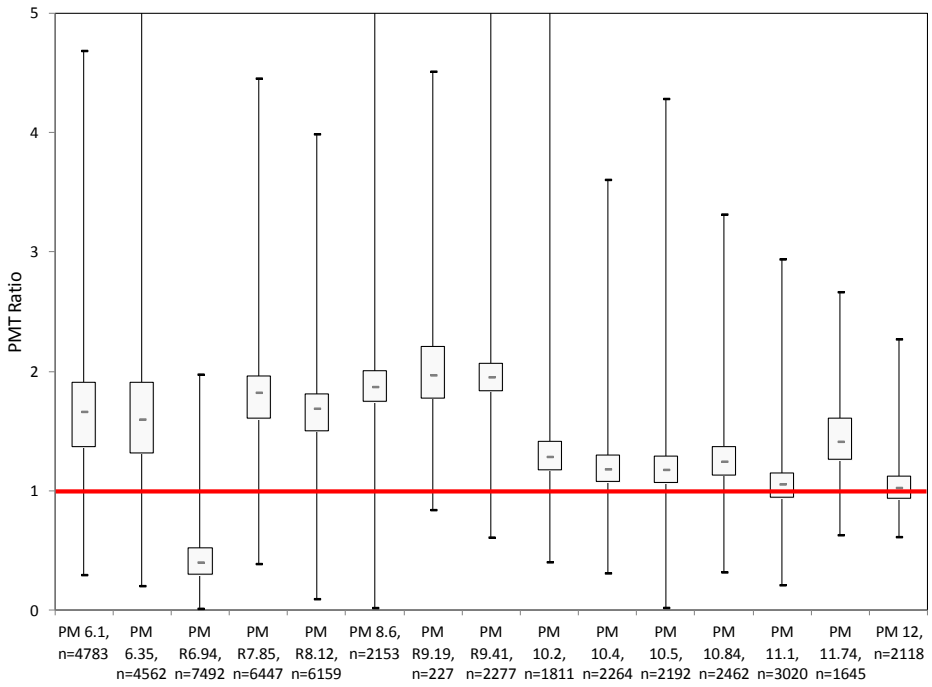

Figure G15. PMT Ratio (by segment, SR-55 Northbound, Continuous)

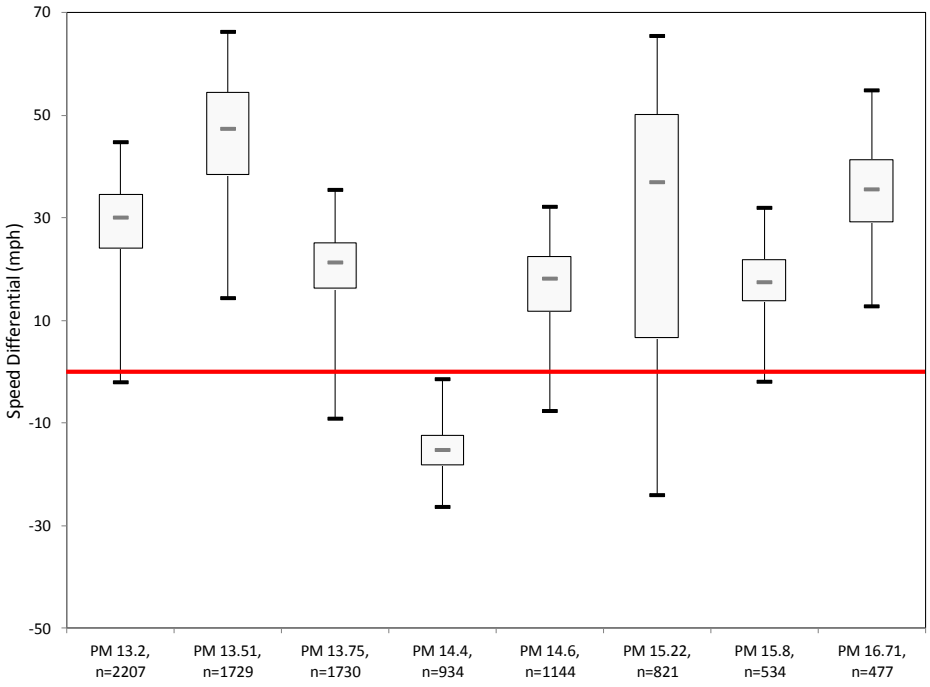

Figure G16. Speed differential (by segment, SR-55 Southbound)

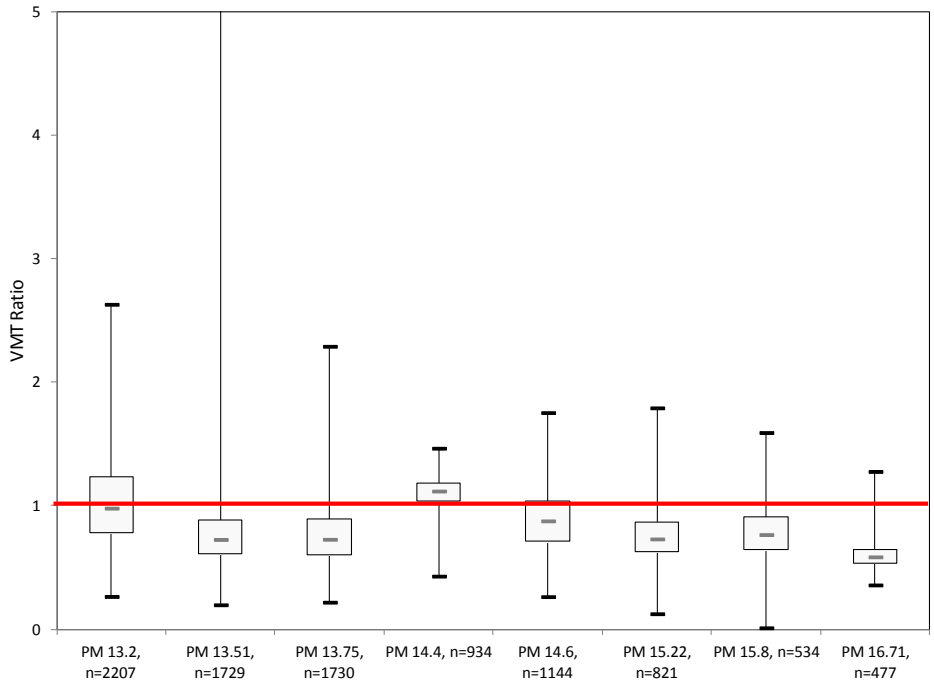

Figure G17. VMT Ratio (by segment, SR-55 Southbound)

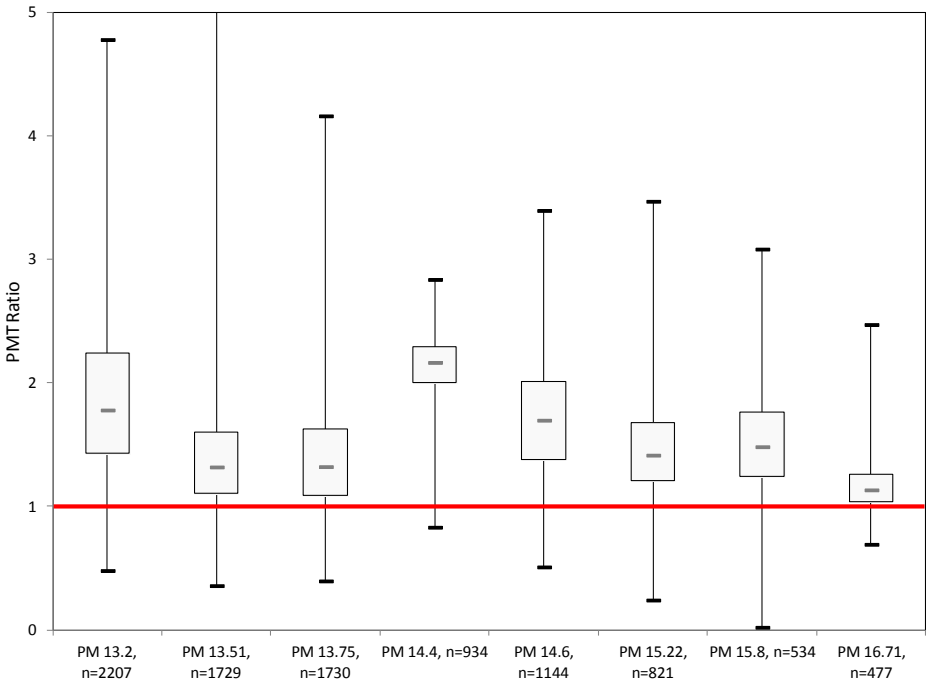

Figure G18. PMT Ratio (by segment, SR-55 Southbound)

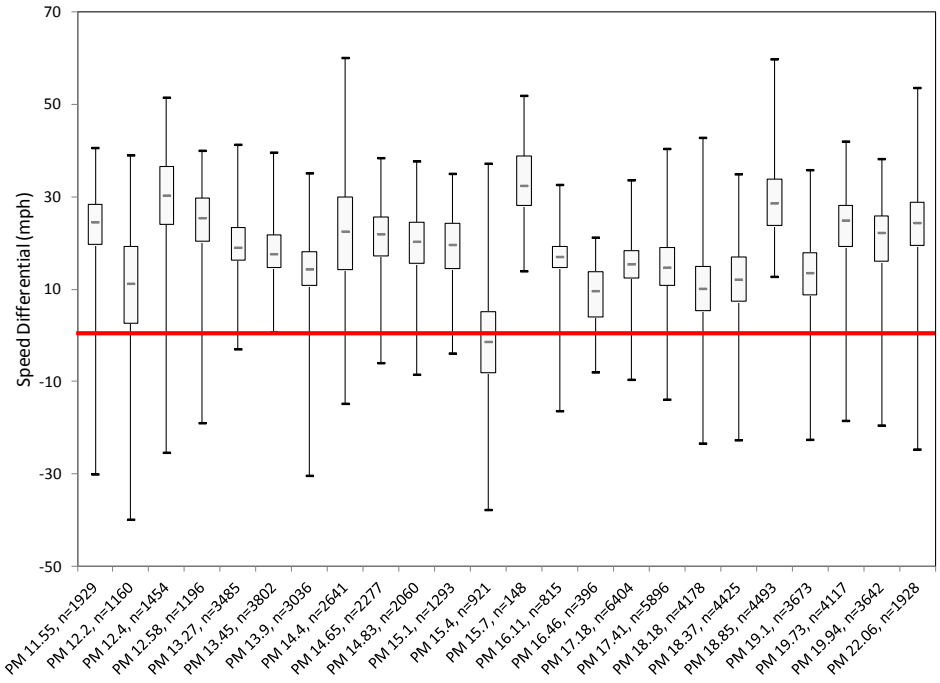

Figure G19. Speed differential (by segment, SR-57 Southbound)

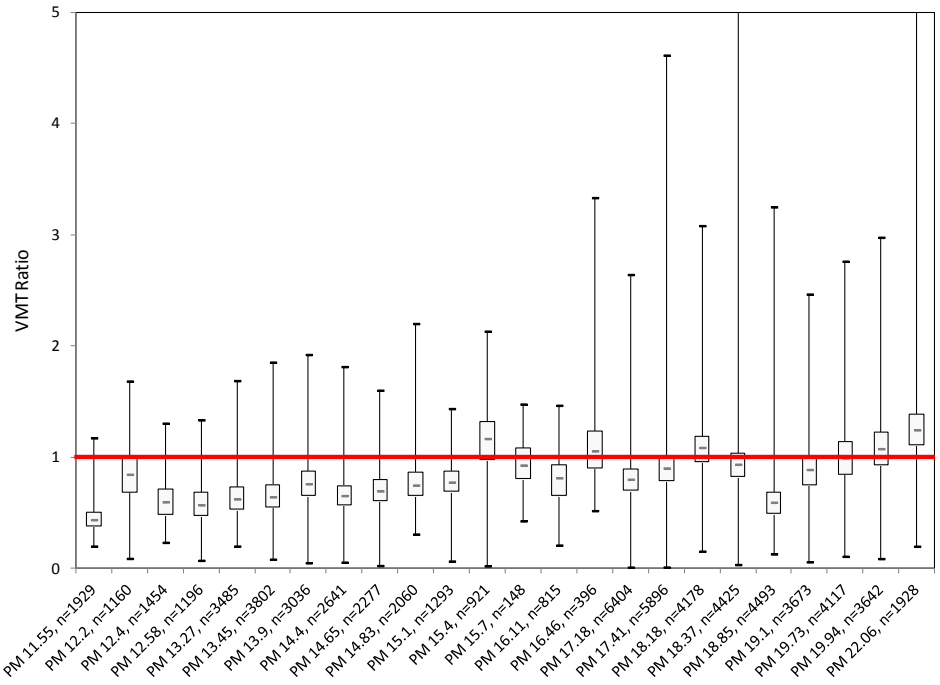

Figure G20. VMT Ratio (by segment, SR-57 Southbound)

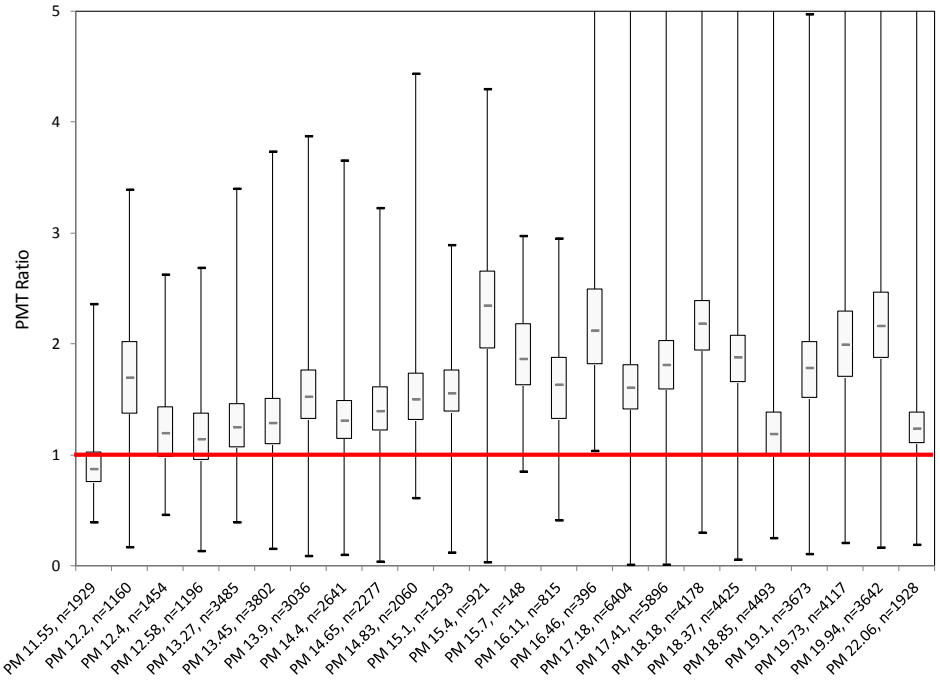

Figure G21. PMT Ratio (by segment, SR-57 Southbound)

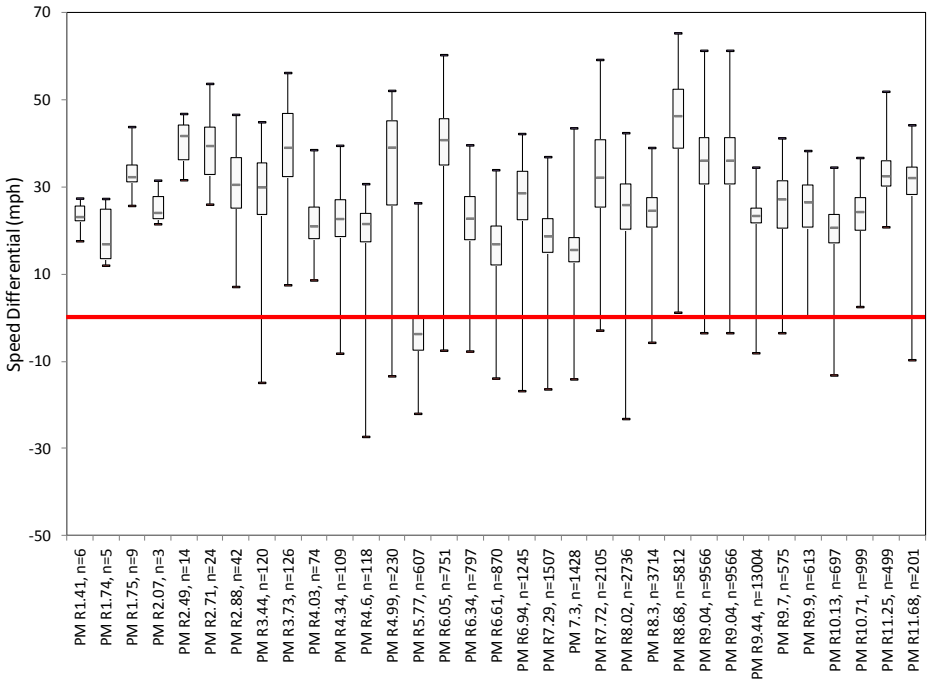

Figure G22. Speed differential (by segment, SR-22 Eastbound)

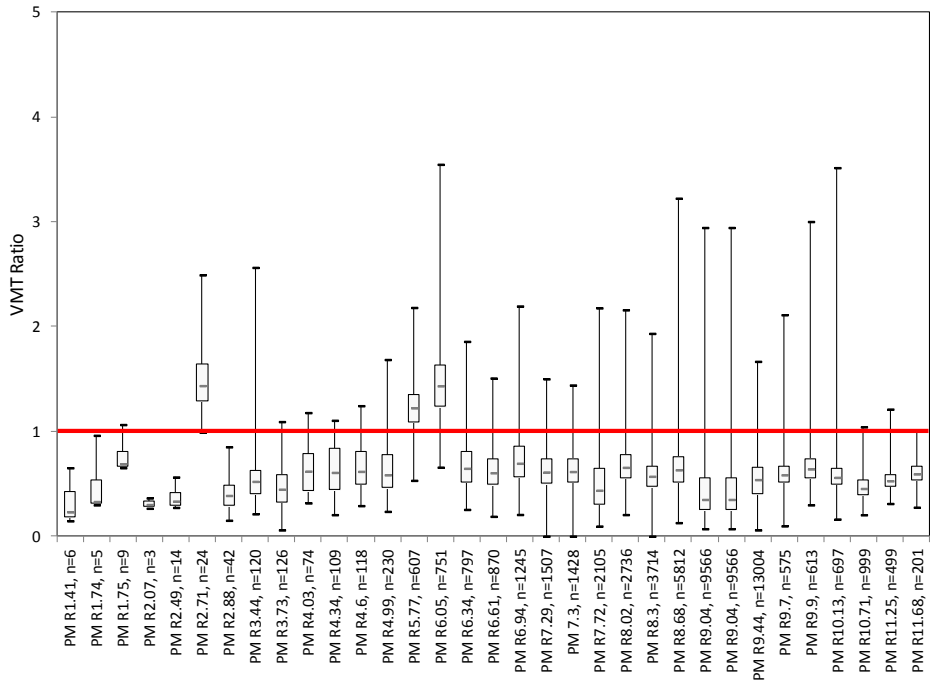

Figure G23. VMT Ratio (by segment, SR-22 Eastbound)

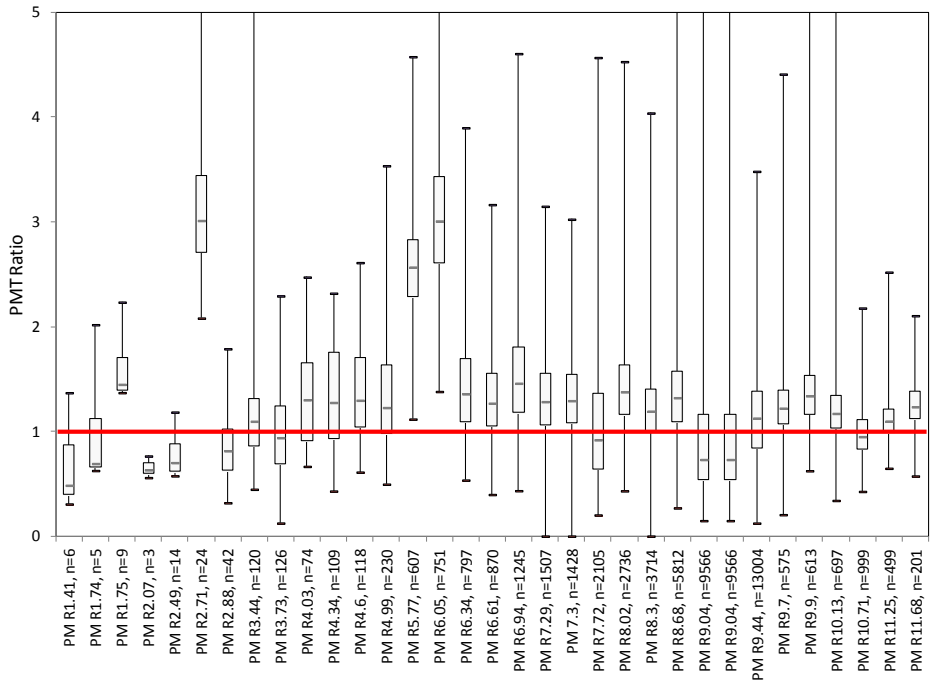

Figure G24. PMT Ratio (by segment, SR-22 Eastbound)

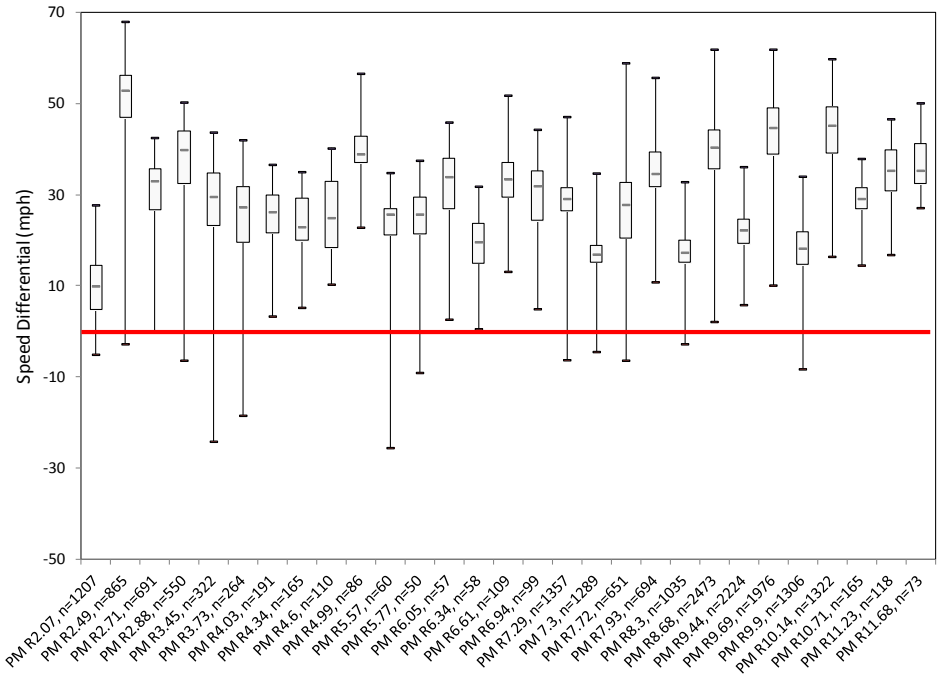

Figure G25. Speed differential (by segment, SR-22 Westbound)

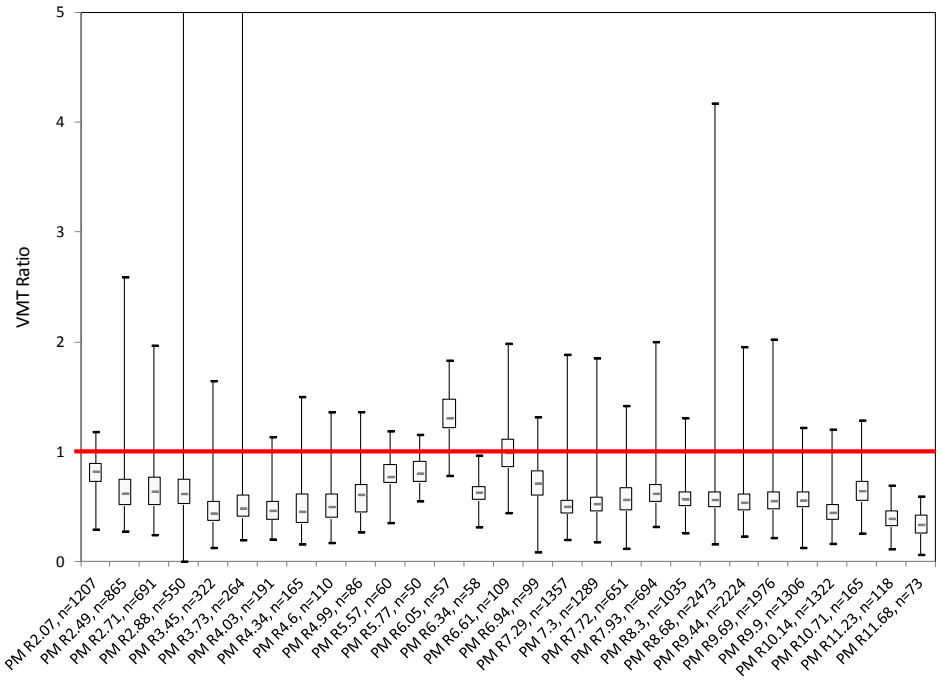

Figure G26. VMT Ratio (by segment, SR-22 Westbound)

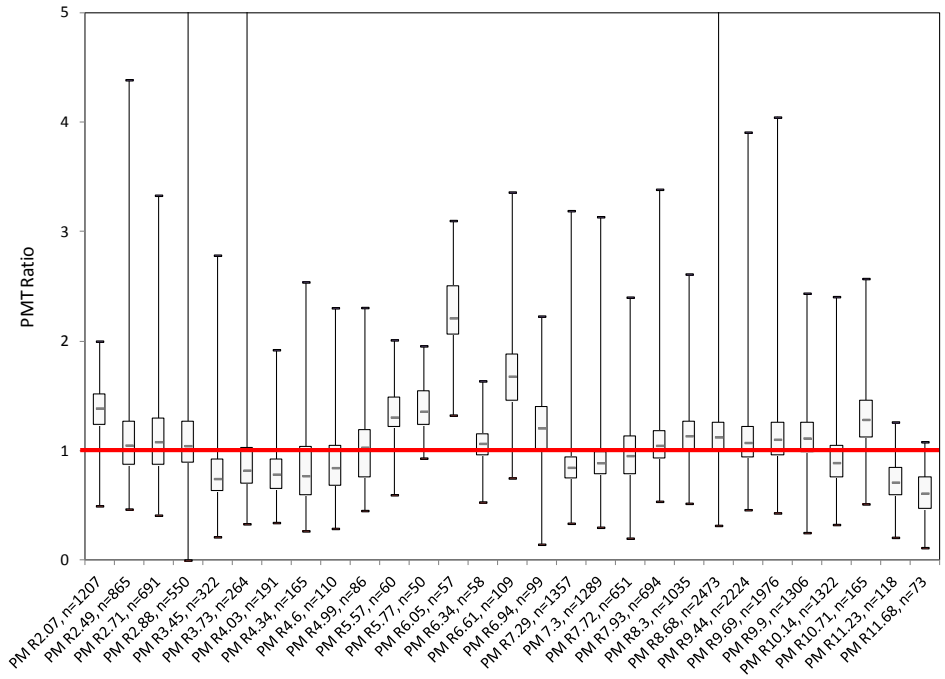

Figure G27. PMT Ratio (by segment, SR-22 Westbound)

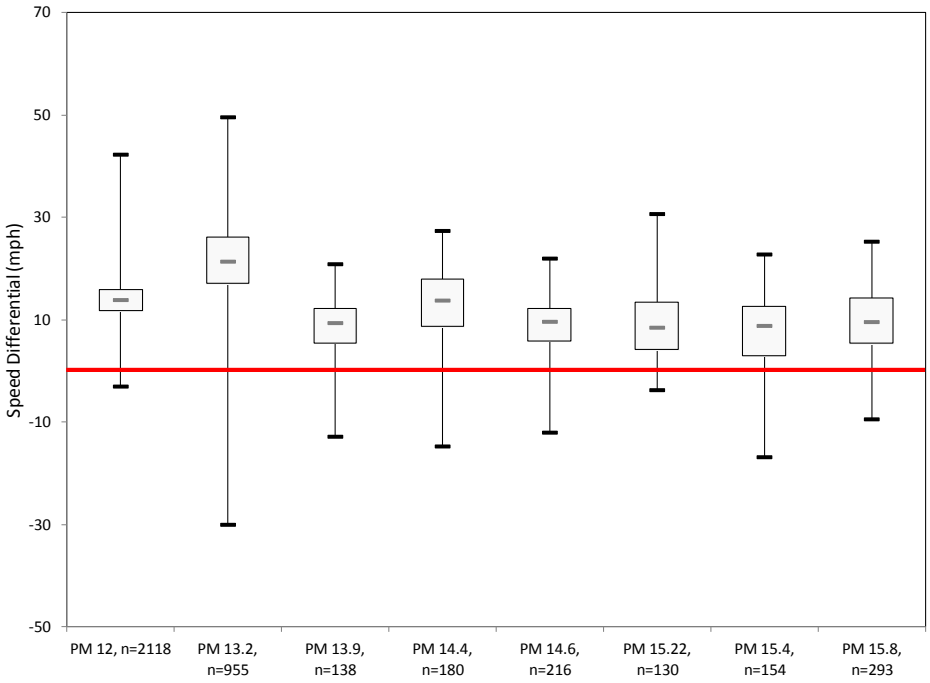

Figure G28. Speed differential (by segment, SR-55 Northbound)

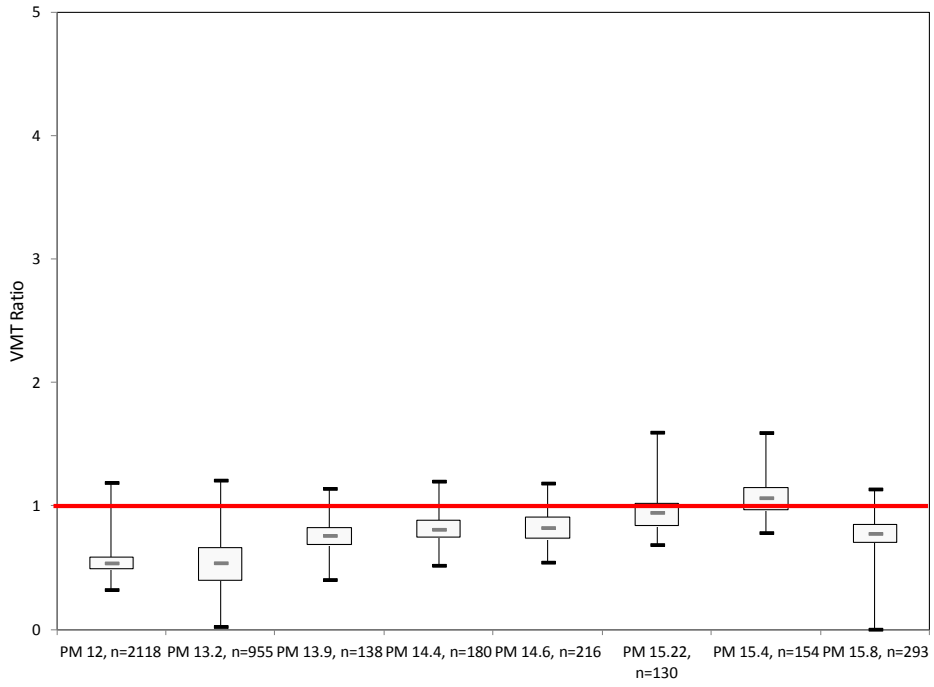

Figure G29. VMT Ratio (by segment, SR-55 Northbound)

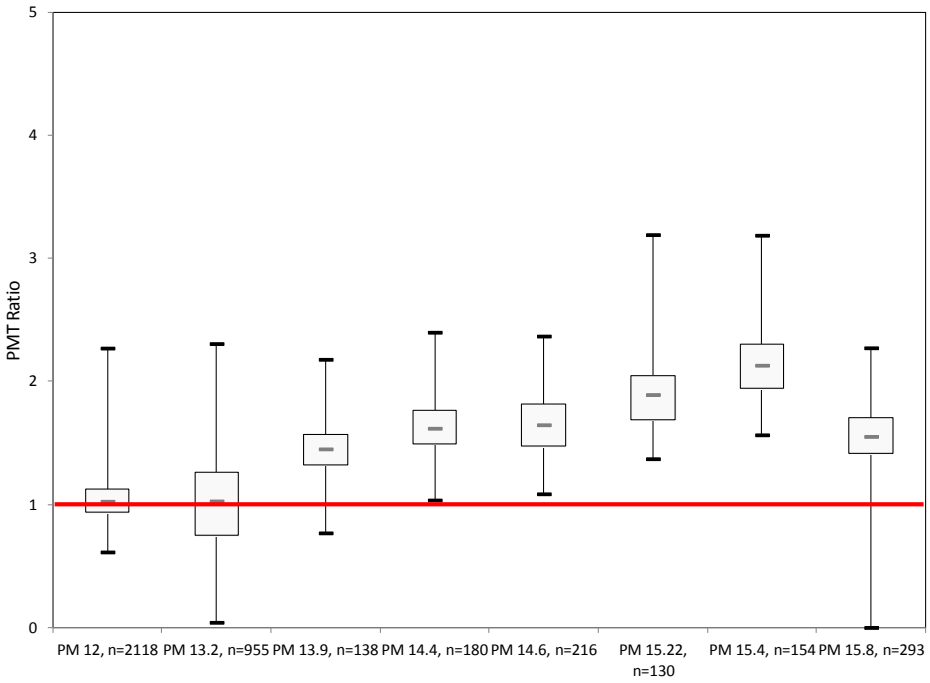

Figure G30. PMT Ratio (by segment, SR-55 Northbound)

Appendix H Different Access Type Parameter Matrix

In this Appendix, the calculation of flow, person-flow, VMT and PMT ratios for GP lanes and HOV lane are based on the following definitions and observations.

- Definition
    - Flow = Flow (5 min interval)
    - Person flow = Flow* Vcc (vehicle Occupants)
    - Please note that the continuous access does not include routes I-80E and I-80W, since it has the special feature of HOV3+..
- The performance Measures (Flow, Person-Flow, Speed Differential, VMT ratio and PMT ratios) are plotted against the average general purpose lanes (AGP). These yield the AGP Speed Joint Distribution Matrices.
    - To determine the representative traffic states when AGP lane's speed is lower than 45 mph, the performance measures- - AGP Speed Joint distributions have been plotted for different HOV access type.
    - The colored vertical bar on the right side is the range of probability density for the corresponding defined joint cell. The AGP speed is separated by 9 levels, each cell is 5mph.
    - The speed differential matrix shows that continuous access has higher speed than limited access when AGP speed is between 15-30mph. There is no difference when AGP speed is lower than 15 mph.
    - In contrast, the VMT ratio of continuous access is higher than limited access at level 10-15mph. But the PMT ratio is at comparable level.

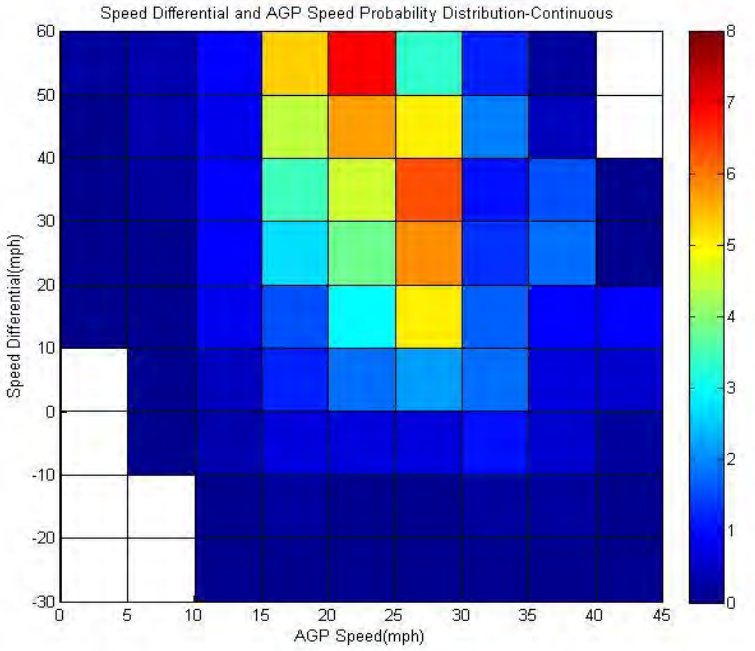

(a) Continuous Type

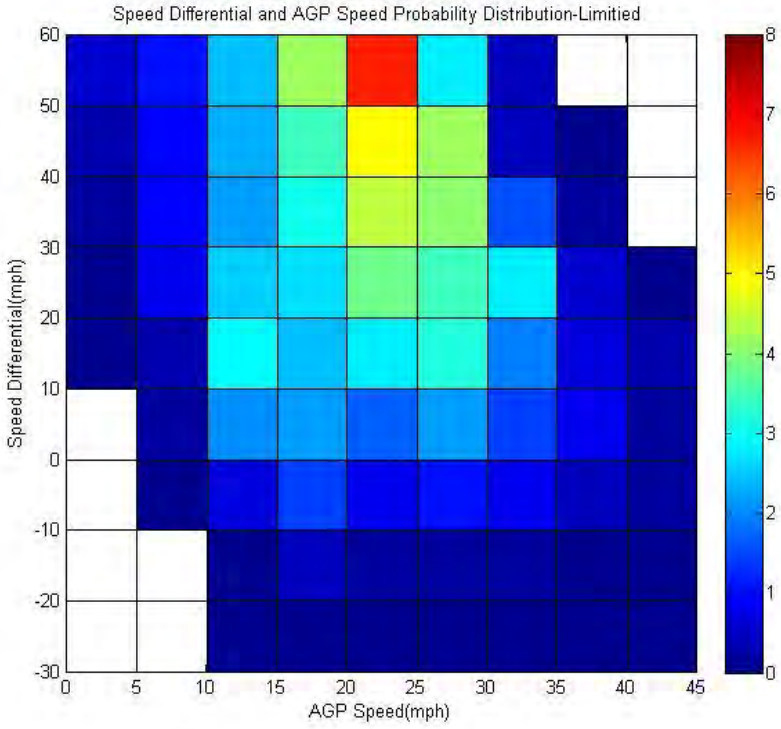

(b) Limited Type

Figure H1. Speed Differential Matrix (a) Continuous, and (b) Limited

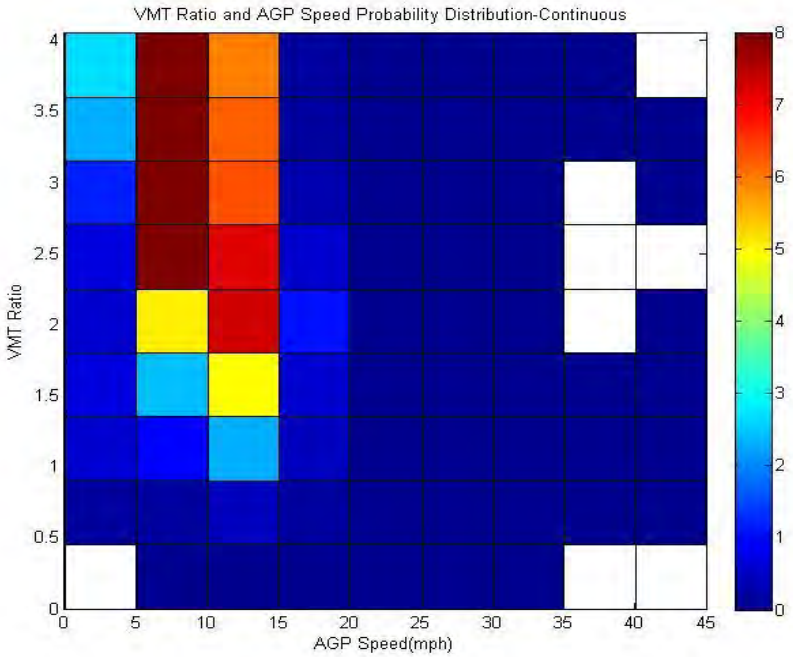

(a) Continuous Type

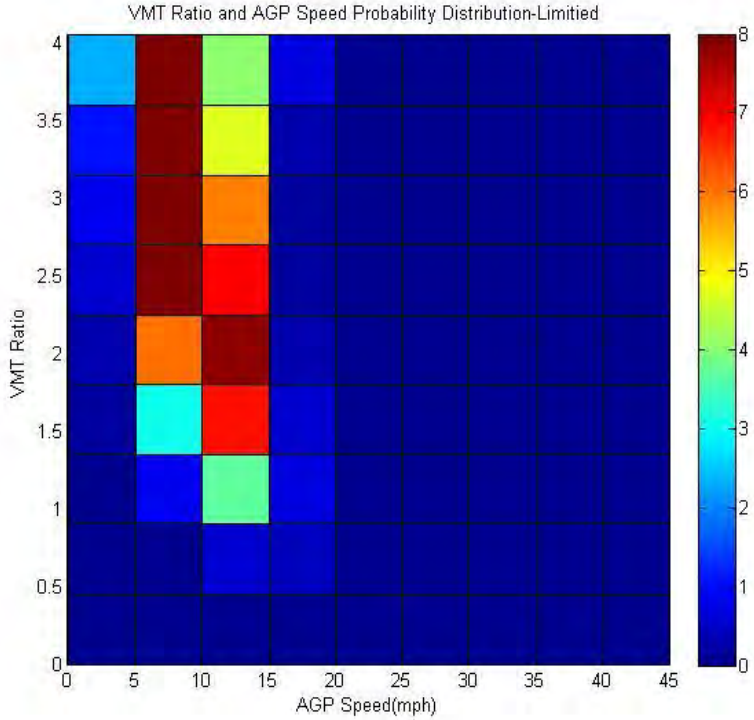

(b) Limited Type

Figure H2. VMT Ratio Matrix (a) Continuous, and (b) Limited

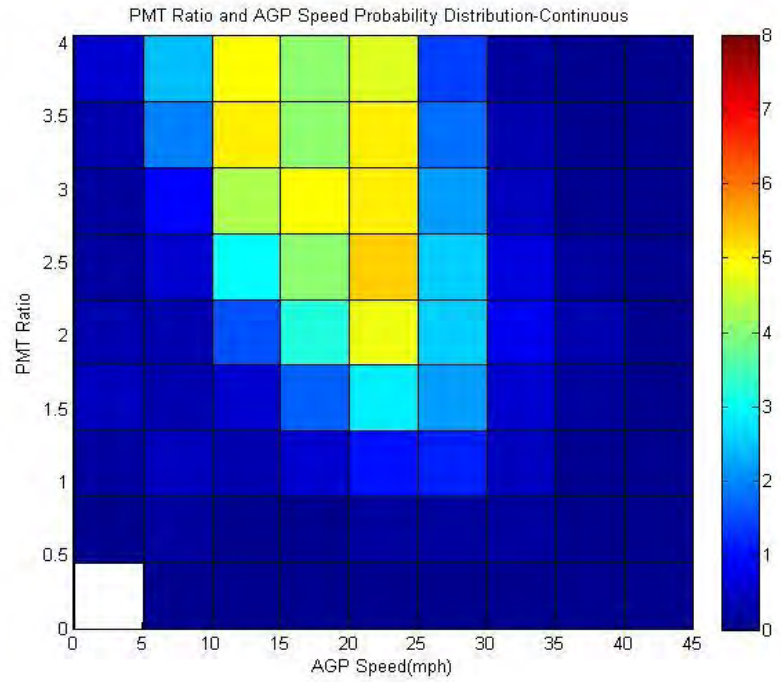

(a) Continuous Type

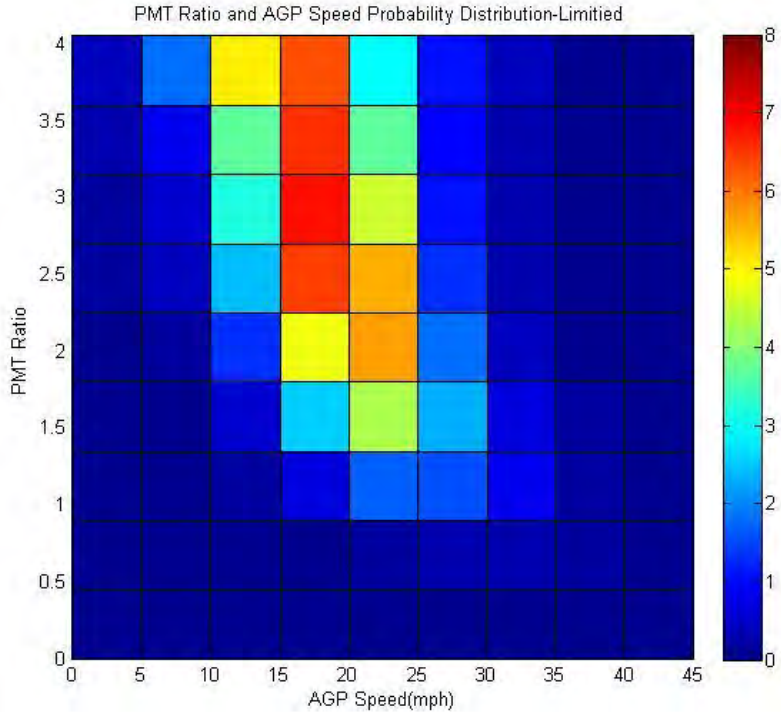

(b) Limited Type

Figure H3. PMT Ratio Matrix (a) Continuous, and (b) Limited

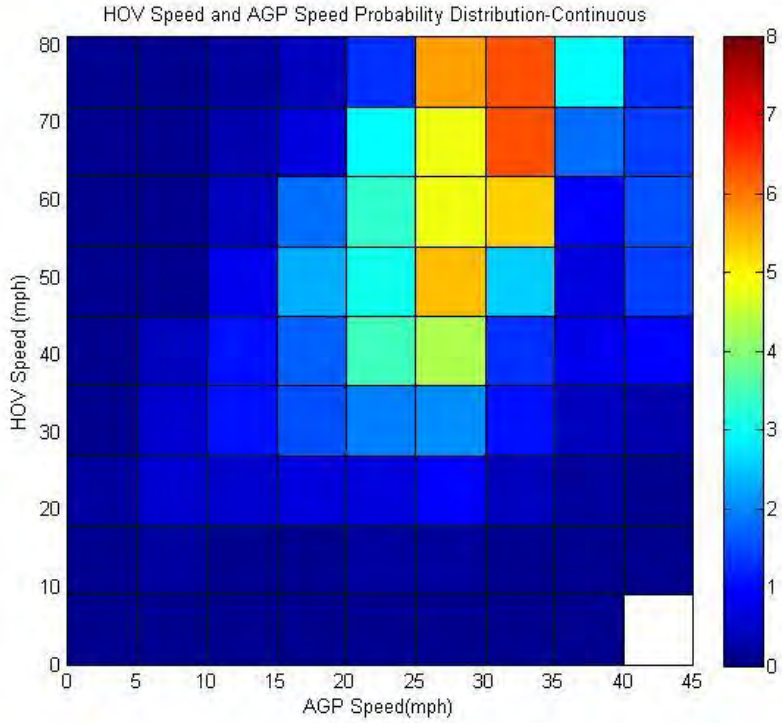

(a) Continuous Type

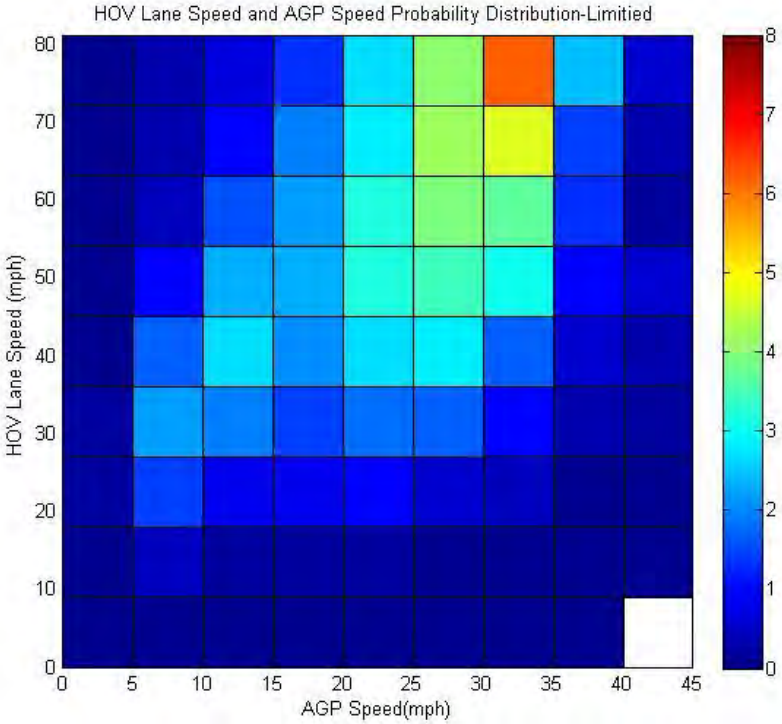

(b) Limited Type

Figure H4. HOV Speed Matrix (a) Continuous, and (b) Limited

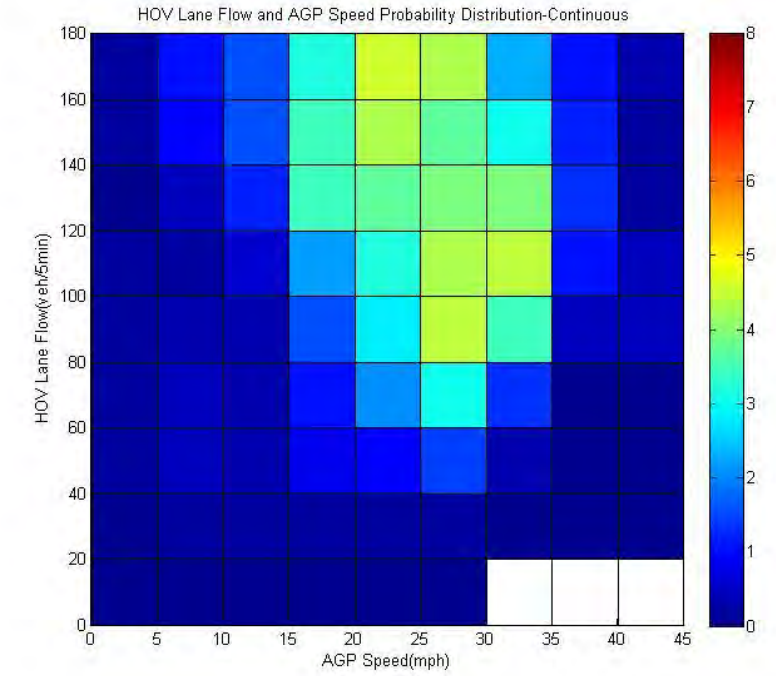

(a) Continuous Type

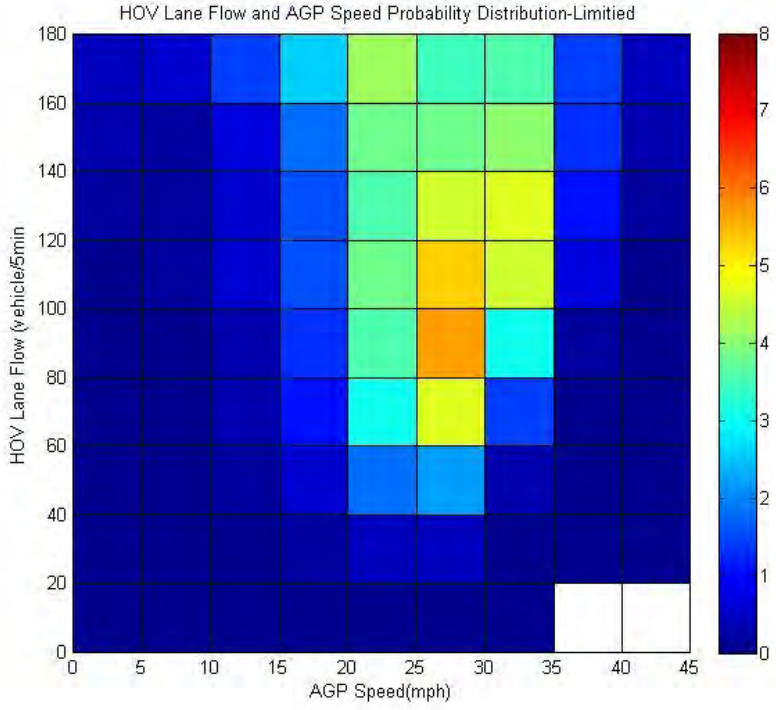

(b) Limited Type

Figure H5. HOV Lane Flow Matrix (a) Continuous, and (b) Limited

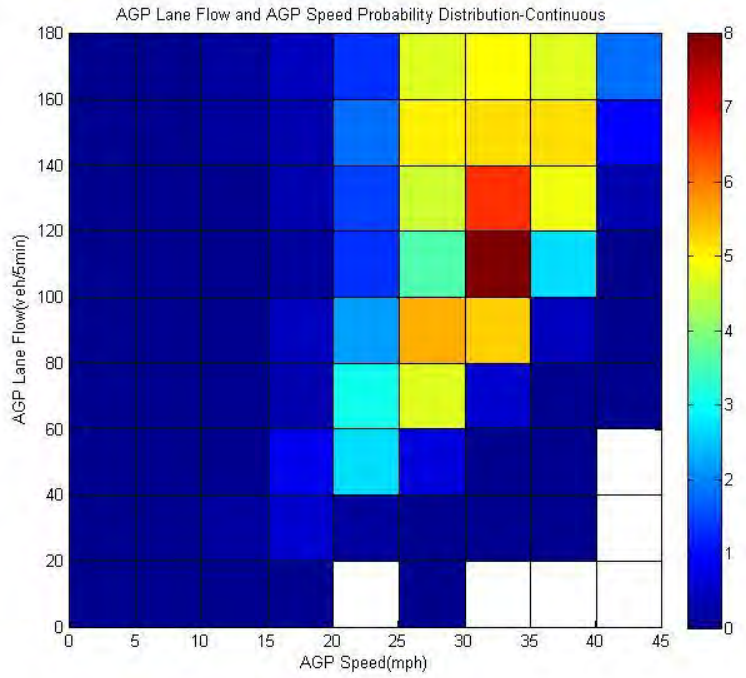

(a) Continuous Type

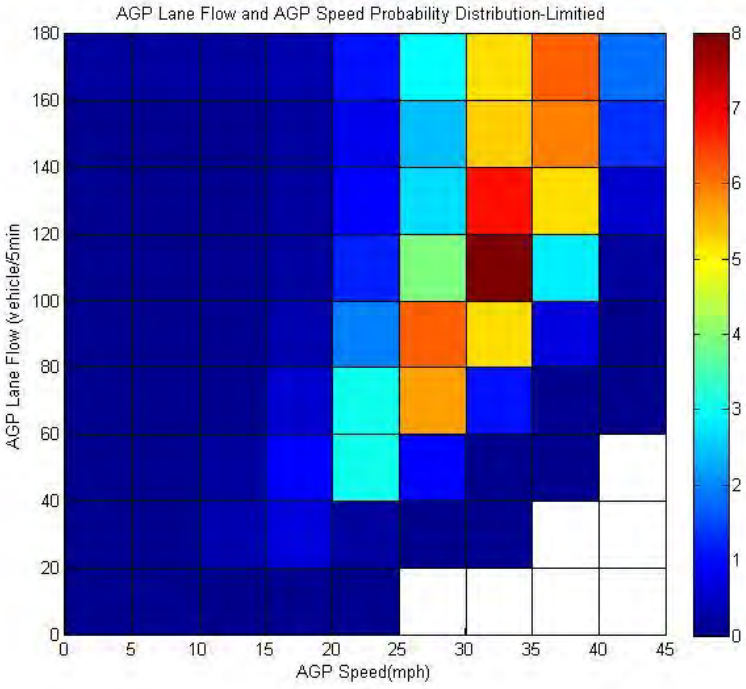

(b) Limited Type

Figure H6. AGP Lane Flow Matrix (a) Continuous, and (b) Limited

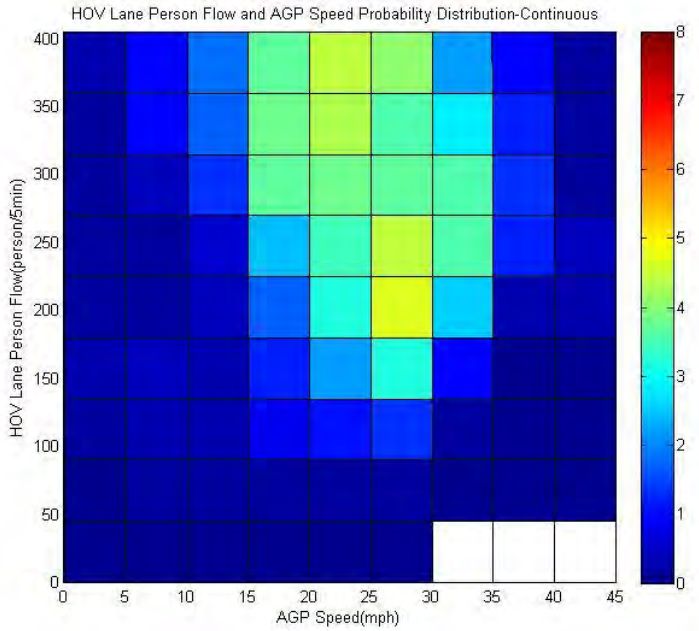

(a) Continuous Type

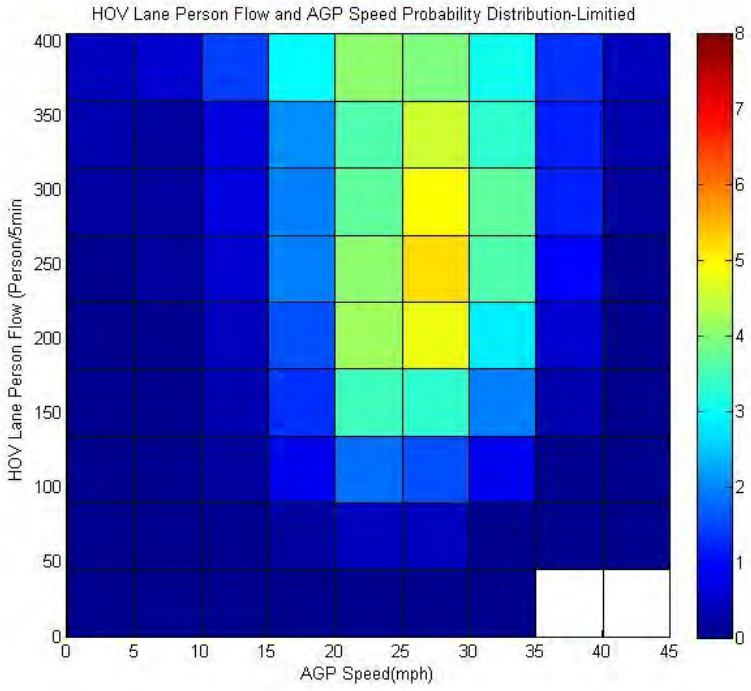

(b) Limited Type

Figure H7. HOV Lane Person Flow Matrix (a) Continuous, and (b) Limited

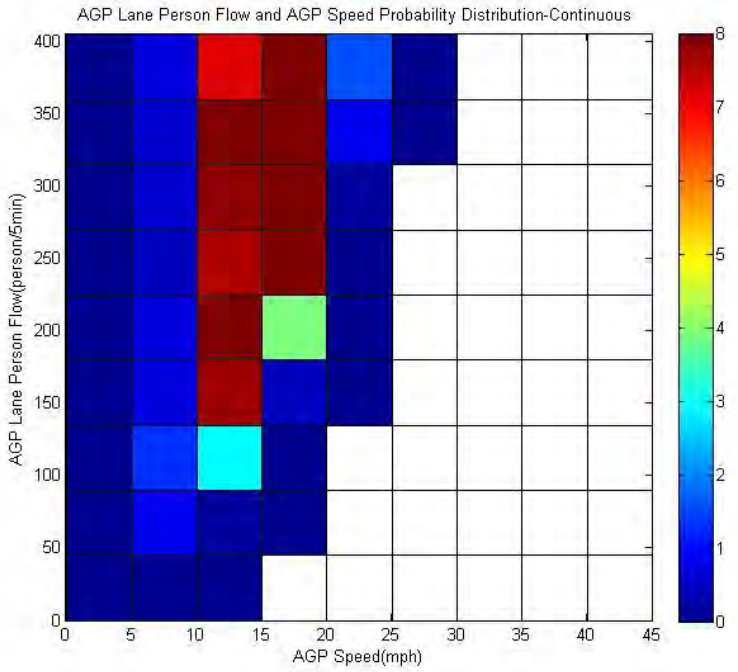

(a) Continuous Type

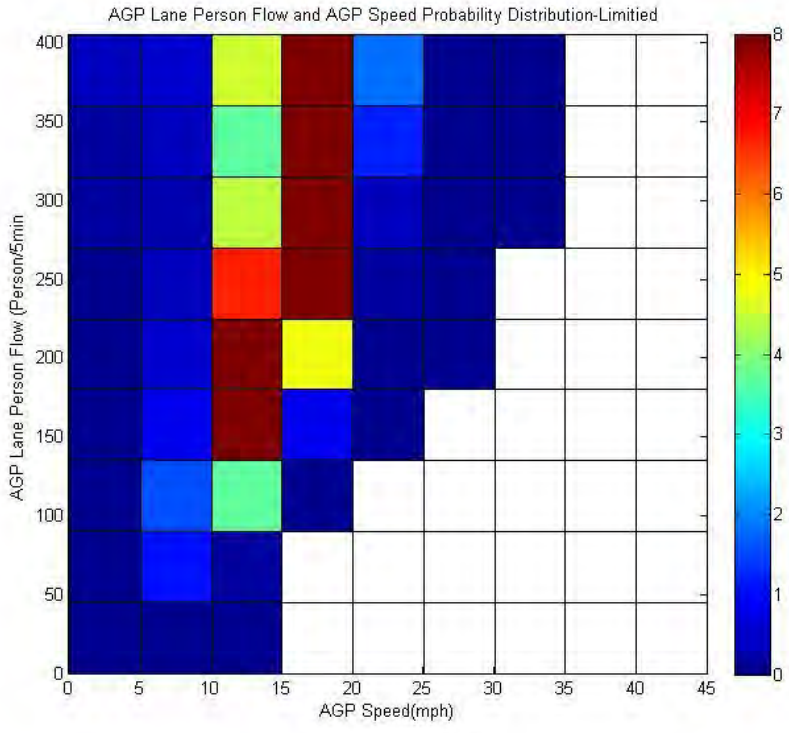

(b) Limited Type

Figure H8. AGP Lane Person Flow Matrix (a) Continuous, and (b) Limited

Appendix I Performance Comparison for Additional Study Sites

A. SR-55 SB2

a) Speed Contour

Figure I-1 shows the speed contours for both GP lanes and HOV lanes before and after the HOV lane conversion. The study limit of the site is from absolute postmile 11.6 to 7.0. However, the speed contours in the figures cover a longer segment from the Lincoln interchange (postmile 16.7) to the Dyer interchange (postmile 8.0) to provide an overview of the traffic condition. We found that the SR-55 SB2 site has a major bottleneck around postmile 9 and 10 at the I-5 interchange, located within the study area. The freeway mainline traffic condition after the HOV lane conversion appears to be more congested with slightly longer duration.

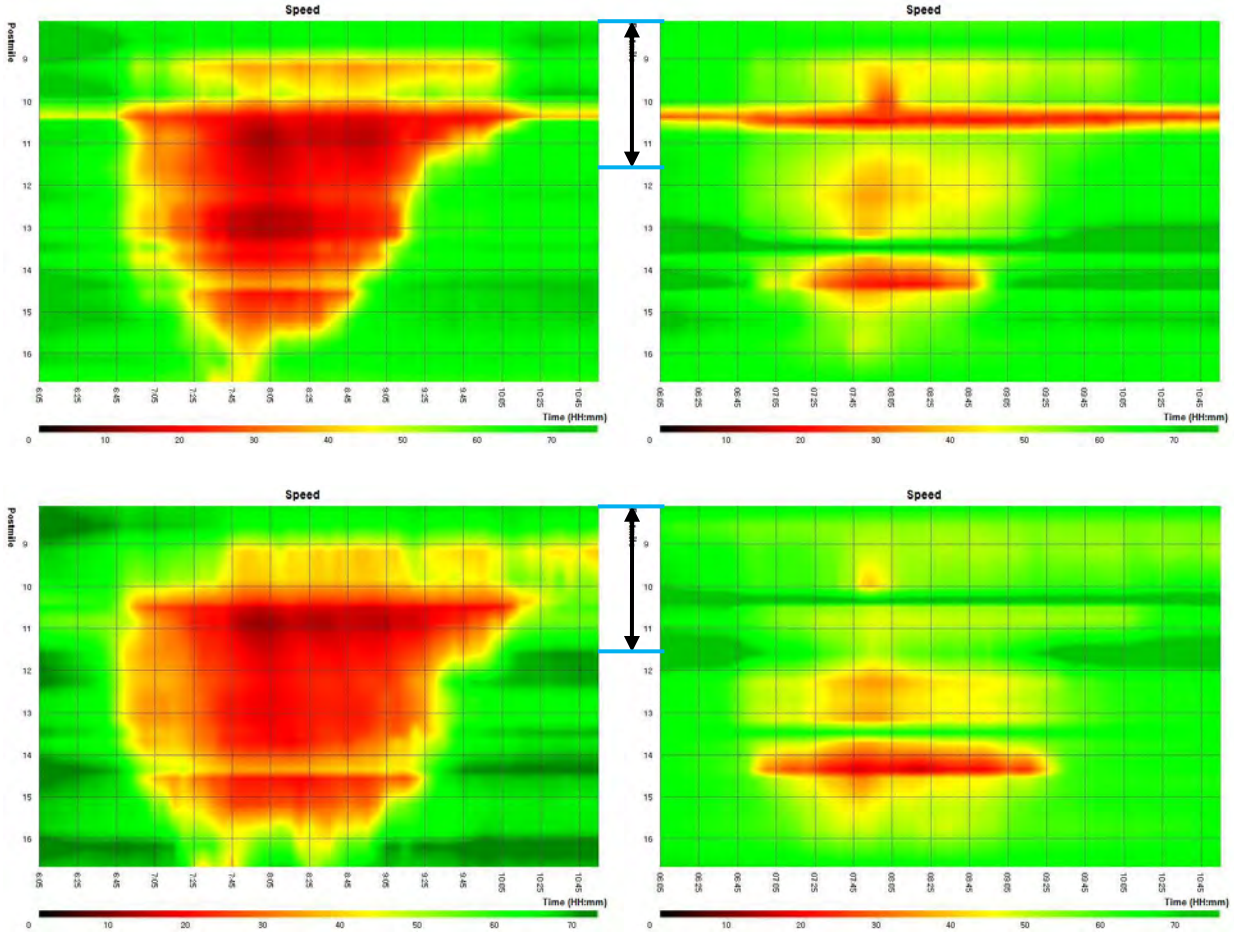

(a) Before (top) and After GP Lanes (b) Before (top) and After HOV Lanes

Figure I-1. SR-55 SB2 Speed Contours Before and After HOV Lane Conversion

b) Speed Differential

The distribution of speed differential between the HOV lane and the GP lane average for the SR-57 SB2 site is presented in Figure I-2. We found the distribution of speed differential was polarized after the conversion for all periods and congestion.

(a) Speed Differential Boxplot (all periods)

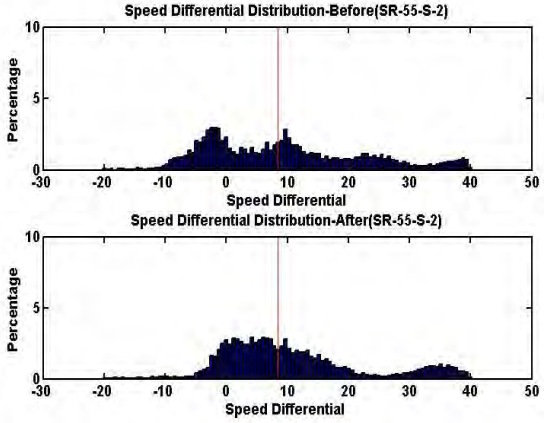

(b) Speed Differential Distribution (all periods)

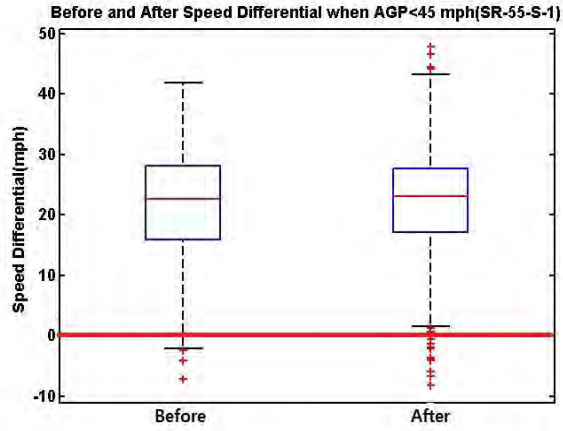

(c) Speed Differential Boxplot (congestion)

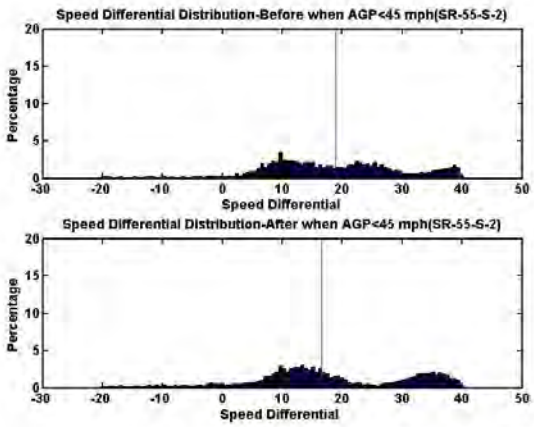

(d) Speed Differential Distribution (congestion)

Figure I-2. Speed Differential for SR-55 SB2

c) VMT ratio

From Figure I-3, it can be seen that the distribution of the VMT ratio barely changes after the conversion in the congested periods analyses and the all periods analyses.

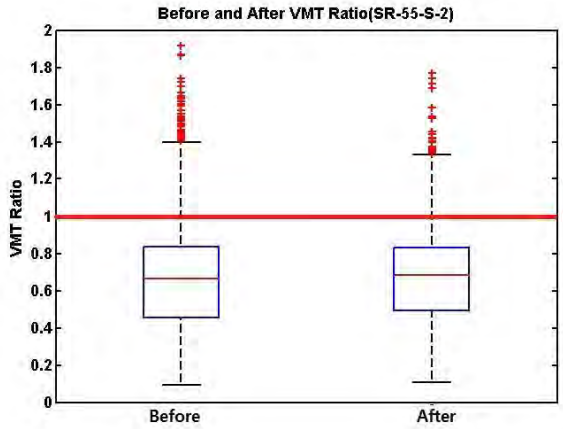

(a) VMT Ratio Boxplot (all periods)

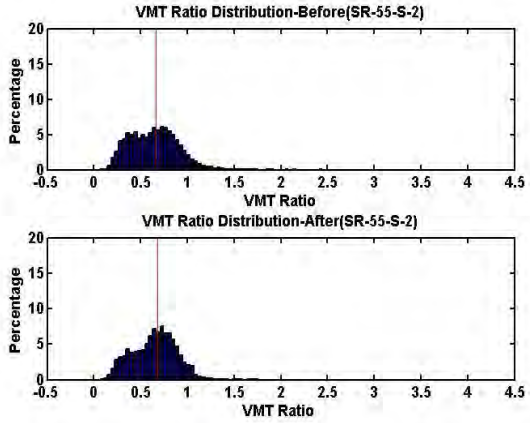

(b) VMT Ratio Distribution (all periods)

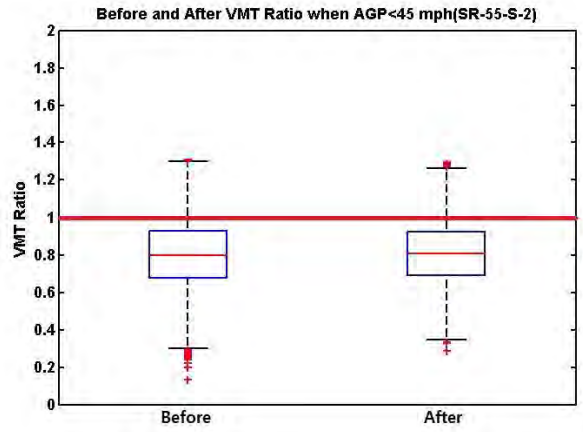

(c) VMT Ratio Boxplot (congestion)

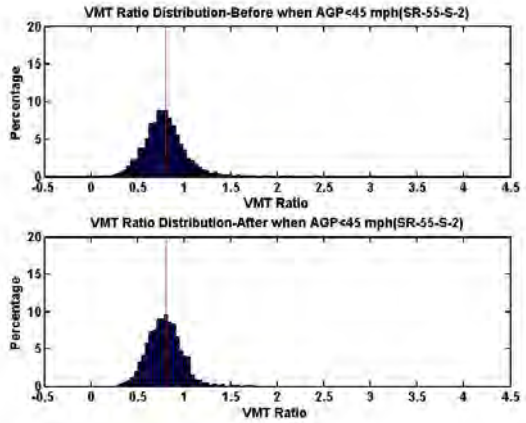

(d) VMT Ratio Distribution (congestion)

Figure I-3. VMT Ratio for SR-55 SB2

d) Demand Flow

For the SR-55 SB2 site, demand flows at all detector locations were analyzed for the a.m. peak period (from 6:00 a.m. to 11:00 a.m.). Table I-1 shows that the site has higher flows on both GP lanes and HOV lanes after the conversion. In total, the demand flow, which is equal to the total GP lane flow plus the total HOV lane flow, are 2%-4% higher after conversion.

Table I-1. Demand Flows for SR-55 SB2

	GP Lanes			HOV Lane			Total			
PostMile	Before	After	Change	Before	After	Change	Before	After	Change	Change %
10.822	15108	15515	407	3392	3731	339	18500	19246	746	4.0%
9.84	31021	31928	907	5688	5905	217	36709	37832	1123	3.1%
9.19	30313	31019	706	4990	5171	181	35303	36190	887	2.5%

e) Traffic Flow Fundamental Diagram Parameters

Because demand flows are higher and traffic congestion is more severe, we were unable to determine whether or not the HOV lane conversion to continuous-access operation provided more operational benefits. The proposed traffic flow fundamental diagram based approach was taken to compare before and after performance.

Table I-2 and Table I-3 compare the key traffic flow fundamental diagram parameters at all mainline VDS locations for the formulation phase and dissipation phase, respectively. Since postmiles 9 and 10 are the bottleneck locations and postmile 9.84 is located at a spot with limited-access under both before and after conditions, we chose the detector station at postmile 9.19 as the key location. Figure I-4 shows the traffic flow fundamental diagram parameters estimated for the formulation phase and dissipation phase at this location. Based on the analysis of the traffic flow diagram parameters, we found

- Critical volume remains the same, which means that there is almost no capacity improvement.
- Shockwave speed is faster in the dissipation phase, which means that the queue is able to be dissipated at faster speeds.

Table I-2. SR-55 SB2: Traffic Flow Diagram Parameters in the Formulation Phase

	PostMile	Ingress /Egress	Before	After	Diff	% Diff	Before V.S. After
Critical Occupancy	10.822	No	0.123	0.121	-0.002	-1.6%	Equivalent
	9.19	Yes	0.126	0.128	0.002	1.6%	Equivalent
Critical Volume	10.822	No	425.1	418.7	-6.4	-1.5%	Equivalent
	9.19	Yes	725.8	731.7	5.9	0.8%	Equivalent
Shockwave Speed	10.822	No	-9.9	-9.4	0.5	-5.1%	After: Lower
	9.19	Yes	-13.6	-16.2	-2.6	19.1%	After: Higher

Table I-3. SR-55 SB2: Traffic Flow Diagram Parameters in the Dissipation Phase

	PostMile	Ingress /Egress	Before	After	Diff	% Diff	Before V.S. After
Critical Volume	10.822	No	353.2	348.2	-5	-1.4%	Equivalent
	9.19	Yes	688.3	685.6	-2.7	-0.4%	Equivalent
Shockwave Speed	10.822	No	-4.9	-9.3	-4.4	89.8%	After: Higher
	9.19	Yes	-22.6	-27.4	-4.8	21.2%	After: Higher

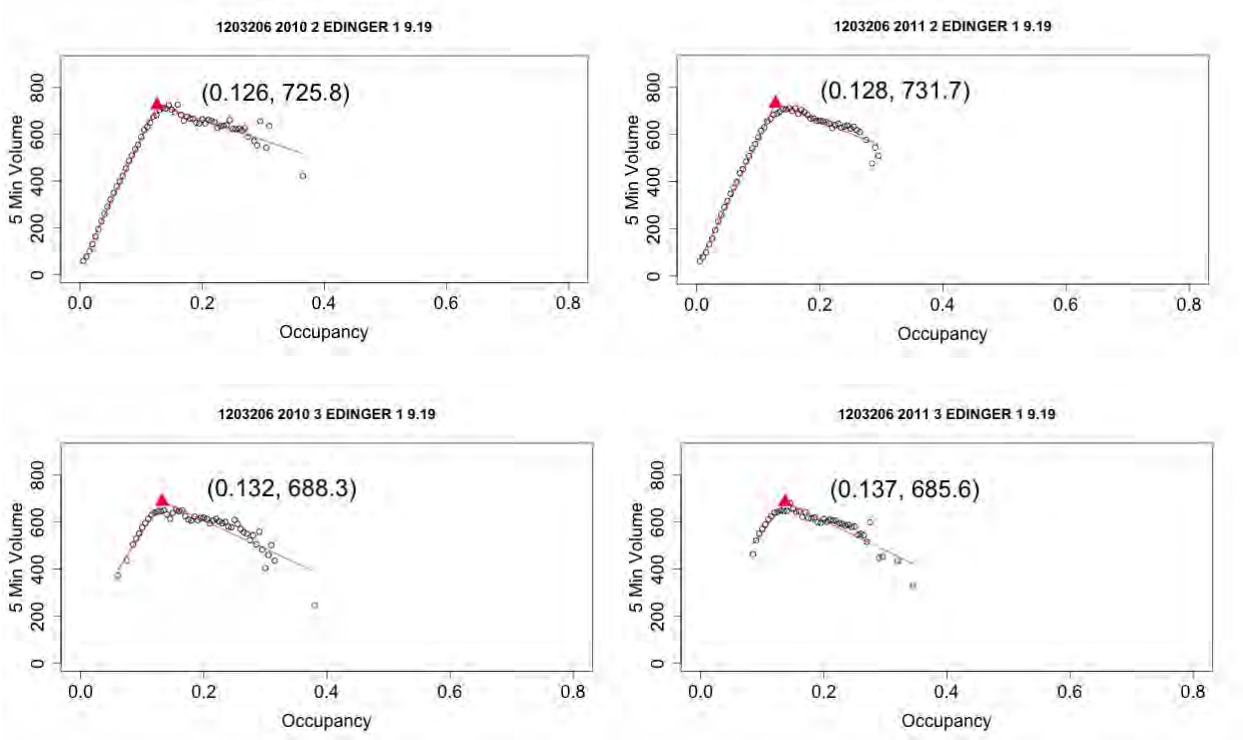

Figure I-4. SR-55 SB2: Estimated Traffic Flow Diagram Parameters using Data in Formulation Phase (Top) and Dissipation Phase (Bottom) at Postmile 9.19

To summarize, the site performs similarly before and after HOV lane conversion. Detailed traffic flow performance analysis shows that the dissipation phase has faster shockwave speed, which means the congestion can dissipate at a faster speed.

B. SR-57 SB2

a) Speed Contour

Figure I-5 shows the speed contours for both GP and HOV lanes before and after HOV lane conversion. The limit of the study site is from absolute postmile 1.93 to 1.4. However, the speed contours in the figures show a longer segment from postmile 2.8 to postmile 0 (corresponding to the I-5/SR-22 interchange) in order to provide an overview of the traffic conditions beyond the study site. We found that the SR-57 SB2 site has a major bottleneck at postmile 0, the connector to I-5 SB, located 1.4 miles downstream of the study area. The freeway mainline traffic condition after the HOV lane conversion is more congested within the study area perhaps because the I-5 bottleneck has become more pronounced.

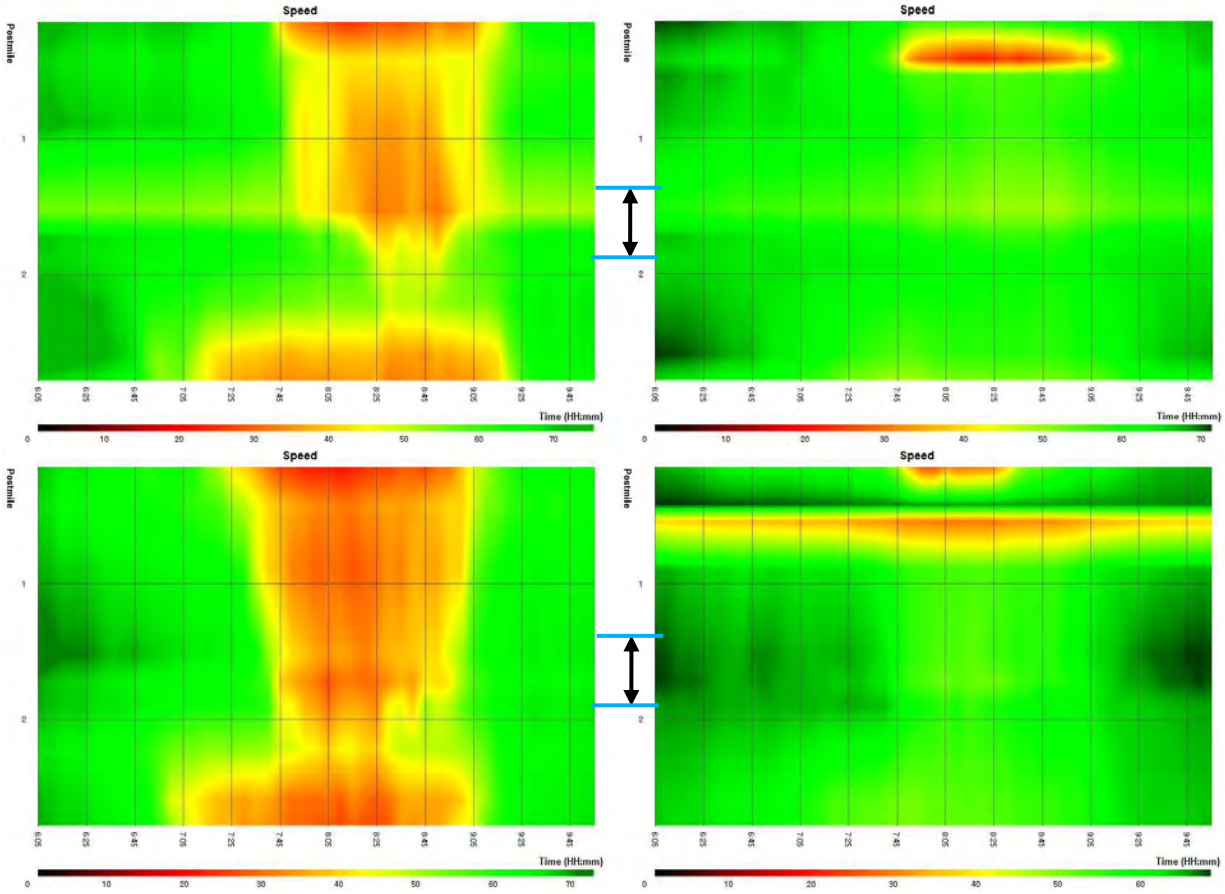

(a) Before (top) and After GP Lanes (b) Before (top) and After HOV Lanes

Figure I-5. SR-57 SB2 Speed Contours Before and After the HOV Lane Conversion

b) Speed Differential

The distribution of speed differential between the HOV lane and the GP lane average for the SR-57 SB2 site is presented in Figure I-6. All plots show a positive speed differential, which implies that the speed in the HOV lanes was higher than the average speeds across GP lanes for a majority of the situations. For all periods (subplots a and b), the speed differential becomes larger after HOV lane conversion. For congested periods when the GP lanes speed is below 45mph, the distributions for before-and-after cases are similar.

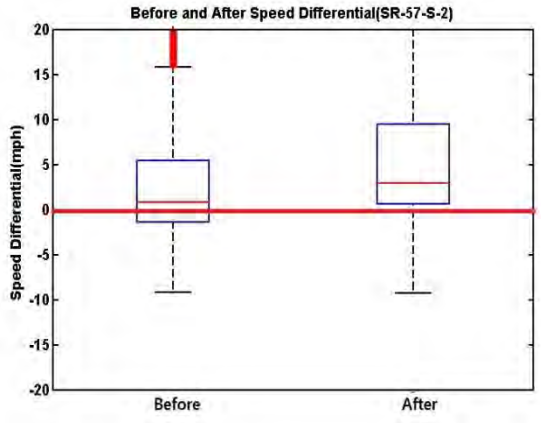

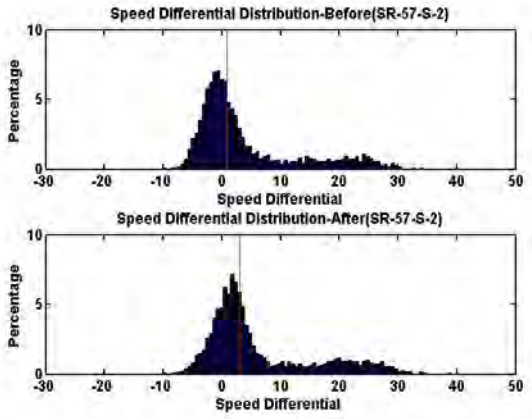

(a) Speed Differential Boxplot (all periods) (b) Speed Differential Distribution (all periods)

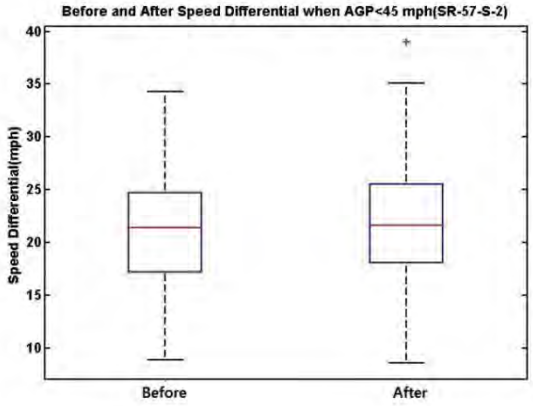

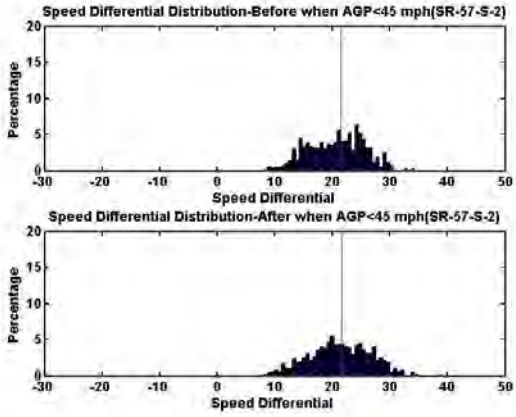

(c) Speed Differential Boxplot (congestion) (d) Speed Differential Distribution (congestion)

Figure I-6. Speed Differential for SR-57 SB2

c) VMT ratio

From Figure I-7, after the conversion, the VMT ratio is shown to be slightly higher in the congested periods analyses and the all periods analyses.

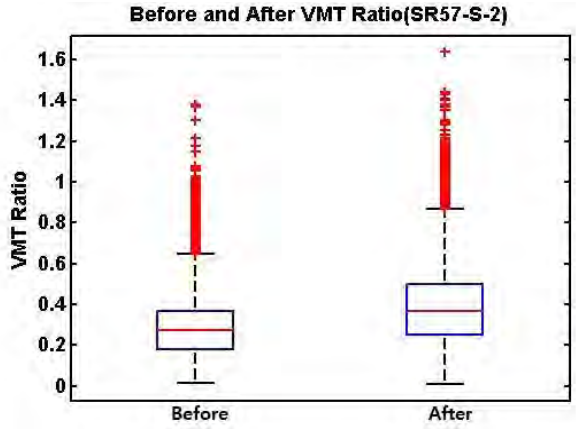

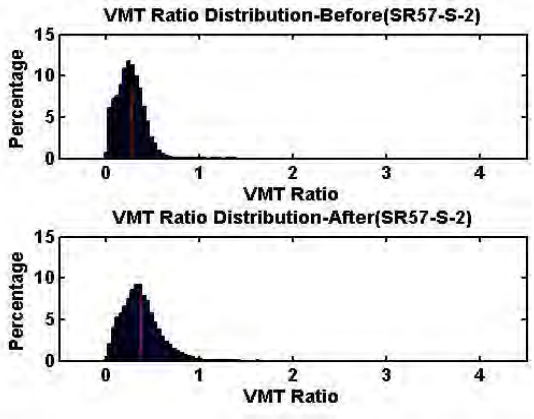

(a) VMT Ratio Boxplot (all periods) (b) VMT Ratio Distribution (all periods)

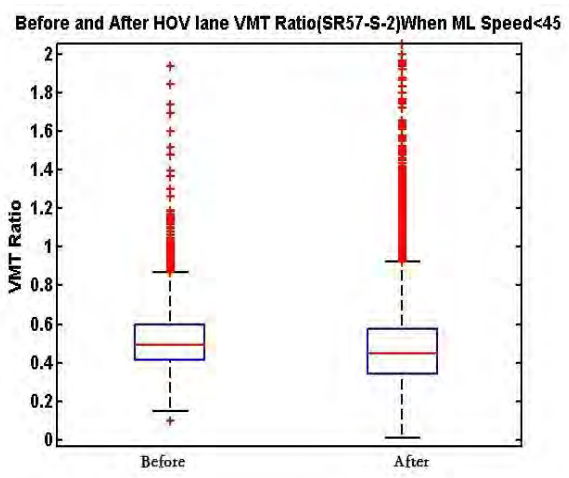

(c) VMT Ratio Boxplot (congestion)

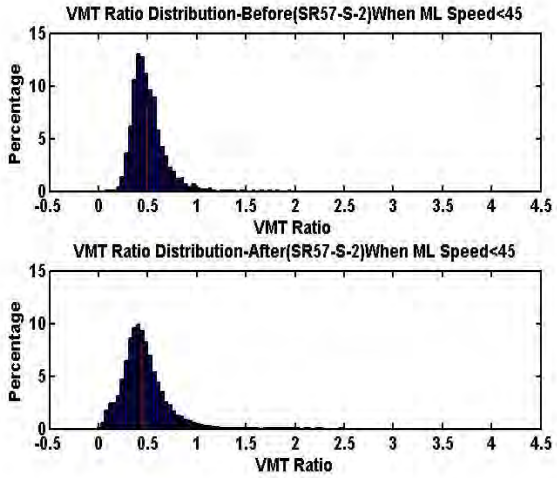

(d) VMT Ratio Distribution (congestion)

Figure I-7. VMT Ratio for SR-57 SB2

d) Demand Flow

For the SR-57 SB2 site, demand flows at all detector locations were analyzed for the a.m. peak period (from 6:00 a.m. to 10:00 a.m.). Table I-4 shows that the site has lower flow for GP lanes and equivalent flow for HOV lanes. In total, the demand flows, which are equal to the total GP lane flow plus the total HOV lane flow, are 2.4% – 2.5% lower after the conversion.

Table I-4. Demand Flows for SR-57 SB2

	GP Lane			HOV Lane			Total			
PostMile	Before	After	Change	Before	After	Change	Before	After	Change	Change %
1.931	28422	27568	-854	2823	2882	59	31245	30450	-795	-2.5%
1.751	29146	28343	-804	3089	3129	40	32235	31471	-764	-2.4%

e) Traffic Flow Fundamental Diagram Parameters

Because the demand flows are lower (as shown in Figure I-5) and traffic congestion is more severe (as shown in Table I-4), it may indicate that the HOV conversion to continuous-access makes the site perform worse. It may be due to the stronger downstream bottleneck at the I-5 interchange. The proposed approach was used to further analyze the operational performance of the site before and after the conversion, to verify the above result, and to explain the result from the perspective of traffic flow theory.

Table I-5 and Table I-6 compare the key traffic flow fundamental diagram parameters at all mainline VDS locations for the formulation phase and dissipation phase, respectively. Based on the analysis of the traffic flow diagram parameters, we found the performance of these traffic flow parameters is mixed, mainly because the study site is not a bottleneck location and its congestion is caused by the I-5 SB bottleneck located 1.4 miles downstream of the site. Detector station at postmile 1.751 is regarded as the key location of the site. Its representative volume-occupancy plots and the traffic flow parameter estimation results are shown in Figure I-8. Although this location shows equivalent performance in terms of critical occupancy and critical volume in both phases, the actual values are slightly lower after the conversion. The slightly lower performance at the location is amplified at the upstream mainline detector station (postmile 1.931) in both formulation and dissipation phases.

In addition, the shockwave speeds at both mainline detector stations in the formulation phase is slower after the conversion, which means the queue builds up at a slower speed and thus is better for operations. Shockwave speed in the dissipation phase is faster after the conversion, which means the queue is able to dissipate at a faster speed and thus is better for operations.

Table I-5. SR-57 SB2: Traffic Flow Diagram Parameters in the Formulation Phase

	PostMile	Ingress /Egress	Before	After	Diff	% Diff	Before V.S. After
Critical Occupancy	1.931	Yes	0.144	0.138	-0.006	-4.2%	After: Lower
	1.751	No	0.146	0.144	-0.002	-1.4%	Equivalent
Critical Volume	1.931	Yes	679.4	652.3	-27.1	-4.0%	After: Lower
	1.751	No	699.9	688.7	-11.2	-1.6%	Equivalent
Shockwave Speed	1.931	Yes	-14.2	-12.3	1.9	-13.4%	After: Lower
	1.751	No	-14.2	-13.1	1.1	-7.8%	After: Lower

Table I-6. SR-57 SB2: Traffic Flow Diagram Parameters in the Dissipation Phase

	PostMile	Ingress /Egress	Before	After	Diff	% Diff	Before V.S. After
Critical Volume	1.931	Yes	646.2	633.4	-12.8	-2.0%	After: Lower
	1.751	No	652.4	649.9	-2.5	-0.4%	Equivalent
Shockwave Speed	1.931	Yes	-15.2	-17.9	-2.7	17.8%	After: Higher
	1.751	No	-12.2	-14.3	-2.1	17.2%	After: Higher

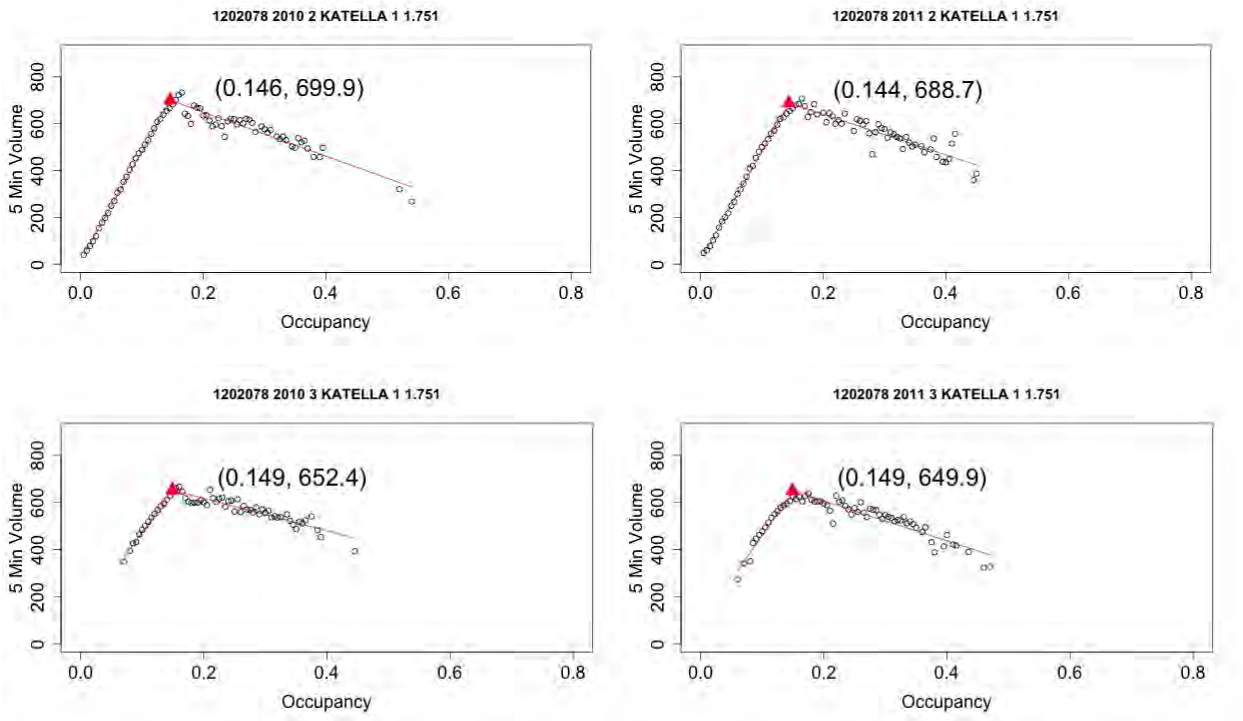

Figure I-8. SR-57 SB2: Estimated Traffic Flow Diagram Parameters using Data in Formulation Phase (Top) and Dissipation Phase (Bottom) at Postmile 1.751

To summarize, the SR-57 SB2 site performed slightly worse after the HOV lane conversion. Since this site is very short and does not have a bottleneck location, the inferior performance might be caused by the bottleneck at the I-5 interchange, located downstream from the site.

C. SR-55 NB2

a) Speed Contour

Figure I-9 shows the speed contours for both GP lanes and HOV lanes before and after the HOV lane conversion. The study limit of the site is from Dyer (absolute postmile 7.6) to the 17th St. interchange (absolute postmile 12). However, the speed contours in the figures show the speeds from postmile 4.7 (the Baker underpass) to postmile 12.682 (the Fairhaven overpass) to provide an overview of traffic conditions beyond the study site.

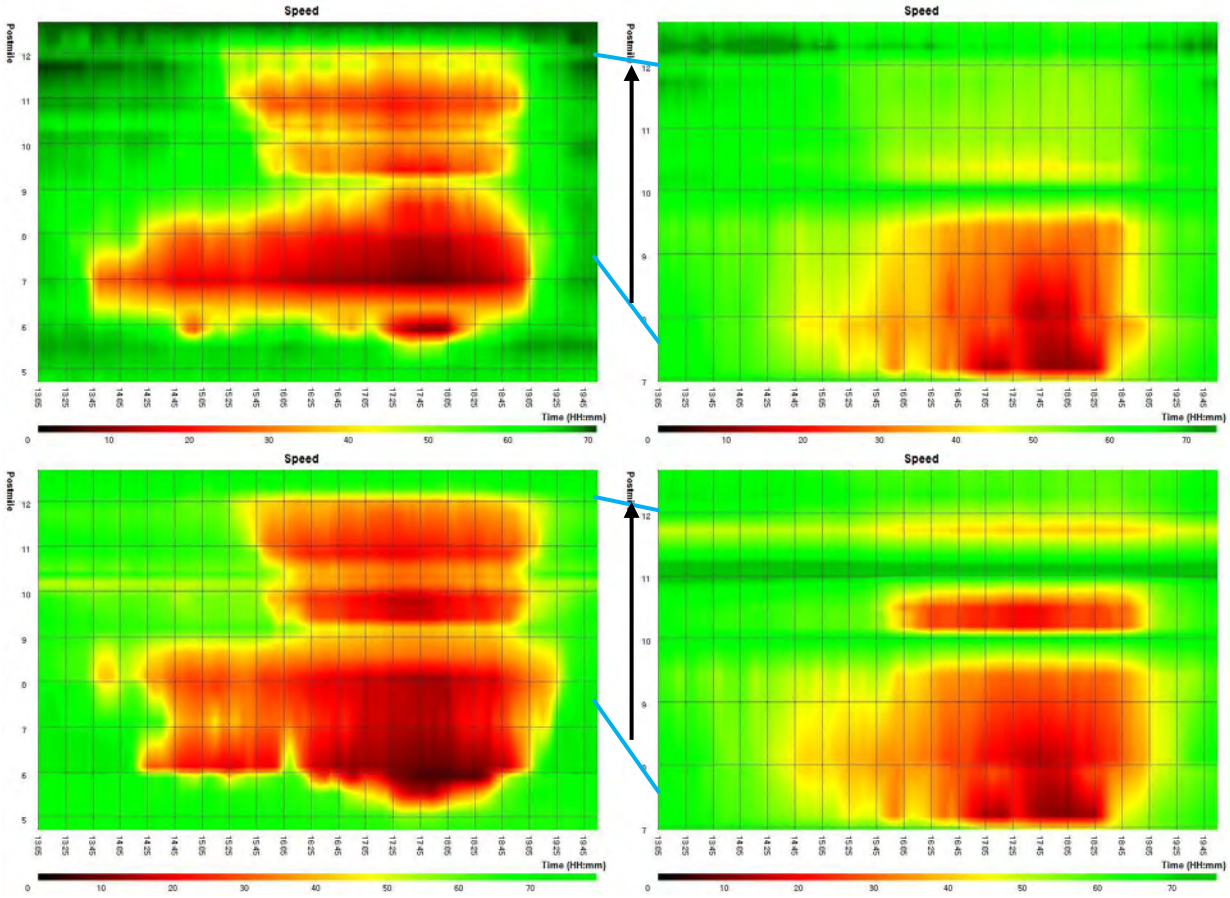

(a) Before (top) and After GP Lanes (b) Before (top) and After HOV Lanes

Figure I-9. SR-55 NB2 Speed Contours Before and After the HOV Lane Conversion

For SR-55 NB2, there are two major bottlenecks within the study site. One is located at postmile 12, the 17th St. interchange. Another is located at postmile 8.12, the Dyer interchange (please note postmile 8.6 has 0% observed data but PeMS provides an estimated speed for this location.).

b) Speed Differential

The distribution of speed differential of the SR-55 NB2 site is presented in Figure I-10. The median value and the distribution of speed differentials increase significantly for all data periods after the conversion. For congested periods, as shown in subplot (c) and (d), the distribution of speed differential has more samples in the higher value range while the median value is only slightly higher.

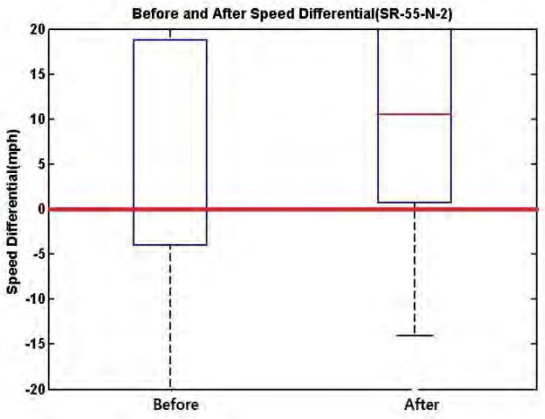

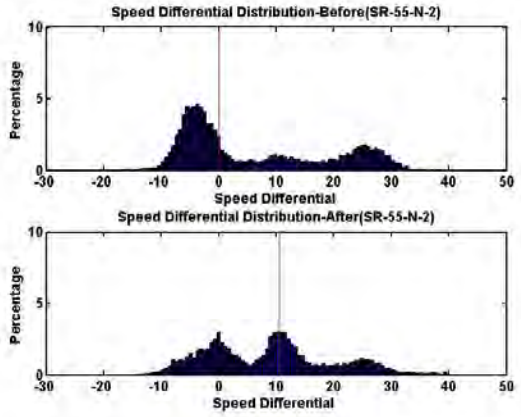

(a) Speed Differential Boxplot (all periods) (b) Speed Differential Distribution (all periods)

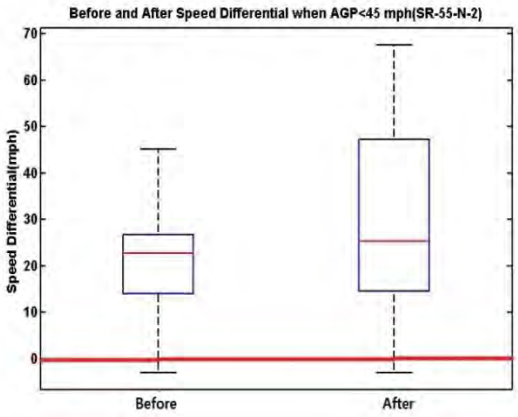

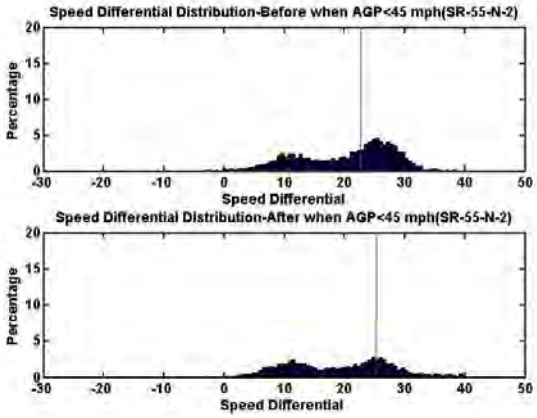

(c) Speed Differential Boxplot (congestion) (d) Speed Differential Distribution (congestion)

Figure I-10. Speed Differential for SR-55 NB2

c) VMT ratio

In Figure I-11, VMT ratio for all periods and congestion are shown to have similar distributions in the before and after study periods.

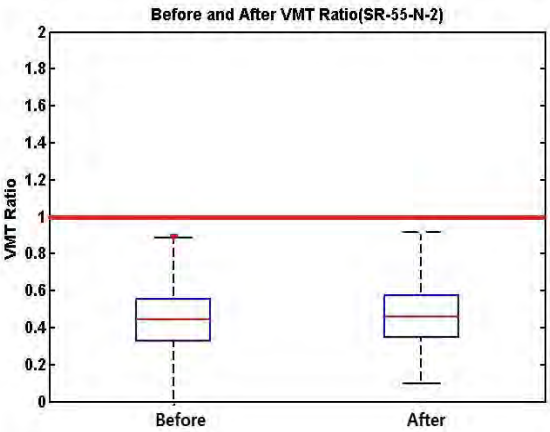

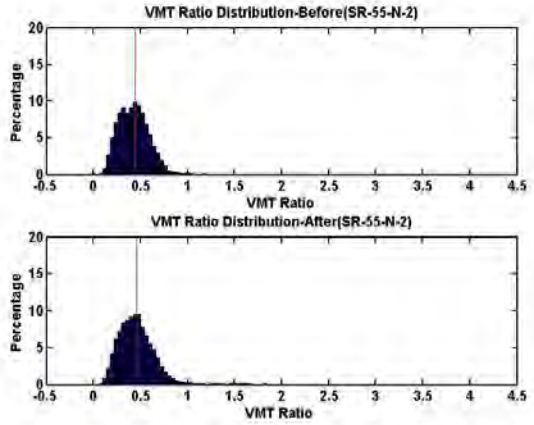

(a) VMT Ratio Boxplot (all periods) (b) VMT Ratio Distribution (all periods)

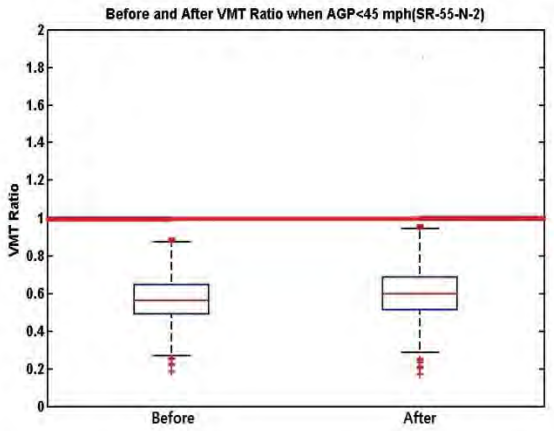

(c) VMT Ratio Boxplot (congestion)

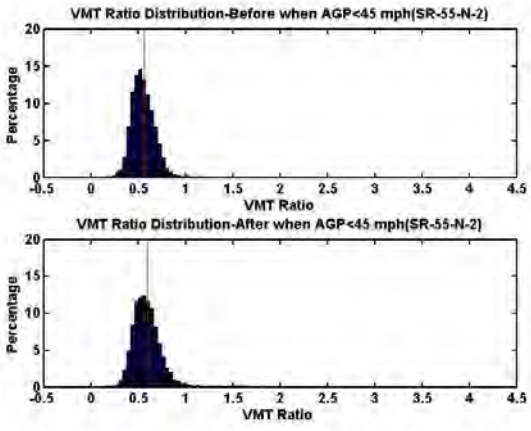

(d) VMT Ratio Distribution (congestion)

Figure I-11. VMT Ratio for SR-55 NB2

d) Demand Flow

We analyzed demand flows at all detector locations for the p.m. peak period (from 1:00 p.m.to 8:00 p.m.). Table I-7 shows that the site has slightly higher (less than 1%) demand flows during the "after conversion" time period. However, the increase is negligible.

Table I-7. Demand Flows for SR-55 NB2

	GP Lane			HOV Lane			Total			
PostMile	Before	After	Change	Before	After	Change	Before	After	Change	Change %
9.41	46727	46910	183	9720	9551	-169	56447	56461	14	0.0%
10.822	30429	30511	83	5121	5164	43	35550	35675	126	0.4%
11.082	47195	47250	55	5097	5282	185	52292	52532	240	0.5%
11.982	51008	50921	-87	5372	5636	264	56380	56557	177	0.3%

e) Traffic Flow Fundamental Diagram Parameters

Because demand flows are a little bit higher and traffic congestion is more severe, we were unable to determine if conversion of HOV lanes to continuous-access provides any operational benefit. Thus, the proposed traffic flow fundamental diagram based approach was used to compare the performance before and after the conversion.

Table I-8 and Table I-9 compare the key traffic flow fundamental diagram parameters at all mainline VDS locations for the formulation phase and dissipation phase, respectively. Among all mainline detector stations, the station at the 17th interchange (postmile 11.982) is a key location.

Its representative volume-occupancy plots and the traffic flow parameter estimation results are shown in Figure I-12.

Based on the analysis of the traffic flow diagram parameters, we found:

- All mainline detector locations have equivalent or higher critical occupancy in the formulation phase, which means that the freeway mainline is less likely to break down.
- All mainline stations have similar or higher critical volumes in both formulation and dissipation phases.
- Most mainline stations have higher shockwave speed for both phases after the HOV conversion, which means that the queue is built up and/or dissipated at a faster speed under congested condition.
- The performance at the key location, the 17th St. interchange (postmile 11.982) is very similar before and after the conversion, which means there is almost no operational difference.

Table I-8. SR-55 NB2: Traffic Flow Diagram Parameters in the Formulation Phase

	PostMile	Ingress / Egress	Before	After	Diff	% Diff	Before v.s. After
Critical Occupancy	8.12	No	0.154	0.154	0	0.0%	Equivalent
	9.41	Yes	0.128	0.128	0	0.0%	Equivalent
	10.822	No	0.132	0.138	0.006	4.6%	After: Higher
	11.082	No	0.137	0.14	0.003	2.2%	After: Higher
	11.982	No	0.165	0.166	0.001	0.6%	Equivalent
Critical Volume	8.12	No	660.1	650	-10.1	-1.5%	Equivalent
	9.41	Yes	663.5	663.2	-0.3	-0.1%	Equivalent
	10.822	No	462.3	476.4	14.1	3.1%	After: Higher
	11.082	No	718.2	732.8	14.6	2.0%	After: Higher
	11.982	No	746	742.7	-3.3	-0.4%	Equivalent
Shockwave Speed	8.12	No	-13.7	-15.1	-1.4	10.2%	After: Higher
	9.41	Yes	-16.7	-16.6	0.1	-0.6%	Equivalent
	10.822	No	-11.8	-13.9	-2.1	17.8%	After: Higher
	11.082	No	-18.6	-20.2	-1.6	8.6%	After: Higher
	11.982	No	-16.8	-17	-0.2	1.2%	Equivalent

Table I-9. SR-55 NB2: Traffic Flow Diagram Parameters in the Dissipation Phase

	PostMile	Ingress / Egress	Before	After	Diff	% Diff	Before v.s. After
Critical Volume	8.12	No	608.8	614.1	5.3	0.9%	Equivalent
	9.41	Yes	636	645.4	9.4	1.5%	Equivalent
	10.822	No	426.5	434	7.5	1.8%	Equivalent
	11.082	No	690.9	686.6	-4.3	4.6%	Equivalent
	11.982	No	708	701.4	-6.6	-0.9%	Equivalent
Shockwave Speed	8.12	No	-14.2	-14.5	-0.3	2.1%	After: Higher
	9.41	Yes	-16.4	-17.3	5.5%	-16.4	After: Higher
	10.822	No	-8.1	-8.5	-0.4	4.9%	After: Higher
	11.082	No	-14.5	-16.6	-2.1	14.5%	After: Higher
	11.982	No	-13.9	-14.1	-0.2	1.4%	Equivalent

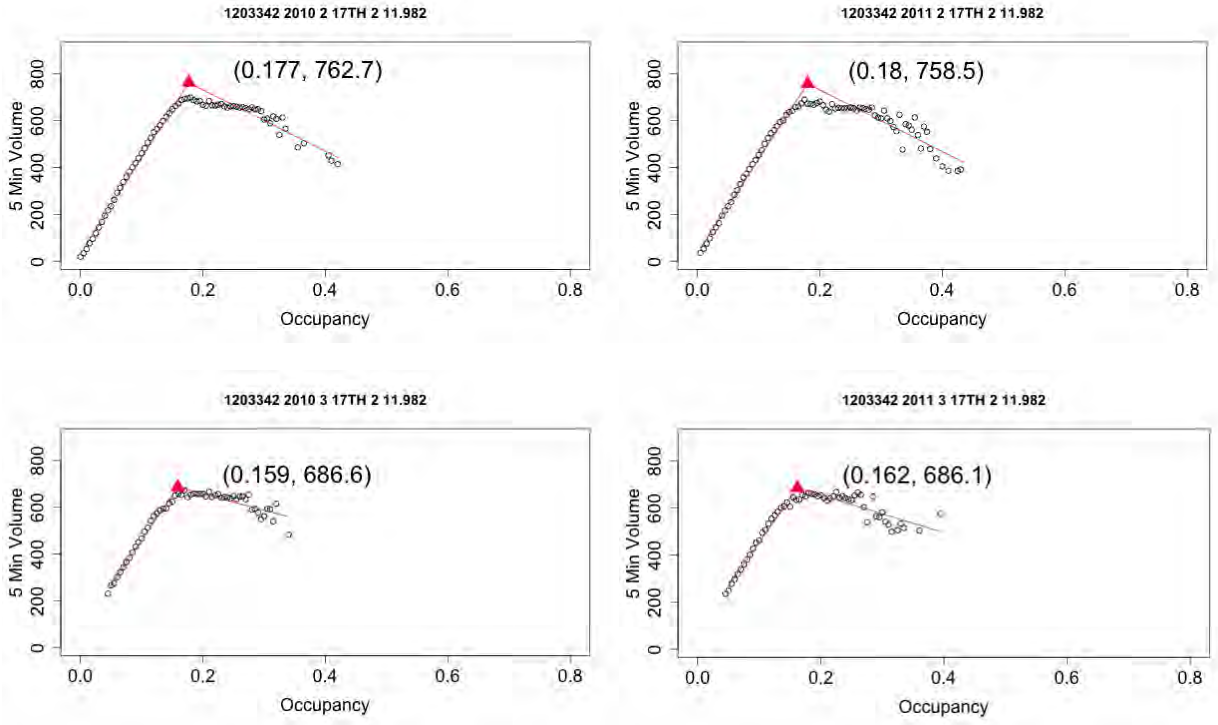

Figure I-12. SR-55 NB2: Estimated Traffic Flow Diagram Parameters using Data in Formulation Phase (Top) and Dissipation Phase (Bottom) at Postmile 11.982

To summarize, the site seems to perform similarly before and after HOV lane conversion, although the actual performance is mixed at different detector stations. Detailed traffic flow performance analysis shows that the formulation and dissipation phases have faster shockwave speed, which means the traffic congestion is able to be built up and dissipated at a faster speed.

Appendix J Comparison of Flow, Density and Speed in Simulation

Table J-1 compares the average speeds on GP and HOV lanes under the existing and alternative simulation scenarios. Under the existing scenario, the average speed differences are 33% for buffer-separated areas and 26% for ingress/egress areas. Under the alternative scenario, the HOV lane does not have congestion and thus average speed differences are increased to 59% and 45% for buffer-separated areas and ingress/egress areas, respectively. The last column of the table measures the improvement of the speed differential from the existing to the alternative scenarios. As indicated earlier, the alternative scenario has higher throughput (because of the use of a low headway factor) along the continuous-access HOV lane and thus its results are too optimistic to be trusted.

Table J-2 compares the average densities on GP and HOV lanes for existing and alternative simulation scenarios. Under the existing scenario, the average density differences are 43% and 44% for buffer-separated areas and ingress/egress areas, respectively. Under the alternative scenario, the average density differences are increased to 53% and 52% for buffer-separated areas and ingress/egress areas, respectively. The last column of the table measures the improvement of the density difference from the existing to the alternative scenarios. As indicated earlier, the alternative scenario has higher HOV lane throughput because of the use of low headway factor and thus its results are too optimistic to be trusted.

Table J-3 compares the average flows on GP and HOV lanes for the existing and alternative simulation scenarios. Under the existing scenario, the average flow differences are 23% for both buffer-separated areas and ingress/egress areas. Under the alternative scenario, the average flow differences are decreased to 16% for both buffer-separated areas and ingress/egress areas. The last column of the table measures the improvement of the flow difference from the existing scenario to the alternative scenario. As indicated earlier, the alternative scenario has higher throughput because of the use of a low headway factor along HOV lanes and thus its results are too optimistic to be trusted.

Table J-1. Comparison of speeds on GP and HOV lanes for existing and alternative scenarios (unit: mph)

Time	Segment Type	Existing (Limited-access)				Alternative (Continuous-access)				% Improve-ment
		GP	HOV	Diff	% diff	GP	HOV	Diff	% diff	
6-7 am	Buffer-separated areas	44.6	55.9	11.4	26%	47.9	71.8	23.9	50%	110%
	Ingress/egress areas	48.3	60.0	11.7	24%	51.5	70.6	19.1	37%	63%
7-8 am	Buffer-separated areas	34.7	47.5	12.8	37%	38.4	69.9	31.5	82%	146%
	Ingress/egress areas	39.2	51.7	12.5	32%	40.8	69.7	28.9	71%	132%
8-9 am	Buffer-separated areas	37.1	55.9	18.8	51%	42.6	70.8	28.2	66%	51%
	Ingress/egress areas	40.5	57.3	16.8	41%	46.7	70.7	23.9	51%	43%
9-10 am	Buffer-separated areas	55.3	65.9	10.6	19%	53.5	74.0	20.5	38%	94%
	Ingress/egress areas	60.2	63.5	3.3	5%	58.8	71.3	12.5	21%	281%
Average	Buffer-separated area	42.9	56.3	13.4	33%	45.6	71.6	26.0	59%	95%
	Ingress/egress area	47.1	58.1	11.1	26%	49.5	70.6	21.1	45%	91%

Table J-2. Comparison of average densities on GP and HOV lanes for existing and alternative scenarios (unit: veh/mile/lane)

Time	Segment Type	Existing (Limited-access)				Alternative (Continuous-access)				% Improve-ment
		GP	HOV	Diff	% diff	GP	HOV	Diff	% diff	
6-7 am	Buffer-separated areas	39.8	25.5	14.3	36%	35.6	19.7	15.9	45%	11%
	Ingress/egress areas	40.6	25.1	15.5	38%	37.1	20.5	16.6	45%	7%
7-8 am	Buffer-separated areas	51.3	32.1	19.2	37%	45.6	19.9	25.7	56%	34%
	Ingress/egress areas	53.8	34.5	19.3	36%	51.5	20.6	30.9	60%	60%
8-9 am	Buffer-separated areas	48.1	23.3	24.8	52%	40.2	16.7	23.5	59%	-5%
	Ingress/egress areas	52.0	23.1	28.9	56%	41.6	16.6	25.0	60%	-14%
9-10 am	Buffer-separated areas	27.7	14.4	13.3	48%	27.8	13.4	14.3	52%	8%
	Ingress/egress areas	25.5	13.3	12.2	48%	25.8	14.1	11.6	45%	-5%
Average	Buffer-separated area	41.7	23.8	17.9	43%	37.3	17.4	19.9	53%	11%
	Ingress/egress area	43.0	24.0	19.0	44%	39.0	18.0	21.0	52%	11%

Table J-3. Comparison of flows on GP and HOV lanes for existing and alternative scenarios (unit: veh/hr)

Time	Segment Type	Existing (Limited-access)				Alternative (Continuous-access)				% Improve-ment
		GP	HOV	Diff	% diff	GP	HOV	Diff	% diff	
6-7 am	Buffer-separated areas	1596	1271	325	20%	1551	1407	143	9%	-56%
	Ingress/egress areas	1655	1336	320	19%	1607	1469	138	9%	-57%
7-8 am	Buffer-separated areas	1484	1265	218	15%	1470	1385	85	6%	-61%
	Ingress/egress areas	1518	1321	198	13%	1513	1433	81	5%	-59%
8-9 am	Buffer-separated areas	1458	1166	292	20%	1423	1175	248	17%	-15%
	Ingress/egress areas	1507	1179	327	22%	1471	1189	282	19%	-14%
9-10 am	Buffer-separated areas	1463	939	524	36%	1425	990	434	30%	-17%
	Ingress/egress areas	1502	951	551	37%	1466	1037	429	29%	-22%
Average	Buffer-separated areas	1500	1160	340	23%	1467	1239	228	16%	-33%
	Ingress/egress areas	1546	1197	349	23%	1514	1282	232	16%	-33%